HYDRAULIC FILL PERFORMANCE IN HONG KONG

GEO REPORT No. 40

C.K. Shen & K.M. Lee

GEOTECHNICAL ENGINEERING OFFICE
CIVIL ENGINEERING DEPARTMENT
HONG KONG

HYDRAULIC FILL PERFORMANCE IN HONG KONG

GEO REPORT No. 40

C.K. Shen & K.M. Lee

This report was originally produced in March 1994
under Consultancy Agreement CE 31/92

First published, June 1995

Prepared by:

Geotechnical Engineering Office,
Civil Engineering Department,
Civil Engineering Building,
101 Princess Margaret Road,
Homantin, Kowloon,
Hong Kong.

This publication is available from:

Government Publications Centre,
Ground Floor, Low Block,
Queensway Government Offices,
66 Queensway,
Hong Kong.

Overseas orders should be placed with:

Publications (Sales) Office,
Information Services Department,
28th Floor, Siu On Centre,
188 Lockhart Road, Wan Chai,
Hong Kong.

Price in Hong Kong: HK$90
Price overseas: US$16 (including surface postage)

An additional bank charge of **HK$50** or **US$6.50** is required per cheque made in currencies other than Hong Kong dollars.

Cheques, bank drafts or money orders
must be made payable to **HONG KONG GOVERNMENT**

PREFACE

In keeping with our policy of releasing information of general technical interest, we make available some of our internal reports in a series of publications termed the GEO Report series. The reports in this series, of which this is one, are selected from a wide range of reports produced by the staff of the Office and our consultants.

Copies of GEO Reports have previously been made available free of charge in limited numbers. The demand for the reports in this series has increased greatly, necessitating new arrangements for supply. Henceforward a charge will be made to cover the cost of printing.

The Geotechnical Engineering Office also publishes guidance documents and presents the results of research work of general interest in GEO Publications. These publications and the GEO Reports may be obtained from the Government's Information Services Department. Information on how to purchase these publications is given on the last page of this report.

A. W. Malone
Principal Government Geotechnical Engineer
June 1995

FOREWORD

This report is the first volume of a set of four study reports on the performance of hydraulic fill in Hong Kong. The study was carried out by Professor C.K. Shen and Dr K.M. Lee of the Hong Kong University of Science and Technology (HKUST) as consultants to the Geotechnical Engineering Office (GEO) of the Civil Engineering Department. Professor J.K. Mitchell of the University of California at Berkeley, USA, and Professor M. Jamiolkowski of the University of Turin and ENEL (Ente Naxionale Per I'Energia Electtrica), Italy assisted as sub-consultants. The project was partly funded by a Research Infrastructure Grant from HKUST.

The study was coordinated and reviewed by Mr Y.C. Chan, Dr J. Premchitt, Mr H.N. Wong and Dr Philip Chen of the Special Projects Division, GEO. Dr Richard Pang and the staff of Public Works Central Laboratory, GEO provided assistance in the laboratory work.

Mr Hugh Childers of Binnie Consultants Limited, Mr John Mckinlay, Mr Vijith DeMel, and Mr Philip Smith of Mott MacDonald Hong Kong Limited, and Mr A.C.H. Bradley of Maunsell Consultants Asia Limited provided site specific data and assistance in field investigation and sampling at the Tin Shui Wai, West Kowloon and Tseung Kwan O Reclamation Sites respectively.

Postgraduate students Mr Derrick H.K. Leung, Mr David C.K. Yu, Mr Kevin Y.Y. Keung and Ms Y. Wang, and Senior Technician Mr Kenny Ma of the Department of Civil and Structural Engineering, HKUST assisted the authors in carrying out most of the field and experimental work, computer analysis, and preparation of figures and drawings presented in the report. The Drafting Unit of the Special Projects Division, GEO converted the figures and drawings into GEO format for the printing of this report.

The Geotechnical Information Unit, GEO provided assistance and access to library facilities for the collection of information. The Soil Mechanics Laboratory, University of Hong Kong made available facilities for and assisted in part of the experimental study presented in the report.

Detailed test results and other information relevant to this report are provided in Appendices in Volumes 2 to 4 of the study reports. They are available for viewing in the Civil Engineering Library.

J.B. Massey
Government Geotechnical Engineer/Development
June 1995

CONTENTS

1. INTRODUCTION

This report presents the results and findings of an investigation on "A Study of Hydraulic Fill Performance in Hong Kong" under the Agreement No. CE 31/92 with the Civil Engineering Department of the Hong Kong Government. The final objective of this study is to develop guidelines for the Geotechnical Engineering Office for quality control of landfill placement applicable to reclamation works in Hong Kong. This, as the self-contained first stage work covering a period of 12 months, was mainly a feasibility and exploratory study for the purpose of developing a pertinent and substantially broad data base for quality control of land reclamation. The scope of work for the one-year study included the following:

(a) literature review on hydraulic fill placement, control and performance,

(b) field investigation on a selected number of sites to gather relevant information,

(c) laboratory testing of selected marine sands for reclamation in Hong Kong including the basic physical property determinations, and triaxial static and cyclic testing,

(d) calibration chamber tests to study the CPT Versus D_r relationship(s) for Hong Kong marine sands, and

(e) preliminary assessment of the dynamic stability of hydraulic fills in Hong Kong.

This study was directed by Professor C.K. Shen and Dr. K.M. Lee of the Department of Civil and Structural Engineering and assisted by four geotechnical engineering postgraduate students at HKUST. The Calibration Chamber tests were conducted at ENEL in Milano, Italy supervised by Professor Jamiolkowski and Dr. Bellotti. Other consultants included Professor James K. Mitchell, Mr. Clarence Chan of the University of California, Berkeley, and Dr. X.S. Li of the University of California, Davis.

Chapter Two contains a comprehensive literature review on hydraulic field placement methodology, control, and performance. A description of field testing conducted on the three selected sites is given in Chapter Three.

The results of the classification tests of samples from the three sites are presented in Chapter Four. In Chapter Five all the triaxial test results are summarized and discussions are given to illustrate the general static and cyclic behaviour of Hong Kong marine sands. A limited number of tests performed on specimens retrieved from sampling tubes using the Mazier samplers are also included.

Chapter Six is devoted to the study of seismic stability of hydraulic fills in Hong Kong; a brief discussion is also given to address the response of fill under other dynamic loads.

The Calibration Chamber tests conducted by ENEL together with a reasonably detailed description of the testing procedure and data interpretation are reported in Chapter Seven.

A comprehensive discussion and summary of the study with emphasis on engineering behaviour and quality control of land reclamation in Hong Kong is presented in Chapter Eight.

2. LITERATURE REVIEW

2.1 General Considerations

Sand hydraulic fills are very young, freshly deposited, water-borne sediments. With some exceptions, they are usually characterized by low relative density, low strength, and high liquefaction potential unless they are densified during or after placement. Density, grain size, segregation during placement, and drainage will all affect performance. The method used for placement and the details of its application, the distance from discharge points, the presence of ponded water, and variability of source materials are all important in determining the resultant fill properties. The placement technique is probably the most important single factor controlling the relative density of a given sand when placed as a hydraulic fill.

Some aspects of dredging in relation to different soil types and transportation methods is given in Table 2.1. A classification of hydraulic fills based on methods of deposition have been developed by Morgenstern and Kupper (1988) and is reproduced in Figure 2.1. It can be seen that this scheme classifies the hydraulic fills primarily on the basis of method of deposition, although other factors such as homogeneity and fine content are also considered. The emphasis on placement method is appropriate, as it can be shown that fills that have performed unsatisfactorily, that is those that have been prone to liquefaction under some form of loading, can be associated primarily with certain methods of deposition.

The first distinction in this classification is made between above water and under water deposition. In general, subaqueous fills tend to be looser than sub-aerial, although this can be an oversimplification. The next distinction that is made is whether or not the depositional process leads to the creation of a beach, which moves forward as a front, as deposition proceeds.

For sub-aerial non-beach deposition, the final component of the classification reflects the end product in terms of degree of homogeneity. Sand infilling refers to the sluicing of sand into the voids of rockfill. Patterned refers to the filling of cells to form a structure. Random refers to the type of filling commonly used in land reclamation and the hydraulic backfilling sometimes adopted in underground mines. Thickened discharge refers to procedures to inhibit segregation by adjusting the placement water content so that a stable pile can be achieved.

With regard to sub-aerial beach deposition, the distinction is made between whether or not the resulting structure is composed of homogeneous fill. The final component of this portion of the classification refers to the geometry of the end product and design and construction aspects such as the need to ensure separation of fines, pool design and type of drainage system required. It should be noted that the terms "central core", "upstream", "centre-line", and "downstream" all refer to different methods for hydraulic fill dam construction. These terms are not relevant to sub-aerial hydraulic fills of the type used for land reclamation in Hong Kong. A contained heterogenous fill refers simply to the beaching of the hydraulic fill between containment dykes that might be of rockfill. Homogeneous fill structures arise either from the deposition initially of fill material without fines or heterogeneous material with

fines being removed during construction.

With regard to sub-aqueous non-beach deposition, a further distinction is made whether the hydraulic fill is placed gradually or dumped. As discussed later in this chapter, it can have a dramatic impact on the in place density of the resulting fill. Sladen (1990) suggested that material beached below water is typically looser than material beached above water even if neither is subject to construction traffic.

2.2 Methods of Deposition

Sladen (1990) discussed the fill placement methods employed for the construction of sand islands in the Canadian Beaufort Sea, these sub-aqueous non-beached deposition methods are very similar to that being employed in Hong Kong as illustrated in Figure 2.2. Hopper dredgers can bottom dump sand (see Figure 2.2a) by discharging through large valves or doors located on the underside of the vessel. Such dumping involves discharging up to 8,000 m^3 of sand in a period of several minutes. Figure 2.2b shows the gradual placement by pump-out from floating pipeline. Relatively steep slopes can be formed by constructing perimeter containment bunds (i.e. low dykes) and infilling the central area as illustrates in Figure 2.2c. The bunds are placed using controlled pipeline discharge techniques. This is accomplished by pumping material from either a hopper or cutter suction dredge through a floating pipeline to an anchored barge. The sand is then discharged through a modified discharge nozzle during controlled winching of the barge or by drag arm pump-out method.

Several other methods of deposition are illustrated schematically in Figures 2.3 and 2.4. In the foreground of Figure 2.3, an embankment is being constructed by means of the cell construction or "patterned" method of non-beach sub-aerial deposition. In this procedure, perimeter bunds are pushed up and maintained by means of bulldozers. An important feature of this construction method is that the cell placed material is subject to traffic loading during the deposition process. Behind the cell construction in Figure 2.3 (see also Figure 2.4) a beach formation is shown. Depending upon water level (or sea level), a significant beach may form below water. When the beach is raised above water level, further compaction is introduced by bulldozers working on the slope to guide the mixture flow. As suggested by Verkerke and Volbeda (1991), this compaction effort could result in Proctor densities of 95% or above.

2.3 Effects of Dredging Methods on Grading of the Materials

Control of the fill gradation and fine content can be achieved by careful borrow selection. Suitable fill source material can be delineated by means of site investigation prior to excavation. Many natural deposits are however heterogeneous and it is often impracticable to select a borrow area that completely conforms to specific criteria. Near real-time monitoring of the excavated material has been adopted in the construction of some artificial islands in the Canadian Beaufort Sea. By continuously screening material, it is possible to direct deleterious material to relatively non critical areas. It should be noted that, however, selective dredging by trailing suction dredgers may not be feasible for larger vessels as usually employed in Hong Kong, since much time is lost in turning to dredge smaller borrowing areas which render it to be uneconomical.

During loading of dredged materials on board, the density of the dredged sand-water mixture (slurry) in the hopper may be increased by means of an overflow system, whereby the unwanted fine suspension is displaced overboard. This is achieved by discharging through an overflow outlet in the hull of the vessel. In this way, the significant quantities of silt and clay can be removed from the sandy deposits. To achieve the required result, the water level in the hopper should be kept close to the level of the settled sand fraction, but not so close as to produce undue sand losses. Jet water systems in the hopper can also be used to keep the settled sand in a liquefied state near the end of the loading period. In some cases hydrocyclones or sand separators have been used (Lyell and Prakke, 1988) to separate fine and coarse materials, but the throughput was generally quite small. Upgrading of the source material is not possible on board of hydraulic pipeline dredgers as the sand-water slurry is continuously pumped directly from the borrow area to the fill area.

2.4 Insitu Density of Hydraulic Fill

Sladen (1990) examined various data concerning the insitu density of subaqueous hydraulic fills, and suggested the following comments which can be considered representative of general experience in the use of subaqueous hydraulically placed sand fills:

(a) Dense sand cannot be obtained by simple hydraulic placement. (Insitu densification has been a commonly accepted practice in land reclamation projects).

(b) At best, relative densities of up to 60 percent can be achieved by hydraulic placement but generally they will be less than 50 percent.

(c) Relative density can vary within a given fill from about 10 to 70 percent.

(d) Other factors being equal, sub-aerially placed fills are generally denser than subaqueous fills.

(e) The factors affecting insitu density are little understood.

A recent evaluation by McNeilan (1993) of several sand hydraulic fills having mean grain sizes, d_{50}, in the range of 0.2 to 0.7mm and placed below water showed (a) average relative densities in the range of 30 to 60 percent, (b) increasing average relative density with increasing d_{50}, and (c) for a given d_{50}, the more uniform the sand, the lower the relative density.

Pipeline discharge to a beach below water gives a looser fill than is obtained if the same material is beached above water. Sand that is bottom dumped from a barge through water is usually denser than material placed by pipeline discharge. According to Sladen (1990) the relative density of hopper placed sand is typically 20 to 30 percentage points higher than that of pipeline placed sand. This means that the loosest zone in a sand hydraulic fill is likely to be just below the free water surface, if bottom dumping is used for placement of fill material in deeper water.

A general sequence for highest to lowest post-placement density for a given material according to placement method is (Sladen, 1990):

1. Above water with traffic compaction.
2. Hopper dumping below water.
3. Beach above water - no compaction.
4. Below water deposition from pipeline onto fill surface.
5. Beach below water.
6. Below water - pipeline deposition above fill surface.

When the source material is variable, then, to the extent possible, the poorest material (usually silts and clays) should be directed to non-critical areas if the operating procedures can accommodate selective dredging and placement methods. Mixed fine-grained and cohesionless dredged material will incorporate the worst features of each.

Experience to date in the Canadian Beaufort Sea has shown that placement technique has an important influence on the insitu density of hydraulically placed sands. This is illustrated by reference to CPT data from five artificial sand islands as shown in Figure 2.5. It can be observed that the mean CPT tip resistance in the hopper placed material is always greater than in the pipeline placed material. At all sites, there is a wide range of tip resistance recorded at a given depth. For a given placement method, the maximum tip resistance is typically two to four times of the minimum value. Given that the vertical stress will likely be related to depth at a given site, these variations can be attributed to some combination of variations of insitu density, horizontal effective stress, composition, and fabric. Given the uniform nature of the sand, it can be assumed that insitu density is likely the dominant factor, but it should be recognized that there is some uncertainty as to the cause of the spatial variability.

The exact mechanics that lead to the differences in density between bottom dumping and pipeline placed material are little understood, Sladen (1990) suggested the following factors that may be causing these differences: The sand hopper dredge, though relatively loose and nearly saturated, probably has a bulk density of around 18 to 19 KN/m^3. On the other hand, a typical density of the sand slurry in pipelines is around 13 to 14 KN/m^3. The net negative buoyancy of the discharge from a hopper dredge is therefore at least twice that of the discharge from a pipeline. As a result, the sand from the hopper falls as a slug rather than as individual particles. Further, the simultaneous opening of all the valves or doors of the hopper dredge inhibits the entrainment of "fresh" water into the slug that would reduce its fall velocity and expand its size. The fall energy of this discharge is likely dissipated in compaction to the berm through impact and shearing. In effect, the bottom dumping method is in itself a form of soil compaction.

Pipeline placement intuitively results in less compaction effort than bottom dumping placement. If the sub-aqueous discharge were a single point held close to the berm surface on the sea floor, there would be little opportunity for "fresh" water into the flow. Virtually all the kinetic energy due to the discharge velocity would be absorbed by the berm. As such one would anticipate some vibratory packing induced by the fluid turbulence in the jet impingement region and some horizontal shearing of the settled sand away from the nozzle. The loosest possible state would likely be achieved if the single point sub-aerial discharge was placed near the sea surface such that maximum "fresh" water entrainment takes place and the

discharge flow become a cloud with a fall velocity close to the fall velocity of individual particles. Each particle would essentially come to rest in the position where it makes contact with the previously placed fill. Subsequently, impacts by other particles may result in some jostling but the impact velocities and forces would be small.

The deposition process of sub-aerial placed sand is quite different from the sub-aqueous deposition. After leaving the pipeline, the sand-water mixture will form a crater lined with the coarsest fraction of the soil. The soil water mixture will flow over the edge of the crater and the sand will deposit on the outside slopes (see Figure 2.6). The slope angle depends on grain size of filling material, mixture concentration and discharge velocity (de Groot et al 1988). Along the slope individual grain settles in a turbulent current while the sand mass is subjected to a downward seepage due to the drainage effect of the sand body. Each grain will only stay in position when it has found a stable position, forming a sand body with a lower void ratio than in submerged deposition. Compaction is further increased by the bulldozers which work on the slope to guide the mixture flow. Usually this will result in a relative density of about 60 to 80 percent (or in Proctor densities of 95 percent or above) as suggested by Verkerke and Volbeda (1991).

Segregation in hydraulic fills above water level will inevitably take place, with the coarse fractions mainly settling in the upper parts of the slope and the finer fractions mainly at the lower parts. In the end, the top layers of the fill will consist of coarser material than the lower layers closer to water level. If fine fraction is presented in open fills, it may be washed out of the fill area and settled below the water level. In closed fills the finer fraction will settle near the overflow weir. If the formation of such deposits of fines are to be prevented, careful planning of the filling method is required. The free water level in the fill area should be kept as low as possible to minimize the quantity of stagnant water and to maximize the layer thickness with high compaction.

2.5 Improvement of Hydraulic Fills

Densification of sand hydraulic fills either during or after placement is often required to insure their stability under static and dynamic loads and to prevent excessive settlements. If liquefaction of a sand hydraulic fill occurs from any cause, then rupture of containment dikes becomes a possibility. Large deformations can cause pipeline rupture and damage to other infrastructure systems; e.g., roadways, drainage channels, buried communication lines. In the consensus report on geotechnical, structures, and construction developed as part of a planned major expansion of the Port of Los Angeles (POLA, 1990), it was stated that:

(a) Hydraulic fill should be "engineered", not simply dredged and placed.

(b) Guidelines for the fill should be at least as demanding as those for the structure that it supports.

Almost all of the available ground improvement and modification methods may be used for the improvement of hydraulic fills. The selection of the appropriate ones for a project depends on detailed evaluation of the following factors:

(a) intended use of the treated ground, level of improvement needed,

(b) area and depth of fill to be treated,

(c) hydraulic fill material type,

(d) availability of required special materials, equipment, and skills,

(e) environmental considerations and constraints,

(f) prior experience,

(g) time available, and

(h) cost

Hydraulic fills may be viewed as freshly deposited, very young water-borne sediments. As a result, their densification and improvement is likely to be easier from the standpoint of structure breakdown and particle rearrangement than is the case for most natural sediments of comparable composition and density. This is because time-dependent strength gain and inter-particle cementation may not yet be as well developed as for older sediments. On the other hand the work may be more difficult to execute owing to the poor equipment trafficability and support properties of the soft fill.

Suitable methods and their characteristics relative to treatment of hydraulic fills are summarized in Table 2.2. Detailed descriptions of these methods are given in readily available literature; e.g., ASCE (1978), Mitchell (1981), ASCE (1987). In Table 2.2 the different methods are organized into the following categories:

Densification during placement
Deep densification by vibration
Deep densification and reinforcement
Precompression
Admixtures
Injection and Grouting

In this table methods for treatment of hydraulic fills of all types are indicated; those pertaining to sand fills are of most significance to the present study.

Densification of shallow lifts during placement is likely to be far easier, more reliable, and less costly for fills placed above water than treatment of fill below water. In most cases below-water densification is not undertaken until the fill surface has been brought above the water surface. Little study seems to have been made of the potential usefulness of underwater densification methods that can be used during fill placement. The concurrent placement and densification of material underwater could result in operational problems during construction; however, the possibilities for selective area densification in lifts below water warrants further evaluation.

Qualitative, comparative costs for the different methods are given in Table 2.2. More specific values for some of the methods, from Welsh (1987), are given in Table 2.3. The values (in 1987's U.S. dollar and assumed a treatment depth of about 10 m) are likely to increase considerably by now, it is given herein only as information of comparative costs for different methods.

Several general observations may be made about each of the categories of improvement methods.

Densification During Placement. Surface compaction of fairly clean sand hydraulic fills during placement is likely to be easier, more effective, and less expensive than deep densification later. Vibratory rollers and heavy construction equipment working on the beach surrounding the hydraulic fill discharge pipes can maintain optimum surface profiles for fill spreading and deposition, and compact concurrently to high relative densities; e.g. 85-90 percent.

Underwater surface compaction has been little used, but is possible by several means, including surface pounder, tamping plates attached to the end of a pile, and underwater vibrating plate compactors operated by barge mounted equipment. For example, a Dynapac unit was developed in Sweden (CM&E, 1976) that weighs 1.8 tons and develops a 9.6 ton vertical force on a 3 ft x 3½ ft (0.9 m x 1.1 m) plate at a frequency of 24 Hz.

Underwater roller compactors are a reasonable expectation for densification of large volume hydraulic fills in the future. A crawler-tractor type unit was designed and patented by the late Arthur Casagrande for use on rockfill and thick soil layers in water depths to more than 100m.

An experimental technique is recently developed by Hodge (1988) for improving the engineering characteristics of underwater sand fills during placement. This technique involving the idea of pumping water out of submerged sand fills concurrently with fill placement, in order to generate inward seepage flows through the sand mass as a possible means of producing higher densities, steeper side slopes and enhanced erosion resistance. This technique, although seems very promising, is only in early stage of development, and it is not yet ready to apply in the field.

Deep Densification by Vibration. Vibratory methods are very well suited for deep densification of clean sand hydraulic fills. Deep dynamic compaction is likely to be the simplest and most economical method for densification of layers up to 10 to 12m thick. The current state of practice using dynamic compaction is described in detail by Lukas (1986).

Vibratory probe densification of clean sand hydraulic fills, using probes of various types suspended from vibratory pile driving hammers, has been very effective in several cases, with maximum relative densities to more than 80 percent being achieved. Two recent cases have been described by Leycure and Schroeder (1987) which illustrate both the magnitude of improvement and the distribution of relative density with depth. Figure 2.7, from their paper, shows the distribution of relative density with depth after vibratory probe densification of a clean medium sand on two sites at the Port of Portland. Maximum density was developed at a depth corresponding to an effective overburden pressure of about 55 kPa.

The observed density distribution with depth is explained by Leycure and Schroeder (1987) on the basis that at shallow depths the confinement needed for maximum densification is not available. At large depth the higher confining pressure increasingly resists the breakdown of the sand structure that is needed to start the densification process.

A similar variation of properties with depth has been found for densification by dynamic compaction. Figure 2.8 is an example. The same confining pressure effects are important as for vibratory probe densification. In addition, the amplitude of vibration caused by the impacting weight diminishes with depth below the ground surface, and this further restricts the effective depth of densification by dynamic compaction.

Blasting may be an effective and economical means for densifying clean sand hydraulic fills, and may have application for special problems. It can be used at depths greater than reachable by other deep densification methods. Successful application to depths of 45m at the Jebba Hydroelectric Development was described by Solymar (1984). Blasting was used to densify the hydraulic fill sand to a depth of 23m inside deep caissons constructed at the Molikpaq's Mobile site in the Arctic. Headroom constraints beneath the deck of the caisson prevented the utilization of other methods for deep densification.

Deep Densification and Reinforcement. Vibro-compaction of cohesionless soils using a vibrofloat and a backfill differs from vibratory probe compaction in that not only is the soil densified by vibration, but a densely compacted column of backfill is produced as well. Thus, the densified sand is further strengthened by the reinforcing action of the compacted sand or gravel piles.

Compaction piles and vibro-replacement stone columns are more suitable for hydraulic fills of silty or clayey sand and cohesive soil hydraulic fills. Since compaction piles and stone columns are considerably stronger than the soils in which they are installed, thus they act as reinforcing elements.

An additional contribution to increased strength and liquefaction resistances as a result of deep densification and reinforcement of cohesionless soils by vibratory and vibro-displacement methods is the increase in effective lateral earth pressure due to vibration.

Precompression. Precompression using preloading and surcharge fills has probably been the most widely used technique for the improvement of cohesive soil hydraulic fills. The use of sand drains for acceleration of the consolidation process has been almost completely supplanted by the use of prefabricated band-shaped drains. The theory and technology for precompression are both well-developed and comprehensively described in readily accessible literature; they are not discussed further here.

Electro-osmosis is a feasible means for consolidation of soft, fine-grained hydraulic fills. Except in special cases, however, the economics may not be favourable. One such case might be when time is not critical and wind power could be used for generation of the needed electrical power.

The potential for densification of fine-grained dredge spoil by seepage consolidation to underdrains was analyzed by Johnson et al (1977). The effective stress profiles in a soil layer corresponding to different drainage and drying conditions are illustrated in Figure 2.9.

It may be seen that downward seepage forces may be used to develop significant effective stress for consolidation.

Previous experiences indicated that seepage consolidation is very economical compared to other techniques, provided, of course, that the underdrain system is installed prior to hydraulic filling. It may be noted also that the use of vertical drains essentially doubles the cost of surcharge loading.

A unique method for improving the liquefaction resistance of a sand hydraulic fill beneath existing oil storage tanks in Kawasaki, Japan involved dewatering to increase the effective confining pressure (Ryan, 1988). The zone of soil to be strengthened by this form of precompression was surrounded by a slurry wall. The water level inside the encapsulated zone was then lowered until the increase in vertical effective stress was sufficient to give the hydraulic fill the required liquefaction resistance.

Admixtures. Structural fills produced by stabilizing the upper few feet of soil using cement, lime, or chemical admixtures can be used for support over soft hydraulic fills. This technology, available in Europe and Japan for a number of years, for construction of deep mix-in-place piles and walls was introduced into the U.S.A. in 1987 for foundation stabilization at Jackson Lake Dam in Wyoming. Equipment is available for construction of piles up to about a meter in diameter to depths up to 30m. Adjacent mix-in-place piles can be used to form walls or cells for encapsulation of liquefiable soil. The high strength of the piles themselves means that they can be used for direct support of structures over soft hydraulic fill. This rather expensive option of the formation of mix-in-place walls or cells may be comparable to the use of deep foundation over soft hydraulic fills.

Injection and Grouting. Permeation grouting using particulate and chemical grouts can be used to eliminate the liquefaction potential of cohesionless soils. Because of its high cost, however, permeation grouting is not likely to be used extensively in hydraulic fills. Jet grouting gives results similar to those obtained using mix-in-place piles and walls. The high cost of jet grouting, Table 2.3, precludes its large scale use in hydraulic fills except for local support of structures.

On the other hand compaction grouting can be used to advantage in silty or clayey sand fills of large void ratio. Compaction grouting may have its greatest utility for filling voids in hydraulic fills composed of clay balls in a loose sand and clay matrix.

2.6 Characterization

Insitu tests are usually used for characterization of hydraulic fills after placement, with the SPT and the CPT being the most common. The CPT is particularly well-suited for use in sandy hydraulic fills, because it is rapid and low cost, it provides a continuous profile through the fill, the results are amenable to rational quantitative analysis, and other useful information can be obtained concurrently with the cone penetration resistance; e.g., shear wave velocities, pore water pressures. In many cases, however, sophisticated analyses of the test results are not required, with simple correlations between measured values and the properties providing a suitable means for establishing whether the specified placement densities have been attained.

Although the cone penetration test (CPT), the standard penetration test (SPT), and the pressuremeter test (PMT) are most commonly used on soil improvement projects, a number of other techniques, tests, and observations can also yield useful information.

Visual Observations. Much can be learned from the direct observation of soil improvement work in progress. Efficient and uniform procedures probably presage satisfactory results. Such things as probe penetration and withdrawal rates and energy consumption during vibrocompaction can be useful indicators.

Settlement Measurement. When the soil improvement involves densification, the ground surface settlement can be used to compute an average density increase over the depth of treatment. No information is obtained about the densification distribution with depth unless settlement devices are installed at different levels.

Backfill Consumption. When deep densification is by vibrocompaction, compaction piles, compaction grout, or dynamic compaction with backfilled craters, a knowledge of the amount of imported fill that is placed into the ground enables estimation of average density increases. Variations with depth can be computed if records are maintained of backfill consumption with depth. However, variations in radial directions from the compaction points cannot be determined from knowledge of backfill consumption alone.

Plate Load Tests (PLT). Plate bearing tests done at the ground surface or at depth in test pits or by the screw plate test provide information about deformation or strength properties from analysis of the load Versus settlement curve (Mitchell and Gardner, 1975). It is essential in the interpretation of the PLT to take into account the soil volume that is stressed and the accompanying drainage conditions.

Seismic Wave Velocity. Before and after measurements of wave velocities provide a direct measure of ground improvement in the zone traversed by the waves. For a given level of excitation, the measured wave velocity depends on modulus, mass density, and Poisson's ratio; with the modulus having by far the greatest influence. Thus, vibroseismic methods can be used to evaluate the effect of ground improvement on modulus. Vibroseismic methods are available that can be employed in many cases; e.g., refraction, Rayleigh wave dispersion, uphole and downhole methods, and crosshole methods. A state-or-the-art evaluation of these methods has been presented by Ballard and McLean (1975). Probably the factor restricts the use of these techniques for application to ground improvement evaluation the most is their relatively high cost.

Two recent developments may help overcome this disadvantage and allow for more routine use of seismic wave velocity methods. Stokoe and Nazarian (1983) describe a method which involves measurement of transiently excited Rayleigh waves propagating along the ground surface. It is reported to be fast, nondestructive, requires no boreholes, and can be fully automated. It can be used to evaluate ground improvement to depths of several meters. A piezometer-friction-bearing cone with a set of geophones or accelerometers built in is described by Robertson et al (1992). A downhole seismic test is done during pauses in penetration. The shear wave source is located at the ground surface. A shear wave velocity profile is obtained which can be used for estimation of the dynamic shear modulus.

Acoustic Emission Monitoring. Koerner and Lord (1985) describe recent developments

in the application of acoustic emission technology for determination of insitu stress by means of an acoustic pressure-meter. As an increase in the insitu lateral stress may be one of the most important results accompanying insitu deep densification of soils, this technique may have potential for supplementing normal PMT measurements that are used for ground improvement evaluation. Acoustic emission monitoring has been used successfully also for monitoring of compaction grouting operations. Koerner and Lord (1985) show how it can be used to locate grouting sources and points where hydrofracturing is occurring.

Downhole Density Measurements. Downhole nuclear density devices have been under development for some time. Their potential for evaluation of ground improvement is great as a specific density increase is often required for site improvement. A nuclear insitu density cone having a cross sectional area of 1500 mm^2 has been developed by the Delft Soil Mechanics Laboratory (Tjelta et al, 1985). The potential usefulness of a device that could be incorporated as a part of a standard CPT evaluation of ground improvement is obvious. There are disadvantages, however, in that special precautions are required when radioactive sources are used, and the loss of such a device in the ground would necessitate special recovery operations.

Penetration Tests. As noted earlier, penetration testing, using either the SPT or the CPT, is the most frequently used means for evaluating insitu deep densification. The CPT is particularly useful because it provides a continuous record with depth, it is fast, it is well-suited for evaluation of sands and silts, and it is cost effective. It is now more widely used in these materials than the SPT. The SPT continues to be used, however, because of its availability and the existence of various experience-based correlations between N-values and properties. It can also be used in ground that cannot be readily penetrated by the CPT.

Pressuremeter and Dilatometer Tests. The PMT has had extensive application for ground improvement evaluation, particularly for projects where deep dynamic compaction has been used. It offers the advantage that estimates can be made of the lateral stress, the modulus, and the shear strength. On the negative side are the facts that holes must be bored, and a large number of separate tests must be done, if a detailed profile is to be obtained. (Although the use of self-boring pressuremeters, SBPMT, will eliminate the need to bore holes. In the authors' opinion, however, these devices are primarily research tools, and to use them on a routine basis for fill evaluation and characterization would be very time consuming and costly.) The flat plate dilatometer can also be used for evaluation of ground improvement, provided it can be pushed or driven to the desired depth. This device, which in effect is a plane strain pressuremeter that yields two points on the expansion curve, can be used in soils that are free of large particles or other obstructions.

The quality and trends of the results obtained using the CPT, the SPT, and the PMT are likely to be comparable in many cases. An example given by Mayne et al (1984) is shown in Figure 2.8. The proportionate increases in SPT N-value, CPT tip resistance, and PMT limit pressure are about the same in each case, as are also the indicated depths of improvement.

As concluding comments on ground improvement evaluation, it is important to keep in mind when using and interpreting insitu test results that:

(a) Measurements and interpretations are separate issues.

(b) Apparatuses and procedures are subject to variability.

(c) Some measurements, such as CPT sleeve friction, are difficult to reproduce.

(d) The "reasonableness" of results should always be checked.

(e) Local ground variability is common, especially in sands.

(f) Time-dependent property changes (in terms of an increase in stiffness and strength and a decrease in compressibility) in sands after disturbance and densification are common.

2.7 Time Effects in Hydraulic Fills

Many sands will develop significant stiffening and strength increase during the first several weeks following their deposition or densification (Mitchell and Solymar, 1984; Dowding and Hryciw, 1986; Schmertmann et al, 1986). As an example Figure 2.10 shows the cone penetration resistance at several locations in a 10m thick clean sand hydraulic fill placed in the Niger River during construction of the Jebba Dam. The fill was dredged from the river bottom and pumped in suspension to the discharge points. The left CPT record of each pair in Figure 2.10 pertains to a CPT measurement between 4 and 10 days after fill placement; whereas, the right CPT record of the pair pertains to a CPT measurement between 50 and 80 days after fill placement. During the several week aging period the penetration resistance about doubled. Deep blasting, to depths of 45m, for densification of this river sand caused immediate densification, as evidenced by settlement of the ground surface. Significant increases in penetration resistance were not measured, however, until several weeks later, by which time the development of inter-particle bonding had produced a strength increase (Mitchell and Solymar, 1984). There is some evidence that a cementation-type bonding can develop in sands in the absence of fines. The exact cause of the time-dependent strength gains in any case has not been conclusively established. Mesri et al (1990) argued for a secondary compression-like process and possibly some changes in effective confining pressure; e.g. increased lateral stress, and some type of silica bonding cannot be ruled out. It is still an open question; however, there is little doubt that time-dependent increases in penetration resistance have occurred in the field.

An excellent illustration of the time-dependent strength increase following densification of a medium to coarse sand hydraulic fill by dynamic compaction is given by Dumas and Beaton (1988). The clean sand fill was placed into the sea by end dumping. The average grain size of the sand is 0.79 mm, and the uniformity coefficient is 3.06. Increases in CPT resistance of up to 100 percent of the immediate post-compaction values were measured during the first 18 days following dynamic compaction.

Results of CPT tests at a point where the hydraulic fill thickness was 15m and the dynamic compaction energy was 330 ton/m^2 are shown in Figure 2.11. The very low values of penetration resistance prior to treatment by dynamic compaction imply that the sand fill

must have been in a very loose state initially. The greater time-dependent strength increase near the surface and diminishing effect with depth are noted by Dumas and Beaton (1988). As this diminishing strength increase parallels the attenuation of dynamic stresses with depth during dynamic compaction, the authors suggest that the time-dependent strength increase may be related to the level of dynamic stress increase. It may be dependent on the static stresses as well, as are the time-dependent strength increase and densification that result from ground improvement using a particular type and magnitude of dynamic input energy.

The time-dependent strength gain in cohesionless hydraulic fills is of practical importance in the following ways:

(a) The properties of freshly deposited or densified hydraulic fill are likely to improve with time, even without a detectable increase in density. This improvement can be assessed by penetration tests; however, presently there is no generally accepted analytical means for predicting the magnitude and rate.

(b) Densification of hydraulic fill is the easiest during or immediately after its placement. The longer the time elapsed before densification, the greater is the input energy needed to break down the initial structure and thus less energy is available for the densification process.

(c) The *quality control testing* to insure that the specified placement density is attained should be conducted at a standardized time after fill placement.

(d) Measurements of a hydraulic fill obtained at a short time after placement or densification are conservative compared to those obtained from the same fill at a later date, provided there is no disturbance of material during the intervening period.

2.8 Equivalent Relative Density

Ground improvement design criteria and specifications are often developed in terms of relative density. A direct conversion of a penetration resistance to relative density is uncertain, because penetration resistance also depends on factors other than density. The correlations between penetration resistance and relative density of fill are dependent upon the lateral pressure, the length of time of a fill under pressure, the stability of the fill structure, and prior strains of the fill (Seed, 1979). Significant increases in penetration resistance with time after densification have been measured even though there is no accompanying increase in density (Mitchell and Solymar, 1984). Fortunately, these same factors lead also to increased resistance to settlement and liquefaction. Thus, it is the penetration resistance values themselves that are important, not the actual relative density. Because of this, it has been found useful in some cases to work with an "equivalent relative density", which is the true relative density that a

sand would have to possess to exhibit the measured penetration resistance if it were freshly deposited, saturated, and normally consolidated.

2.9 Sand Property Correlations

It is relevant to note that it is difficult to measure insitu density of sand with accuracy. The problem is that it is extremely difficult to recover a sample of sand with any certainty that its density has not changed during the sampling process. The assessment of insitu state of sand and the difficult in measuring the insitu density of sand have been discussed by Sladen (1989) and Sobkowicz and Handford (1990) with reference to the Canadian Beaufort Sea experience.

The cone penetration test has been widely used for insitu assessment of sand state. The basic approach has been to calibrate the CPT in large chambers in which sand density and stress state can be controlled. Such a correlation between relative density and mean effective stress measured in large scale chamber tests for Ticino Sand has been presented by Baldi et al (1986), and it is reproduced in Figure 2.12. In which contours of relative density are shown in a plot of cone tip resistance (q_c) Versus mean effective stress (p'). Relationship similar to Figure 2.12 would be entirely plausible and very useful in practice.

2.10 Conclusion and Recommendations

Cohesionless hydraulic fills have low relative density, low strength, and high liquefaction potential when placed. Consequently, densification and improvement of hydraulic fills are required before they can be used for most purposes.

Densification by vibration has been the most commonly used technique for improvement of cohesionless hydraulic fills, whereas, precompression has been used the most for fine-grained hydraulic fills. Surface compaction of clean sand hydraulic fills during placement is usually easier, more effective, and less expensive than deep densification later. Underwater compaction during placement appears not to have been much used but warrants consideration for new projects.

Insitu tests form an essential part of virtually all ground improvement and land reclamation projects. Before and after measurements yield a direct indication of what has been accomplished without the need for sampling, laboratory testing, and analytical studies. The CPT, SPT, and PMT are the most commonly used tests, with the CPT being preferred in many recent projects for rapid, routine and cost-effective insitu evaluation of sands. Other observations and tests can be very useful for ground improvement evaluation as well.

For future development of hydraulic fills for land reclamation projects in Hong Kong, it is suggested that careful consideration should be given to placement methods at the design stage. Many of the factors that affect liquefaction potential can be influenced by decisions made during the construction phase. As recommended by Sladen (1990) for the Port of Los Angeles Harbour project, which is generally true for the situations in Hong Kong, potential fill areas could be zoned according to end use and special techniques may be warranted in more critical areas. Judicious selection of materials and methods, particularly in critical areas

can reduce the cost of post depositional ground improvement. Although post-depositional investigation will remain essential, greater emphasis should be placed on "real-time" quality control procedures during fill placement. If selective borrowing of relatively clean material is impracticable, consideration should be given to various techniques for improving fill quality.

For critical areas, it is likely that some form of post construction densification will be required. For less critical areas, proper selection of placement method may make densification unnecessary. For below water deposition, an improved density can generally be achieved by bottom dumping from split barge/hoppers rather than pipeline or beach placement. For above water construction, a significant advantage can generally be achieved by maintaining good drainage and imparting modest compaction by construction equipment.

There is a pressing need to develop means of increasing the confidence with which insitu state can be assessed. Determination of the insitu properties of hydraulic fills will likely require extensive insitu testing, sampling and laboratory testing. The development of a correlation between insitu CPT measurements and calibration chamber tests could significantly increase our confidence in the use of CPT tests. This correlation could further be supplemented by more direct measurements of insitu density such as advanced samplers perhaps in conjunction with ground freezing, grouting or nuclear methods.

3. SELECTED HYDRAULIC FILL SITES IN HONG KONG

In an effort to familiarize ourselves with the general knowledge of Hong Kong hydraulic fills, it was decided that a number of existing sites be selected and a limited on-site investigation be conducted to provide the needed information for understanding, in general terms, the characteristics of Hong Kong hydraulic sand fills.

With the help of the Geotechnical Engineering Office, three existing sites were selected for this purpose. These are the West Kowloon (CS1), the Tin Shui Wai (TSW) and the Tseung Kwan O (TKO) reclamation sites. The locations of the sites are indicated on the map shown in Figure 3.1. Aside from their accessibility and yet to be fully developed status, the marine sand fills of these sites came from three different sources in the Territory waters, representing a broad spectrum of Hong Kong marine sands used in reclamation.

Several visits were made to the sites prior to field investigations for purposes of:

(a) carrying out discussions with site engineers,

(b) gathering relevant data and information of the sites,

(c) familiarizing with site conditions and construction progresses of the sites, and

(d) selecting locations for field testing and sampling.

Due largely to time and budgetary constraints the extent of the field testing programmes was rather limited. Every effort however was made to locate the field testing locations as close as practically possible to the borrow pits for bulk samples except at the West Kowloon

site where extensive construction activities nullified any possibility to locate the field test site next to the borrow pit.

The field work was carried out between 22 December 1992 and 15 January 1993. On each of the three sites, the following site investigation works were carried out :

(a) one borehole, where SPT was carried out at 1.5m intervals and "undisturbed" samples were taken in-between the intervals using a Mazier sampler (76mm in diameter, one-meter long using polymer drill mud),

(b) one 15 sq.cm CPT hole with pore water pressure measurements, and

(c) one 10 sq.cm CPT hole with pore water pressure measurements.

A total of four holes were drilled by the Bachy Soletance Group for SPT and sampling, and a total of six cone penetration tests(CPT) were carried out by the Fugro McClelland Ltd. The locations of these field investigation work are given in Figures 3.2, 3.3 and 3.4 for CS1, TSW and TKO, respectively. It should be noted that one extra hole was made at the Tin Shui Wai site to a depth of 6m and a SPT was conducted to better define the bottom of the sand fill at the site.

3.1 Results of Drilling

Boreholes were logged by the technical staff of the Bachy Soletanche Group in accordance with Geoguide 2 "Guide to Site Investigation" and Geoguide 3 "Guide to Rock and Soil Description". The boring logs are shown in Figures 3.5, 3.6 and 3.7 for CS1, TSW and TKO respectively. A summary of the stratigraphy is given in Table 3.1.

As revealed from the boreholes, hydraulic sand fill overlying marine or pond deposits were recovered on all sites. The thickness of fill materials are approximately 25m , 6m and 16m for CS1, TSW and TKO respectively. Noticeable segregation marks of fine to coarse sands were observed at the West Kowloon and Tseung Kwan O; likewise fine gravel and sand layers were observed at the Tin Shui Wai site. The gravel layers were generally 10mm to 30mm thick, while the thickness for the sand layers were about 150mm to 300mm.

3.2 Standard Penetration Tests (SPT)

SPTs were carried out at 1.5m intervals on the three sites. The results of penetration resistance (N) value Versus depth are plotted in Figures 3.8, 3.9 and 3.10 for CS1, TSW and TKO respectively. It is generally found that the penetration resistance of the fills above the mean sea level are much higher than that below the mean sea level. This finding is consistent with the results obtained from cone penetration tests which will be discussed in section 3.4.

3.3 Tube Sampling of Hydraulic Sand Fill

Tube samples (76mm diameter) were taken by the Mazier sampler. The Mazier sampler which has been successfully used in coring CDG samples in Hong Kong, is a triple-core-barrels which contains detachable plastic PVC liners within the inner barrel that protect the core from drilling fluid and damage during transportation and sample extrusion (see Figure 3.11). To carry out the sampling work in reclaimed sand fills, a polymer stabilizer of Sodium Carbomethylcellulose was used as drilling fluid and a spring core-catcher was attached at the inner barrel cutting shoe. The percentage of total core recovery of Mazier samples for the three sites are shown in Figure 3.12. It seemed that this sampling technique is capable of yielding relatively high core recovery for fine to medium sand fills (i.e. at the West Kowloon and Tseung Kwan O Reclamation sites), but fails to obtain good samples of loose to medium dense, layered sands of fine to coarse material (i.e. at the Tin Shui Wai Site). The core recovery above the sea level is generally better than that below it (due to wash-out effect when sampling under water). It should be noted that the sea levels indicated in Figure 3.12 were different from the mean sea levels due to tidal levels at the time of sampling.

All Mazier samples were freely drained before they were waxed and capped to avoid damage due to liquefaction and disturbance during transportation and extrusion. One of the Mazier samples was opened and inspected on the site. Based on the observation of the marks left by the spring core-catcher on the sample's surface and the general appearance of the sample (see Plate 3.1), the core sample can be considered to be relatively intact and of high quality (Class 1). However, it is doubtful that insitu densities can be correctly determined from these samples. All Mazier samples were subsequently shipped and stored at the Government Public Works Central Laboratory, Kowloon Bay.

3.4 Cone Penetration Tests (CPT)

Two continuous cone penetration tests (one 15 sq. cm cone and one 10 sq.cm cone) were carried out at each reclamation site. The 15 sq.cm (7.5 tonne) cone was spaced at 3 meters apart from the 10 sq.cm (5.0 tonne) cone. The penetration rate was set at a constant speed of 2cm/sec with a data sampling frequency of 1 second for both tests. The position of the porous element was on the shaft between the piezocone and the sleeve (U2 cone filter position) and glycerine was used as the system de-airing fluid.

The results of tip resistance (q_c) with depth for the $10cm^2$ and $15cm^2$ cones at the West Kowloon site are shown in Figures 3.13 and 3.14, respectively. It appears that there is no significant difference between the readings obtained by the two different cone sizes. The results of tip resistance above the sea level were significantly greater than those below the sea level, which are consistent with the results obtained from the standard penetration tests. Figure 3.15 shows the relationship between relative density (D_r) and cone resistance (q_c) of uncemented, normally-consolidated quartz sands developed by Jamiolkowski et al (1985). These values were derived from calibration chamber tests and they require correction for chamber size. The correction for chamber size is made by dividing q_c by K_q , where the correction factor K_q, is given by :

$$K_q = 1 + \frac{0.2\ (D_r - 30)}{60} \qquad \ldots\ldots\ldots\ldots\ldots\ldots \quad (3.1)$$

Because K_q is a function of D_r, it is necessary to determine D_r from Figure 3.15 first and substitute into Equation 3.1 to obtain the correction factor, K_q. The final value of D_r can then be determined by :

$$q_c \text{ (corrected for chamber size)} = \frac{q_c \text{ (field value)}}{K_q \text{(base on } D_d \text{ by Eq. 3.1)}} \quad \ldots . \quad (3.2)$$

With the corrected q_c determined from Eq. 3.2, final value of D_r can then be estimated from Figure 3.15. Based on this correlation technique, the relative density values along the hydraulic sand fill profile can be estimated and plotted as shown in Figures 3.13 and 3.14. It should be noted that the relative densities of the calibration chamber tests given in Figure 3.15 were determined using the maximum and minimum densities according to the ASTM specifications (Designation: D4253-91 and D4254-91, respectively). In this report, a symbol $D_{r\,(ASTM)}$ will be used to designated the relative density values determined by the ASTM based technique, while $D_{r\,(BS)}$ is used for the British Standard based technique. Using the West Kowloon site as an example, three regions of the sand fill can be identified :

(a) a region of dense to very dense fill above sea level (about 10 m thick) with $D_{r\,(ASTM)}$ of 60% to 90%,

(b) a region of loose sand just below the sea level (about 5m thick) with $D_{r\,(ASTM)}$ of 35% to 40%, and

(c) a region of medium dense sand fill beneath the loose sand layer (about 8m thick) with $D_{r\,(ASTM)}$ of 40% to 50%.

According to the construction record of West Kowloon Reclamation site, three distinct placement methods were employed during the reclamation process. The bottom 8m of fill was bottom dumped by direct discharge of fill material from the base of a hopper using valves or doors. This was followed by high velocity discharge of sand fill from a nozzle at some distance above the fill surface (this process is called spigotting as illustrated in Plate 3.2). The spigotting placement method was stopped when the fill was about 1m below the sea level. This was then followed by a low velocity discharge of sand fill as a slurry from a pipe located close to the placement level (this method is called pump-out as illustrated in plates 3.3 and 3.4). Because of the discharging of a large quantity of fill material (in the order of 4000 m^3 to 8000 m^3) at a relatively short period of time in bottom dumping, a medium dense fill will result. A review of other published data (Jefferies et al , 1988; Massarch, 1985; and Wallays, 1983) indicates that, for depths of water up to about 20m, the bottom dumping method is reflected by CPT tip resistance value ranging from 7-12 MPa, which is consistent with the results shown in Figures 3.13 and 3.14 at the West Kowloon Reclamation site. The hydraulic filling process of spigotting would produce the least dense fill because of the hydrodynamic effect as the sand disperse and settle below water. This hydraulic placement method is reflected by the CPT tip resistance values ranging from 5 to 8 MPa. Higher fill densities can be achieved above the sea level due to the compaction brought about by seepage of water in the fill carrying finer material into the voids between coarser material. (Reilly, 1991). Fill densities above the sea level could also be increased by mechanical compaction due to the levelling operations of bulldozers near the discharge nozzle. For the West Kowloon site, CPT tip resistance value as high as 35 MPa was recorded in fill located above the sea level. As

a consequence of these three distinct fill placement methods, variations in the density with depth is evident. Similar results were also obtained at the Tin Shui Wai and Tseung Kwan O sites as shown in Figures 3.16 through 3.19.

3.5 CPT Versus SPT

There is a considerable amount of interest to correlate the SPT N values with CPT tip penetration resistance q_c. The results of q_c (in MPa) obtained from the three sites were plotted against the SPT N value in Figure 3.20. It can be seen that a reasonable correlation between the cone resistance values and N values can be obtained. For the hydraulic sand fills investigated in this study, a relationship between q_c and N is proposed as follows:

$$q_c = 0.7\ N \quad \ldots\ldots\ldots\ldots\ldots\ldots \quad (6.3)$$

where q_c is in MPa and N is the number of blows for a 0.3m penetration.

The results obtained from the three sites are also plotted on the q_c/N Versus average grain size, D_{50}, relationship as proposed by Burland and Burbidge (1985) in Figure 3.21. The proposed relationship of q_c=0.7N seems to be in good agreement with the results obtained from Burland and Burbidge (1985) and Robertson et al (1982).

4. PHYSICAL PROPERTIES DETERMINATION

Materials used for laboratory testing and for shipment to ENEL, Italy for calibration chamber testing were taken from the sites between 9 and 11 November 1992. Locations on the three sites where samples were taken are shown in Figures 3.2, 3.3 and 3.4. These samples from a depth of 2 to 3 meters were obtained using a mechanical excavation (see Plate 4.1) and filled into steel barrels for transport (see Plate 4.2).

All the laboratory tests described in the following sections were conducted on well mixed samples. They passed the 5 mm sieve. All the classification tests (except permeability test) were conducted at the Public Works Central Laboratory, some of the tests were later repeated in the Geotechnical Laboratory, HKUST to check for reliability. The results of all the classification tests were summarized in Table 4.1.

It is interesting to note that segregation of fine to coarse sands were clearly visible from pits left by excavation on the three sites (see plates 4.3, 4.4 and 4.5 for CS1, TKO and TSW, respectively). The segregation in the fill is created by the hydraulic filling processes, thus it serves to indicate that the sampling sites were free from previous construction disturbance and ground compaction. It however also indicates that the physical properties reported herein can only be considered as "gross property values" of the fills, not the individual layer properties existing in the field.

4.1 Sieve Analysis

The well-blended mixture from each of the three sites were quartered down to provide representative samples for particle size distribution test (7B of BS 1377, 1975 for dry-sieving). Grading curves for samples from all three sites are given in Figure 4.1. Similar grading curves for bulk samples shipped to Italy for stress chamber testing are given in Figure 4.2 for cross comparison. The difference between the bulk samples and laboratory samples are generally very small, except for unknown reasons, the bulk sample obtained from TSW is slightly finer than that of the laboratory sample.

The basic constituents of the three batches of samples are very similar, all comprising mainly siliceous material deriving from the weathering of granite. The TSW sample is a well graded gravelly sand (about 44% gravel size and 56% sand particle size), it contains less than 1% fines. The coarse size material is generally of quartz type. The particle shapes of the TSW sample are sub-angular. The particle sizes of the CS1 sample are coarse to fine sand with about 20% fine gravel, some shell fragments, and less than 1% fines. The TKO sample is made of clean medium sand with some shell fragments. The particle shapes of both CS1 and TKO are sub-angular to sub-rounded. The coefficient of uniformity C_u defined as

$$C_u = \frac{D_{60}}{D_{10}} \quad \ldots\ldots\ldots\ldots\ldots\ldots \quad (4.1)$$

where D_{60} = grain size (in mm) corresponding to 60% passing, by weight,
and D_{10} = grain size (in mm) corresponding to 10% passing, by weight;

the coefficient of curvature, defined as

$$C_c = \frac{(D_{30})^2}{(D_{10})\ (D_{60})} \quad \ldots\ldots\ldots\ldots\ldots\ldots \quad (4.2)$$

where D_{30} = grain size (in mm) corresponding to 30% passing by weight;

and the average grain size, D_{50} (= grain size in mm corresponding to 50% passing by weight), are calculated based on Figure 4.1 and summarized as in the following:

	Tin Shui Wai TSW	West Kowloon CS1	Tseung Kwan O TKO
Average Grain Size, D_{50}	2.0 mm	0.72 mm	0.28 mm
The Coefficient of Uniformity, C_u	6.0	6.4	2.1
The Coefficient of Curvature, C_c	1.15	0.42	0.92
Unified Soil Classification	SW	SP	SP

4.2 Specific Gravity (G_s)

A minimum of three specific gravity tests in accordance with Test 6 of BS 1377 (1975) on oven-dry samples were conducted for each site. The results of G_s were found to be:

West Kowloon (CS1)	G_s	= 2.628
Tseung Kwan O (TKO)	G_s	= 2.635
Tin Shui Wai (TSW)	G_s	= 2.634

4.3 Minimum Density

Minimum density tests in accordance with Part 4:43 of BS 1377(1990) were performed. This test was devised by Kolbuszewski, it is the minimum density of a clean dry sand that can be obtained in a measuring cylinder. After shaking, the soil in the cylinder is allowed to fall freely, and in so doing it entraps air and forms a loose structure enclosing a maximum volume of voids. At least five individual trials were performed on samples from each of the three sites, the results of minimum density $\rho_{D,min}$ are summarized as follows:

West Kowloon (CS1)	$\rho_{D,min}$	= 1.61 g/cm^3
Tseung Kwan O (TKO)	$\rho_{D,min}$	= 1.40 g/cm^3
Tin Shui Wai (TSW)	$\rho_{D,min}$	= 1.55 g/cm^3

4.4 Maximum Density

Maximum density tests in accordance with Part 4:42 of BS 1377 (1990) were preformed. The maximum density is determined by compacting the soil with a vibrating hammer under submerged condition into a CBR compaction mould. At least three maximum density tests were performed on samples from each of the three sites. By selecting the maximum value out of each batch of samples, the maximum density $\rho_{D,max}$ for the three sites are as follows:

West Kowloon (CS1)	$\rho_{D,max}$	= 1.98 g/cm^3
Tseung Kwan O (TKO)	$\rho_{D,max}$	= 1.77 g/cm^3
Tin Shui Wai (TSW)	$\rho_{D,max}$	= 2.01 g/cm^3

4.5 Compaction Tests

The relationship between dry density and moisture content for the CS1, TKO and TSW samples were determined by the standard compaction test, as detailed in test 12 of BS 1377 (1975). The results are shown in Figures 4.3, 4.4 and 4.5 for CS1, TKO and TSW, respectively. The 100% saturation (zero air-void) line is also plotted for reference. The maximum dry densities (Maximum Proctor) and optimum water contents determined for each site are summarized as follows:

	West Kowloon (CS1)	Tseung Kwan O (TKO)	Tin Shui Wai (TSW)
Maximum Dry Density (g/cm^3)	1.88	1.67	1.84
Optimum Moisture Content (%)	11.8	20.6	13.12

It should be noted that compaction curves for clean sands (especially poorly graded sand like TKO) are generally not well defined (Johnson and Sallberg, 1960). Therefore, the optimum moisture contents defined in the above table is subject to individual interpretation.

4.6 Permeability Test

Constant head permeability tests were performed in the Soil Mechanics Laboratory, University of Hong Kong. The constant head permeability cell was manufactured by Wykeham Farrance Engineering Limited. The sample size is 75 mm in diameter and 200 mm in length with two tapered outlets at 100 mm vertical pitch. The basic procedure adopted in this study was very similar to that outlined by Akroyd (1969). For each type of soil, three constant head tests were performed at three difference relative densities. The air pluviation sample preparation technique was utilized to produce specimens of different densities. This sample preparation procedure is very similar to that used for making cylindrical triaxial specimens. The results are summarized in the following table, and the relationships between coefficient of permeability and void ratio for the three soils are shown in Figure 4.6. The effect of void ratio, e (or relative density, D_r) on the coefficient of permeability, k for TSW soil is much more pronounced than the other two soils.

West Kowloon (CS1)			Tseung Kwan O (TKO)			Tin Shui Wai (TSW)		
D_r (%)	e	k (cm/s)	D_r (%)	e	k (cm/s)	D_r (%)	e	k (cm/s)
65	0.42	$5.62\ 10^{-3}$	58	0.63	$7.14\ 10^{-3}$	58	0.44	$5.97\ 10^{-2}$
45	0.48	$6.20\ 10^{-3}$	36	0.71	$1.20\ 10^{-2}$	36	0.53	$7.18\ 10^{-2}$
18	0.57	$1.38\ 10^{-3}$	25	0.76	$2.08\ 10^{-2}$	22	0.59	$1.31\ 10^{-1}$

5. LABORATORY TRIAXIAL TESTING

The triaxial tests were performed using the automated triaxial testing system which was developed at the University of California at Davis and Berkeley Campuses. In the automated triaxial testing system, the computer programmed electronic signal for frequency and magnitude of loading is applied to an electro-pneumatic transducer which then controls pneumatic amplifiers for the application of loads. All modes of loading are controlled by closed-loop feedback schemes. The system is designed for performing both static and dynamic testing with independent and/or synchronized adjustment of axial load and chamber pressure.

A photograph and a schematic diagram of the automated system are shown in Plate 5.1

and Figure 5.1, respectively. The system includes a loading frame, a triaxial cell, a load piston, a volume-measuring device with three pressure transducers, a dual channel pneumatic loading unit, a signal-conditioning unit, a process interface unit, a 486 PC, and a dot-matrix printer. Detail descriptions of the various elements can be found elsewhere (Li et al, 1988). Both static and cyclic tests were performed on reconstituted specimens of Hong Kong marine sands obtained from CS1, TSW and TKO.

5.1 Specimen Preparation

Soil Deposition :

In this study, uniform triaxial test specimens were prepared by the air (dry) pluviation technique. Deposition by pluviation involves the free fall of soil grains through air so that the particles come to rest in a repeatable configuration. The intensity of deposition, expressed as mass per unit area per unit time, is controlled by the diameter of the aperture through which the soil particle flows. The pluviation technique has advantages over other techniques of fabrication because of its simple operation and its approximation to the natural deposition process. A similar dry pluviation method of specimen fabrication is also used at ENEL for calibration chamber testing.

The basic design of the pluviation apparatus is shown schematically in Figure 5.2. The sand fall in "jets" through funnels of different openings onto a stack of diffuser sieves. The diffuser sieves create a uniform rain of sand for the deposition of sand into the cylindrical mould. The distance from the diffuser sieves to the top of the deposited sand must be at least 50 cm in order to achieve free falling of sand particles. By using funnels of different openings, relative densities of about 30%, 40%, 60% and 70% were obtained (It should be noted that all the relative density values reported in this chapter are based on the minimum and maximum dry densities determined by the British Standard based technique).

Preparation of the Testing Apparatus:

The basic procedure is outlined as in the following :

1. Preparing the cell base and end platens, porous stone(s), membranes, O-rings, and supplemental evacuation apparatus to receive the specimen.

2. Checking the saturation of the pore pressure measuring device and its flexibility by measuring the compliance.

3. Mounting the specimen on base.

4. Sealing the specimen and assemble the cell.

5. Applying the back pressure for saturation and measuring the "B" value.

6. Performing triaxial consolidation.

7. Performing shear loading to failure.

Because of the highly automated nature of the system, the "B" value check, triaxial consolidation, and shear loading to failure can be programmed by computer software routinely; they will not be discussed in any detail. The procedure of achieving high degree of saturation by using the dual-evacuation-chambers method will be discussed next.

Saturation :

Saturation of a triaxial specimen is achieved by first evacuating the drain lines, porous stone(s) and specimen under a high vacuum, then allowing the de-aired water to fill the lines and the specimen, and finally increasing the back pressure and cell pressure by equal (usually small) increments until all air in the specimen is flashed out. The degree of saturation is monitored during and at the end of the process by checking the "B" value.

The dual-evacuation-chambers method for specimen saturation is shown schematically in Figure 5.3. A photo of the device is shown in Plate 5.2. The step-by-step procedure to saturate a specimen is given as follows:

1. Select the effective consolidate pressure (σ'_{3C}) to be applied to the specimen before shear loading. If σ'_{3C} is greater than or equal to 100kPa, a full vacuum should be used in the subsequent steps.

2. Close valve B before connecting the vacuum line to valve A, and apply a regulated vacuum to the evacuation chamber of the amount $(-)\sigma'_{3C}$ or (-) 100 kPa, whichever is less. Bubbling is seen initially in the water which should stop in a few minutes. The water in the evacuation chamber 1 is de-aired when bubbling stopped.

3. Close valve A and switch vacuum line to valve D of evacuation chamber 2. Make sure valve C is closed. Open valve D and apply a regulated vacuum to the evacuation chamber 2 of the amount $(-)\sigma'_{3C}$ or (-) 100kPa, whichever is less. Bubbling in the water is seen initially which should stop in a few minutes unless a leak in the fittings exists. Repair the leak if necessary.

4. Open valve C and now the specimen is being vacuumed. A significant amount of bubbling will first be observed which will be reduced and eventually stopped in a few minutes. If bubbling continues, the rubber membrane could be leaking. Leaks can usually be sealed by painting over with rubber cement, liquid

latex rubber, or other pliable sealants.

5. Keep valve D open and continue to apply vacuum through evacuation chamber 2. The specimen is now almost fully de-aired but may still have a small amount of air entrapped inside.

6. Open valve B and adjust the vacuum gauge of evacuation chamber 1 so that there is always a small pressure difference between the two evacuation chambers (by a difference of about 10 to 20 kPa) with a higher vacuum in evacuation chamber 2.

7. Water will start to flow through the drain line of evacuation chamber 1 into the specimen. Some bubbling can be observed at evacuation chamber 2 as the entrapped air is forced out of the specimen.

8. Adjust the vacuum valves A and D so that a differential vacuum pressure (in the order about 10 to 20 kPa) is maintained between the two chambers at all times.

9. Once the specimen is filled with "de-aired" water (bubbling should stop by now), close valves B and C. Detach evacuation chamber 1 from the triaxial cell, and connect the vacuum line to valve D.

10. The cell is now ready for back pressure saturation and "B" value check. By using this method normally, a back pressure of 100KPa or less is needed to saturate the specimen.

5.2 Static Triaxial Tests

Undrained triaxial tests were performed on saturated specimens (with a "B" value of at least 0.97) to establish the stress-strain, and strength characteristics of the hydraulic fill sands. Two groups of specimens with relative densities (in British Standard) of approximately 30% and 70% were tested under a range of isotropic consolidation pressures of 100kPa, 200kPa and 300kPa. To better define the strain-stress characteristics, especially for the case of strain-softening material, the strain-controlled static triaxial testing with pore pressure measurement was employed. The strain rate is kept constant at 0.5%/min for all tests.

The p'-q stress path plot of the West Kowloon sand with relative density of approximately 35% is shown in Figure 5.4. The failure state was defined by the failure envelop, and the effective angle of internal friction (ϕ') for the material was found to be about 35°. The stress-strain, pore water pressure response for each undrained test are plotted in Figures 5.5, 5.6 and 5.7 for consolidation pressures of 100kPa, 200kPa and 300kPa,

respectively. The results indicate that shearing will first cause the sand to decrease in volume (compression) thus a corresponding increase in pore pressure, upon reaching the phase transformation line (volume change tendency reverses from compression to dilation) at an axial strain level of about 2 to 3%. Further loading will cause the sand to increase in volume (dilation) thus a corresponding decrease in pore pressure. The net change in pore water pressure (Δu), during undrained testing, however, remains positive for all three tests. The results of these three tests are summarized in Table 5.1.

Figure 5.8 shows the p'-q stress path plot for the West Kowloon sand with relative density of approximately 73%. The effective angle of internal friction was found to be about 40°. The stress-strain, pore water pressure response for each undrained test are plotted in Figures 5.9, 5.10 and 5.11 for consolidation pressures of 100kPa, 200kPa and 300kPa, respectively. The results clearly indicate that before reaching the phase transformation line, shearing of specimens also cause a decrease in volume thus a corresponding increase in pore pressure. As the specimen approaches failure, further loading will cause an increase in volume thus a corresponding decrease in pore pressure. The net change in pore water pressure (Δu) however, is negative in this case indicating a net volume increase tendency during shearing. Table 5.2 summarizes the stress-strain and strength response of the sand at a relative density of about 73%.

Tables 5.3 and 5.4 summarize the static test results of the TKO and TSW sands respectively. The ranges of confining pressure and relative density adopted are similar to those used for the CS1 sand. The p'-q stress path plots for TKO and TSW sands are presented in Figures 5.12, 5.13, 5.14 and 5.15 respectively.

5.3 Cyclic Triaxial Tests

Specimens same as those used in static loading tests were prepared for cyclic triaxial testing. After consolidation to an effective stress (σ_c') of 150kPa, a cyclic axial loading was applied to the specimen while holding the cell (consolidation) pressure constant. The undrained response is monitored and recorded in terms of the variations of axial load, axial deformation, and pore pressure against loading cycles.

A total of thirty (30) stress-controlled cyclic loading tests at a frequency of 1Hz were performed on the West Kowloon hydraulic fill sand for relative densities (in British Standard) about 35%, 45%, 65% and 75%. Different cyclic deviator stresses (σ_{dp}) were applied to evaluate the liquefaction potential. The cyclic stress level applied to the specimen is commonly quantified by the stress ratio, SR, defined as :

$$SR + \frac{\sigma_{dp}}{2(\sigma'_c)} \quad \ldots\ldots\ldots\ldots\ldots\ldots \quad (5.1)$$

where σ_{dp} = cyclic deviator stress, i.e., the amplitude of the applied cyclic axial loading.
σ'_c = effective mean normal stress at the end of isotropic consolidation.

Thus a normalized liquefaction curve (SR Versus number of loading cycles to liquefaction , N) can be established for a given relative density.

For all the test results reported herein (including both static and cyclic tests), the relative density values were calculated based on the density of the specimen obtained after isotropic consolidation.

The results of cyclic triaxial tests for the CS1 specimens are summarized in Table 5.5. The normalized liquefaction curves (SR Versus N) for $D_{r\,(BS)}$ of 35%, 45%, 65% and 75% under an isotropic consolidation pressure of 150kPa are shown in Figure 5.16. When the level of cyclic deviator stress was increased, the number of cycles needed to cause liquefaction decreased, and vice versa. At a constant stress ratio, the number of cycles needed to cause initial liquefaction increased as the relative density of the sand increased. These findings are consistent with those reported by DeAlba et al (1976) and Seed and Lee (1966).

The results of a typical cyclic loading test of loose sand from West Kowloon site (with $D_{r\,(BS)}$ = 37.5% and SR=0.095) are shown in Figures 5.17(a) to 5.17(g). In this test, a cyclic deviator stress, σ_{dp}, of constant amplitude (±30 kPa), was applied under a confining pressure of 150kPa. Figures 5.17(a), (b) and (c) show the changes in stress, strain, and pore-water pressure with loading cycles. It can be noted that, during the first seventeen cycles of stress applications, the specimen showed no noticeable deformation although the pore-water pressure built up gradually. However, during the eighteen cycles, the pore pressure suddenly increased to a value equal to the externally applied confining pressure (i.e., back pressure of 100kPa plus the consolidation pressure of 150kPa to give a total pressure of 250kPa) and the specimen developed large strains in excess of 20 percent . In fact, the soil had liquefied and the effective confining pressure had been reduced to zero (Figures 5.17(d) and (e)).

Figures 5.17(f) and 5.17(g) show the effective stress paths and the shear stress-shear strain loops. Large shear strains are associated with stress paths approaching the phase transformation line under small effective confinement. The shear strain build up is slow and gradual before reaching the phase transformation. The reduction in shear resistance with increasing loading cycles is also evident.

The cyclic triaxial test results for TKO and TSW are summarized in Tables 5.6 and 5.7 respectively. The cyclic stress ratio ($\sigma_{dp}/2\sigma_c'$) Versus the number of loading cycles to initial liquefaction (N) relationships of these two sands are plotted for different relative densities, as shown in Figures 5.18 and 5.19. A number of observations of the results can be made as follows:

(a) The cyclic behaviour of the TKO sand is quite similar to that of the CS1 sand.

(b) The TSW sand is less susceptible to liquefaction compared to the other two sands. This phenomenon seems to agree with information reported in the literature (Seed and Idriss, 1967); e.g. in general, coarse and more uniformly graded material is less likely to liquefy.

(c) It was noticed that for relatively dense ($D_{r\,(BS)} \approx 65\%$) specimens of TSW sand, the pore water pressure increases as the number of loading cycles is increased; however, unlike the other cases, the pore water pressure

ceases to increase before it reaches the state of initial liquefaction (i.e. $\sigma_3 = u$, $\sigma'_3 = 0$). This phenomenon is not uncommon for dense granular soil where large cyclic deformation can take place without causing drastic failure (Seed and Lee, 1966). In presenting the information in Figure 5.19, the $D_r \approx 65\%$ curve was established by taking the N value where the pore water pressure reading was very close to the confining pressure and remained more or less constant with additional loading cycles.

5.4 Insitu Tube Sample Versus Reconstituted Specimens

Differences in liquefaction resistance between the undisturbed and the reconstituted specimens is always a concern to geotechnical researchers and practitioners, particularly for sandy soils. Sandy soils are prone to disturbance during sampling, transporting, and specimen preparation. It is doubtful that accurate and representative density determinations can be achieved from samples taken by conventional sampling techniques including the use of Mazier sampler. In addition, sandy deposits such as hydraulic fills are known to have density and grain size segregation resulting from placement methods and other field conditions. One must therefore be aware of the discrepancies and shortcomings in laboratory results.

A number of insitu specimens retrieved from sampling tubes obtained on the CS1 site were prepared. The insitu specimens were first saturated and then isotropically consolidated under a cell pressure of 150MPa. They were then subjected to cyclic loading until liquefaction failures occurred. The results are plotted as shown in Figure 5.20. Not knowing the true density (or relative density) of the insitu specimens, the results were plotted based on the applied cyclic deviator stress and the number of loading cycles to failure. It is interesting to note that the data points from insitu specimens fall to the right of the laboratory established curves of specimens prepared by the air pluviation method. The dry and bulk densities of the nine insitu specimens were determined and listed in Table 5.8.

Material of the insitu specimen U2 was saved and re-used to form specimens of the same density by two different sample preparation methods. One was prepared by the air pluviation method as described in the previous section; the other was by wet tamping. These two specimens were tested following the same procedure and condition as the insitu U2 specimen. It was found that the wet tamping specimen M2 has even higher liquefaction resistance than the insitu specimen; whereas, the air pluviated specimen A2 is weaker, and falls into the zone of laboratory established curves as described in section 5.3.

The information presented here further substantiates the concern regarding the differences in strength between the insitu and the reconstituted specimens. It also sheds some light to the fact that different methods of sample preparation (i.e. air pluviation Versus wet tamping) can drastically influence the liquefaction resistance of a specimen. It however is comforting to note that specimens prepared using the air pluviation method which has been adopted for this study, have the least resistance to liquefaction. Such test results would be on the conservative side if they were adopted to be used as the basis for design considerations.

It should be mentioned that the U2 specimen was from a depth approximately 8 meters below the ground surface; whereas, the bulk sample for laboratory testing was obtained at a depth of 2 to 3 meters. The gradations shown in Figure 5.21 speak well of the non-uniformity and segregation of particles in hydraulic fills.

6. DYNAMIC STABILITY OF HONG KONG RECLAMATION SITES

Hydraulic fills in Hong Kong are made mainly of sandy soils. As noted in the literature review, the density of sandy fills varies greatly with placement methods used during a reclamation process. For instance, sand that is bottom dumped below water is usually denser than those placed by sub-aerial pipeline discharge. The existence of loose layers (with relative density less than about 35%) in the fill may cause settlement related instability problems; consequently, fill improvement measures are normally required to densify loose layers.

As settlement in sandy soil is caused primarily by dynamic loads, in this Chapter an attempt has been made to assess the dynamic response of the fill, in terms of liquefaction potential to seismic events, and surface settlements due to earthquake, pile driving, or other impact loads.

6.1 Seismic Response Analysis

Two of the three selected sites were studied to evaluate the site response under earthquake loads. The TSW site was excluded because of its relatively shallow hydraulic fill. In the seismic response analysis, the liquefaction potential and the ground settlement of the CS1 and TKO sites were carefully examined.

6.1.1 Soil Profile

The generalized soil profiles for TKO and CS1 are shown in Figures 6.1 and 6.2 respectively. The pertinent soil properties of each layer were either determined in the laboratory, or deduced from available site information.

It is noted that at the TKO site the fill is placed directly on top of a layer of sea mud approximately 4 to 9 meters thick; whereas, in West Kowloon CS1 area, the sea mud layer was completely dredged and the hydraulic fill (which is much thicker than that at TKO) is placed directly on the alluvium.

6.1.2 The SUMDES Computer Code

In this study, the seismic response analysis was carried out by a computer programme SUMDES (Li et al 1992). This is a fully coupled effective stress 1-D finite element code formulated on the basis of vectored motion and generalized material stiffness. The code is capable of predicting multi-directional motions and pore pressure responses of level grounds. The soil skeleton of each element can be modeled individually. One of the special features of the code is the incorporation of the highly sophisticated bounding surface hypoplasticity soil

model for granular soil (Wang et al, 1990) into the finite element program. In calibrating the model parameters as input to the program, the cyclic triaxial test results reported in the previous chapter were used.

6.1.3 Input Motion

As indicated in the GEO Publication No.1 (1991) "Earthquake Data for the Hong Kong Region" previous earthquakes within 200km of Hong Kong had magnitudes less than 6.0, and larger magnitude earthquakes have only occurred outside the 200km region. The fact that Hong Kong is not a seismically active zone and typhoon being the most formidable environmental hazard to engineering structures, earthquake loading has seldom been seriously considered in local design codes. The stability of hydraulic fill is of course immune to wind load, seismic loads being the cause for concern must now be considered.

In this study a downhole acceleration time history recorded at Lotung, Taiwan during a major earthquake in November 1986 was chosen as the input excitation. The epicentre of the earthquake was originated at E121° 50.17', N23° 57.65' near Hualien, Taiwan, and the earthquake was measured at M=7.0 on the Richer scale. The focal depth was approximately 6km deep. The Lotung monitoring site was approximately 80km NW of the epicentre. Figures 6.3(a)-(c) shows the three components of the acceleration time history record. The two horizontal acceleration-time history components were used as the outcropping rock motions near the site. The shaking was more than 50 seconds long with peak acceleration values of 0.09g and 0.08g at N-S and E-W directions respectively. Undoubtedly the magnitudes of the input motions far exceed what might be expected in Hong Kong; thus the analyses presented in the next section serve to assess, in general terms, the response of hydraulic fills under a rather severe seismic shaking. A more meaningful assessment can be carried out when more representative acceleration records become available.

6.2 Response Analysis of the TKO Site

6.2.1 Ground Motions and Site Response

The procedures to develop the input parameters for the SUMDES finite element code at the TKO site are given in a separate report. Using the original Lotung earthquake records of N-S (direction 1) and E-W (direction 2) horizontal motions as input, the acceleration time history records at the bottom boundary (35m) and at the ground surface were calculated and are shown in Figures 6.4 through 6.7 for directions 1 and 2 respectively. It can be seen that the maximum ground surface acceleration is approximately 0.14g in direction 1 and 0.1g in direction 2. These calculated ground motion accelerations are approximately twice as much as that commonly adopted for seismic analysis in Hong Kong. The time history of the induced ground settlement is shown in Figure 6.8. The total amount of settlement at the end of the earthquake is approximately 1.5cm. Also predicted are the time history of excess pore water pressure and effective mean normal stress at different depths. Clearly, the pore water pressure increases during shaking and then dissipates gradually after the major shock (Figures 6.9 through 6.14 for depths at 5.5m, 6.5m, 7.5m, 8.5m, 9.5m and 10.5m, respectively).

In addition, the distribution of excess pore water pressure and effective mean normal

stress against depth at different time periods are also plotted as shown in Figures 6.15 through 6.22. All the analytical results seem to indicate that liquefaction is not likely to take place on the site; that the most critical zone of potential liquefaction is located in the hydraulic fill below the sea level (at a depth of 5m) and above the sea mud layer (at a depth of 11m); that the maximum excess pore water pressure in the hydraulic fill takes place at approximately 22 to 27 seconds after the commencement of the earthquake.

It should be pointed out that because of the lateral boundary specified for the free field condition in the analysis, the total stress in the soil element increases during shaking; hence, the amount of pore water pressure change cannot be directly inferred by the changes in effective mean normal stress as would be the case.

6.2.2 Scaled Down Ground Motions and Site Response

A similar analysis was made for the same site except the input ground motion was scaled down from the original input to yield a maximum surface acceleration of 0.07g, which is the recommended design acceleration in Hong Kong. A scaling factor of 0.45 was needed in order to achieve the 0.07g maximum ground acceleration. Figures 6.23 to 6.26 show the calculated scaled down acceleration time history at the bottom boundary and the ground surface in both directions 1 and 2 respectively using the factored earthquake input. Figures 6.27 through 6.32 depict the same information as appeared in 6.2.1; obviously, with less total surface settlement and lower excess pore water pressure generated by the earthquake excitation, the liquefaction potential is very low.

An exercise was carried out to examine how the different scaling factors might affect the total amount of surface settlement and pore pressure increase. Table 6.1 summarizes the results using different scaling factors to the original Lotung input motion while all the other condition remained unchanged. It should be noted that the "settlement" shown in the Table means ground surface settlement at the end of the earthquake. The term "max. acc." represents the maximum induced horizontal ground acceleration during earthquake, whereas the "Peak Value of $(1-P'/P_0')$" is the maximum value of $(1-P'/P_0')$ encountered during an earthquake in which P' is the effective mean normal stress and P_0' is the initial effective mean normal stress. Thus when P' is equal to zero, the value of $(1-P'/P_0')$ will equal 100% which is the condition of liquefaction.

6.2.3 Effect of Permeability of Hydraulic Fill

The coefficient of permeability k of the hydraulic fill was assumed as 1.0×10^{-4} m/sec in all the analyses performed thus far. This value was chosen on the basis of the estimated relationship between the relative density of the fill and the laboratory permeability test results. The actual field coefficient of permeability may vary somewhat due to the heterogeneity and segregation of the fill. Consequently, a number of analyses were carried out using different k values for the hydraulic fill but keeping all other conditions unchanged. The results of this study is summarized in Table 6.2. Generally speaking within the range of permeability values used, it is found that the liquefaction potential of the fill increases as the permeability decreases.

6.2.4 Effect of Thickness of Sea Mud Layer

The sea mud layer beneath the hydraulic fill at the TKO site varies in thickness ranging from 4 to 9 meters. An average thickness of 6.5 meters was adopted for the site response analysis. Table 6.3 listed the results of site response analysis for different assumptions of thickness of the sea mud layer. Since the total thickness of the soil column in the analyses was not altered, the thickness of the alluvium was changed accordingly to keep the total thickness of the soil column unchanged. It can be seen clearly that the relatively soft sea mud layer serves to attenuate the ground motion. This beneficial effect of thicker sea mud layer will therefore result in a reduction of excessive pore water pressure build up in the hydraulic sand fill.

6.3 Response Analysis of the CS1 Site

For this site, analyses as those performed for the TKO site were carried out. The generalized soil profiles for CS1 site is shown in Figure 6.2. The site conditions generally are quite similar to that of the TKO site except that there is no sea mud layer and the hydraulic fill layer is thicker in the CS1 site. The fill was divided into three layers: the top most layer of 9.5 meters is above the sea level and is relatively dense; the middle layer (6.5 meters) formed by pipe-line discharge is very loose; and the lower layer (7.5 meters) formed by bottom dumping is assumed to be loose (based on the field CPT results). Some of the interesting observations pertaining to the analytical results can be summarized as follows:

(a) The site is not likely to liquefy under the original Lotung input.

(b) A scaling factor of 0.6 is needed to adjust the maximum horizontal ground surface acceleration to 0.07g.

(c) The zone most susceptible to liquefaction is located below the sea level in the hydraulic fill.

(d) The dissipation of excess pore water pressure after the major shock is very slow and gradual.

(e) The possible ground surface settlement is small, somewhere between 1 to 2cm.

(f) It appears that the seismic response of the fill will not be significantly affected by the values of permeability assumed in the parametric study.

6.4 Seed and Idriss' Simplified Analysis

The Seed & Idriss' simplified liquefaction analysis is not a rigorous one for detailed study; however, it is probably the most widely used method for feasibility study and/or preliminary liquefaction assessment. Figures 6.33 and 6.34 show the results of the Seed &

Idriss' simplified analysis for the TKO and CS1 sites respectively. The magnitude of the input earthquake motion was assumed to be M=7.2 and the maximum ground accelerations used in the analyses were 0.07g and 0.116g. The results likewise indicated that site liquefaction is not likely to occur.

6.5 Settlement Caused by Dynamic Loads

Currently there is no established procedure to estimate the settlement of sandy fill due to surface imposed dynamic loads. Besides, the undrained cyclic triaxial test results do not give any meaningful information pertaining to the settlement behaviour of fill subjected to such loadings. Consequently, an exploratory investigation to estimate the ground settlement was initiated using the CS1 sand. It involved the testing of a number of loose, saturated specimens under drained cyclic loading conditions. The applied cyclic deviator stresses were small ranging between 5 to 15% of the drained strength. The number of loading cycles Versus the volumetric strain were plotted for each test as shown in Figure 6.35(a) to (d). Because of the relatively low applied stress levels, the resulting volumetric strains are small and the majority of the total strain occurred during the first 10 to 50 loading cycles. The volumetric strain obtained from cyclic triaxial testing cannot be used directly to translate to vertical settlement in the fill.

It has been argued that cyclic simple shear loading can better simulate field conditions: i.e. K_0-stress state, zero lateral displacement and the application of cyclic shear loading. A study on volume changes of dry sands during cyclic simple shear loading was reported by Silver and Seed (1971). The following is an attempt to use their results as the basis to examine the appropriateness of using the volumetric strain data from cyclic triaxial tests for ground settlement prediction. It is understood that this attempt is a simplified one, which can only serve as a reference for preliminary considerations.

As indicated by De Alba (1975) that the conversion of isotropically consolidated cyclic triaxial loading (TX) to the cyclic sample shear loading (CSS) is given by (see Figure 6.36)

$$\left[\frac{\tau_{hp}}{\tau_v c}\right]_{css} = C_r\left[\frac{\tau_{dp}}{2\tau_3 c}\right]_{TX} \qquad \ldots\ldots\ldots\ldots\ldots\ldots \quad (6.1)$$

where τ_{hp} is the applied cyclic horizontal shear stress for cyclic simple shear test.
σ_{vc} is the applied vertical pressure for cyclic simple shear test.
σ_{dp} is the applied deviator stress (i.e., σ_{1c}-σ_{3c}) for cyclic triaxial test.
σ_{3c} is the applied confining (consolidation) pressure for cyclic triaxial test.
C_r is the empirical correction factor.

From large scale shaking table tests, the range of C_r for Monterey No.0 sand is 0.61-0.66 according to DeAlba (1975).

Since $\tau_{hp}=G\gamma_{xy}$

where G is the shear modulus, and γ_{xy} is shear strain; and (referring to Figure 6.36)

$$\tau_{vc} = \tau_{nc} = \tau_{3c} + \frac{\tau_{dp}}{2} \qquad \text{. . . . . (6.2)}$$

Substitute Eq. 6.2 into Eq. 6.1, it can be written as :

$$\frac{G\gamma_{xy}}{\sigma_{3c} + \frac{\sigma_{dp}}{2}} = C_r \frac{\sigma_{dp}}{2\sigma_{3c}}$$

or

$$\sigma_{dp}^2 + 2\sigma_{3c}\sigma_{dp} - \frac{4\sigma_{3c}G\gamma_{xy}}{C_r} = 0 \qquad \text{. . . . . (6.3)}$$

where C_r and σ_{3c} are constants; G is a function of the shear strain γ_{xy} under a given number of loading cycles and confining pressure (overburden). Using this equation the cyclic shear strain γ_{xy} in simple shear can be related to the cyclic deviator stress σ_{dp} in triaxial compression.

Figures 6.37 and 6.38 from Silver and Seed (1971) show the vertical strain of Monterey No.0 sand due to triaxial shearing in 10 cycles under different cyclic shear strain, or different cyclic shear stress respectively. These results were obtained for specimens of different relative densities subjected to a range of overburden pressures. Using the data presented for D_r=45%, it is possible to develop a relationship between shear modulus and vertical (volumetric) strain in 10 cycles under 150kpa overburden as shown in Figure 6.39. Referring to Figure 6.40 from Silver and Seed, the relationships between cyclic shear strain and vertical (volumetric) strain in simple shear under different overburden pressures for 10 loading cycles and 50 loading cycles are given. For the case of D_r=45% and an overburden pressure of σ_{vc}=3133 lb/ft^2 (≈150kpa), the relationship between cyclic shear strain and volumetric strain can be approximated as shown in Table 6.4.

Having the shear modulus variations with shear strain in 10 cycles (Figure 6.39), and the consolidation stress σ_{3c} of 150kpa, values of deviator stresses and the corresponding cyclic shear strains for different C_r values can be calculated according to Eq. 6.3. The results are listed in Table 6.5. Note that the shear moduli shown in Table 6.5 are for N=10; the same moduli however, are also used for N=50. The deviator stress σ_{dp} Versus the volumetric strain relationships from the simple shear results for different C_r values and N values are presented in Figures 6.41 through 6.46. Also plotted are data points from the cyclic triaxial tests (i.e., results as presented in Figure 6.35(a)-(d)). For the range of C_r considered, the volumetric strain due to cyclic simple shear loading is smaller than those due to cyclic triaxial loading. Generally speaking, the former is only half or less of the latter. This comparison seems reasonable as the triaxial specimen is free to deform laterally. Furthermore, for an isotropic and elastic body the ratio between vertical strain and volumetric strain is 1:3. Thus the above justifies the use of drained cyclic triaxial data to roughly estimate the ground settlements.

Assuming that the vertical settlement is about half of the amount of the volumetric

settlement, according to Figure 6.35(d) the maximum vertical strain under a deviator stress 34.5kpa (15% of strength) is 0.2%. For a loose sand layer of 10 meters thick the total settlement would then be 2cm. This is indeed a small amount, which probably can be tolerated under normal conditions. Settlement in the vicinity of pile driving or heavy impact loading must be considered separately because of much higher stress intensities.

7. CALIBRATION CHAMBER TESTS

The cone penetration test results reported in Chapter 3 give a quantitative index of the compactness of reclaimed sand with depth. The CPT sounding is a direct and effective way to assess the competence of hydraulic fill for field control; however, the measured q_c and f_s values are not basic soil parameters commonly used to characterize the state and, to some extent, the engineering behavior of the soil being investigated. For granular soil in the field, its behavior is heavily influenced by the combined effect of overburden pressure (σ_c) and relative density (D_r). To make the penetration test results more meaningful it is desirable if correlation among q_c, σ_c, and D_r can be established. The calibration chamber test is designed to furnish this very information.

The calibration chamber test is performed in a large calibration chamber with the aim of calibrating, under carefully controlled stress and strain conditions, various insitu testing devices in sand . A detailed description of the design, construction and use of the ENEL Calibration Chamber is given by Bellotti, Bizzi and Ghionna (1982). Specimens of approximately 1.20 meters in diameter and 1.40 meters high were prepared in the calibration chamber by the air pluviation method. For specimens tested in this study, two different air pluviation schemes were used. The first six specimens were prepared by the use of a traveling sand spreader. However for the three hydraulic fill sands undertaken in the study, it was found that this technique could not form specimens with high degree of uniformity. To achieve more uniform specimens especially at lower densities, a different technique which uses a deposition tube (22mm in diameter) maintained at a height 7 meters above the plane of deposition was later adopted for all remaining specimens (except for specimen Test no. 446i). A schematic drawing depicting the preparation using a deposition tube is shown in Figure 7.1.

All specimens were saturated by back pressuring (except for Test no. 446i which was tested under dry condition) prior to performing the CPT test with a 20mm diameter cone at a penetration rate of 2cm/sec. Two sets of CPT were performed on each specimen under the boundary condition 1 (BC1, σ_v=constant, σ_h=constant). The penetration of the cone under the first stage stress condition was carried to a depth of 62cm and stopped; the stress condition was increased (normally increased in both σ_v and σ_h) before further penetration of the cone proceeded. A report submitted by the ENEL - Hydraulic and Structural Research Center entitled "Cone Penetration tests on three cohesionless soils from Hong Kong", which provides detail descriptions of the procedure and all the test results, is available for reference.

A typical calibration chamber test record is given in Figure 7.2; the penetration resistance (q_c) Versus depth relationships under two different consolidation pressures are shown on the left side of the Figure. For consistency, it is advised that the q_c values be taken at depths 50-60cm and 90-100cm respectively for the two consolidation pressures. It is considered that the wavy shape of some of the traces, such as the one seen in Test no. 437i to 442i (see Enclosure E-5 of the reference), could be caused by the way the specimens were

formed: i.e. segregation due to pluvial deposition through air and/or "path induced non-uniformity". Table 7.1 summarized all the calibration chamber test results conducted at ENEL in Milano, Italy. Detail test records of all the calibration chamber tests are given in the referenced ENEL report. It should be pointed out that the relative densities of the calibration chamber test specimens do not match closely with the specified conditions in the originally proposed testing program. This should not cause any concern since we are interested in the results of specimens covering a range of relative densities that can give enough meaningful data points to establish a q_c-σ_c-D_r relationship(s) for Hong Kong reclamation sands, not particularly the specific relative densities of specimens.

The choice of q_c (tip resistance) over f_s (shaft resistance) for correlation is due largely to the fact that (1) the values of f_s can be significantly affected by the overconsolidation ratio or stress history of the soil deposit, and (2) the f_s measurements are also affected by the roundness and the alignment of the penetrometer itself; whereas, q_c can be more uniquely related to the relative density of granular soils.

In this study, all the calibration chamber test results were obtained by the use of a miniature 20 mm cone. The use of such a small size cone is aimed at reducing the chamber size effect on CPT readings which is accomplished by increasing the ratio of the diameter of the test specimen to the diameter of the cone. According to the work by Parkin and Lunne (1982), Salgado (1993), and previous studies at the ENEL, the chamber size effect under BC1 can underestimate the free field penetration resistance value (q_{cff}) by an amount of 10 to 15%. Accordingly, all the values of q_c determined by calibration chamber tests were adjusted by multiplying a correction factor of 1.15 to obtain free field penetration resistance (q_{cff}) values as shown in the last column in Table 7.1. It should be noted that this correction factor is based primarily on data from four different sands previously studied by the group at ENEL and others. The relevant information regarding these sands are shown in Table 7.2. Likewise, the corresponding information of the Hong Kong sands are shown in Table 7.3. It is clear that the referenced sands used by the ENEL group were much finer and more uniform than the hydraulic fill sands undertaken in the present study.

In view of the differences in material composition, it seems that additional justification in using the suggested correction factor should be further examined. An analytical solution in the form of a finite element code to correct the chamber size effect for penetration resistance values in sandy soil was recently developed by Rodrigues (1993), which can be used to determine the free field correction factor. Consequently, the calibration chamber test results of the CS1 sand were selected to properly calibrate the required soil parameters using the back calculation approach for computer simulation and validation. Results of the predicted cone penetration resistance values (q_{cp}) under the simulated Calibration Chamber conditions are tabulated in Table 7.4; and were plotted against the corresponding actual chamber test results as shown is Figure 7.3. As seen from the result, the predicted values were in reasonable agreement with the test data. To correct for free field boundary effect, the finite element program also give a q_{cp}/q_{cpff} ratio for each set of test (as indicated in Table 7.4). The corrected free field penetration resistance value q_{cff} can then be determined by multiplying the ratio q_{cp}/q_{cpff} to the calibration chamber test results. A comparison of the predicted free field penetration resistance values q_{cff} to the measured penetration resistance values q_c is shown in Figure 7.4. The simulation study yielded an averaged correction factor 1.13 (slope of the dotted line by regression analysis) for the calibration chamber results, which is very close to the factor 1.15 used in Table 7.1.

Throughout this report, the relative densities determined for Hong Kong sands were based on the maximum and minimum densities specified according to the British Standard (Part 4:42 and Part 4:43 of BS 1377, 1990, respectively). However, the relative densities of the calibration chamber specimens were determined using the maximum and minimum densities according to the ASTM specifications (Designation: D 4253 - 91 and D 4254 - 91, respectively). Significant differences in density values determined by these two methods are noticed, particularly in maximum densities as shown in Table 7.5. It should also be noted that all the tests reported in Chapters 4 and 5 were conducted on sands which passed the 5 mm sieve, while all the Calibration Chamber tests conducted at ENEL were on sands which passed the 4.75 mm sieve. Accordingly conversion scales D_r (ASTM) Versus D_r (BS) and D_r (ASTM) Versus the dry unit weight of the given soil γ_d are developed for reference as shown in Figure 7.5.

Most of the information dealing with relative density reported in the literature are ASTM-based, as it is also true in the literature review presented in Chapter 3. It is therefore decided to use both the ASTM-based D_r and the BS-based D_r values in establishing the q_c-σ_c-D_r relationships for this study. Figures 7.6, 7.7 and 7.8 are charts prepared for CS1, TKO, TSW sands respectively (it should be noted that the BS-based D_r values are given in parentheses), where the q_c values are free field cone penetration resistance values derived from corrected calibration chamber results.

The individual data points marked as (x) in the Figures are results of q_c Versus σ_c obtained by the use of geotechnical centrifuge at the ISMES Laboratories, Bergamo, Italy. It should be noted that the results of q_c determined by centrifuge tests have to be corrected for the rigid lateral boundary condition effect (i.e., BC3, σ_v =constant, σ_h =0). Based on the previous studies at ENEL and Salgado (1993), it is suggested the q_c values determined by centrifuge tests be reduced by 15% to account for the boundary effect. Results of penetration tests performed in the centrifuge (Enclosure E-6 of the reference) seem to show reasonable agreement with those obtained in the calibration chamber. Conducting penetration resistance test in the centrifuge is a new attempt. It is originally intended to simulate higher overburden pressure environment in the test, thus complementing the calibration chamber testing on the higher side of the pressure range. However, there appear to be inherent boundary condition problems and other limitations making the interpretation of results difficult. It is the authors' opinion that more work is needed before the relevance of performing calibration chamber tests in the centrifuge can be established.

Referring to Figures 7.9, 7.10 and 7.11, the "blocked" zones which appear on the charts are regions where the field CPT values (Chapter 3) were plotted. In the absence of reliable field density determinations, the measured CPT values cannot be used to validate the q_c-σ_c-D_r relationships established by the calibration chamber test results; nevertheless, the zones delineating CPT values at various depths seem to fall within the generally recognized relative density range(s) in reclamation work noted in the literature.

8. SUMMARY AND CONCLUSIONS

The first phase of the study aiming at the development of suitable means for the characterization of hydraulic sand fills used for land reclamation in Hong Kong has been completed. In this report an overview of the literature on hydraulic fills for land reclamation

was presented. It was clear that the quality of hydraulic fills in terms of density and uniformity depends on a variety of factors such as the source material, the method of placement, the environment under which deposition was carried out, etc. Variations in placement density and grain size must be recognized in hydraulic fill since different placement methods are employed during the filling process. Generally speaking, other than the selection of suitable fill material and control at the point of discharge, very little can be done to effectively control the quality of hydraulic fill. Compaction or other improvement methods can be employed, usually with high cost, to densify the reclaimed land for engineering purposes. Active control and improvement of the placement density while filling is in progression has not been widely considered.

A limited number of insitu measurements in terms of CPT and SPT were conducted on the three reclamation sites. The results clearly indicated significant variations in placement density and grain size with fill depth on every site due to reasons stated previously. Site specific information regarding the soil profile, fill depth, filling process, site treatment, etc. are available upon request. Physical properties of the three marine sands were carefully determined and reported. These sands cover a broad spectrum of the marine sands used for reclamation in Hong Kong, thus forming a useful source of information. It, however, must be cautioned that a wide variation of grain size distribution and density can be found in reclaimed fills. A good example is shown in the limited "undisturbed" samples obtained from the CS1 site where the grading curves and densities of the fill at different depths vary quite significantly.

An extensive undrained triaxial testing program was carried out, including both static and cyclic loadings on saturated specimens. These specimens were prepared by the dry pluviation method for different relative densities and tested under different confining pressures. The static test results provide a complete set of information of the stress-strain and volume charge characteristics (pore pressure response) of Hong Kong marine sands. The cyclic triaxial test results determined the liquefaction potential of the sands under different cyclic deviator stress levels. Such information is needed to assess the site response to seismic loads. From a limited number of tests, it was discovered that the liquefaction potential of specimens of the same soil with similar density but prepared under different sample preparation techniques are quite different. For the CS1 sand, specimens prepared by the wet tamping method has the highest liquefaction resistance, followed by the "undisturbed" specimen and then the dry pluviated specimen. This is indeed a concern when dealing with the dynamic testing of sandy soils.

The dynamic stability of Hong Kong reclamation sites were analyzed for two types of cyclic loading conditions: i) the site response to seismic loads, and ii) the settlement of sand fill due to other surface imposed cyclic loads. In the seismic response analyses, both the likelihood of liquefaction and the magnitude of seismically induced ground settlement were studied. The study employed a fully coupled effective stress 1-D finite element code which is capable of cooperating multi-directional motions and predicting the settlement and pore water response. Parameters such as the permeability, magnitude of ground motion, and layer thickness were varied to evaluate the influences of these parameters on site responses. The input ground motion was taken from a downhole acceleration-time history recorded at Lotung, Taiwan during a major earthquake in November 1986. The input indeed far exceeded what might be expected in Hong Kong. More realistic assessment could be made if representative acceleration records were available. It should be noted that both horizontal acceleration

components (S-N and E-W) were considered in the analysis. It is believed that this kind of multi-directional ground motions analysis would be more realistic (but more severe) than the commonly employed single acceleration input motion analysis. In addition, drained cyclic triaxial tests were performed to estimate the possible ground surface settlement due to surface imposed loading. Simplified calculations were carried out to approximate the possible ground settlement induced by surface imposed cyclic loading. It appears that the ground settlement would be relatively small for low intensity loadings (less than 15% of the strength).

The σ_v'-q_c-D_r relationships of the three marine sands have been established via results of calibration chamber tests carried out at ENEL. The q_c values were corrected for size and boundary effect using a recently available analytical solution. These relationships can be used to form the basis for identifying the insitu quality of hydraulically placed sandy fill in Hong Kong.

In short, this report gives a comprehensive set of information pertaining to the static and dynamic properties and behaviours of Hong Kong marine sands. It however must be borne in mind that hydraulic fills are almost always heterogeneous. Significant differences can be found in density and gradation of fill material on any reclamation site. The information compiled in this report represents the general behaviour of the fill but not a specific layer or zone.

In light of the above discussion, general statements pertaining to the construction, treatment, control and stability of Hong Kong reclamation site may be summarized as follows:

(a) It is prudent to acknowledge that hydraulic fills are heterogeneous. The method used for fill placement and the details of its application, the conditions of discharge, the presence of ponded water, and variability of source materials are all important in forming the resulting fill properties.

(b) The placement technique is probably the single most important factor controlling the relative density of a given sand when placed as a hydraulic fill. As such, the weakest zone is generally located beneath water level where fill deposition is made by pipeline discharge. This is true for all the three sites selected for this study.

(c) It follows that for economic and effective control of the quality of hydraulic fills, attention must be paid to improve the weakest zone situated right below the water level.

(d) There seems a need to develop techniques capable of densifying the fill during the process of fill deposition and monitoring the improvement for quality control.

(e) Based on the limited amount of information available from calibration chamber tests, correlations of D_r-σ_c-q_c for Hong Kong marine sands can be established and it

is likely that such correlations can be used for fill quality control.

(f) Generally speaking, the Hong Kong hydraulic fills are of good quality. This is supported by the triaxial test results presented in this report. It is believed that the good quality is a direct result of the good source material and good dredging practice.

(g) Because of the excellent source material and the fact that Hong Kong is not a seismically active zone, the dynamic stability of Hong Kong hydraulic fills appears to be sound. Dynamic disturbance, however, can be the cause of extensive local failures of hydraulic fills, as witnessed in the San Francisco Bay area during the Loma Prieta earthquake of 1989, and the failure at the airport site in Nice, France.

(h) It is extremely difficult to correlate the insitu measurements with field density in sandy soils. Disturbance in sampling nullifies the possibility of obtaining undisturbed samples from the field if conventional sampling techniques are employed. It appears that a truly representative correlation of D_r-σ_c-q_c must be carried out in the field and high quality undisturbed samples obtained from advanced sampling techniques must be secured.

Indeed for any planned major reclamation project, the fill must be engineered, not simply dredged and placed. Even so, major buildings or installations may have to be supported by deep foundations extending beyond the fill. For airport runways or any other major track beds, superior fill material such as quarry rock should be used.

9. REFERENCES

Akroyd, T.N.W. (1969), Laboratory Testing in Soil Engineering, Soil Mechanics Ltd., London, 249 pp.

ASCE (1978), Soil Improvement, History, Capabilities and Outlook, Report by the committee on Placement and Improvement of Soils, American Society of Civil Engineers.

ASCE (1987), "Soil Improvement - A Ten Year Update", ASCE Geotechnical Special Publication No. 12, American Society of Civil Engineers.

Baldi, G., Bellotti, R., Ghionna, V., Jamiolkowski, M., and Pasqualini, E. (1986), Interpretation of CPT's and CPTU's Part 2, drained penetration of Sands. Fourth International Geotechnical Seminar. Field instrumentation and insitu measurements, Singapore, pp. 143-156.

Ballard, R.G. and McLean, F.G. (1975), "Seismic Field Methods for Insitu Moduli," Proc. ASCE Specialty Conf. on Insitu Measurements of Soil Measurements of Soil Properties, Raleigh, NC, Vol. 1, 1975, pp. 121-150.

Been, K., Jefferies, M.G., Crooks, J.H.A., and Rothenberg, L. (1987), "The Cone Penetration Test in Sands: Part II, General Inference of State," Geotechnique, Vol. 37, No. 3, pp. 285-299.

Bellotti, R., Bizzi, G. and Ghionna, V. (1982), "Design, Construction and Use of a Calibration Chamber", Proceedings for the Second European Symposium on Penetration Testing, Amsterdam, pp439-446.

Bray, R.N. (1979), Dredging: A Handbook for Engineers, Edward Arnold, London, 276 p.

British Standards Institution (1975), Methods of Testing Soils for Civil Engineering Purposes. (B.S. 1377:1975), British Standards Institution, London, 143 p.

Burland, J.B. and Burbidge, M.C. (1985), "Settlement of Foundation on Sand and Gravel", Proc. Instu. Civ. Engrs., Dec. 1985, 78, Part I, pp. 1325-381.

Burmister, D.M. (1962), "Physical, Stress-Strain, and Strength Response of Granular Soils," Symposium on Field Testing of Soils (STP 322), ASTM Philadelphia, 355 p.

Castro, G., Enos, J., France, J.W., and Poulos, S.J. (1982), "Liquefaction induced by cyclic loading", Report to National Science Foundation, Washington, D.C., No. NSF/CEE-82018, pp. 325.

CM&E (1976), Methods Memo, p. 132, April.

De Alba, P.A. (1975), Determination of Soil Liquefaction Characteristics by Large Scale Laboratory Test, Ph.D. Diss., U.C. Berkeley.

DeAlba, P., Seed, H.B. and Chan, C.K. (1976),"Sand Liquefaction in Large Scale Simple Shear Tests", Journal of Geotechnical Engineering Division, ASCE, Vol. 102, No. GT9, pp. 909-927.

de Groot, M.B., Heezen, F.T., Mastbergen, D.R., and Stefess, H. (1988), "Slopes and Densities of Hydraulically Placed Sands", Proceedings of the Conference-Hydraulic Fill Structures, ASCE, Fort Collins, pp. 32-51.

Dowding, C.H. and Hryciw, R.D. (1986), "A Laboratory Study of Blast Densification of Saturated Sand", Journal of Geotechnical Engineering, ASCE, Vol. 112, No. 2, pp. 187-199.

Dumas, J.C. and Beaton, N.F. (1988), "Discussion to "Practical Problems from Surprising Soil Behaviour ", by J.K. Mitchell, Journal of Geotechnical Engineering, ASCE.

Durgunoglu, H.T. and Mitchell, J.K. (1975), "Static Penetration Resistance of Soils", Proceedings of the ASCE Specialty Conference on Insitu Measurement of Soil Properties, Raleigh, NC, Vol. 1, pp. 151-189.

GEO (1991), Review of Earthquake Data for the Hong Kong Region (GEO Publication No. 1/91), Geotechnical Control Office, Civil Engineering Services Department, Hong Kong.

Gibbs, H.J. and Holtz, W.G. (1957), "Research on Determining the Density of Sands by Spoon Penetration Testing," Proceedings of the Fourth International Conference on Soil Mechanics and Foundation Engineering, Vol. 1, London, pp. 35-39.

Hodge, W.E. (1988), "Construction Method for Improving Underwater Sand Fills", Hydraulic Fill Structures: ASCE Geotechnical Division Specialty Conference, Fort Collins, CO.

Holtz, W.G. and Gibbs, H.J. (1979), Discussion of "SPT and Relative Density in Coarse Sand," Journal of the Geotechnical Engineering Division, ASCE, Vol. 105, No. GT3, pp. 439-441.

Jamiolkowski, M., Ladd, C.C., Germaine, J.T., and Lancellotta, R. (1985), "New Developments in Field and Laboratory Testing of Soils," Proceedings of the 11th International Conference on Soil Mechanics and Foundation Engineering, San Francisco, Vol. 1, pp. 57-153.

Jamiolkowski, M., Baldi, G., Bellotti, R., Ghionna, V., and Pasqualini, E. (1985), "Penetration Resistance and Liquefaction of Sands," Proceedings of the 11th International Conference on Soil Mechanics and Foundation Engineering, San Francisco, Vol. 4, pp. 1891-1896.

Jefferies, M.G., Rogers, B.T. and Stewart, H.R. (1988a), "Island Construction in the Canadian Beaufort Sea", ASCE Geotechnical Special Publication No. 21, Fort Collins, Colorado.

Jefferies, M.G., Rogers, B.T., Stewart, H.R., Shinde, S., James D., and Williams-Fitzpatrick, S. (1988b), "Island Construction, Underwater Soil Sampling, Testing and Construction Control", ASTM, STP501, American Society of Testing and Materials, pp. 122-180.

Johnson, S.J., Cunny, R.W., Perry, E.B. and Devay, L. (1977), "State-of-the Art Applicability of Conventional Densification Techniques to Increase Disposal Area Storage Capacity", Technical Report D-77-4. Soils and Pavements Laboratory, U.S. Army Engineer Waterways Experiment Station, Vicksbury, Miss.

Johnson, A.W. and Sallbery, J.R. (1960), "Factors that Influence Field Compaction of Soils", Bulletin 272, Highway Research Board, 206 pp.

Johnston, S.J., Compton, J.R., and Ling, S.C. (1972), "Control of Underwater Construction, Underwater Soil Sampling, Testing and Construction Control", ASTM, STP501, American Society for Testing and Materials, pp. 122-180.

Koerner, R.M. and Lord, A.E. (1985), "Recent Field Advances Using Acoustic Emissions", Proceedings of the 11th International Conference on Soil Mechanics and Foundation Engineering, San Francisco, Vol. 2, pp. 875-878.

Kulhawy, F.H. and Mayne, P.W. (1990), Manual on Estimating Soil Properties for Foundation Design, EL-6800, Electric Power Research Institute Research Project, 1493-6.

Kulhawy, F.H., Jackson, C.S., and Mayne, P.W. (1989), "First Order Estimation of K_0 in Sands and Clays,"Foundation Engineering: Current Principles and Practices, F. H. Kulhawy, Ed., ASCE, New York, pp. 121-134.

Lambe, T.W. and Whitman, R.V. (1969), Soil Mechanics, John Wiley and Sons, New York, 553 p.

Leycure, P. and Schroeder, W.L. (1987), "Slope Effects on Probe Densification of Sands", Soil Improvement - A Ten Year Update, ASCE Geotechnical Special Publication No. 12, pp. 197-214.

Li, X.S., Chan, C.K. and Shen, C.K. (1988), "An Automated Triaxial Testing System", Advanced Triaxial Testing of Soil and Rock, ASTM STP977, pp. 95-106.

Li, X.S., Wang, Z.L. and Shen, C.K. (1992), User's Manual for SUMDES----A Nonlinear Procedure for Response Analysis of Horizontally-Layered Sites Subjected to Multi-directional Earthquake Loading, University of California, Davis.

Lukas, R.G. (1986), "Dynamic Compaction for Highway Construction, Vol. 1: Design and Construction Guidelines", Federal Highway Adminstration Report No. FHWA/RD-86/133, 230 pp.

Lyell, K.A., and Prakke, H.K. (1988) "Cyclone Deposited Tailings Dam for 300 Million Tonnes", Proceedings of the Conference, Hydraulic Fill Structures, ASCE, Ford Collins, pp. 987-999.

Marchetti, S. (1985), "On the Field Determination of K_0 in Sand", Proceedings of the 11th International Conference on Soil Mechanics and Foundation Engineering, San Francisco, Vol. 5, pp. 2667-2672.

Massarch, K.R. (1985), "Deep Compaction of Sand Using Vibratory Probes", Third International Geotechnical Seminar, Soil Improvement Methods, Singapore.

Mayne, P.W., Jones, J.S. and Dumas, J.C. (1984), "Ground Response to Dynamic Compaction", Journal of the Geotechnical Engineering Division, ASCE, Vol. 110, No. 6, pp. 757-774.

McNeilan (1993), Personal communication, June 15, 1993.

Mesri, G., Feng, T.W., and Benak, J.M. (1990), "Post Densification Penetration Resistance of Clear Sands", Journal of Geotechnical Engineering, ASCE, Vol. 116, No. 7, pp. 1095-1115.

Meyerhof, G.G. (1956), "Penetration Tests and Bearing Capacity of Cohesionless Soils," Journal of the Soil Mechanics and Foundations Division, ASCE, Vol. 82, No. SM1, pp. 1-19.

Mitchell, J.K. (1981) "Soil Improvement: State-of-the-Art", Proceedings of the Tenth International Conference on Soil Mechanics and Foundation Engineering, Stockholm, Vol. 4, pp. 509-565.

Mitchell, J.K. (1986), "Ground Improvement Evaluation by Insitu Tests", Insitu 86, ASCE Geotechnical Special Publication No. 6, pp. 221-236.

Mitchell, J.K. (1988), "Densification and Improvement of Hydraulic Fills", Proceedings of Hydraulic Fill Structures '88, ASCE Geotechnical Special Publication No. 21, p 601.

Mitchell, J.K. and Solymar, Z.V. (1984), "Time-Dependent Strength Gain in Freshly Deposited or Densified Sand", Journal of the Geotechnical Engineering Division, ASCE, Vol. 110, No.11, pp. 1559-1576.

Mitchell, J.K. and Gardner, W.S. (1975), "Insitu Measurement of Volume Change Characteristics", Proceedings of ASCE Specialty Conference on Insitu Measurements of Soil Properties, Raleigh, NC, Vol. 2, pp. 279-345.

Morgenstern, N.R. and Kupper, A.A.G. (1988), "Hydraulic Fill Structures - a Perspective", Proceedings of Hydraulic Fill Structures '88, ASCE Geotechnical Special Publication No. 21, pp. 1-31.

NAVFAC (1982), Soil Mechanics (DM 7.1), Naval Facilities Engineering Command, Alexandria, VA, 355 p.

Parkin, A.K. and Lunne, T. (1982), "Boundary Effects in the Laboratory Calibration of Cone Penetrometer for Sand", Proc. ESOPT, Amsterdam.

Peck, R.B., Hanson, W.E., and Thornburn, T.H. (1974), Foundation Engineering, 2nd Edition, John Wiley and Sons, New York, 514 p.

POLA (1990), Port of Los Angeles Seismic Workshop, Draft Proceedings, March 1990.

Reilly, G.J. (1991), "Design and Quality Control of Hydraulic Fills - A Consultants Perspective", Reclamation Important Current Issues, HKIE Geotechnical Division, Hong Kong.

Richart, F.E., Jr., Hall, J.R., Jr., and Woods, R.D. (1970), Vibrations of Soils and Foundations, Prentice-Hall, Englewood Cliffs, NJ, 414p.

Robertson, P.K. and Campanella, R.G. (1983), "Interpretation of Cone Penetration Tests," Canadian Geotechnical Journal, Vol. 20, No. 4, pp. 718-733.

Robertson, P.K., Campanella, R.G. and Wightman, A. (1982), "SPT-CPT Correlations", Soil Mechanics Series No. 62, University of British Columbia, Civil Engineering Department.

Robertson, P.K., Woeller, D.J. and Finn, W.D.L. (1992), "Seismic Cone Penetration Test for Evaluating Liquefaction Potential Under Cyclic Loading", Canadian Geotechnique Journal, Vol 29, No. 4, pp 686-695.

Ryan, C.R. (1988), "The Fringes of Technology in Geotechnical Construction", Lecture to the Geotechnical Group of the San Francisco Section, ASCE, January 14, 1988.

Salgado, R. (1993), Analysis of Penetration Resistance in Sands, Ph.D. Thesis. University of California at Berkeley.

Schmertmann, J.H. (1975), "Measurement of Insitu Shear Strength", Proceedings of the ASCE Specialty Conference on Insitu Measurement of Soil Properties, Raleigh, NC, Vol. 2, pp. 57-138 (closure: pp. 175-179)

Schmertmann, J.H. (1978), "Guidelines for Cone Penetration Test Performance and Design," Report FHWA-TS-78-209, U.S. Department of Transportation, Washington, 145 p.

Schmertmann, J., Baker, W., Gupta, R. and Kessler, K. (1986) "CPT/DMT QC of Ground Modification at a Power Plant", in Use of Insitu Tests in Geotechnical Engineering, Geotechnical Special Publication No. 6, ASCE, pp. 985-1001.

Seed, H.B. (1979), "Soil Liquefaction and Cyclic Mobility Evaluation for Level Ground During Earthquakes", Journal of the Geotechnical Engineering Division, ASCE, Vol. 105, No. GT2, pp. 201-255.

Seed, H.B. and Idriss, I.M. (1967), "Analysis of Soil Liquefaction, Niigata Earthquake", Journal of Soil Mechanics and Foundation Division, ASCE, Vol 93, No SM3, pp83-108.

Seed, H.B. and Lee, K.L. (1966), "Liquefaction of Saturated Sands During Cyclic Loading", Journal of Soil Mechanics and Foundation Division, ASCE, Vol. 92, No. SM6, pp105-134.

Silver, M.L. and Seed, B.H. (1971), "Volume Changes in Sands During Cyclic Loading", Journal of the Soil Mechanics and Foundation Division, ASCE, SM9, pp. 1171-1182.

Sladen, J.A. (1989), "Problems with Interpretation of Sand State from Cone Penetration Test", Geotechnique, 39, 2, pp. 323-332.

Sladen, J.A. (1990), "Effect of Placement Method on the Liquefaction Potential of Hydraulic Sand Fill," Draft Proceedings of the Port of Los Angeles Seismic Workshop, March 1990.

Sladen, J.A., D'Hollander, R.D., Krahn, J. (1985b), "The Liquefaction of Sands, a Collapse Surface Approach", Canadian Geotechnical Journal, 22, 4, pp. 564-578.

Sladen, J.A., D'Hollander, R.D., Krahn, J., and Mitchell, D.E. (1985a), "Back Analysis of the Nerlerk Berm Liquefaction Slides", Canadian Geotechnical Journal, 22, 4, pp. 579-588.

Sladen, J.A., and Handford, G. (1987), "A Potential Systematic Error in Laboratory Testing of Very Loose Sands", Canadian Geotechnical Journal, 24, 3, pp. 462-466.

Sladen, J.A., and Oswell, J.M. (1989), "The Behaviour of Very Loose Sand in the Triaxial Compression Test", Canadian Geotechnical Journal, 26,1, pp. 103-113.

Sobkowicz, J.C., and Handford, G.T. (1990), The application of state-of-the-art static liquefaction concepts at Syncrude Canada Ltd, Presented at the 43rd Canadian Geotechnical Conference. Quebec City.

Solymar, Z.V. (1984), "Compaction of Alluvial Sands by Deep Blasting", Canadian Geotechnial Journal, Vol. 21., No. 2, pp. 305-321.

Sowers, G.F. (1979), Introductory Soil Mechanics and Foundations: Geotechnical Engineering, 4th Edition, Macmillan Publishing Co., New York, 621 p.

Stokoe, K.H., II, and Nazarian, S. (1983), "Effectiveness of Ground Improvement from Spectral Analysis of Surface Waves," Proceedings of the Eighth European Conference on Soil Mechanics and Foundations, Helsinki, Vol. 1, May 1983, pp. 91-94.

Terzaghi , K. and Peck, R. B. (1967), Soil Mechanics in Engineering Practice, 2nd Ed., John Wiley and Sons, New York, 729 p.

Tjelta, T.I., Tieges, A.W.W., Geise, J.M. and Lunne, T. (1985), "Insitu Density Measurements by Nuclear Backscatter for an Offshore Soil Investigation," Proceedings, 17th Offshore Technology Conference, May 1985, Paper 4917.

Turnbull, W.J., and Mansur, C.L. (1973), "Compaction of Hydraulically Placed Fills", Journal of the Soil Mechanics and Foundations Division, ASCE, SM11, pp. 939-955.

Verkerke, U.F., and Volbeda, J.H. (1991), "Design and Quality Control of Hydraulic Fill - a Contractor's Perspective", Proceeding of the Seminar Reclamation-Important Current Issues organized by the Geotechnical Division, HKIE, May 14, 1991.

Wallays, M. (1983), "Deep Compaction by Vertical and Horizontal Vibration", Geotechnical Engineering, Vol. 14.

Wang, Z.L., Dafalias, Y.F., and Shen, C.K. (1990), "Bounding Surface Hypoplasticity Model for Sand", Journal of Engineering Mechanics, ASCE, Vol. 116, No. 5.

Welsh, J.P. (1987), GKN Hayward Baker Ground Modification Seminar Notes.

Yano, L.T., and Fair, A.E. (1988), "Overview of Hydraulic Construction Techniques. Utilized at the Syncrude Canada Limited Tailings Pond", Proceedings of the Conference, Hydraulic Fill Structures, ASCE, Fort Collins, pp. 971-986.

Youd, T.L. (1973), "Factors Controlling Maximum and Minimum Densities of Sands", Evaluation of Relative Density and Its Role in Geotechnical Projects Involving Cohesionless Soils (STP 523), ASTM, Philadelphia, pp. 98-122.

LIST OF TABLES

Table 2.1 - General Characteristics of Soils and Rocks for Dredging Purposes

Rock/soil type	Excavation characteristics						Suitable as reclamation material	Suitability to pipeline transportation	Often observed bulk density before excavation
	Dipper dredger	Bucket dredger	Suction dredger	Cutter dredger	Trailer dredger	Grab dredger			
ROCK ▲									
I. Igneous	NA	NA	NA	NA	NA	NA	NA	NA	2.0–2.8
II. Sedimentary	Possible in soft rock but difficult	Possible in soft rock but difficult	NA	Difficult to fair in softer rocks	NA	Possible in softer rocks but very difficult	Very good	Fair, large fragments may block pipes	1.9–2.5
III. Metamorphic	NA	NA	NA	NA	NA	NA	NA	NA	2.0–2.8
Boulders	Fair	Very slow may require slinging	NA	NA	NA	Difficult but large units cope	Not acceptable	NA	NA
Cobbles or Cobbles with gravel	Fair	Fair	Difficult	Difficult	Difficult	Fair	Bad to good	Poor	NA
Gravel	Easy	Fair	Difficult to fair	Fair	Difficult to fair	Fair	Good	Fair	1.75–2.2
Sandy gravel	Easy	Fair to easy	Fair	Fair to easy	Fair to easy	Fair to easy	Very good	Fair to good	2.0–2.3
Medium sand	Easy but low production	Easy	Easy	Easy	Fair to easy but High overflow losses likely	Easy	Very good	Good	1.7–2.3
Fine sand							Good	Very good	
Extra fine sand			Fair						
Silty fine sand									
Cemented fine sand	Fair	Fair	NA	Fair to easy	Difficult	Difficult	Good	Bad to good	1.7–2.3
Silt	NA	Easy	Difficult to fair	Easy	Fair to easy but high overflow losses	Fair	Bad	Very good	1.6–2.0
Firm or stiff gravelly or sandy clays (i.e. boulder clays)	Fair	Difficult to fair	NA	Difficult to fair	NA	Difficult to fair	Good	Only possible after disintegration	1.8–2.4
Soft silty clays (i.e. alluvial clays)	NA	Fair to easy	NA	Easy	Fair	Easy	Bad	Fair	1.2–1.8 (fresh harbour sediment 1.15–1.6)
Firm or stiff silty clay	Fair to easy	Easy	NA	Fair to easy	Difficult to fair	Fair	Bad to fair	Only possible after disintegration	1.5–2.1
Peats	NA	Easy	NA	Easy if no gas encountered	Fair	Easy	Unacceptable	Very good	0.9–1.7

Legend :

▲ Weathering of rocks will after form and strength considerably and may allow direct dredging without blasting, etc

NA Not applicable

Notes :

(1) This table only gives a rough indication and should be used with caution.

(2) The feasibility to use a certain type of dredging equipment depends not only on the soil type but also on site conditions, the size strength of construction and power supply of that piece of equipment, etc.

(3) The qualifications used above (bad, poor, fair, easy, very good, etc.) are meant to show the degree of suitability but should not be related to the output or even less as indicative of the cost per excavated unit.

(4) This Table is based on Bray (1979).

Table 2.2 - Summary of Methods for Improvement of Hydraulic Fills (Sheet 1 of 2)

	Method	Principle	Most Suitable Hydraulic Fill Types	Maximum Effective Treatment Depth	Special Materials Required	Special Equipment Required	Properties of Treated Material	Special Advantages and Limitations	Relative Cost
Densification During Placement	Surface Compaction	Compaction in layers as fill is placed	Fairly clean sands (<15% passing No. 200 sieve)	N/A	None	Rollers, Bulldozers	High (85% +) relative density, good uniformity	Simple, low cost, work in the dry	Low
	Underwater Surface Compaction	Tamping of fill surface during placement	Fairly clean sands (<15% passing No. 200 sieve)	N/A	None	Barge mounted tampers, underwater compactors	High relative density, good uniformity	Simple, may interfere with full placement operations	Low to Moderate
	Internal Dewatering by Pumping	Inward seepage force give density increase, allow steeper side slopes, reduce surface erosion	Clean sand	?	None	Suction probe, suction pumps	Increased density	In early stage of development	?
	Surface Drying	Drying shrinkage causes density and strength increase, compressibility decreases	Soft, cohesive soils	1m (?)	None	None	Higher strength, lower compressibility than when placed	Limited depth of effectiveness; very slow placement and improvement rates	Low
Deep Densification by Vibration	Blasting	Shock waves and vibrations cause liquefaction and displacement, with settlement to higher density	Clean sands (<15% passing No. 200 sieve)	>30m	Explosives, hole casing	Jetting or drilling machine	Relative densities to 70-80%; may get variable density; time-dependent strength gain	Rapid, inexpensive, can treat any size area; effective at large depth; variable properties; little improvement near surface; large ground vibrations	Low
	Vibratory Probe	Densification by vibration; liquefaction induced settlement to higher density	Clean sands (<15% passing No. 200 sieve)	20m (Ineffective near suface)	None	Vibratory pile driver, or rod probe	Relative densities of up to 80%. Ineffective in some sands	Rapid, simple, good underwater, soft underlayers may damp vibrations; difficult to penetrate stiff overlayers	Moderate
	Dynamic Compaction	Repeated application of high intensity impacts at surface	Cohesionless soils, waste fills	15m	None	Weights to more than 100 tons, high capacity crane with long boom	Can obtain good improvement and reasonable iniformity, improvement decreases with depth	Simple, rapid, suitable for some soils with fines; usable above and below water; economical for large areas; vibrations in adjacent structures	Low

Table 2.2 - Summary of Methods for Improvement of Hydraulic Fills (Sheet 2 of 2)

	Method	Principle	Most Suitable Hydraulic Fill Types	Maximum Effective Treatment Depth	Special Materials Required	Special Equipment Required	Properties of Treated Material	Special Advantages and Limitations	Relative Cost
Deep Densification and Reinforcement	Vibro-Compaction	Densification by vibration and compaction of backfill material	Clean sands (<15% passing No. 200 sieve)	30m	Granular backfill, water supply	Vibroflot, crane, pumps	High relative densities, good iniformity, increased k_o	Uniformity, control, high level improvement	Moderate
	Compaction Piles	Densification by displacement of pile volume and by vibration during driving	Clean sands, silty or clayey sand	>20m	Pile material (softer sand or soil plus cement mixture)	Pile driver, special sand pile equipment	High densities, good uniformity, piles act as reinforcement	Useful in soils with fines; uniform compaction; easy to check results; slow; limited improvement in upper 1-2m	Moderated to high
	Vibro-Replacement Stone and Sand Columns	Hole in soft, fine-grained soil backfilled with densely compacted gravel or sand	Soft silty or clayey sands, cohesive soils	20m	Gravel or crushed rock backfill	Vibroflot crane	Increases bearing good uniformity, piles act as reinforcement	Facter than precompression; sand pockets densified by vibration; drainage through columns; limited bearing capacity	Moderate to high
Precompression	Proloading	Load is applied sufficiently in advance of construction so that compression of soft soil is completed prior to development of the site	Cohesive soils	--	Earth fill or other material for loading the site; gravel drainage blanket, vertical drains	Earth moving equipment; vacuum drainage systems sometimes used; settlement markers peizmeters	Reduced water content and void ratio, increased strength	Easy, theory will developed uniformity; required long time (vertical drains can be used to reduce consolidation time)	Low (Moderate if vertical drains are required)
	Surcharge Fills	Fill in excess of that required permanently is applied to achieve a given amount of settlement in a shorter time; excess fill than removed	Cohesive soils	--	Earth fill or other material for loading the site; sand or gravel for drainage blanket	Earth moving equipment; settlement markers, piezometer, inclinometers	Reduced water content, void ratio and compressibility; increased strength	Faster than preloading without surcharge, theory well developed; extra material handling; can use vertical drains to reduce consolidation time	Moderate
	Electro-osmosis	DC current causes water flow from anode towards cathods where it is removed	Soft silts and silty clays	--	Anodes (usually rebars or alluminum), cathodes (well points or rebars)	DC power supply, wiring metering systems	Reduced water content and compressibility, increased strength, electrochemical hardening	No fill loading required, can use in confined area, relatively fast; non-uniform properties between electrodes, no good in highly conductive soils	High
	Seepage Consolidation	Seepage forces downward through hydraulic fill to underdrains cause consolidation	Soft clay and silt	a few m.	Underdrains beneath fill	Pumps	Recuded water content, compressibility and void ratio, increased strength	le properties no fill loading required, variable with depth, requires long time	Moderate

Table 2.3 - Costs of Some Ground Improvement Methods

METHOD	Based on Volume of Treated Ground ($/yd^3)	($/m^3)	Based on Length ($/ft)	($/m)
Dynamic Compaction	0.5-2	0.6-2.6		
Vibro-compaction	1-5	1.3-6.5	5-12	15-40
Vibro-replacement stone columns	3-9	3.9-11.8	10-16	30-50
Compaction Grouting	20-150	26-200		
Slurry Grouting	30-60	40-80		
Chemical Grouting	120-400	160-525		
Jet Grouting	100-300	130-400	25-100	80-330
Surface Compaction	2-5	2.5-6.5		
Remove and Replace	5-15	10-20		
Freezing	200-500	260-650		

Note : Data from Welsh, 1987.

Table 3.1 - Summary of the Stratigraphy for the Three Sites

Site	Depth(m)	Soil Type	Description
WEST KOWLOON (CS1)	0.0 to 25.0	Sand Fill	Loose to Medium dense greyish yellow and yellowish light grey segregated layers of fine to medium SAND with occasional shell fragments
	25.0 to 27.0	Disturbed Marine Deposit	Loose to very loose greyish dark green slightly silty clayey fine SAND with occasional fine shell fragments.
	27.0 to End of Hole	Marine Clay Deposit	Very soft, light grey sandy CLAY with occasional shell fragment.
TIN SHUI WAI (TSW)	0.0 to 6.0	Sand Fill	Loose to Medium dense, yellow, fine to coarse SAND with segregated layers of subangular to subrounded fine to coarse quartz gravel.
	6.0 to End of Hole	Pond Silty Deposit	Firm, yellowish grey, mottled black, slightly sandy clayey SILT with some subangular fine gravel and rootlets. Bad odour present.
TSEUNG KWAN O (TKO)	0.0 to 12.0	Sand Fill	Loose to Medium dense, yellow segregated layers of fine to medium SAND with occasional shell fragments.
	12.0 to End of Hole	Marine Clay Deposit	Firm, greenish grey CLAY with occasional shell fragments.

Table 4.1 - Summary of Basic Properties Test Result

	Site		
Test , unit	West Kowloon, CS	Tseung Kwan O, TKO	Tin Shui Wai, TSW
Maximum Dry Density, Mg/m^3	1.98	1.77	2.01
Minimum Dry Density, Mg/m^3	1.61	1.40	1.55
Specific Gravity	2.61	2.62	2.62
Compaction Test :			
Dry Density, g/cm^3	1.88	1.67	1.84
Optimum Moisture Content ,%	11.8	20.6	13.1
Permeability Test :			
Void Ratio, e	0.42 to 0.57	0.63 to 0.76	0.44 to 0.59
Coefficient of permeability, cm/s (T = 20 °C)	$6x10^{-3}$ to $2x10^{-2}$	$7x10^{-3}$ to $2x10^{-2}$	$6x10^{-2}$ to $2x10^{-1}$

Table 5.1 - Summaries of Stress-Strain and Strength Characteristics of West Kowloon Fill Sands with D_r around 35%

Consolidation Pressure, σ'_c (kPa)	Relative Density D_r (BS) (%)	$(\sigma'_1-\sigma'_3)_{max}$ (kPa)	$(\sigma'_1/\sigma'_3)_{max}$	$(\Delta u)_f$ (kPa)	$(\varepsilon_a)_f$ (%)	ϕ' (degree)	E_{30} (Mpa)
100	34.17	158#	3.94	44^	22.4*	35	1.1
200	34.41	360#	3.92	67^	20.5*	35	6.2
300	36.14	504#	3.78	109^	16.8*	35	8.2

Notes :
(1) #$(\sigma'_1-\sigma'_3)_{max.}$determined at the the point just before the termination of the test, which could be slightly underestimated because of the pre-mature termination of test.
(2) ^$(_{\Delta}u)_f$ determined at the point just before the termination of the test, which could be in slightly different with the actural$(_{\Delta}u)_f$ due to the pre-mature termination of test.
(3) *$(\varepsilon_v)_f$ could be underestimated due to pre-mature termination of test.

Table 5.2 - Summaries of Stress-Strain and Strength Characteristics of West Kowloon Fill Sands with D_r around 73%

Consolidation Pressure, σ'_c (kPa)	Relative Density D_r (BS) (%)	$(\sigma'_1-\sigma'_3)_{max}$ (kPa)	$(\sigma'_1/\sigma'_3)_{max}$	$(\Delta u)_f$ (kPa)	$(\varepsilon_a)_f$ (%)	ϕ' (degree)	E_{30} (Mpa)
100	73.69	1193	4.99	-196	5.2	40	33.6
200	72.30	1473	4.71	-195	6.4	40	42.8
300	73.42	1764	4.63	-189	7.4	40	47.7

Table 5.3 - Summary of Static Tests of Site TKO (Tseung Kwan O)

Test No.	D_s (Mg/m^3)	D_r (BS) (%)	σ'_c (kPa)	File name	Friction angle ϕ'
1	1.517	36.98	100	TKS4	35.3°
2	1.518	37.19	200	TKSP1	
3	1.513	35.64	300	TKS5	
4	1.642	70.41	100	TKS7	37.8°
5	1.631	67.68	200	TKS8P2	
6	1.631	67.75	300	TKS6	

Table 5.4 - Summary of Static Tests of Site TSW (Tin Shui Wai)

Test No.	D_S (Mg/m^3)	D_r (BS) (%)	σ'_c (kPa)	File name	Friction angle ϕ'
1	1.693	36.91	100	TWS1	35.3^o
2	1.704	39.49	200	TWS5	
3	1.704	39.49	300	TWS7	
4	1.837	68.27	100	TWS2	39.6^o
5	1.843	69.47	200	TWS3	
6	1.840	68.91	300	TWS8	

Table 5.5 - Summary of Dynamic Tests for West Kowloon Site

Test Number	Relative Density D_T (BS) (%)	Stress Ratio	Initial Liquefaction (no. of cycles)
1	44.10	0.237	0.7
2	39.90	0.100	25
3	41.77	0.150	5
4	42.47	0.122	13
5	62.25	0.205	5
6	55.08	0.152	13
7	70.58	0.130	42
8	63.54	0.110	85
9	79.67	0.177	28
10	20.55	0.057	310
11	11.51	0.093	50
12	12.03	0.130	21
13	17.20	0.182	1.7
14	42.31	0.073	114
15	51.38	0.148	8
16	43.50	0.218	2
17	44.35	0.118	16
18	73.98	0.205	8
19	71.33	0.150	37
20	71.92	0.130	40
21	71.58	0.133	45
22	74.44	0.108	124
23	71.16	0.177	20
24	37.49	0.095	18
25	61.41	0.150	42
26	34.56	0.130	7
27	34.83	0.150	5
28	35.31	0.077	65
29	65.78	0.133	20
30	68.75	0.130	20

Notes : (1) One second period.
(2) Effective consolidation pressure at 150 kPa.
(3) Maximum dry density 1.98 Mg/m^3.
(4) Minimum dry density 1.61 Mg/m^3.

Table 5.6 - Summary of Dynamic Tests of Site TKO (Tseung Kwan O)

Test No.	D_s (Mg/m³)	D_r (BS) (%)	Stress Ratio	Initial Liquefaction (no. of cycles)
1	1.635	68.76	0.207	5
2	1.635	68.78	0.188	6
3	1.616	64.04	0.140	18
4	1.642	70.50	0.122	62
5	1.643	70.68	0.118	63
6	1.626	66.36	0.090	168
7	1.580	54.61	0.190	3
8	1.574	52.94	0.143	12
9	1.582	54.92	0.110	28
10	1.582	54.95	0.090	86
11	1.520	37.80	0.167	3
12	1.515	36.20	0.138	7
13	1.506	33.67	0.090	26
14	1.514	35.93	0.070	93

Note : All tests were conducted at back pressure 100kPa and effective confining pressure 150kPa.

Table 5.7 - Summary of Dynamic Tests of Site TSW (Tin Shui Wai)

Test No.	D_s (Mg/m³)	D_r (BS) (%)	Stress Ratio	Initial Liquefaction (no. of cycles)
1	1.827	66.25	0.300	6
2	1.844	69.67	0.296	6
3	1.841	69.07	0.292	8
4	1.824	65.64	0.265	9
5	1.840	68.87	0.245	12
6	1.843	69.47	0.245	11
7	1.830	66.85	0.192	38
8	1.837	68.35	0.138	904
9	1.765	53.23	0.250	4
10	1.761	52.36	0.190	11
11	1.754	50.82	0.143	37
12	1.762	52.57	0.120	115
13	1.697	37.83	0.185	4
14	1.705	39.72	0.168	8
15	1.699	38.52	0.140	13
16	1.690	36.20	0.115	31
17	1.708	40.42	0.110	43
18	1.699	38.47	0.092	102

Note : All tests were conducted at back pressure 100kPa and effective confining pressure 150kPa.

Table 5.8 - Details of Dynamic Triaxial Tests on 'Undisturbed Samples' of West Kowloon, CS1

							Dry Density (Bulk Density in Mazier) (Mg / m^3)			Stress Ratio Number of cycles (Initial Liquefaction)		
Sample No.	Depth (m)	q_c (MPa) 10 cm^2	15 cm^2	D_{min} (Mg/m^3)	*D_r (BS) (%)	Void Ratio, e	Group A (Air-pluviated)		Group U (Undisturbed)		Group M (Moist-tamped)	
1	13.75	7.5	8			0.711			1.5250	0.150		
									(2.001)	1600		
2	7.79	27	26	1.449	56	0.595	1.6370	0.20	1.6368	0.200	1.6346	0.207
								6	(1.927)	50		1692
3	7.63	30	33			0.555			1.6788	0.25	1.6254	0.255
									(1.945)	15		970
4	10.76	15	10			0.528			1.7080	0.18		
									(2.041)	1014		
5	3.03	24	16	1.250	86	0.676	1.4578	0.280	1.5574	0.265		
								1.1	(1.977)	13		
6	4.95	20	24	1.346	65	0.667			1.5659	0.172		
									(1.902)	107		
7	6.34	25	25	1.481	57	0.562			1.6706	0.215		
									(1.969)	9		
8	9.45	23	22.5	1.347	74	0.631			1.6005	0.233		
									(1.934)	5		
9	9.28	26	25	1.361	71	0.629			1.6020	0.16		
									(1.933)	121		

Legend :

* The relative density (D_r) is calculated by assuming the maximum dry density equal to 0.37 plus minimum dry density (i.e. Assume the range between maximum dry density and minimum dry density for all 'undisturbed samples' is equal to which is found from material used in analysis)

Table 6.1 - Result of Different Input Motions by Different Scaling Factors

scaling factor	1.00	0.90	0.75	0.60	0.45
depth (m)	Peak Value of (1 - p' / p_o') in %				
5.5	5.1	4.8	4.4	4.7	4.7
6.5	22.9	178	14.7	13.0	11.5
7.5	41.8	29.5	22.4	19.6	16.8
8.5	48.8	36.7	26.5	23.1	20.0
9.5	52.3	39.4	27.8	23.9	20.9
10.5	51.6	38.4	26.2	22.8	19.8
settlement *	1.39 cm	1.22 cm	1.00 cm	0.79 cm	0.55 cm
max. acc. (g) ▲	0.130	0.117	0.103	0.089	0.071

Legend :

* Settlement at the end of earthquake

▲ Maximum ground acceleration

Table 6.2 - Effect of Permeability of Hydraulic Fill Layer

k (m/s)	5.0×10^{-5}	1.0×10^{-4}	2.0×10^{-4}	3.0×10^{-4}
depth (m)	Peak Value of (1 - p' / p_o') in %			
5.50	6.0	4.7	3.2	2.2
6.50	15.4	11.5	8.4	6.5
7.50	22.2	16.8	11.8	9.5
8.50	25.3	20.0	13.8	10.9
9.50	25.9	20.9	14.6	11.4
10.50	24.6	19.8	13.8	10.7
settlement	0.48 cm	0.55 cm	0.60 cm	0.64 cm
Note : Settlement at the end of the earthquake.				

Table 6.3 - Effect of Thickness of Sea Mud Layer

thickness of sea mud (m)	0	3.9	6.5	9.3	12.1
depth (m)	Peak Value of (1 - p' / p_o') in %				
5.5	4.4	4.5	4.7	4.6	4.3
6.5	11.1	11.4	11.5	11.3	11.0
7.5	16.7	16.8	16.8	16.5	16.0
8.5	19.7	20.0	20.0	19.6	19.1
9.5	20.6	20.8	20.9	20.5	20.0
10.5	19.6	19.8	19.8	19.5	19.9
settlement	0.52 cm	0.54 cm	0.55 cm	0.53 cm	0.54 cm

Notes : (1) Settlement denotes the ground settlement at end of the earthquake.
(2) The change in thickness of sea mud layer is compensated by the thickness of the alluvium to keep a constant total thickness of the column.

Table 6.4 - Volumetric Strain with Different Cyclic Shear Strain

Cyclic Shear Strain γ_{xy}, %	Volumetric Strain ε_v, %					
	σ_{vc} = 2000 lb/ft^2 Overburden Stress		σ_{vc} = 4000 lb/ft^2 Overburden Stress		σ_{vc} = 3133 lb/ft^2 ($\cong$ 150 kPa)	
	N = 10	N = 50	N = 10	N = 50	N = 10	N = 50
0.06	0.138	0.406	0.207	0.366	0.177	0.389
0.05	0.094	0.310	0.168	0.302	0.136	0.307
0.04	0.063	0.210	0.122	0.220	0.096	0.216
0.03	0.031	0.110	0.086	0.143	0.062	0.129
0.02	0	0.044	0.037	0.061	0.021	0.054

Note : Data from Silver & Seed, 1971.

Table 6.5 - Transformation from Cyclic Shear Strain of Cyclic Simple Shear Test to Deviator Stress of Cyclic Triaxial Tests by Equation (6.3)

Cyclic Shear Strain γ_{xy}, %	Shear Modulus G, MPa	Deviator Stress σ_{dp}, kPa					
		C_r = 0.61	C_r = 0.62	C_r = 0.63	C_r = 0.64	C_r = 0.65	C_r = 0.66
0.06	33.16	55.11	54.34	53.59	52.86	52.15	51.46
0.05	35.32	49.68	48.97	48.29	47.63	46.98	46.35
0.04	37.58	43.09	42.48	41.88	41.29	40.72	40.17
0.03	39.74	35.00	34.49	34.00	33.51	33.04	32.59
0.02	41.87	35.32	24.94	24.57	24.21	23.87	23.53

Table 7.1 - Summary of ENEL Calibration Chamber Test Results (Sheet 1 of 3)

A. CS1 SAND (BC1)						
Test Number (ENEL)		**Density (kN/m^3)**	**D_r (ASTM) (%)**	**σ_v' (kPa)**	**q_c (MPa)**	**q_{cff} (MPa)**
437i	**a**	16.85	58.9	106.1	6.07	6.98
	b	16.89	60.1	204.0	10.50	12.08
438i	**a**	16.86	59.1	36.0	2.95	3.39
	b	16.90	60.6	70.8	4.89	5.62
440i	**a**	16.83	58.0	36.6	2.32	2.67
	b	16.87	59.5	70.4	3.45	3.97
442i	**a**	16.75	54.7	205.9	6.85	7.88
	b	16.78	55.9	300.7	9.88	11.36
443i	**a**	16.17	31.7	51.8	1.34	1.54
	b	16.22	33.7	101.1	2.66	3.06
444i	**a**	16.19	32.5	198.8	5.44	6.26
	b	16.24	34.5	301.0	7.73	8.89
453i	**a**	17.41	79.0	100.9	7.68	8.83
	b	17.46	80.8	301.0	16.91	19.45
455i	**a**	16.66	51.4	50.7	1.77	2.04
	b	16.70	53.1	100.7	3.71	4.27
456i	**a**	17.09	67.6	99.3	4.85	5.58
	b	17.10	67.9	299.8	12.07	13.88

Table 7.1 - Summary of ENEL Calibration Chamber Test Results (Sheet 2 of 3)

B. TKO SAND (BC1)						
Test Number (ENEL)		**Density (kN/m^3)**	**D_r (ASTM) (%)**	**σ_v' (kPa)**	**q_c (MPa)**	**q_{cff} (MPa)**
439i	**a**	15.27	62.0	103.9	8.08	9.29
	b	15.31	63.2	200.0	12.14	13.96
441i	**a**	15.04	54.7	51.0	3.61	4.15
	b	15.11	56.9	203.9	8.99	10.34
445i	**a**	14.07	22.0	50.9	1.56	1.79
	b	14.10	23.1	102.3	2.38	2.74
450i	**a**	14.38	33.1	199.8	5.38	6.19
	b	14.40	33.8	250.6	5.79	6.66

Table 7.1 - Summary of ENEL Calibration Chamber Test Results (Sheet 3 of 3)

C. TSW SAND (BC1)						
Test Number (ENEL)		**Density (kN/m^3)**	**D_r (ASTM) (%)**	**σ_v' (kPa)**	**q_c (MPa)**	**q_{cff} (MPa)**
447i	a	16.44	35.7	56.5	2.54	2.92
	b	16.48	37.0	154.6	6.73	7.74
449i	a	17.58	71.7	49.0	6.16	7.08
	b	17.60	72.3	150.4	12.20	14.03
452i	a	17.09	56.9	52.2	4.40	5.06
	b	17.14	58.2	152.2	8.93	10.27
454i	a	17.43	67.3	49.9	6.15	7.07
	b	17.47	68.4	149.0	11.54	13.27

Table 7.2 - Properties of the Sands Used in the Calibration Chamber Tests

SAND	$\gamma_{d,min}$	$\gamma_{d,max}$	G_S	e_{min}	e_{max}	C_u	D_{50} (mm)	D_{10} (mm)
H	14.28	17.25	2.724	0.5485	0.8706	1.91	0.45	0.21
M0	14.03	16.60	2.650	0.57	0.86	1.60	0.37	0.25
T1	13.64	16.73	2.685	0.5738	0.9306	-	0.58	0.36
T2	13.64	16.73	2.685	0.5738	0.9306	-	0.58	0.36
T4	13.64	16.67	2.677	0.5747	0.9245	1.50	0.54	0.36
T9	13.64	16.40	2.684	0.6048	0.9296	1.35	0.55	0.36
Y	13.09	16.13	2.65	0.6111	0.9852	1.27	0.23	-

Legend :

H	Hokksund	Y	Toyoura Sand
M0	Monterey No. 0	T	Ticino Sand

Notes : (1) Maximum and minimum dry densities were determined by ASTM method.
(2) All sands for Calibration Chamber Tests were passed sieve at 4.75mm.
(3) Data after LoPresti (1987), Crippa, Lopresti & Pedroni (1992), Drnevich et al (1984), and Verdugo & Ishihara (1992). Maximum density obtained using ASTM D4253-83 for Monterey No. 0 sand and by pluviation (Miura & Toki, 1982) for all others; minimum density, by ASTM D4254-83 (from Rodrigues, 1993).

Table 7.3 - Properties of the Hong Kong Hydraulic Fill Sands Used in the Calibration Chamber Tests

SAND	γ_d, min (kN/m^3)	γ_d, max (kN/m^3)	G_S	C_u	D_{50} (mm)	D_{10} (mm)
CS1	15.43	18.02	2.654	4.9	0.73	0.21
TKO	13.48	16.63	2.662	2.1	0.30	0.18
TSW	15.45	18.59	2.649	5.8	1.19	0.26

Notes : (1) Maximum and minimum dry densities were determined by ASTM method.
(2) All sands for Calibration Chamber Tests were passed sieve at 4.75mm.

Table 7.4 - Summary of the Computer Predicted Cone Penetration Resistance Values for CS1 Sand

Actual chamber test data					Predicted values		Corrected for free field
Test	D_r (%)	σ'_v (kPa)	σ'_h (kPa)	q_c (kPa)	q_{cp} (kPa)	q_{cp}/q_{cpff}	$q_{eff} = \frac{q_{cpff}}{q_{cp}} \times q_c$ (kPa)
1	67.6	99.3	62.1	4850.6	5929.6	0.878	5524.6
2	67.9	299.8	186.3	12066.0	12898.8	0.894	13496.6
3	51.4	50.7	33.2	1773.1	3263.3	0.878	2019.5
4	53.1	100.7	61.8	3709.5	5183.7	0.908	4085.4
5	58.9	106.1	65.6	6073.0	5712.0	0.886	6854.4
6	60.1	204.0	135.0	10496.5	9543.0	0.891	11780.6
7	59.1	36.0	20.1	2952.4	2680.8	0.789	3742.0
8	60.6	70.8	38.8	4886.4	4460.2	0.860	5681.9
9	58.0	36.6	20.6	2314.7	2691.1	0.794	2915.2
10	59.5	70.4	39.1	3450.8	4432.8	0.861	4007.9
11	54.7	205.9	118.9	6847.9	7728.6	0.912	7508.7
12	55.9	300.7	172.1	9882.3	10707.0	0.918	10765.0
13	31.7	51.8	33.5	1338.3	2269.7	0.925	1446.8
14	33.7	101.1	65.9	2659.7	4007.4	0.945	2814.5
15	32.5	198.8	113.0	5438.2	5691.2	0.952	5712.4
16	34.5	301.0	171.7	7726.5	8149.4	0.954	8099.1
17	79.0	100.9	63.1	7682.9	6730.4	0.848	9060.0
18	80.8	301.0	184.7	16907.2	14311.2	0.864	19568.5

Table 7.5 - Comparison of Minimum and Maximum Dry Densities Determined by ASTM Method $_{u.c.}$ BS Method

SAND	ASTM		BS	
	γ_d, min (kN/m^3)	γ_d, max (kN/m^3)	γ_d, min (kN/m^3)	γ_d, max (kN/m^3)
CS1	15.43	18.02	15.78	19.40
TKO	13.48	16.63	13.72	17.35
TSW	15.45	18.59	15.19	19.70

LIST OF FIGURES

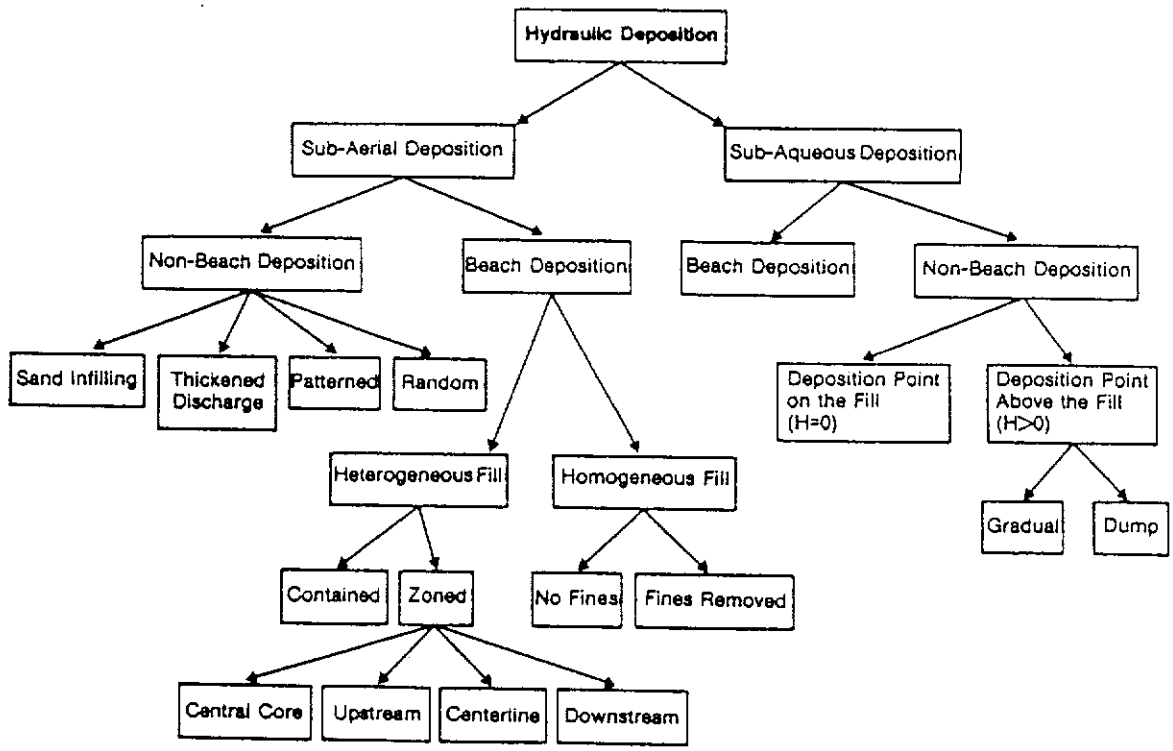

Figure 2.1 - Classification of Hydraulic Deposition (from Morgenstern & Kupper, 1988)

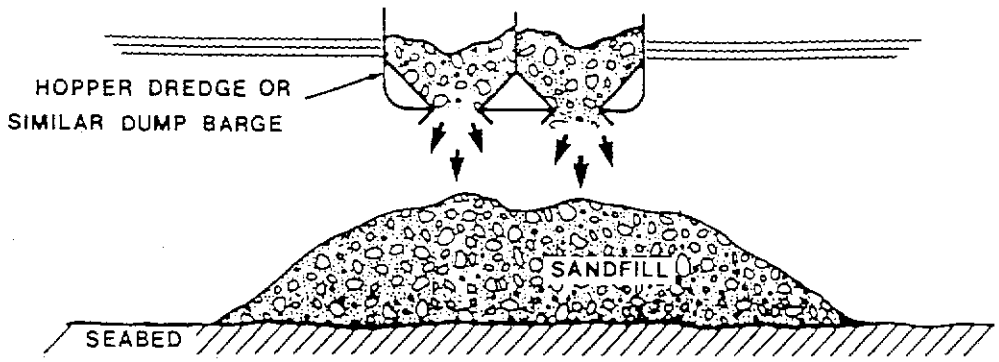

(a) Hopper or Dump-barge-placed Dredged Fill (Bottom Dumping)

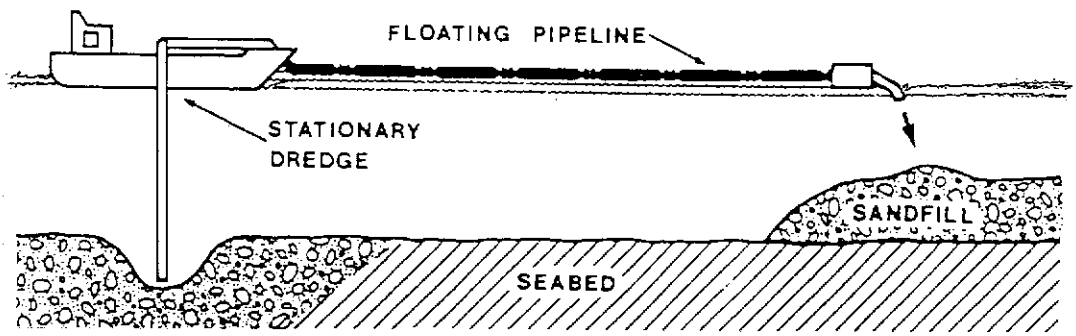

(b) Pipeline-placed Dredged Fill (Pipeline Placement)

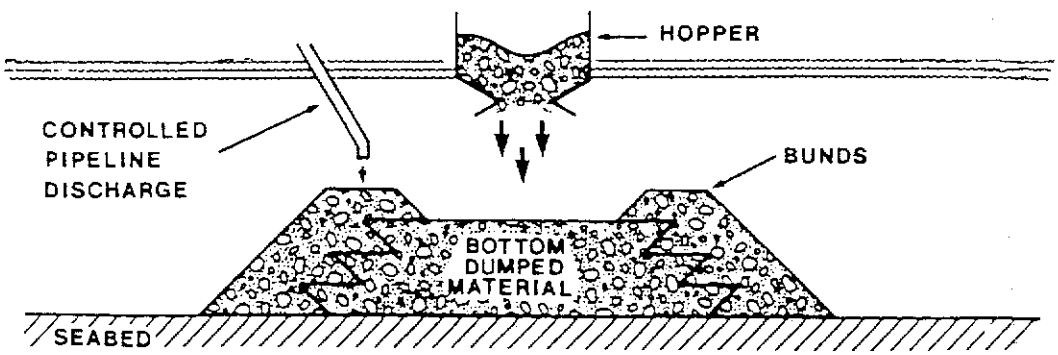

(c) Bund Construction Method

Figure 2.2 - Schematic Illustration of Hydraulic Placement Methods for Sand (after Sladen & Hewitt, 1989)

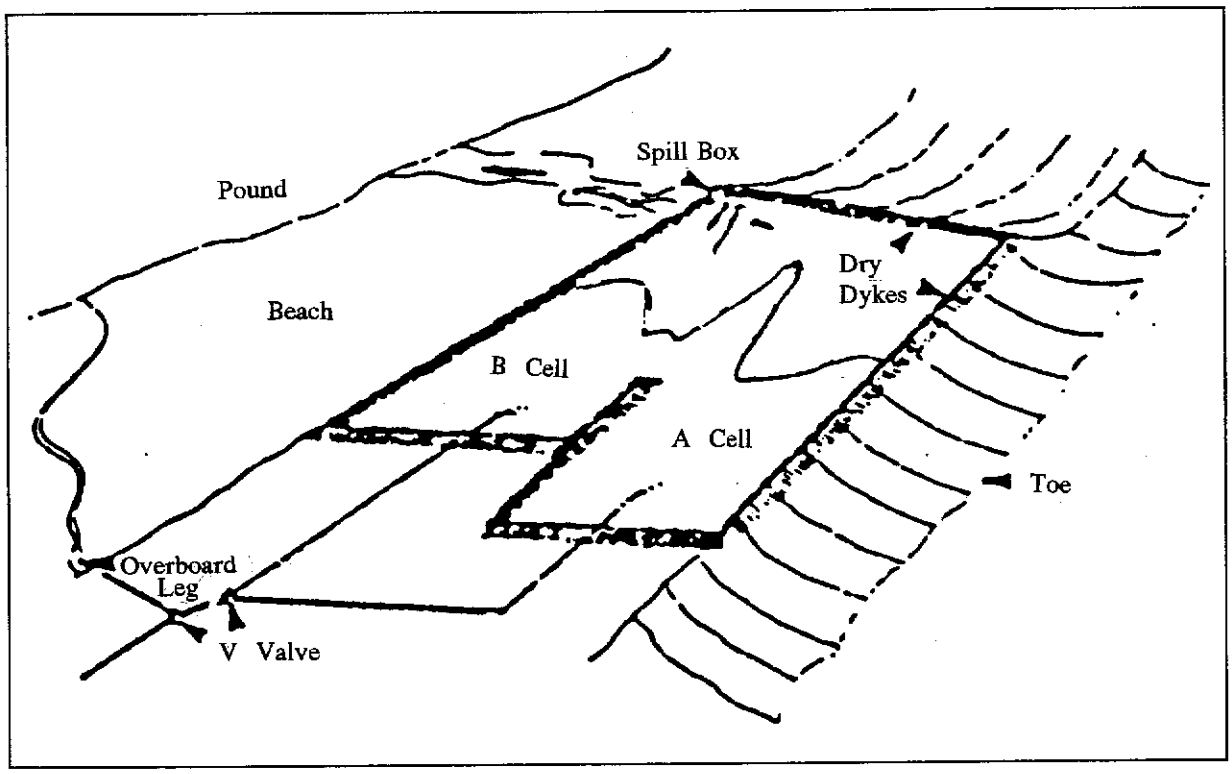

Figure 2.3 - Schematic Illustration of Cell Construction (Patterned) and Subaerial and Subaqueous Beach Construction Methods (from Yano & Fair, 1988)

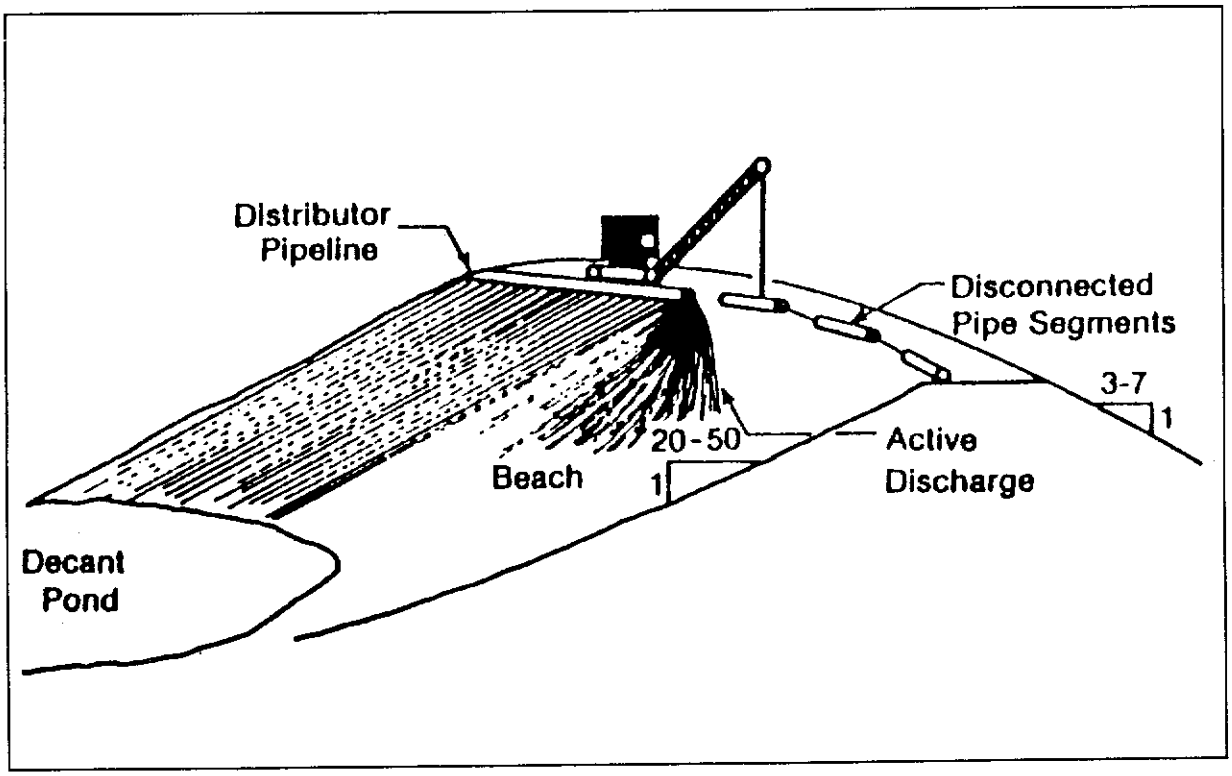

Figure 2.4 - Fill Placement by Pipeline and Single Point Discharge (after Morgenstern & Kupper, 1988)

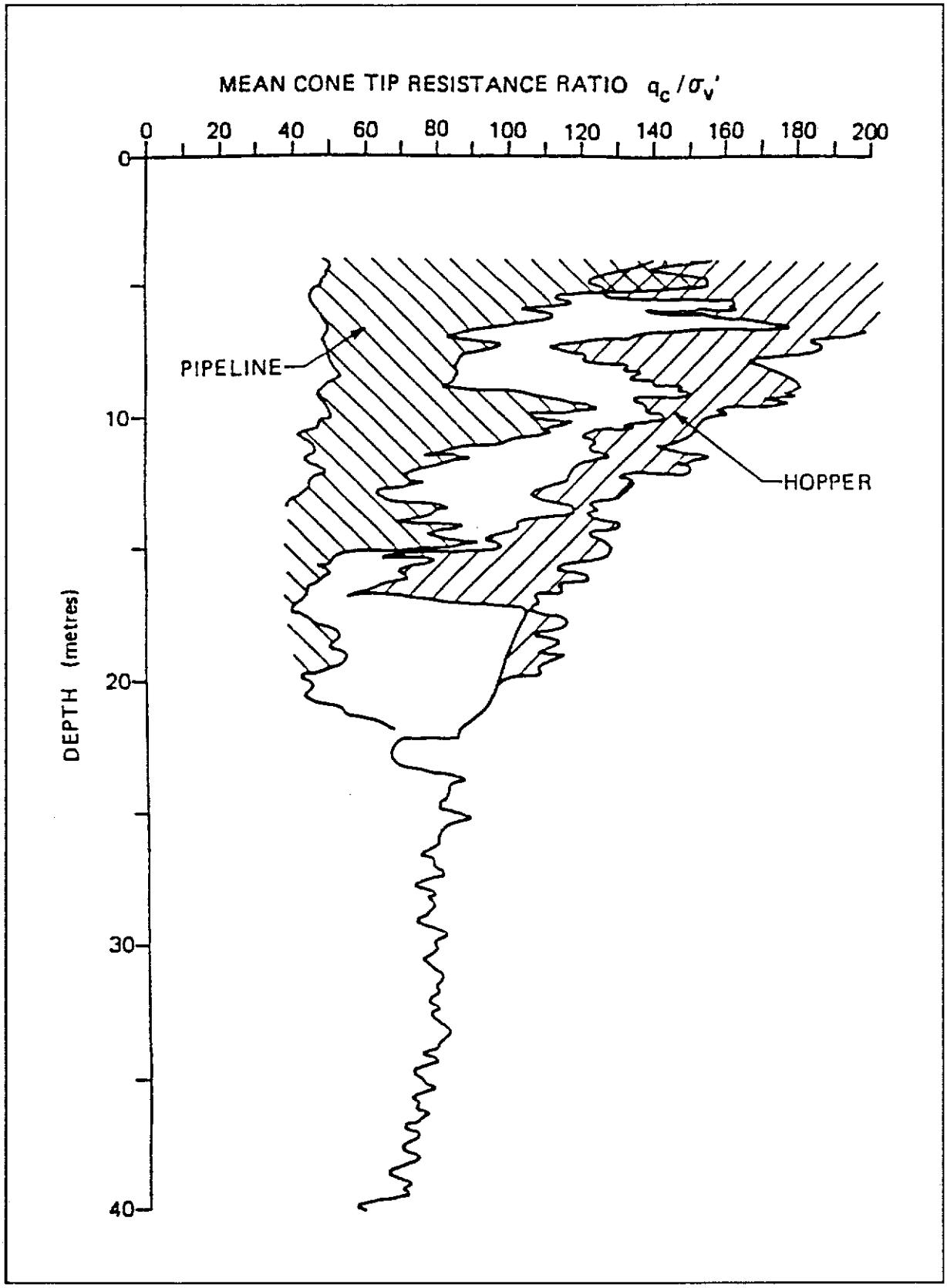

Figure 2.5 - Range of Mean Tip Resistance Normalized by Effective Overburden Pressure for Hopper Placed Sands Compared to Pipeline Placed Sands (after Sladen, 1990)

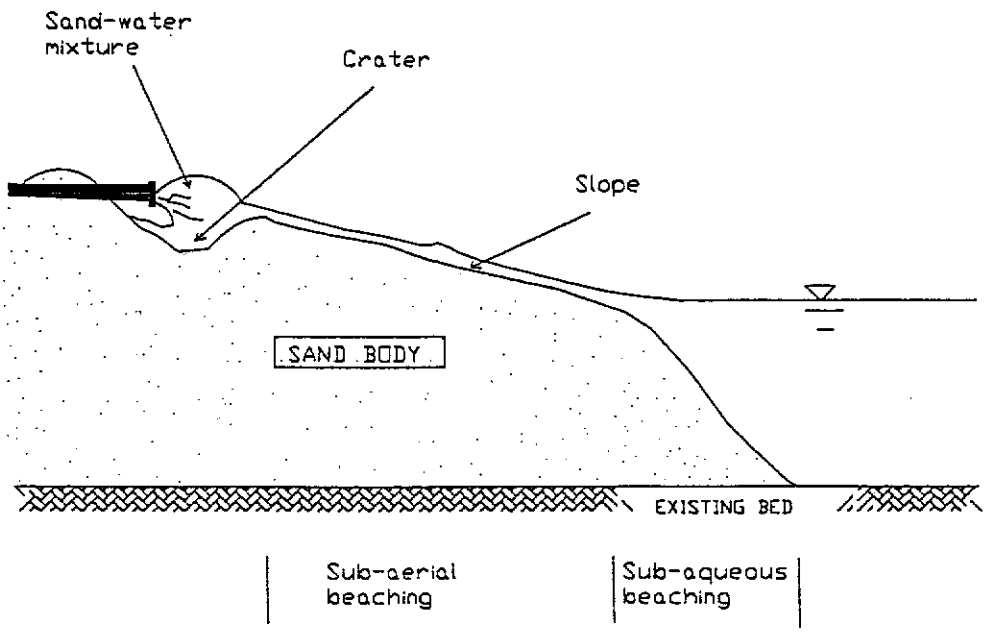

Figure 2.6 - Construction Method (Longitudinal Profile)

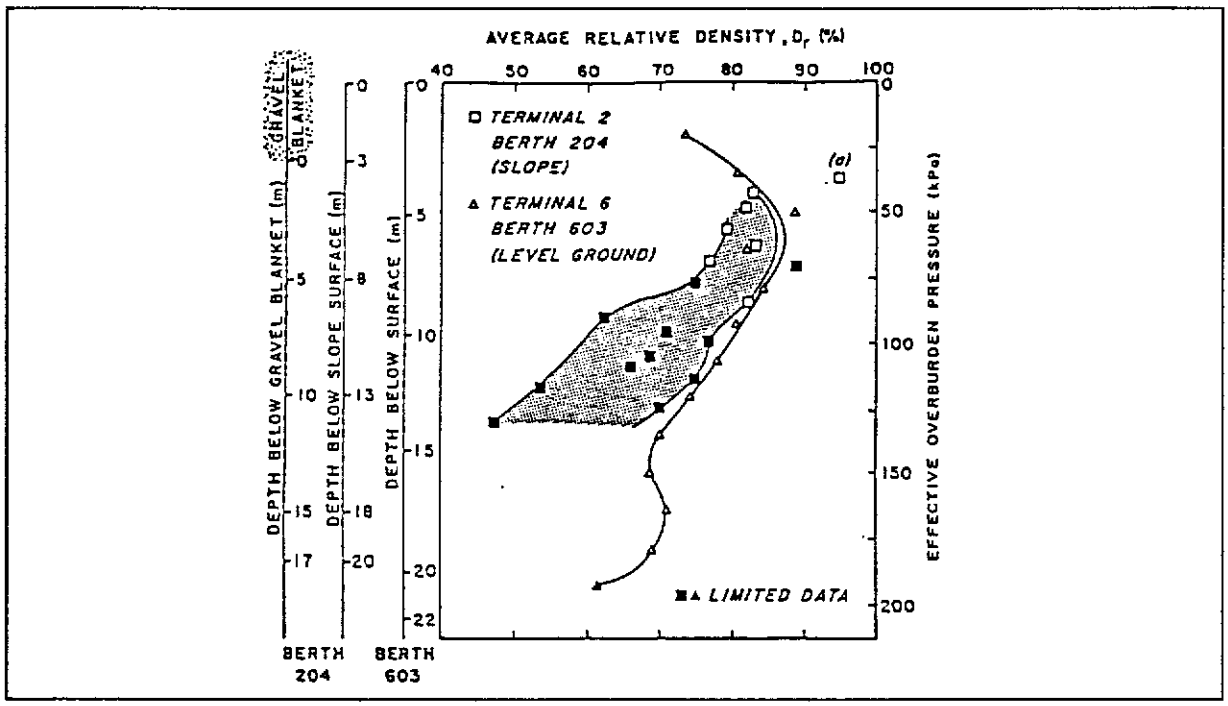

Figure 2.7 - Relative Density Distribution as a Function of Effective Overburden Pressure and Depth after Densification of a Clean Sand Hydraulic Fill by Vibratory Probe Compaction (from Leycure & Schroeder, 1987)

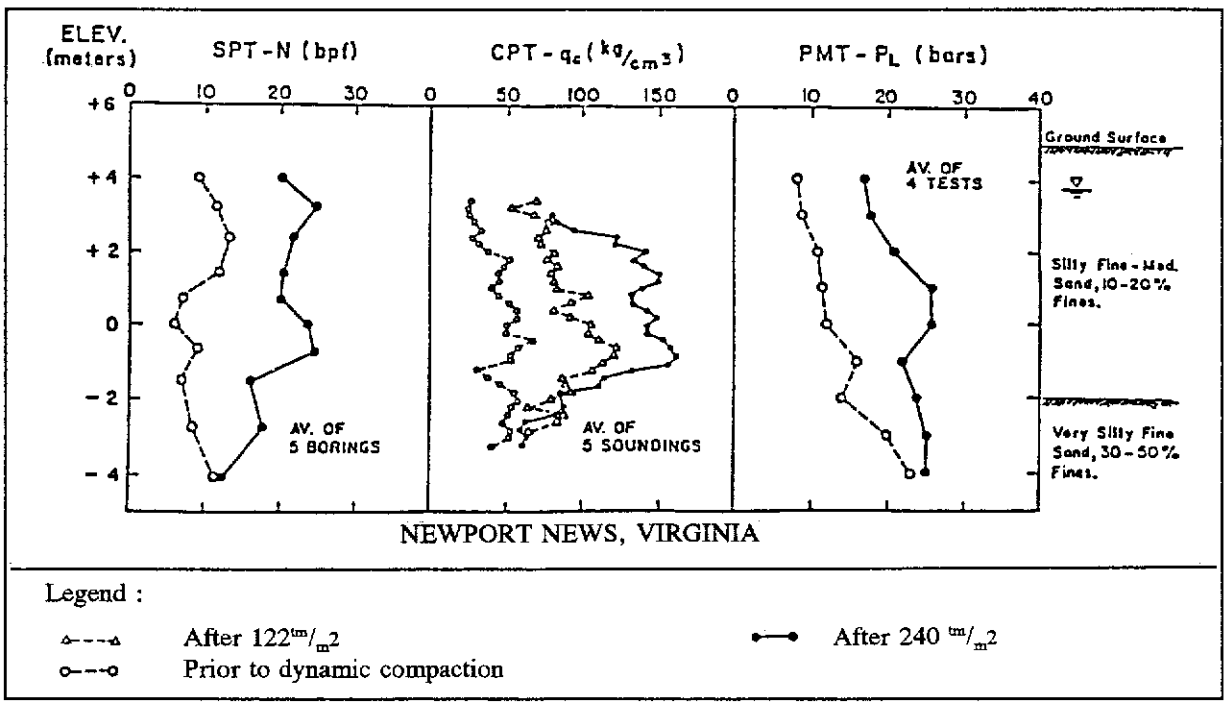

Figure 2.8 - Variation of CPT Resistance, SPT Resistance, and Pressuremeter Limit Pressure with Depth after Densification by Dynamic Compaction (from Mayne et al , 1984)

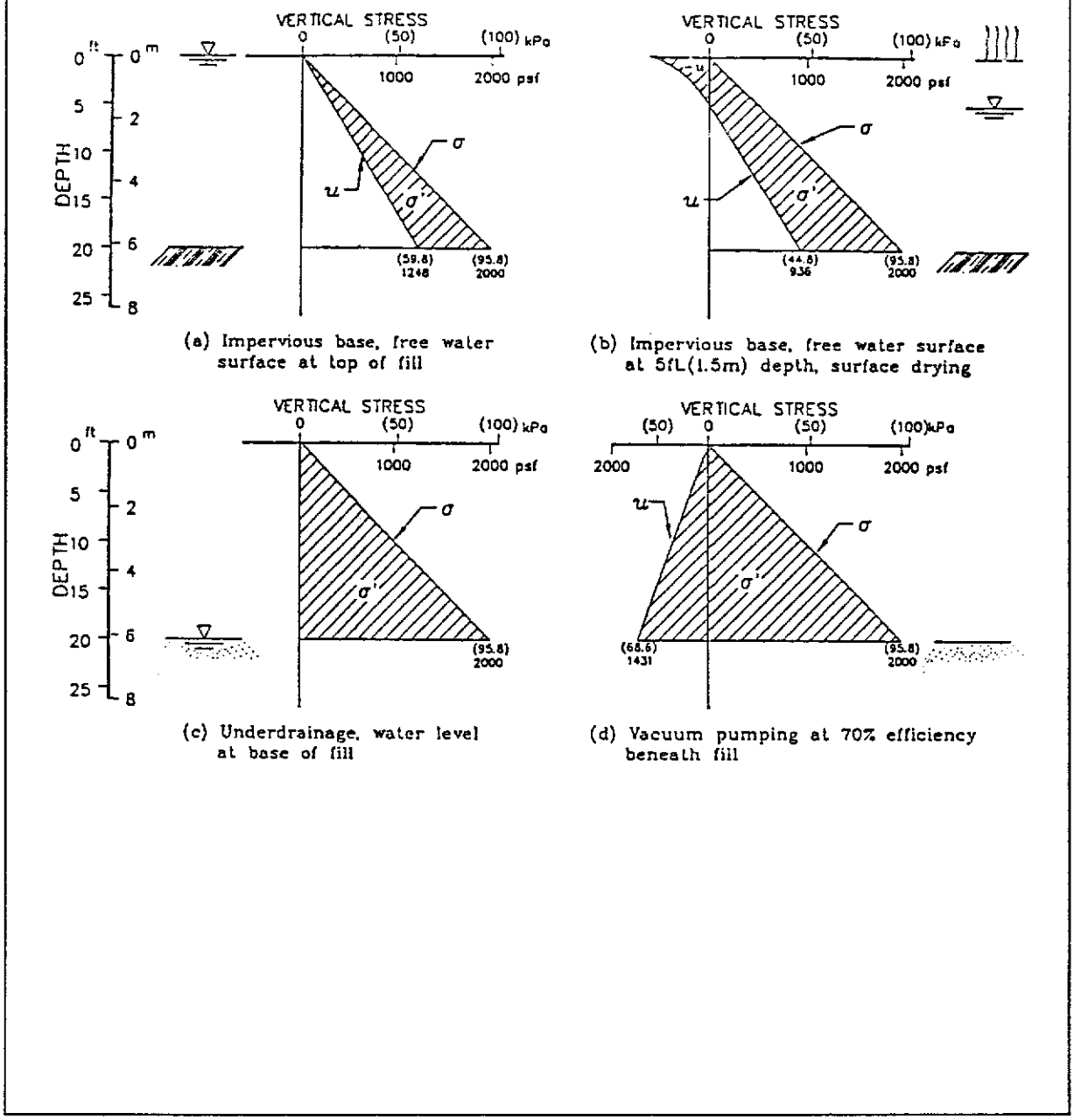

Figure 2.9 - Vertical Stress Profile at the End of Consolidation for Different Drainage Condition in a Fine-grained Hydraulic Fill. Total Unit Weight of Fill is 100 pcf (15 kN/m^3)(after Johnson et al , 1977)

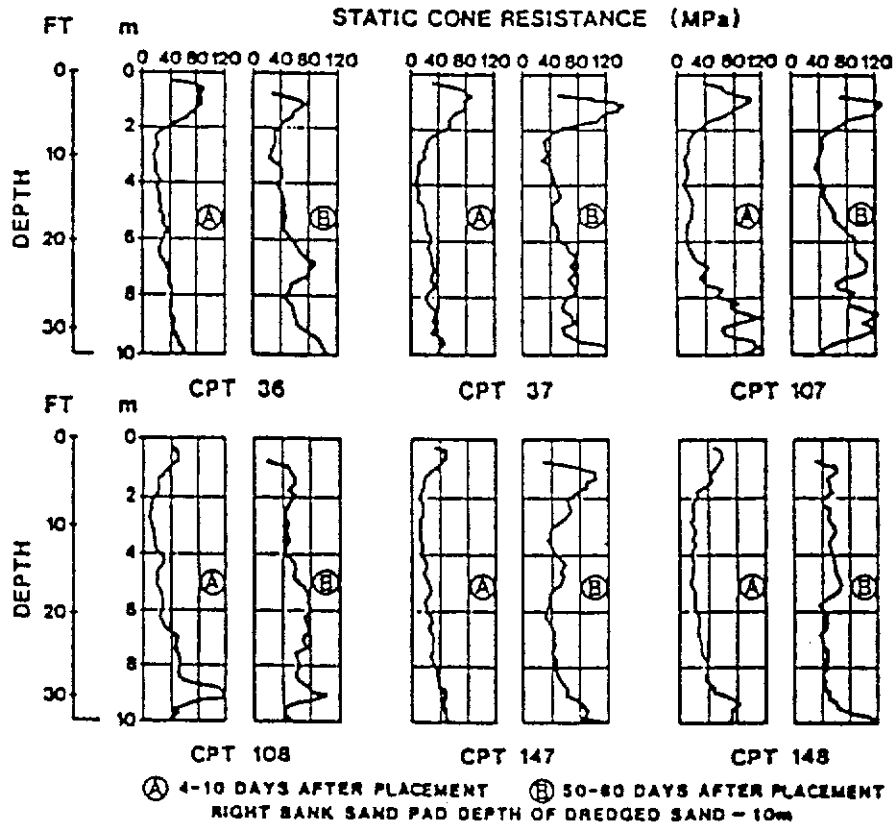

Figure 2.10 - Effect of Time on the Cone Penetration Resistance of Hydraulic Fill at the Jebba Dam

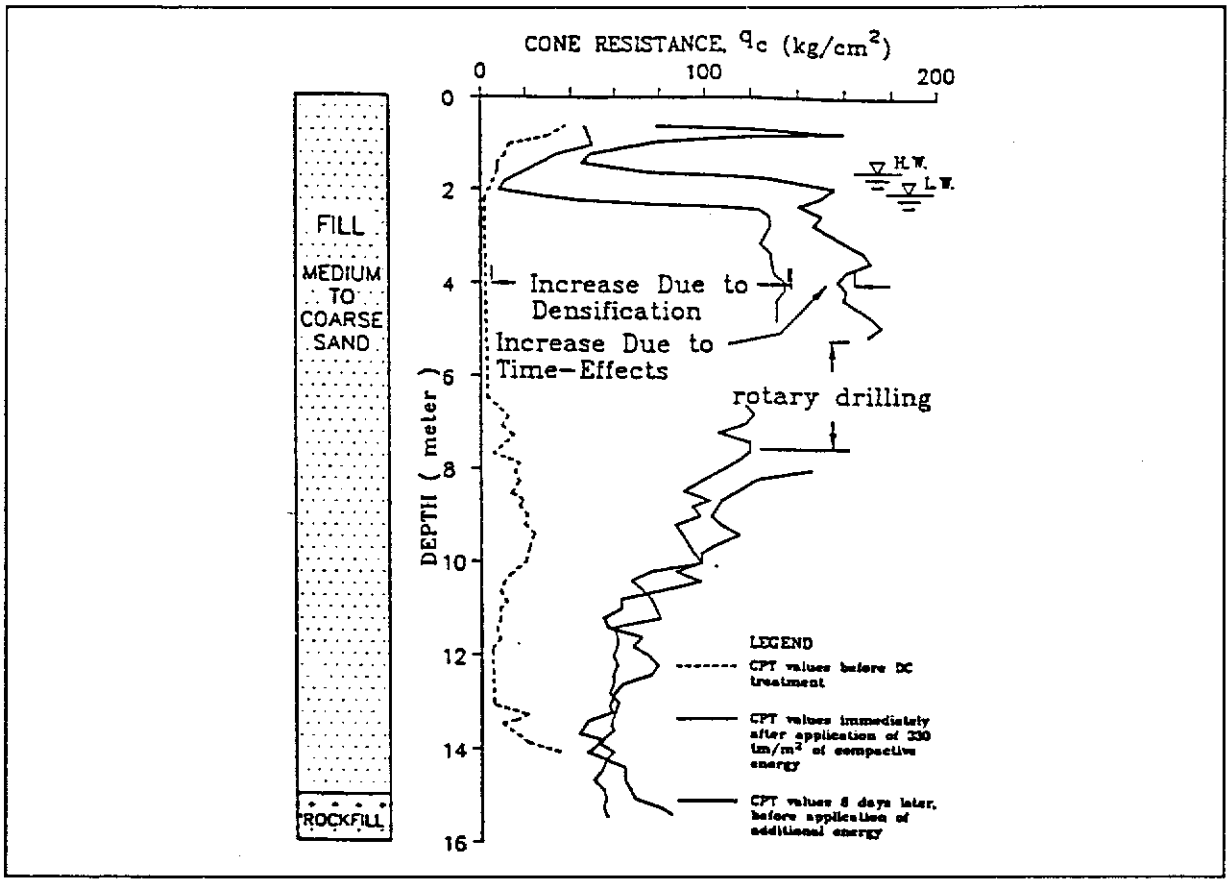

Figure 2.11 - Results of CPT Testing at Impact Point No. 40-34 at New Harbour Facility of Port Canada, Pointe Norie, Sept-Iles, Quebec Showing Strength Gain from Dynamic Compaction and Time Effects
(Redrawn from Dumas & Beaton, 1988)

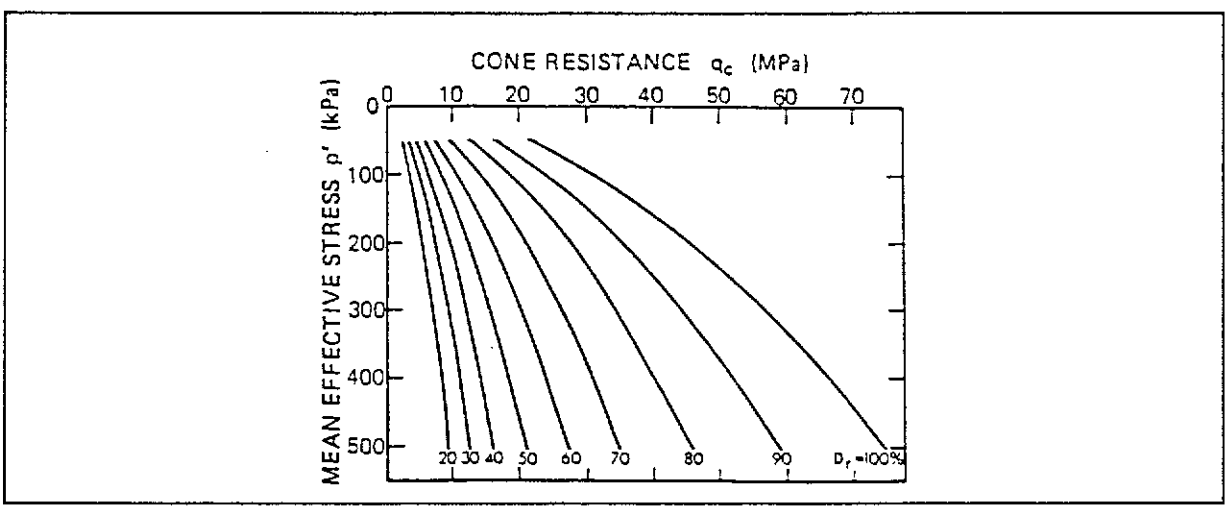

Figure 2.12 - The Relationship between Relative Density and Mean Effective Stress Measured in Large-scale Chamber Tests for Ticino Sand
(after Baldi et al, 1986)

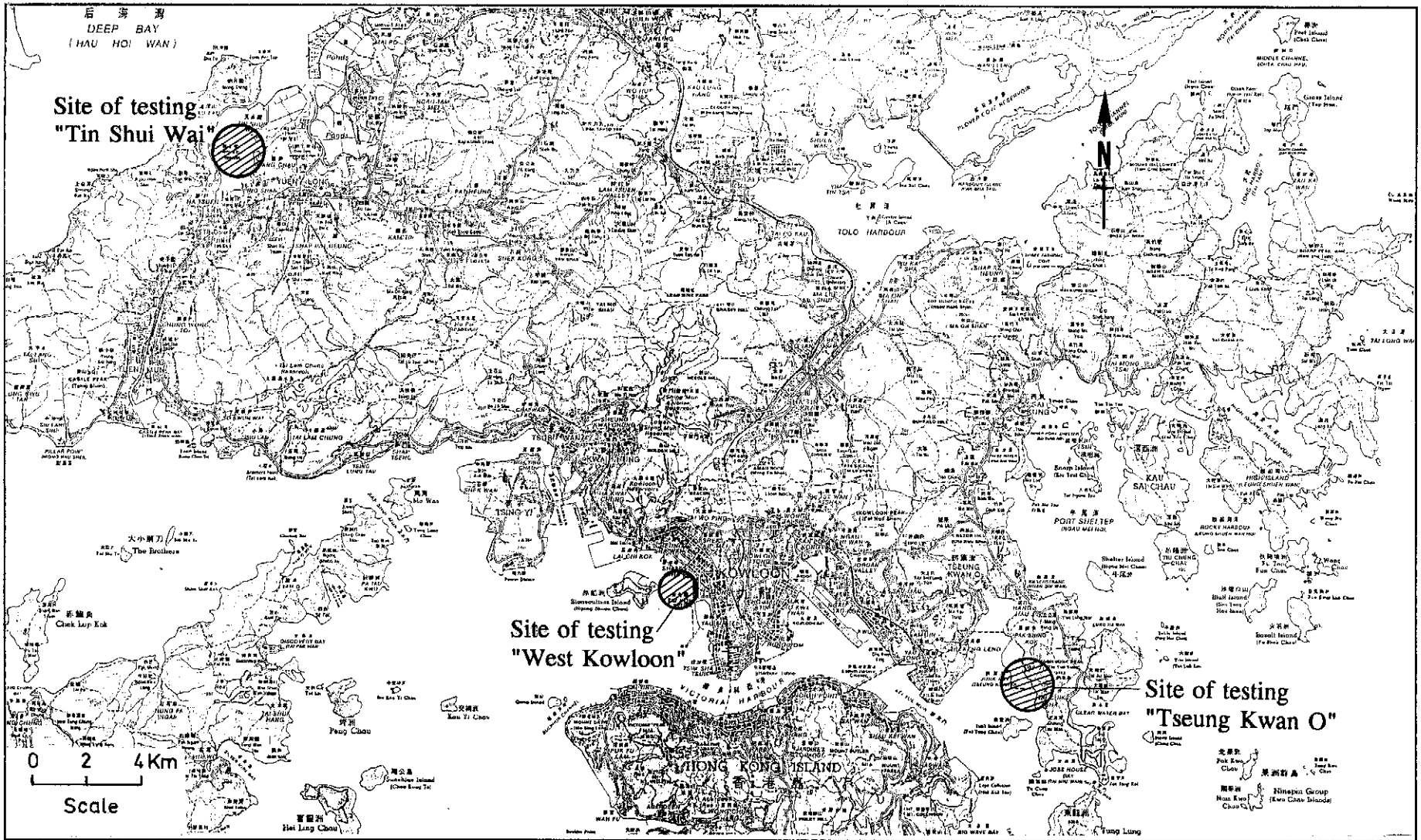

Note : Hydraulic Fill Study - Works Order No.33.126.

Figure 3.1 - Key Plan Showing Sites of Investigation

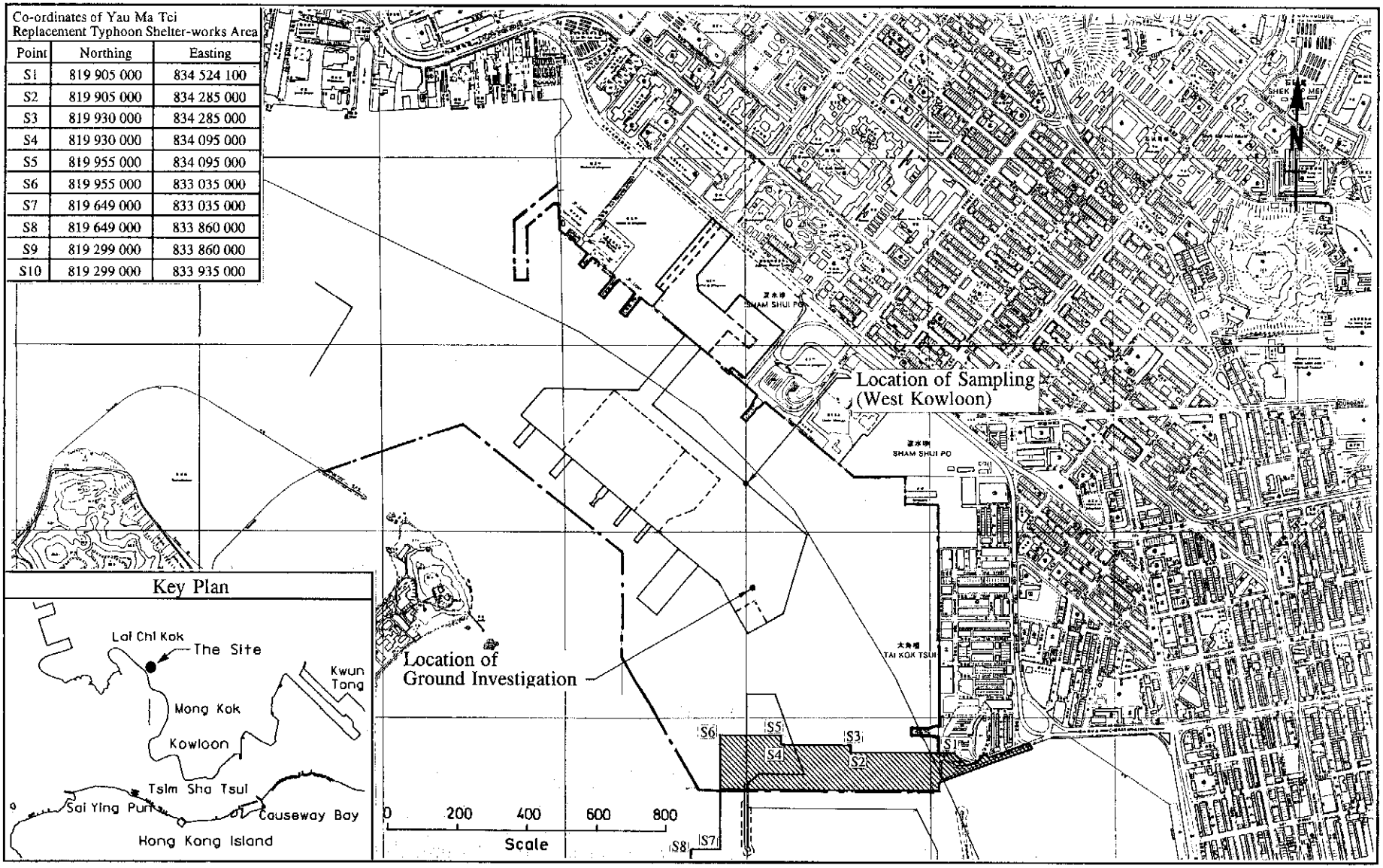

Figure 3.2 - Site Location Plan (West Kowloon Reclamation, North Section)

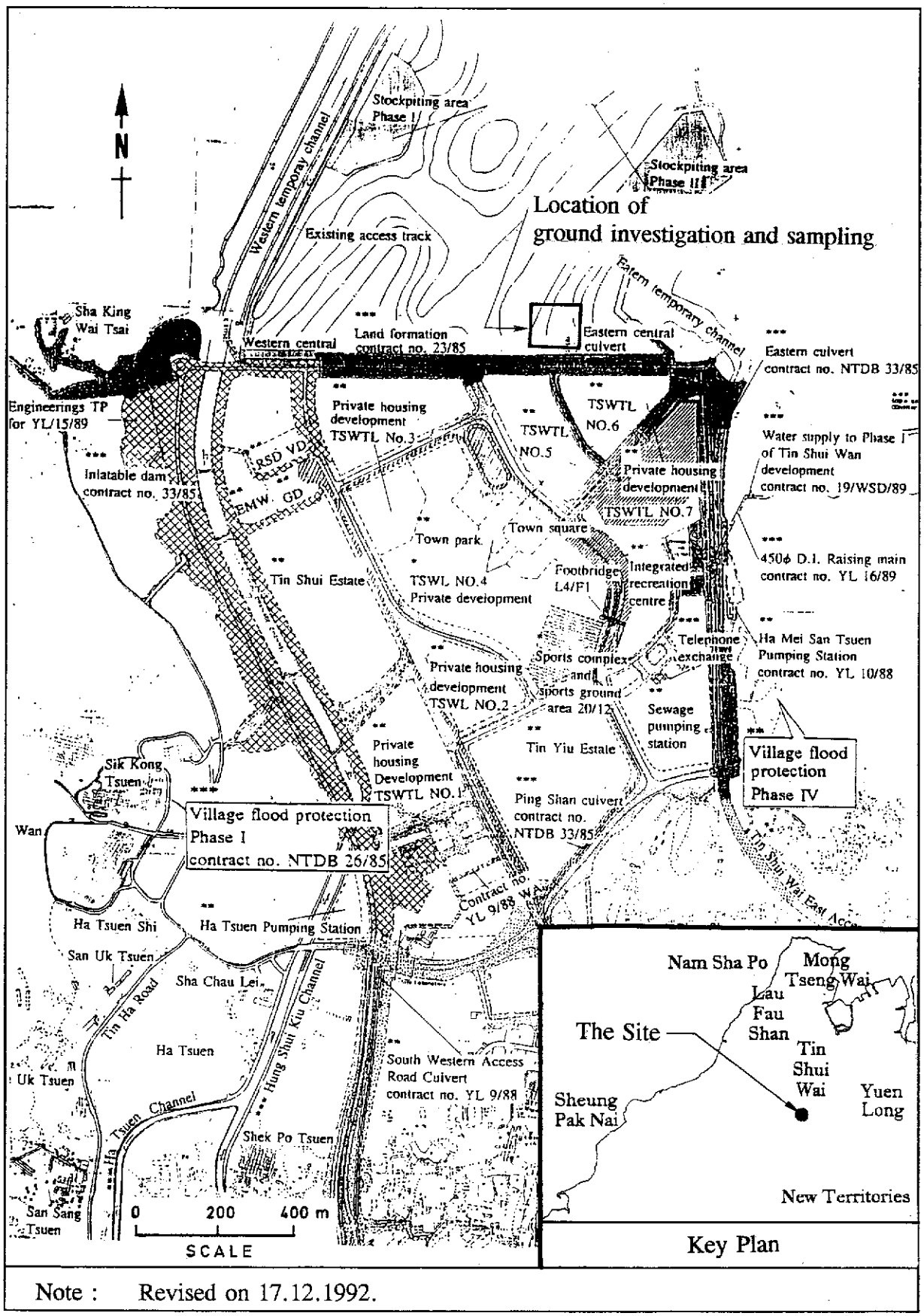

Note : Revised on 17.12.1992.

Figure 3.3 - Site Location Plan (Tin Shui Wai Development Reclamation)

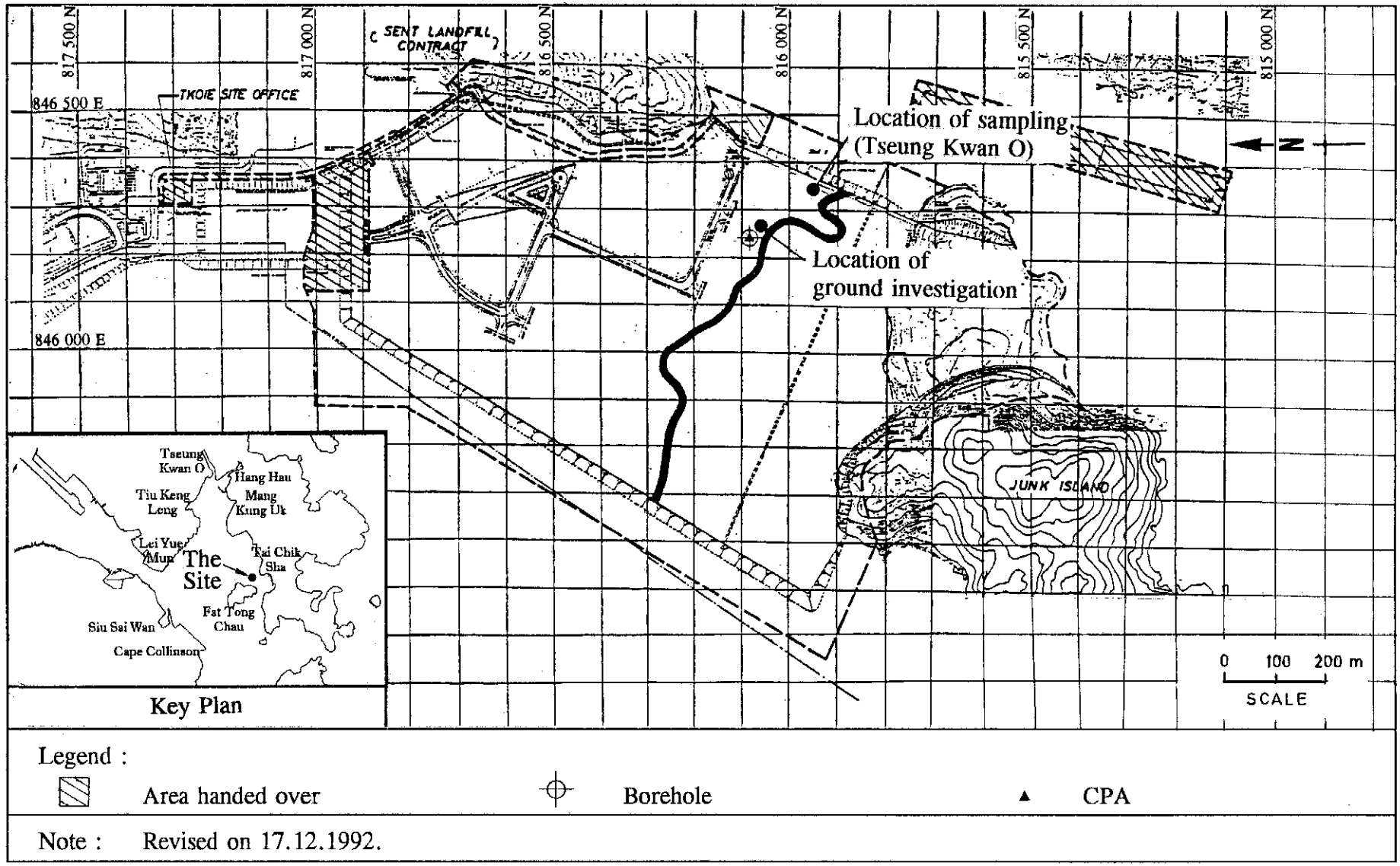

Figure 3.4 - Site Location Plan (Tseung Kwan O Industrial Estate Reclamation)

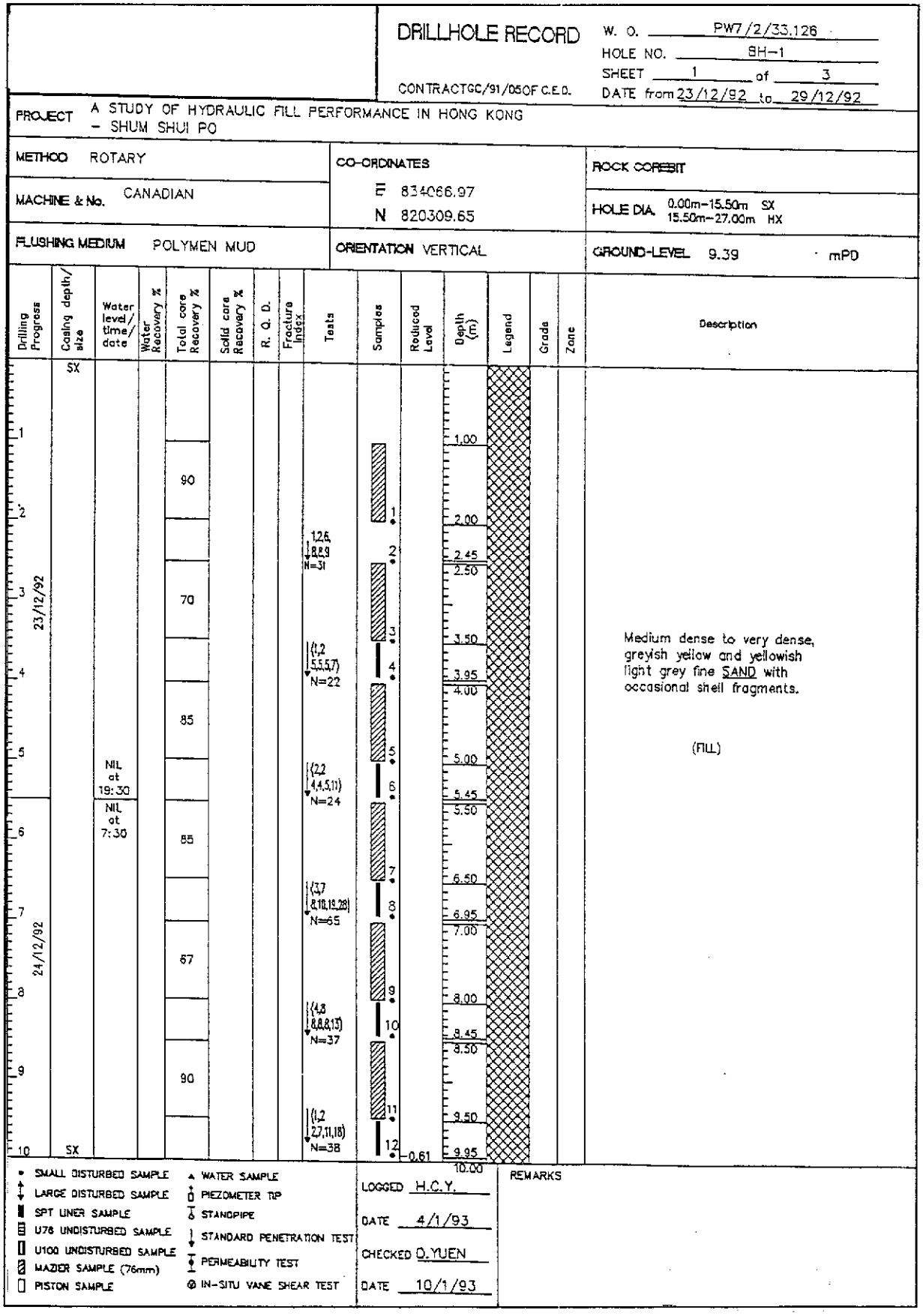

Figure 3.5 - Drillhole Logs at the West Kowloon Reclamation Site (Sheet 1 of 3)

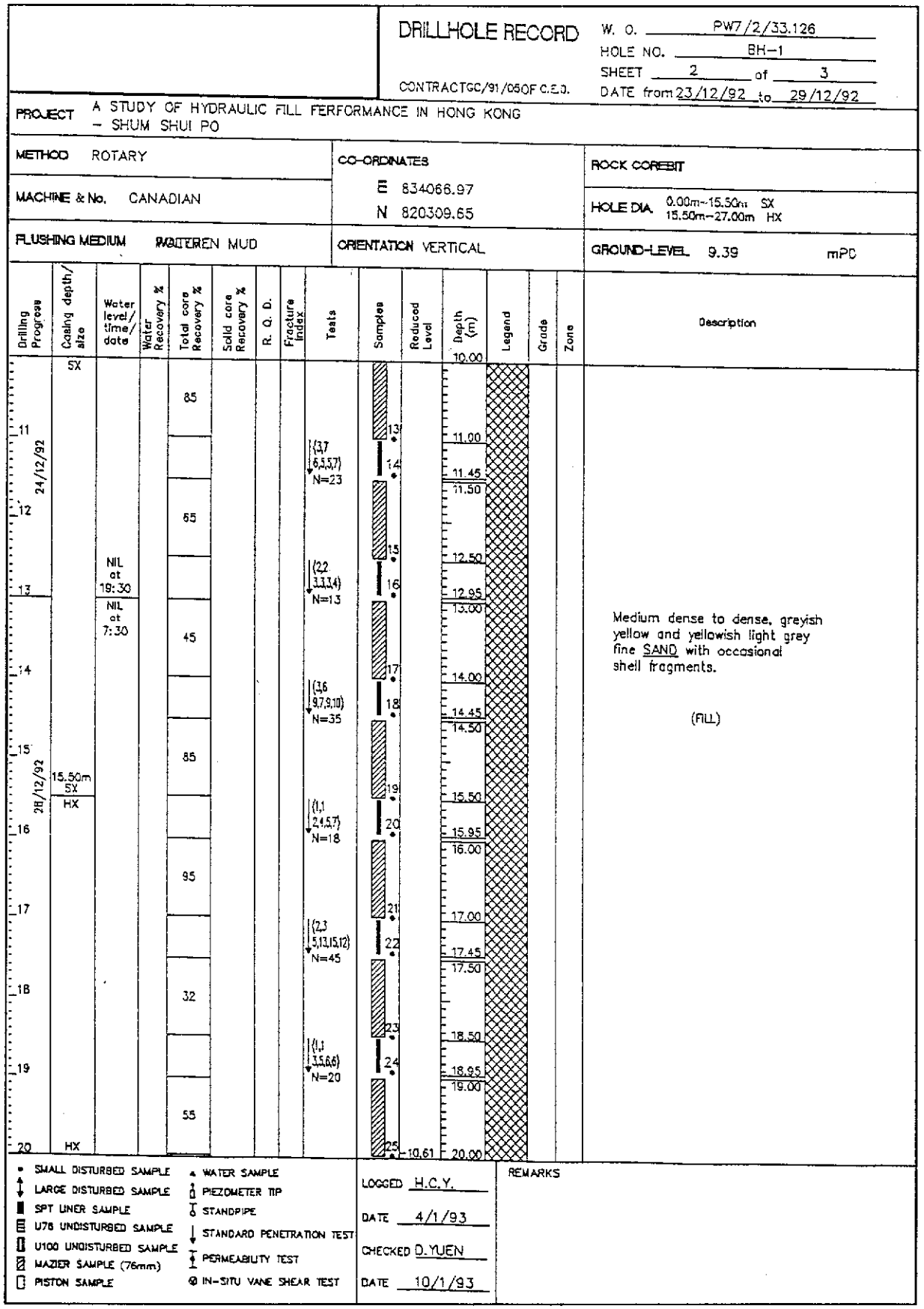

Figure 3.5 - Drillhole Logs at the West Kowloon Reclamation Site (Sheet 2 of 3)

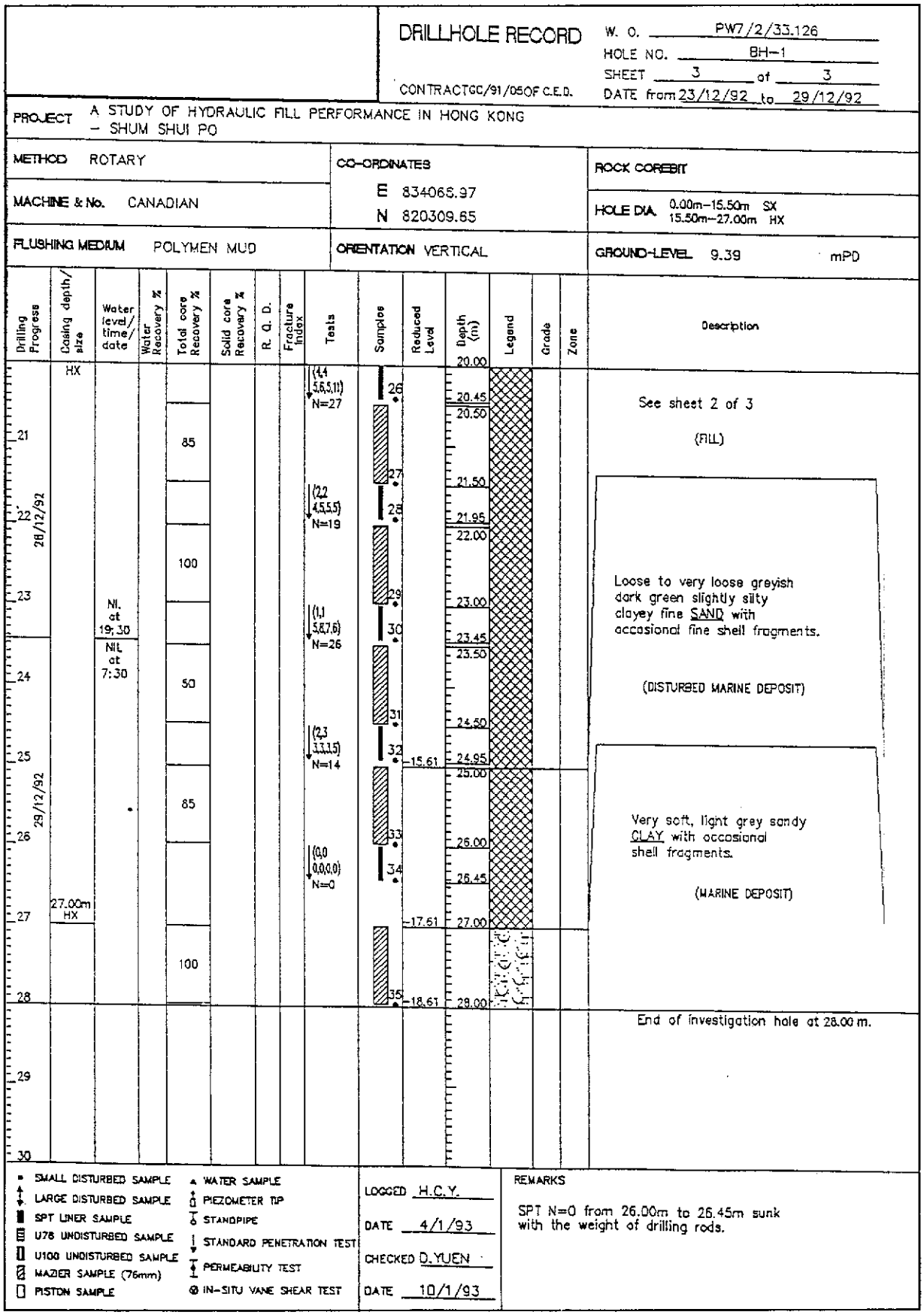

Figure 3.5 - Drillhole Logs at the West Kowloon Reclamation Site (Sheet 3 of 3)

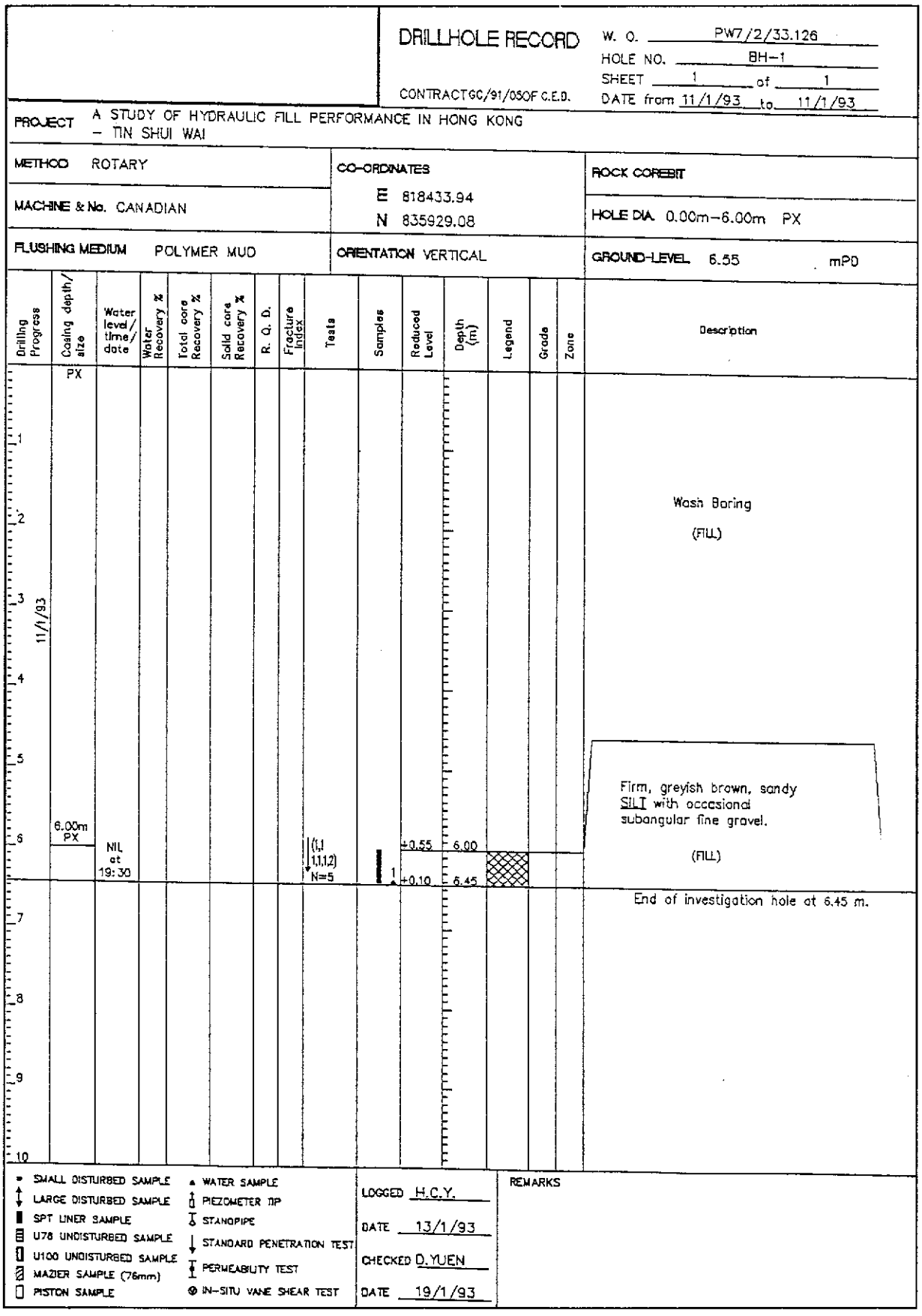

Figure 3.6 - Drillhole Logs at the Tin Shui Wai Reclamation Site (Sheet 1 of 2)

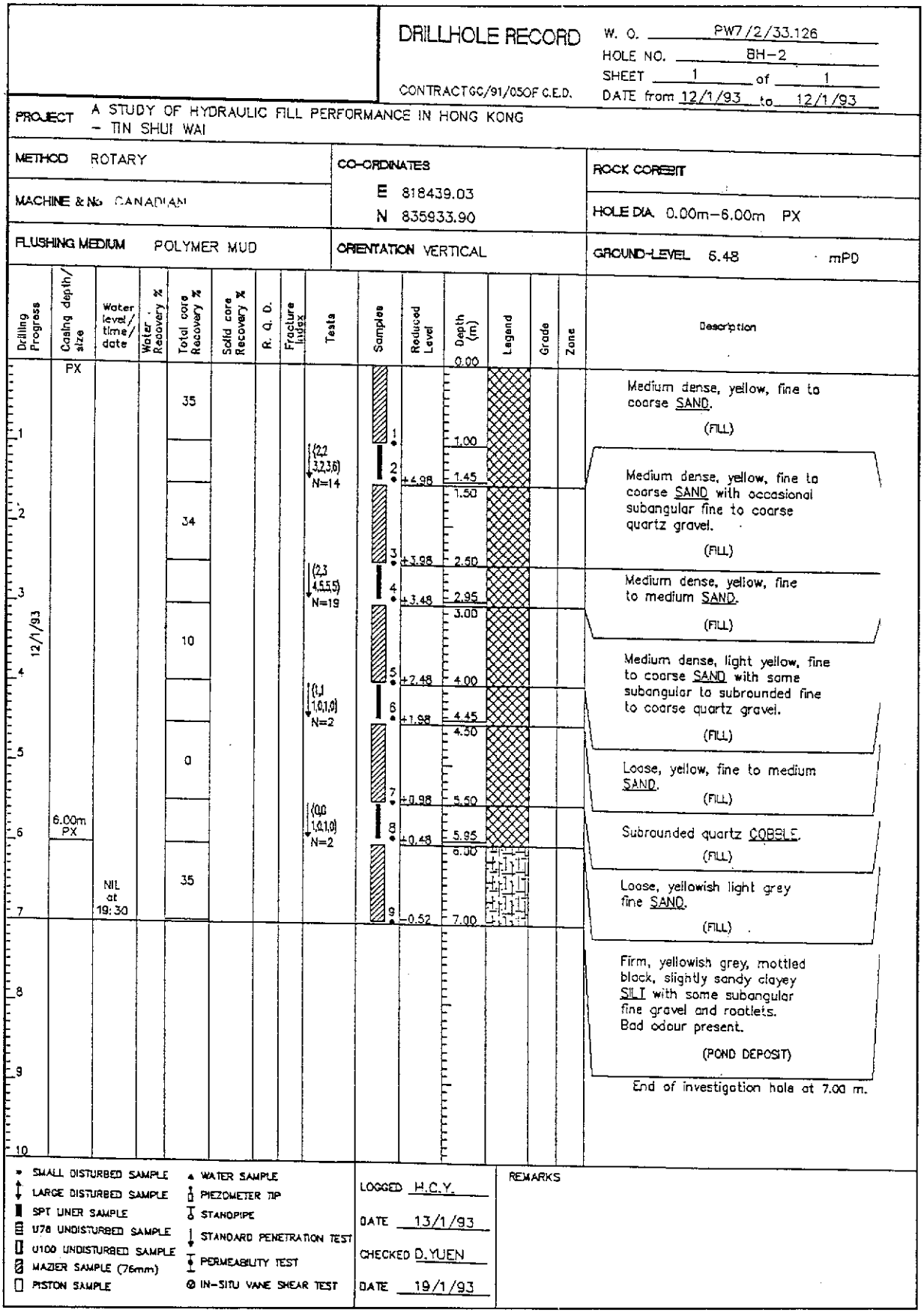

Figure 3.6 - Drillhole Logs at the Tin Shui Wai Reclamation Site (Sheet 2 of 2)

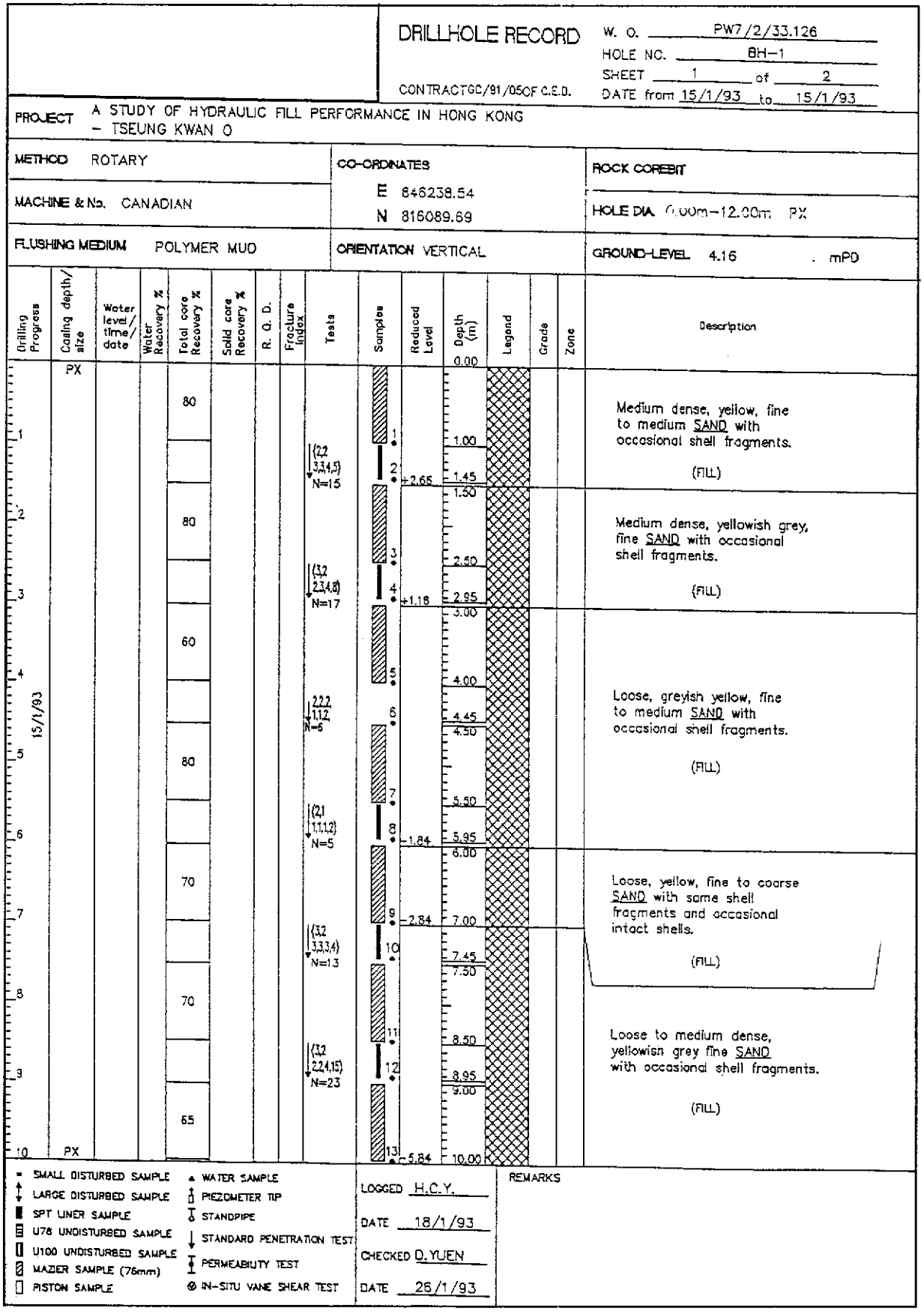

Figure 3.7 - Drillhole Logs at the Tseung Kwan O Reclamation Site (Sheet 1 of 2)

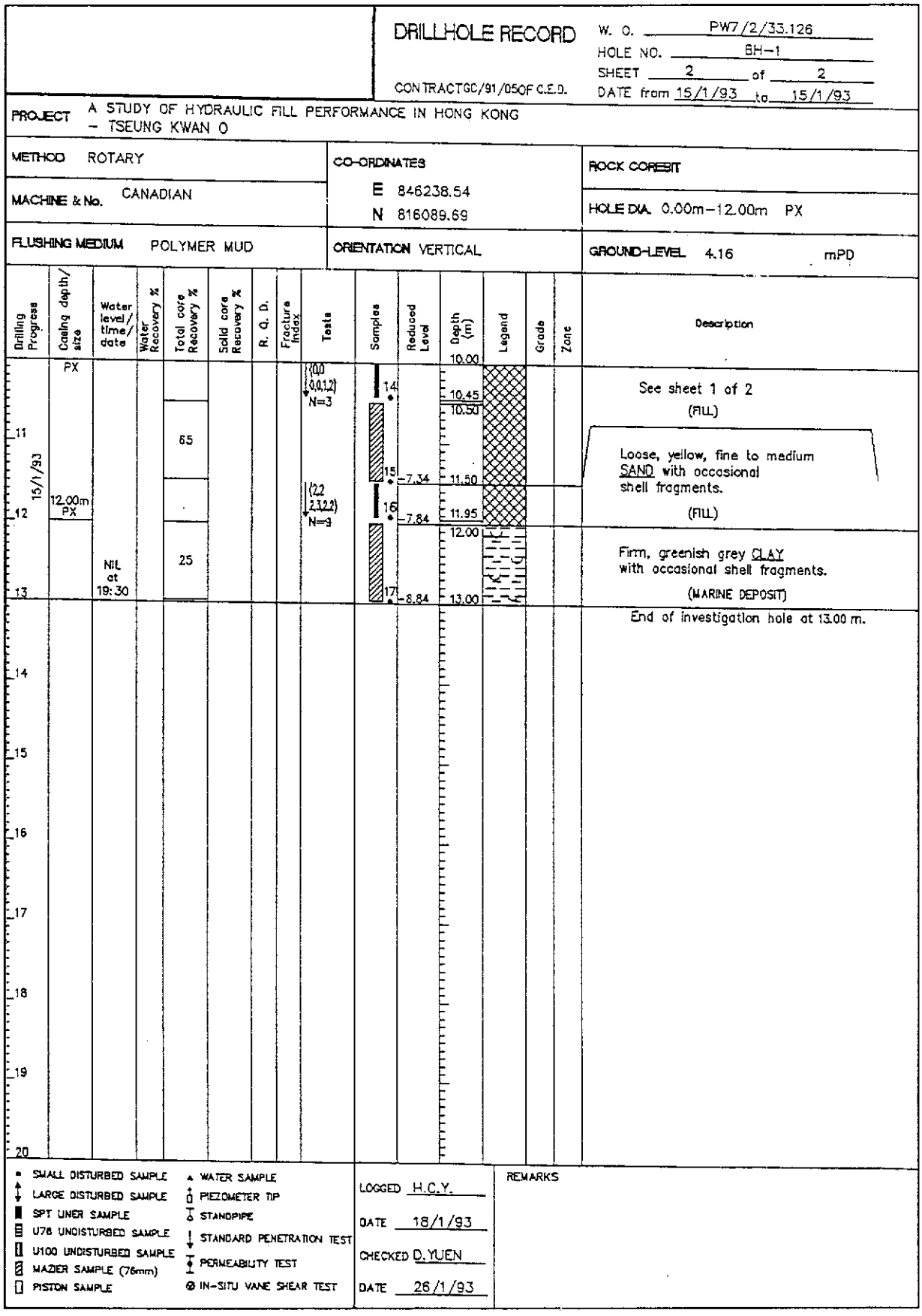

Figure 3.7 - Drillhole Logs at the Tseung Kwan O Reclamation Site (Sheet 2 of 2)

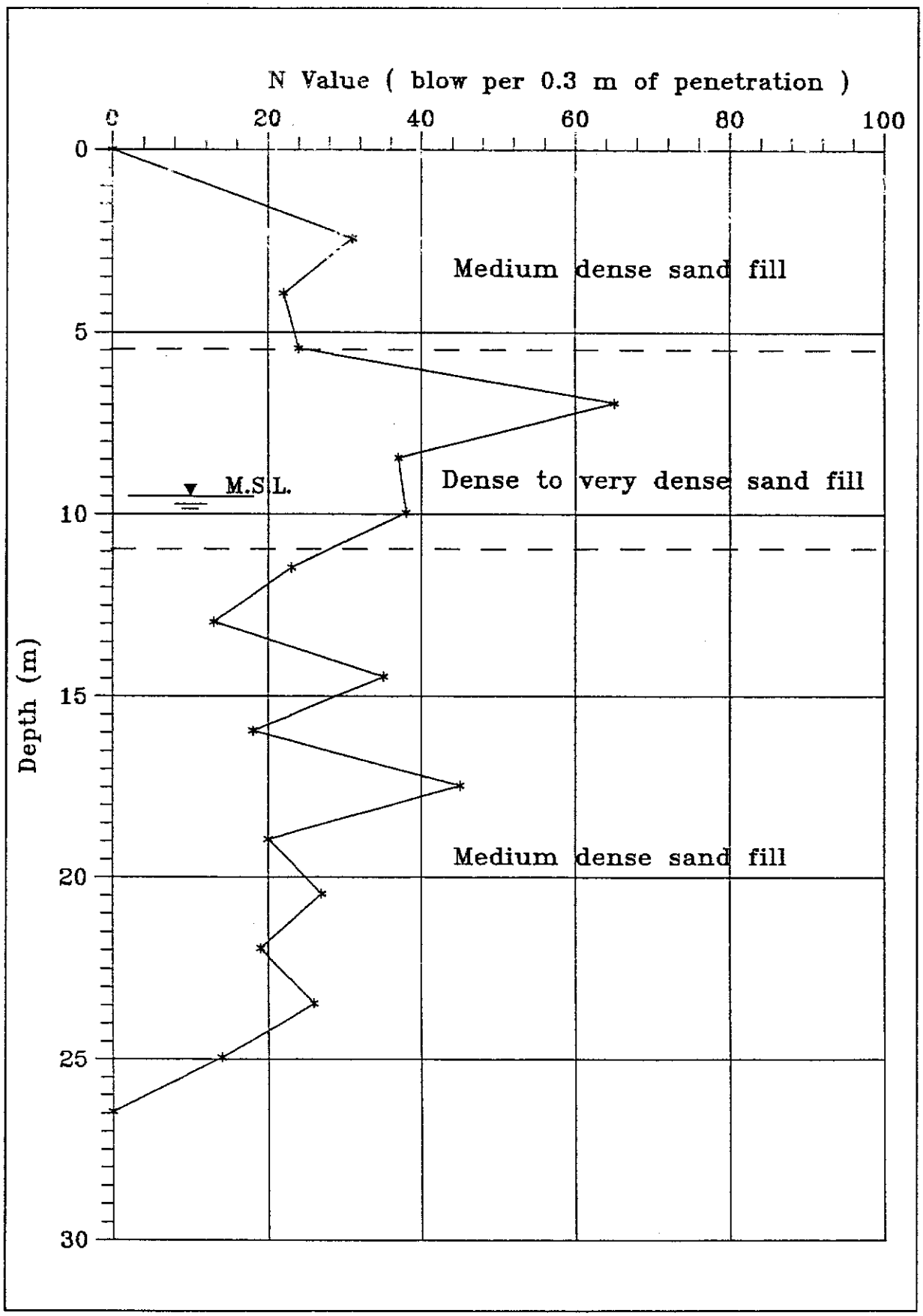

Figure 3.8 - SPT-N Value Versus Depth for the West Kowloon Reclamation Site

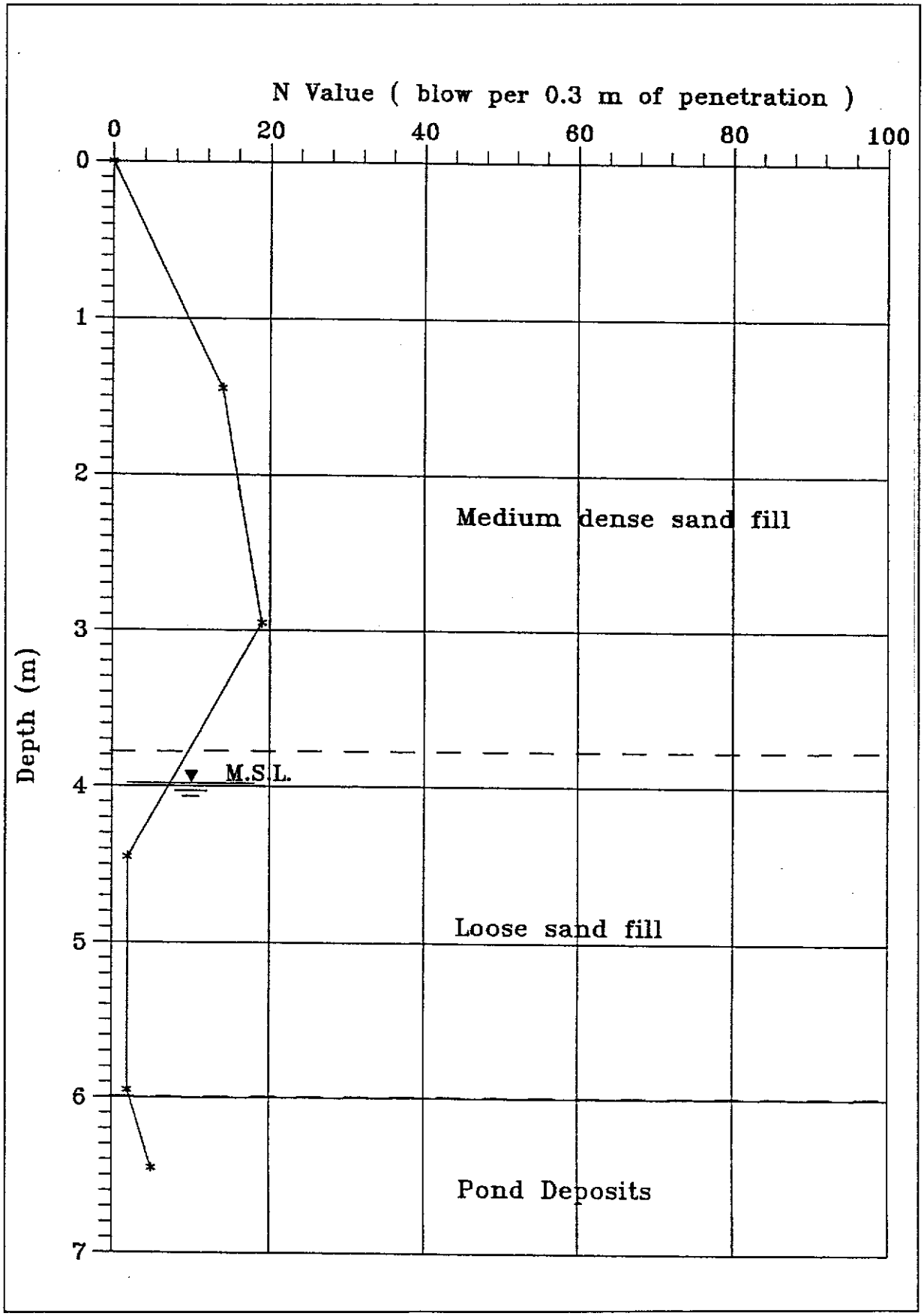

Figure 3.9 - SPT-N Value Versus Depth for the Tin Shui Wai Reclamation Site

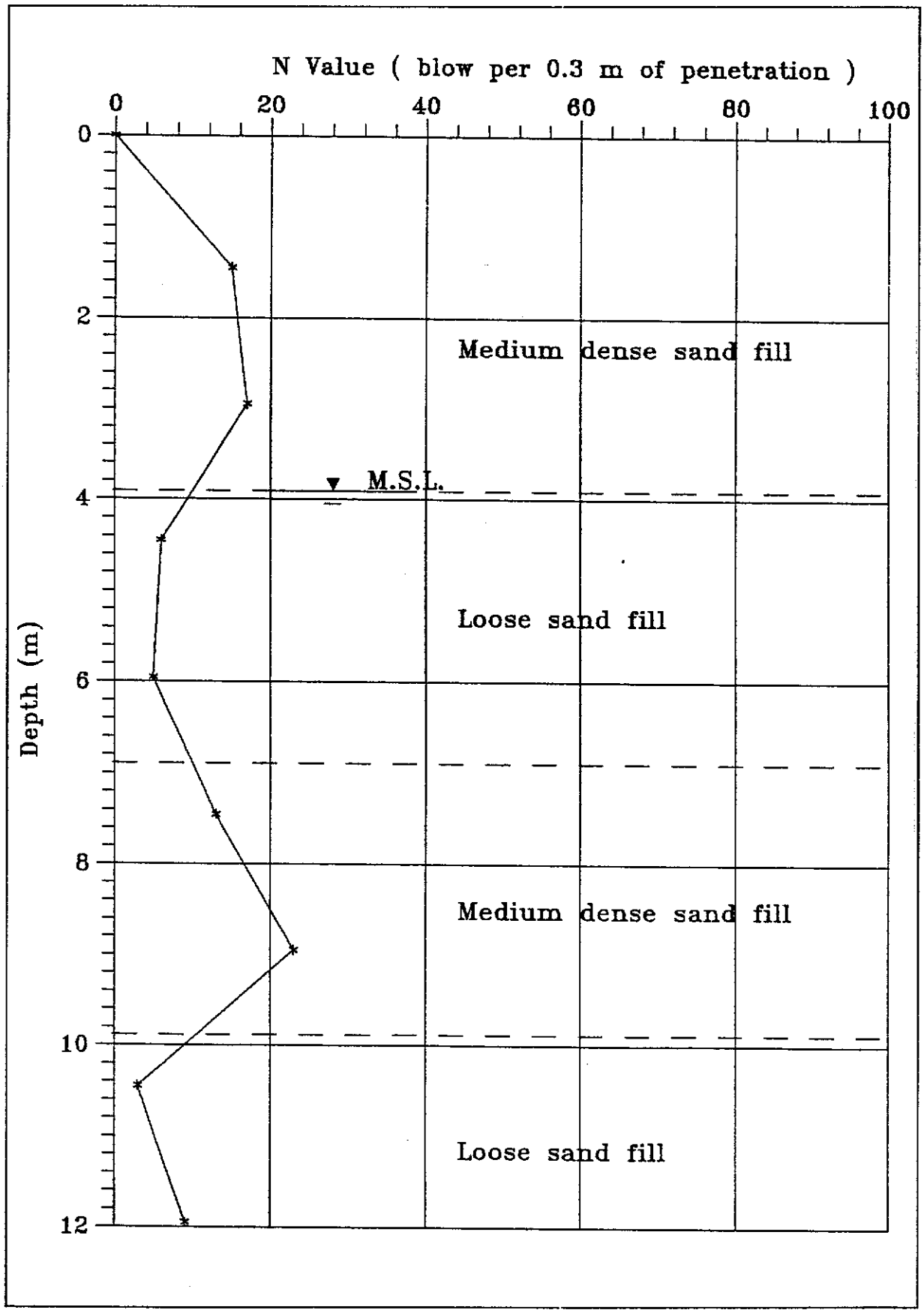

Figure 3.10 - SPT-N Value Versus Depth for the Tseung Kwan O Reclamation Site

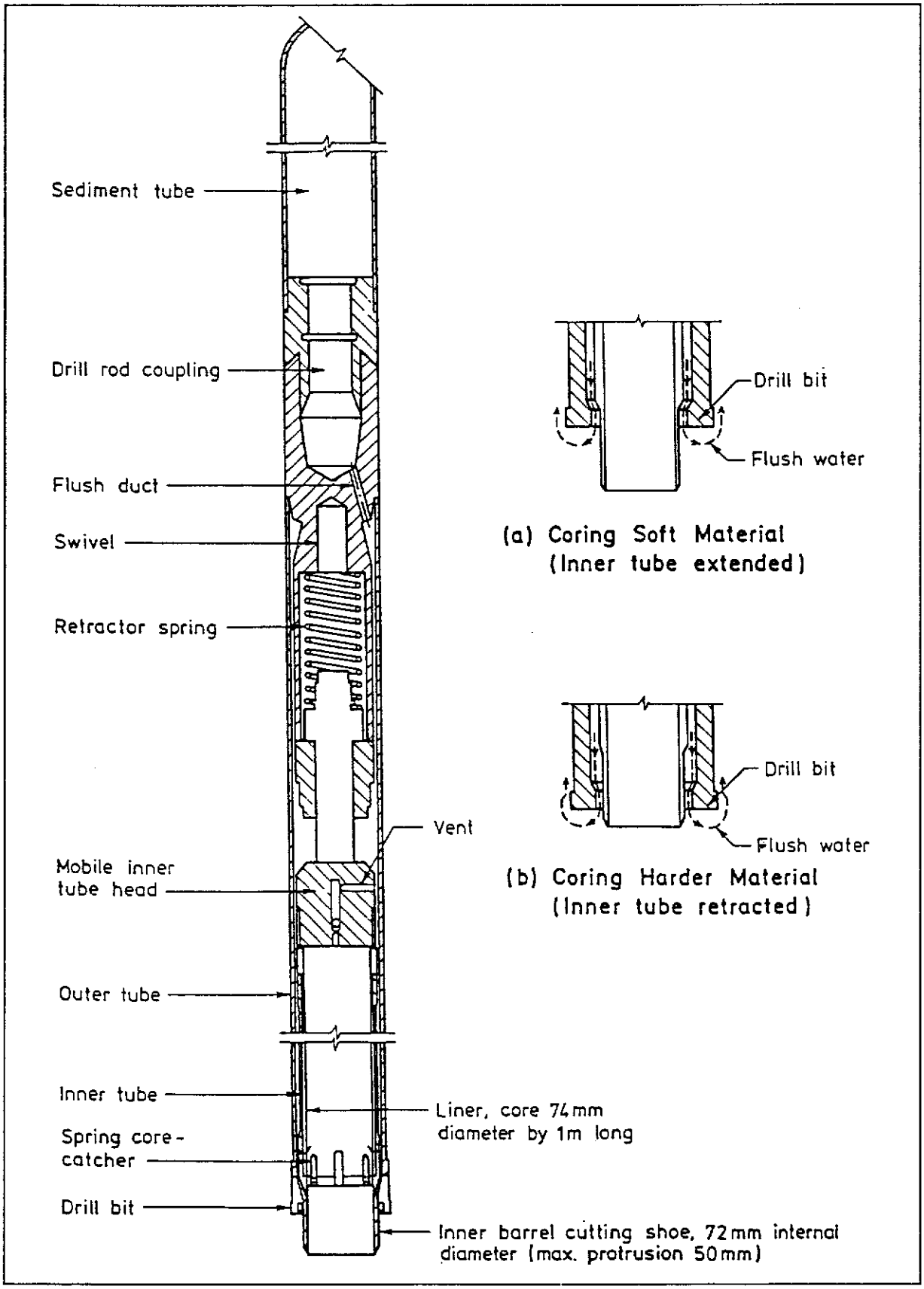

Figure 3.11 - Example of a Retractable Triple-tube Core-barrel (Mazier)
(Guide to Site Investigation, GEO)

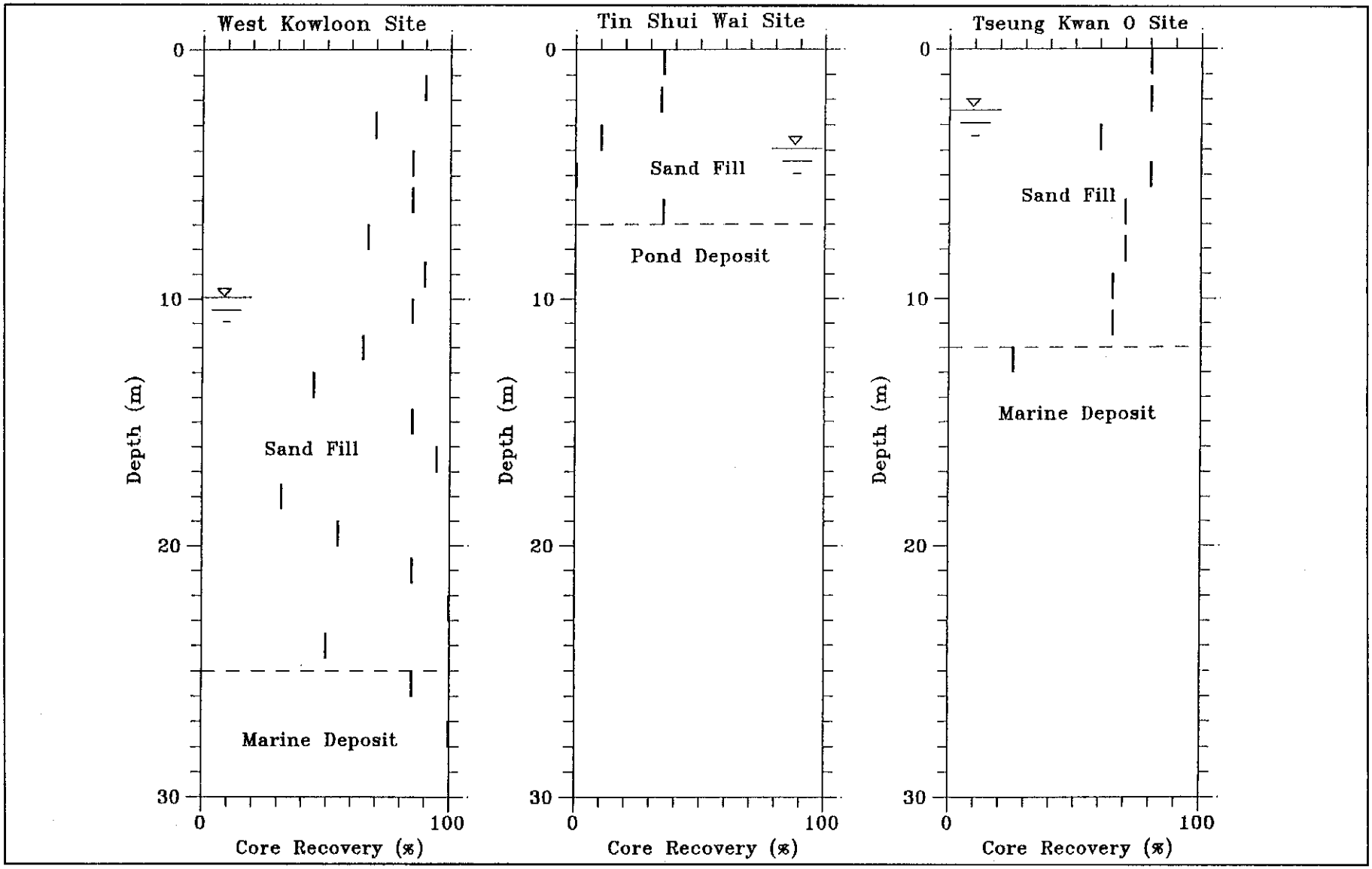

Figure 3.12 - The Percentage Total Core Recovery of Mazier Samples at the Three Sites

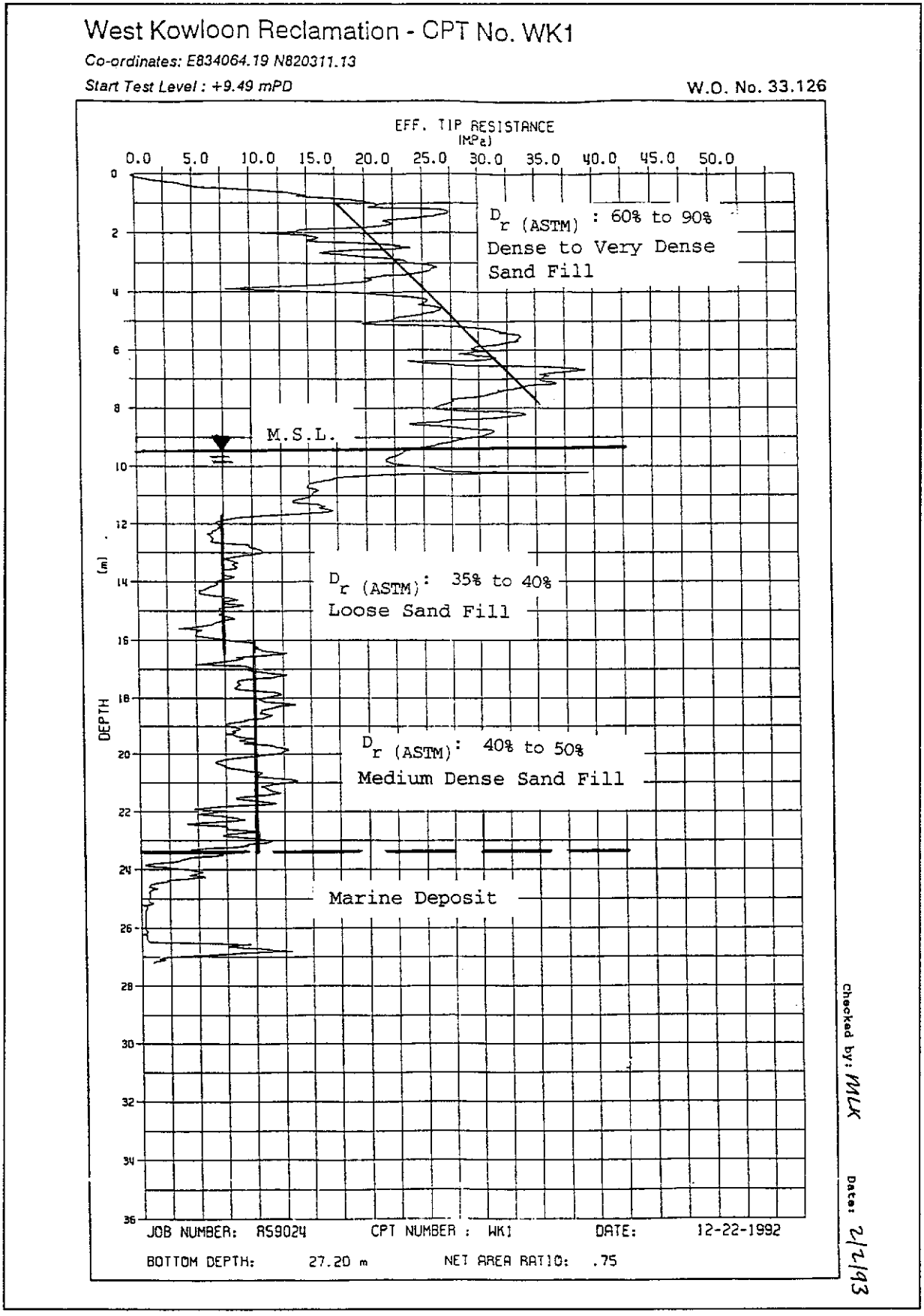

Figure 3.13 - Record of q_c' Versus Depth for the 10 cm^2 (5 ton) Cone at CS1

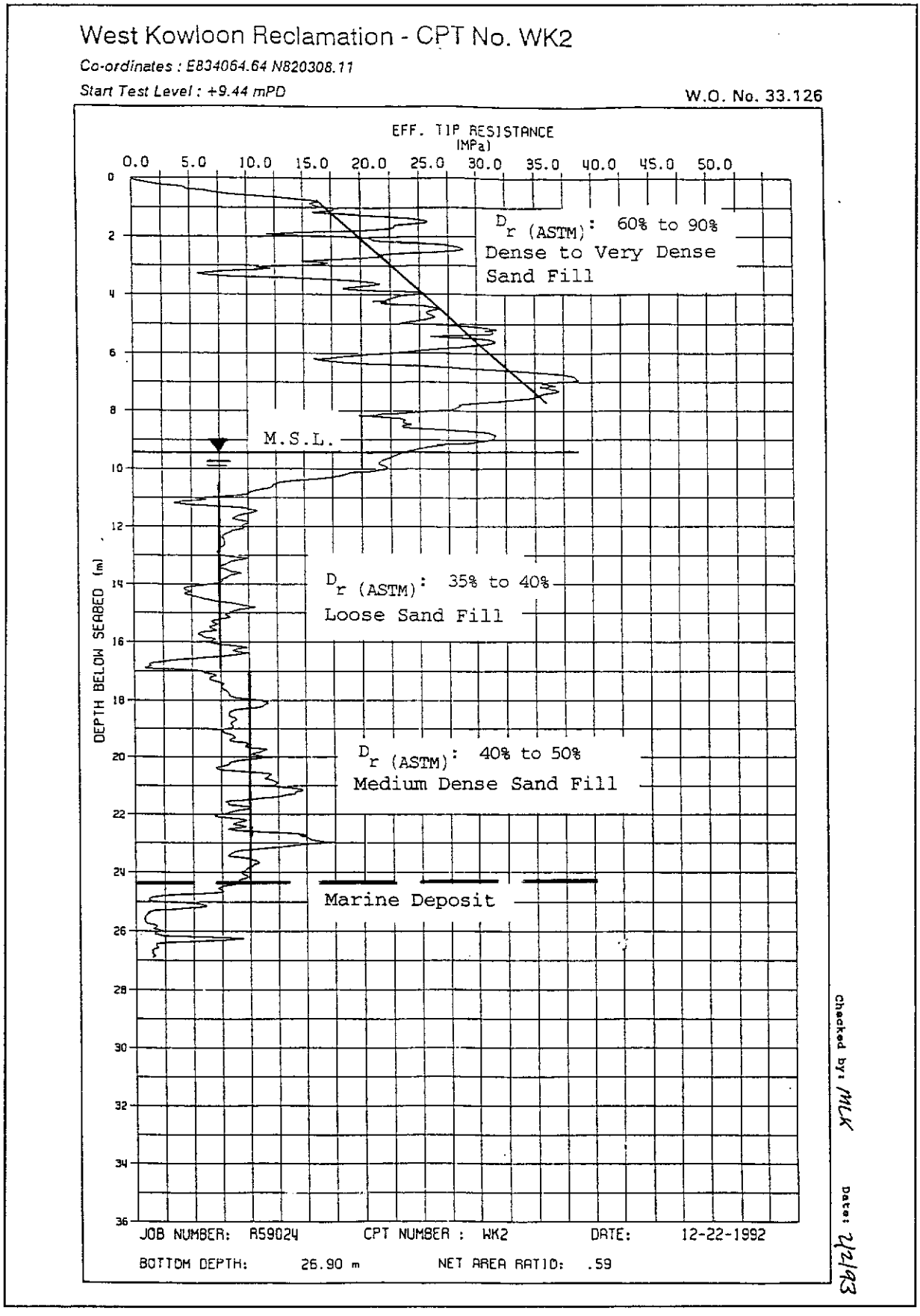

Figure 3.14 - Record of q_c' Versus Depth for the 15 cm^2 (7.5 ton) Cone at CS1

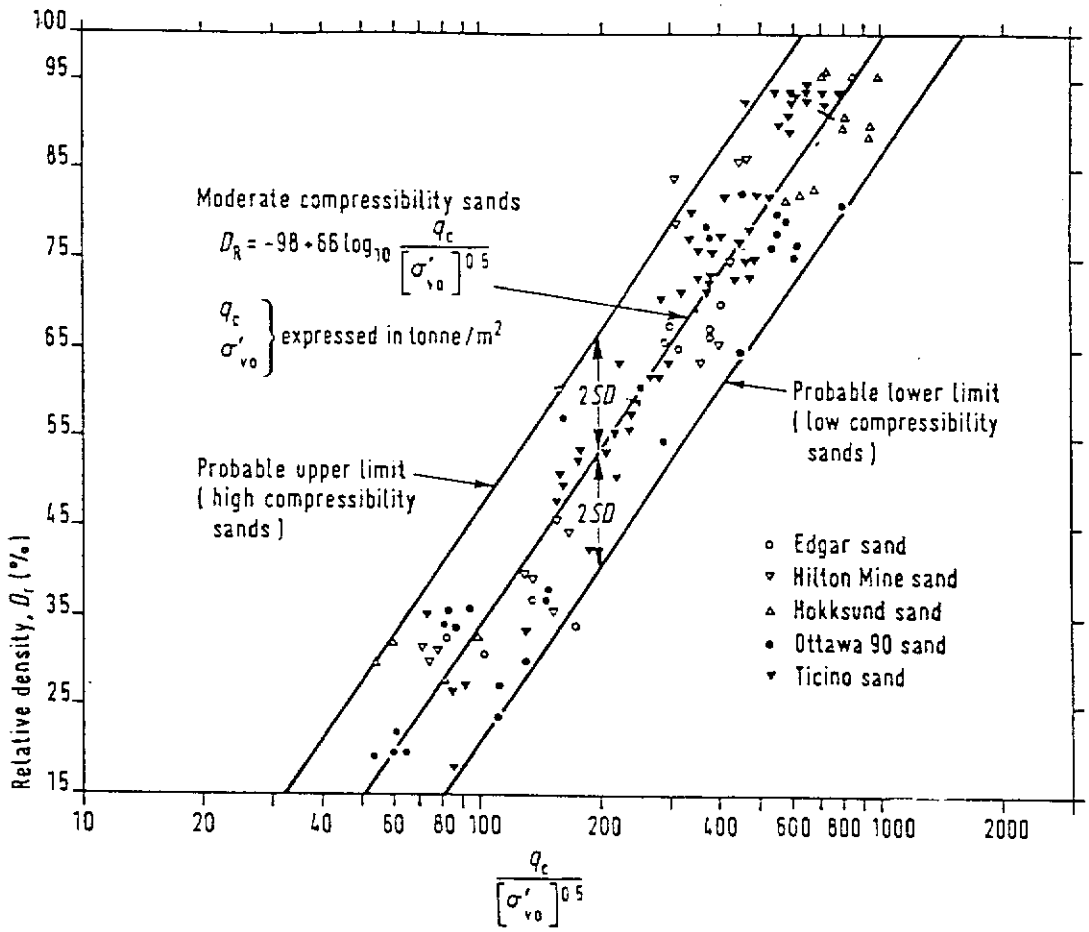

Note : Correction required for chamber size.

Figure 3.15 - Relationship between Relative Density and Cone Resistance of Uncemented, Normally-consolidated Quartz Sands (after Jamiolkowski et al , 1985)

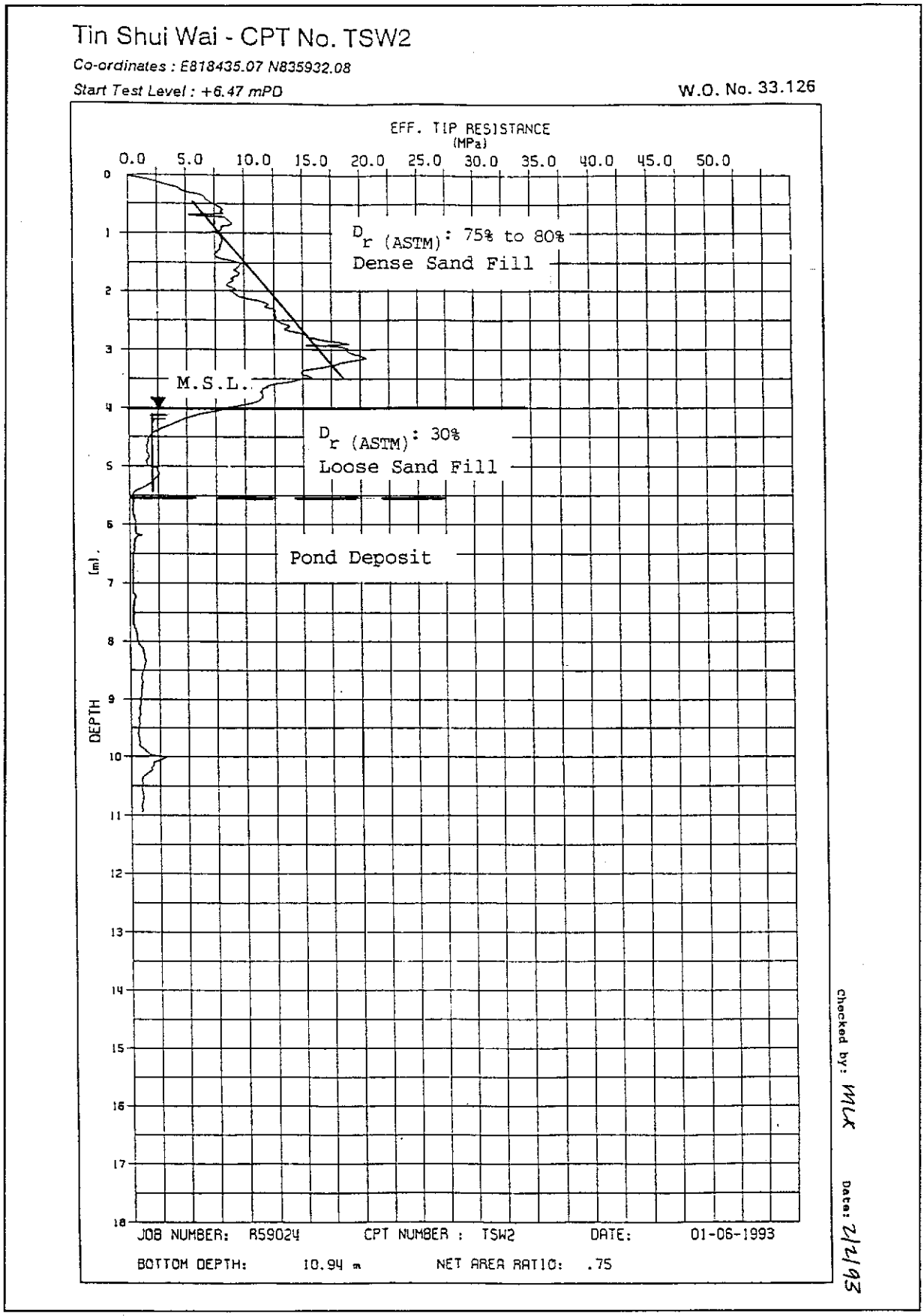

Figure 3.16 - Record of q_c' Versus Depth for the 10 cm^2 Cone at TSW

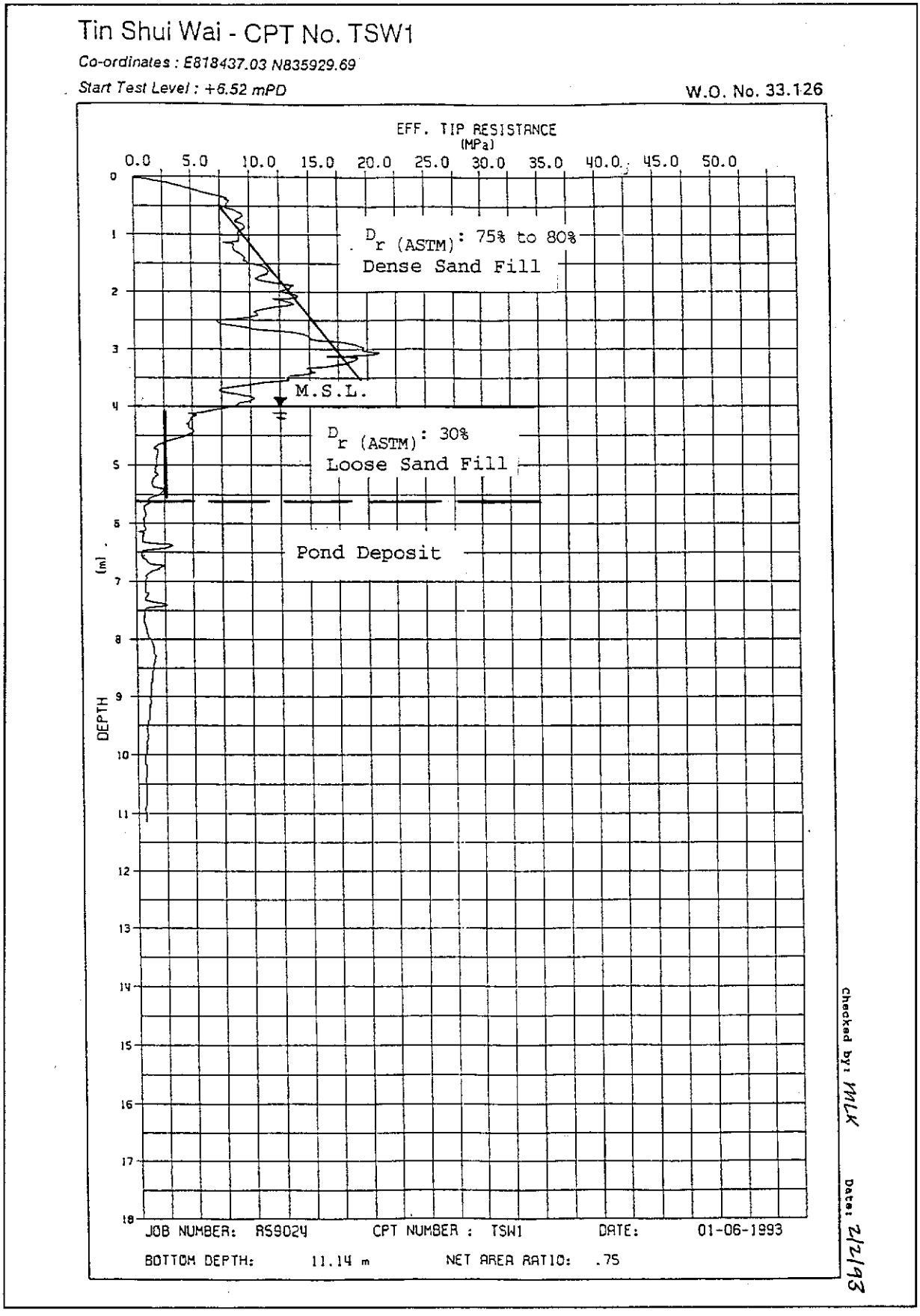

Figure 3.17 - Record of q_c' Versus Depth for the 15 cm^2 Cone at TSW

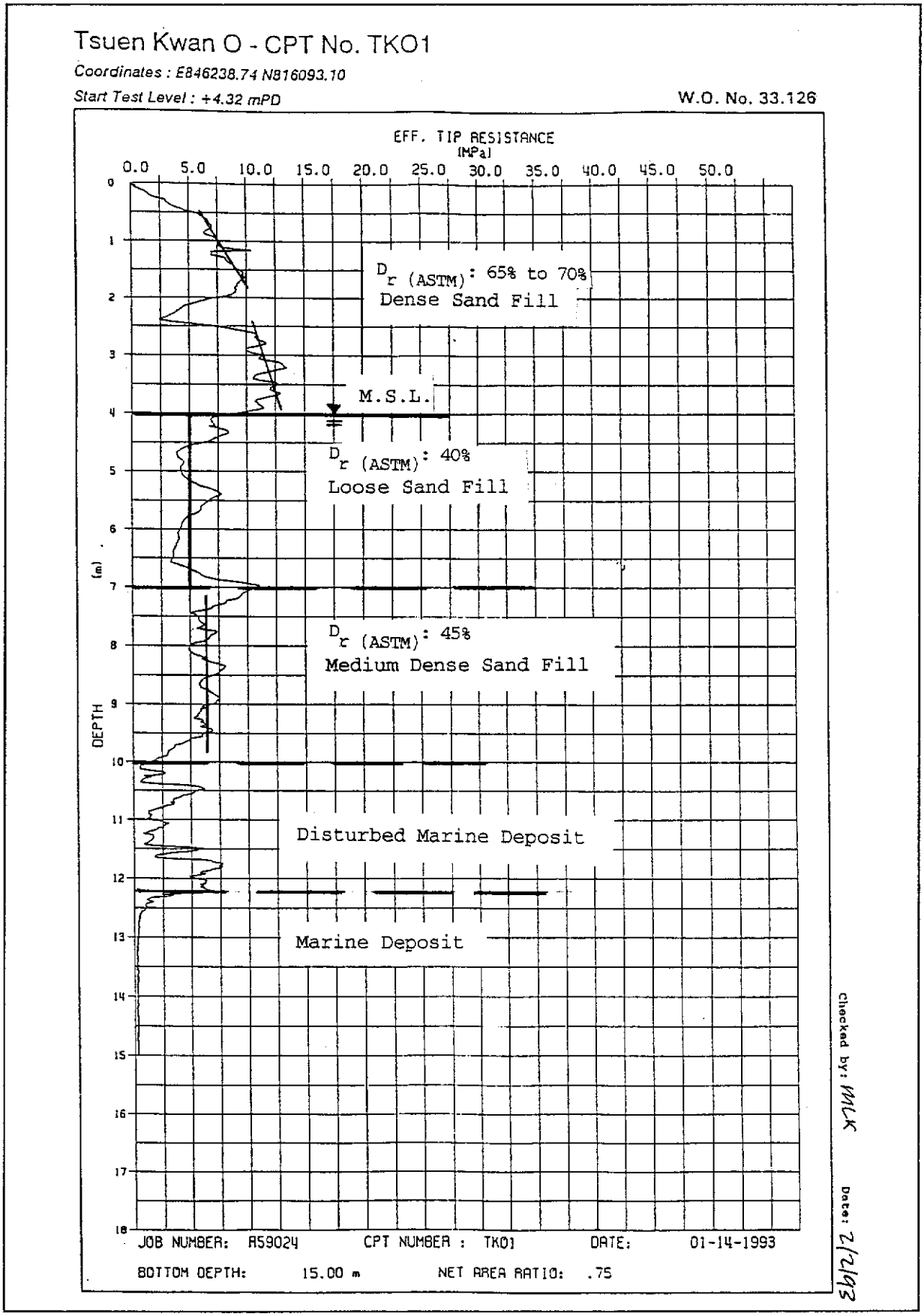

Figure 3.18 - Record of q_c' Versus Depth for the 10 cm^2 Cone at TKO

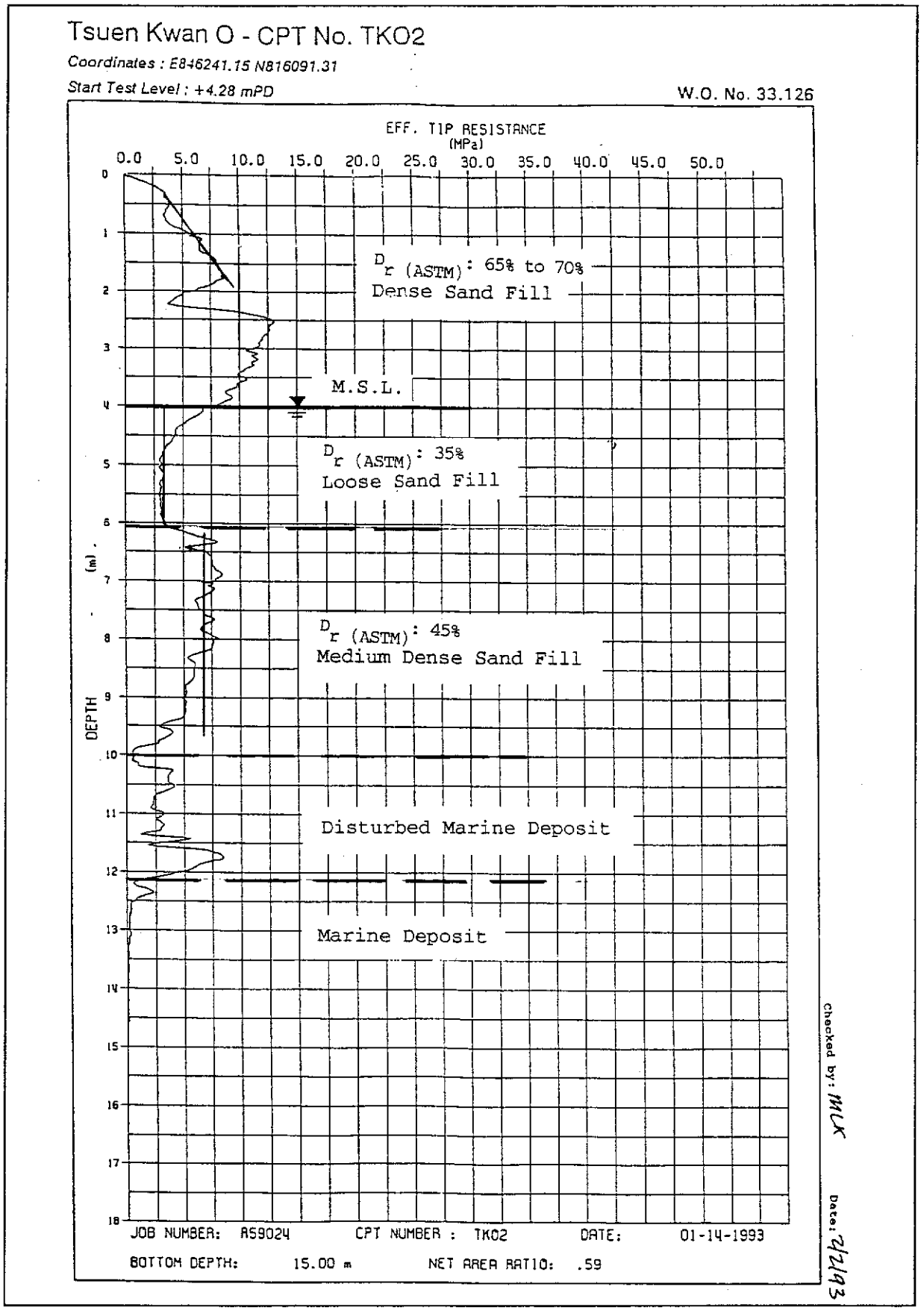

Figure 3.19 - Record of q_c' Versus Depth for the 15 cm^2 Cone at TKO

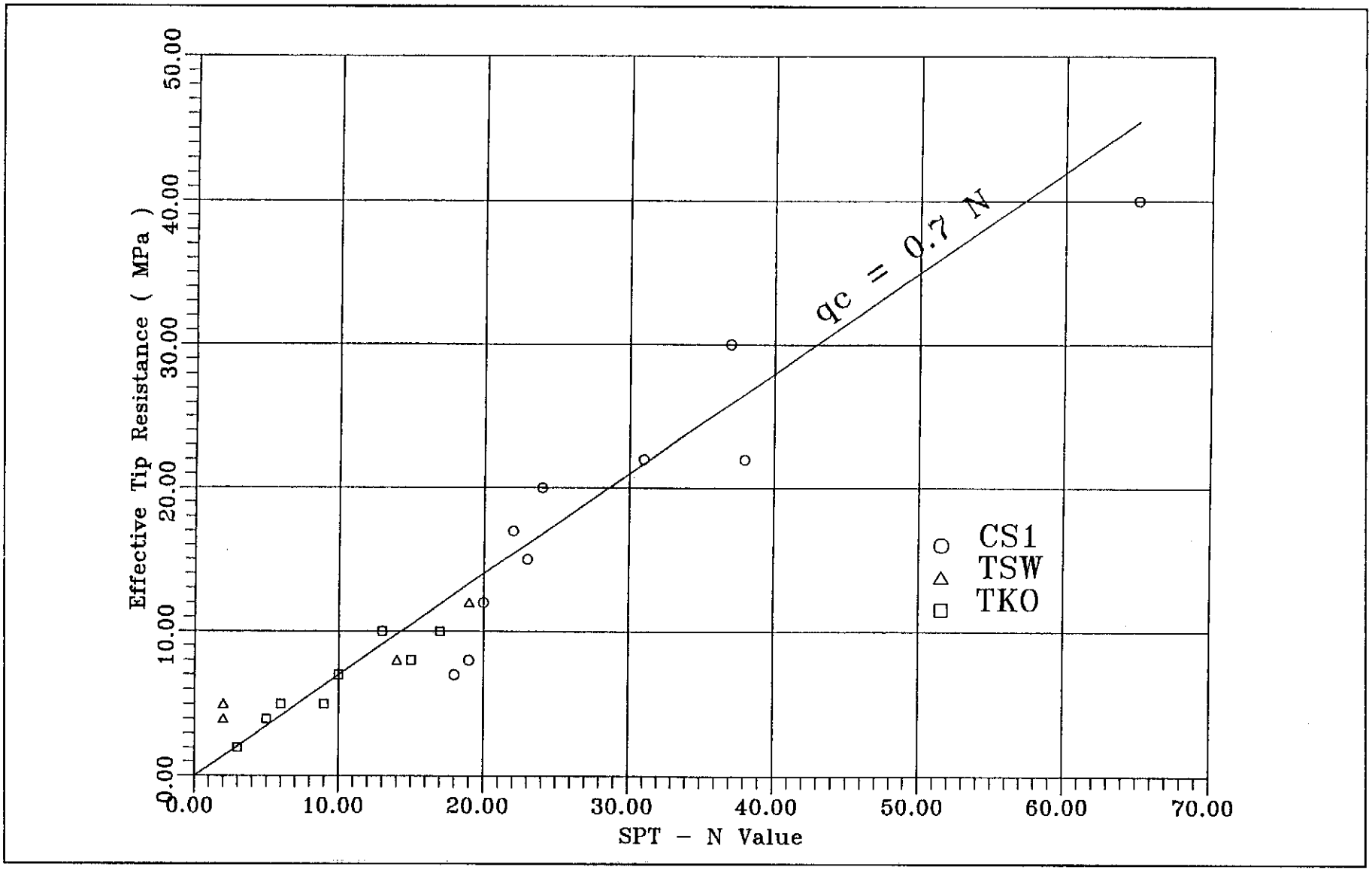

Figure 3.20 - Correction between CPT Penetration Resistance and SPT-N Value

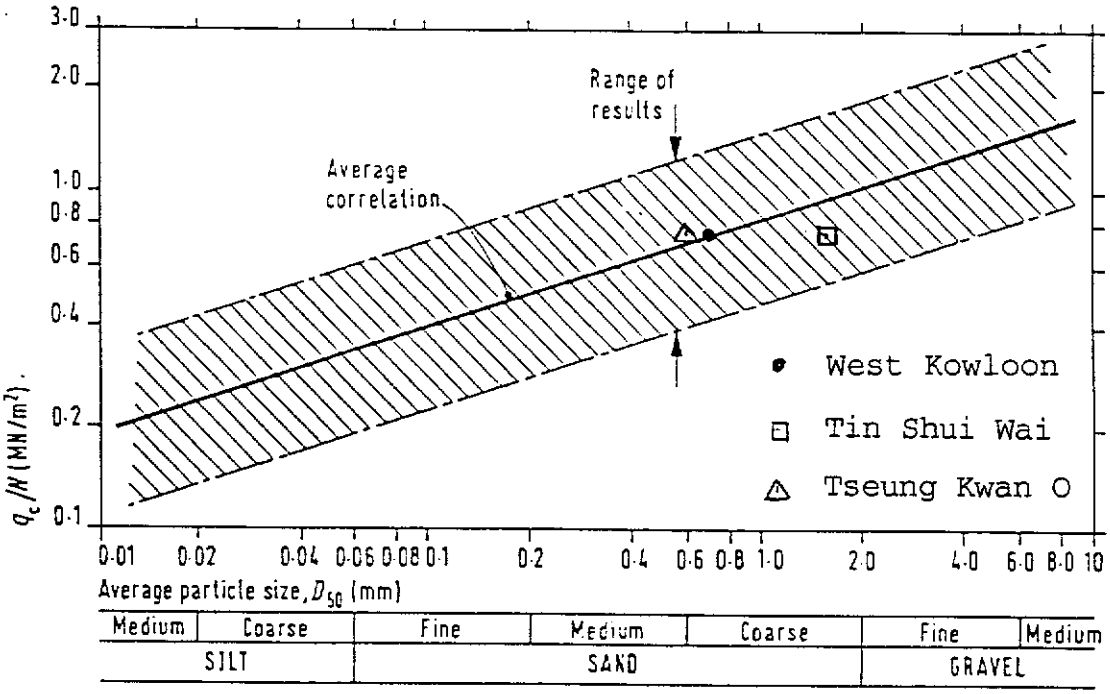

Figure 3.21 - Relationship between Cone Penetration Test and Standard Penetration Test (from Burland & Buridge, 1985)

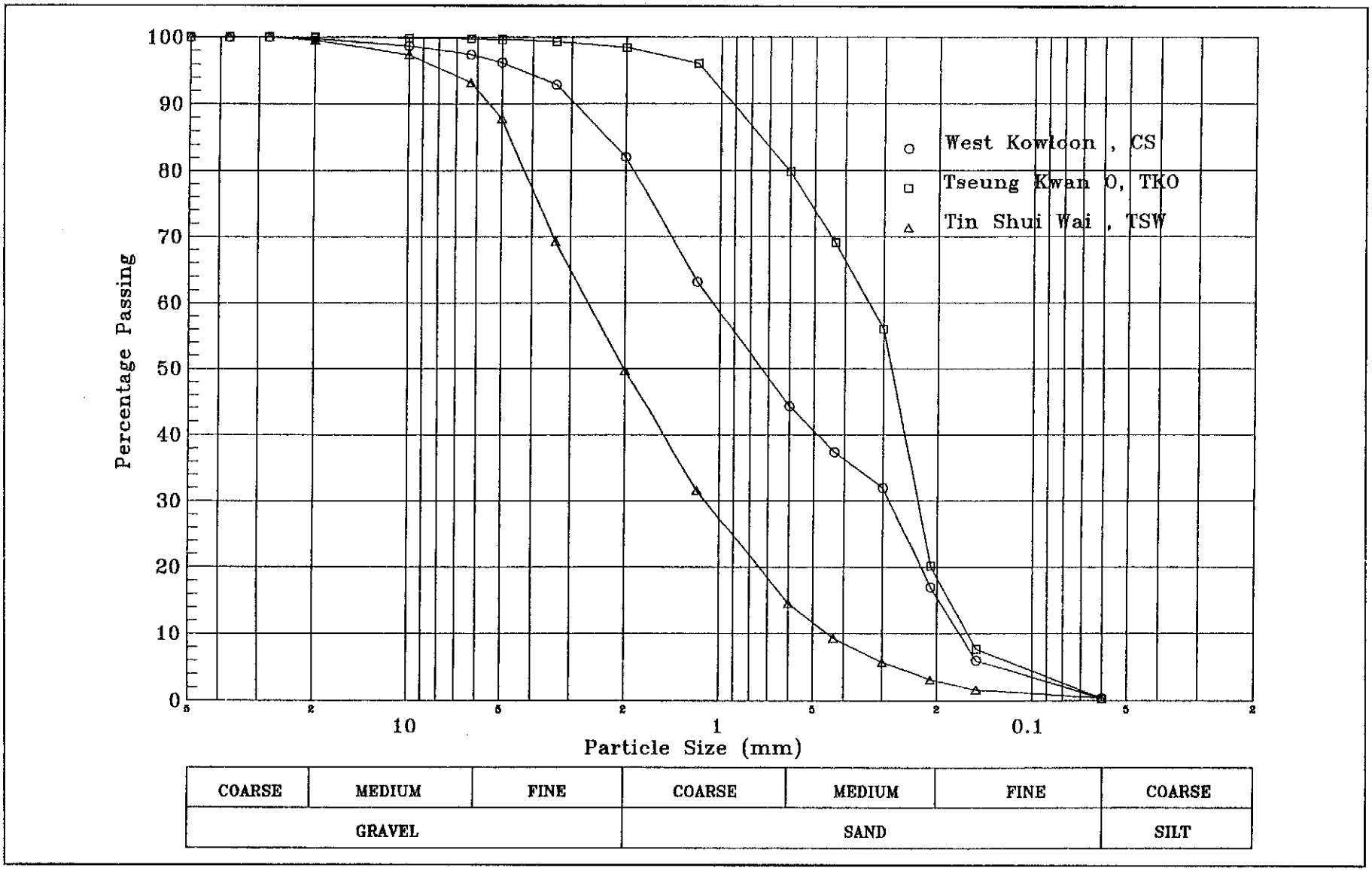

Figure 4.1 - Particle Size Distribution Determination (Origin Material, before Screening out Particle Greater than 5 mm)

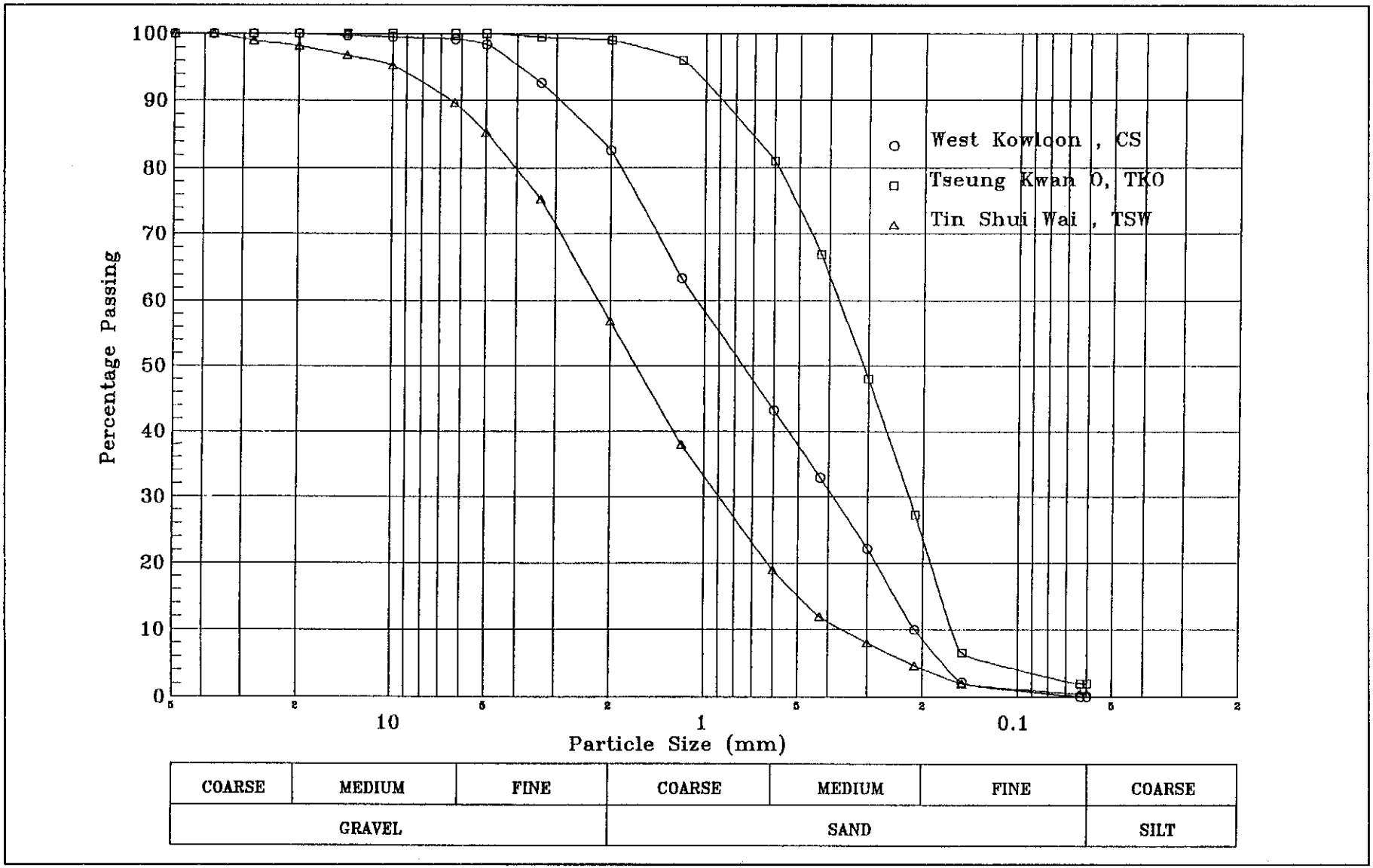

Figure 4.2 - Particle Size Distribution Determination (Material Shipped to Italy for Calibration Chamber Test)

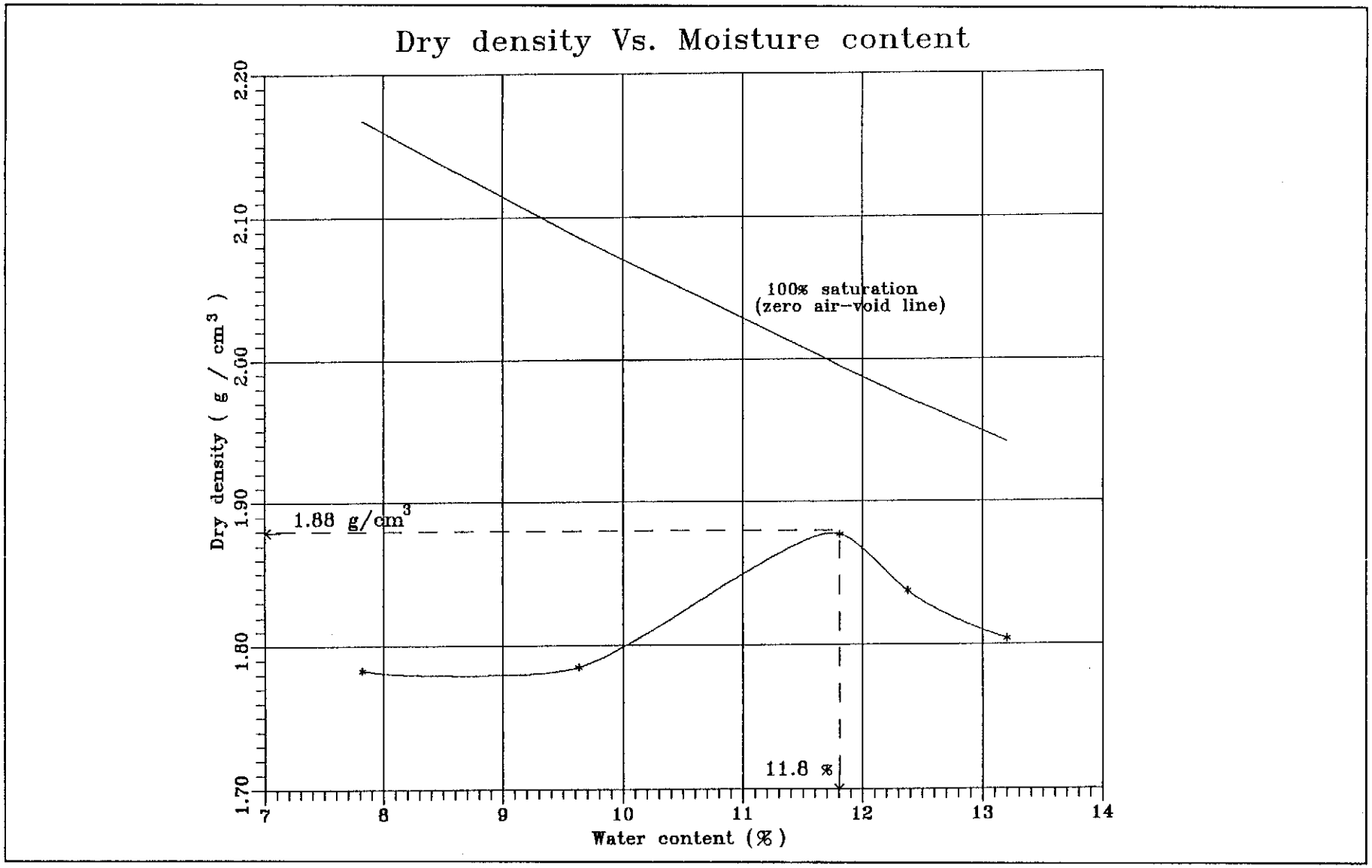

Figure 4.3 - Result of Compaction Test for West Kowloon (CS1) Sample

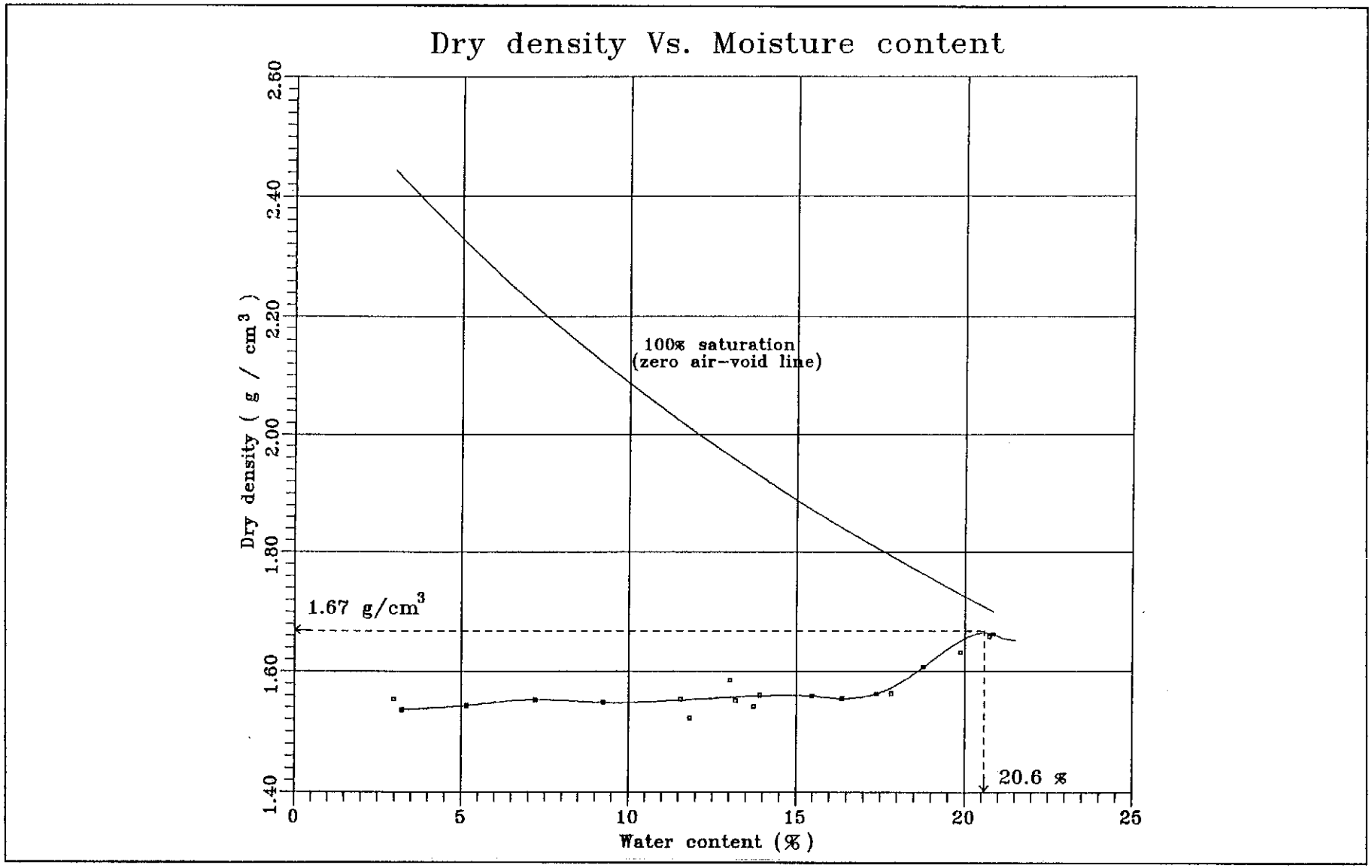

Figure 4.4 - Result of Compaction Test for Tin Shui Wai (TSW) Sample

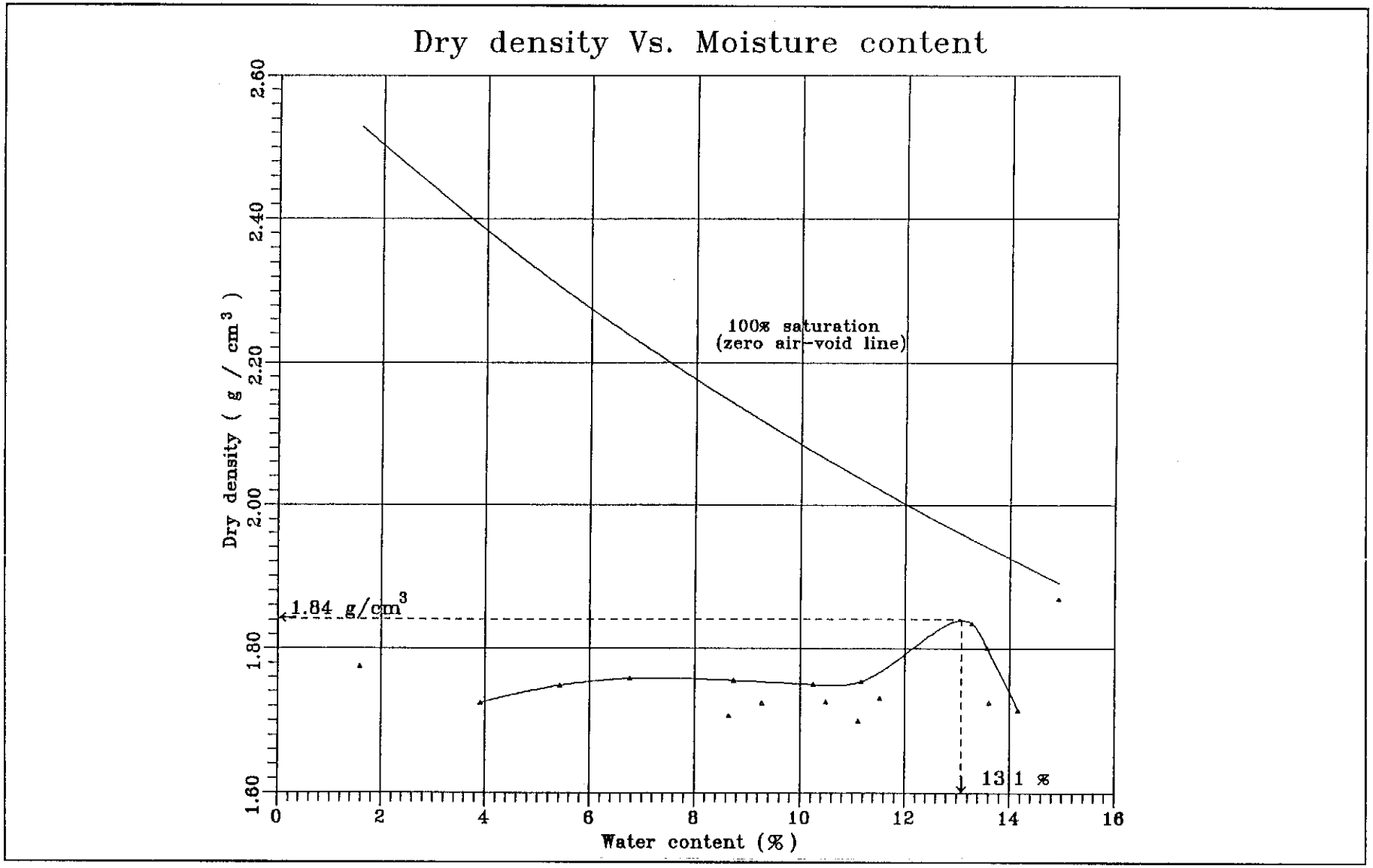

Figure 4.5 - Result of Compaction Test for Tseung Kwan O (TKO) Sample

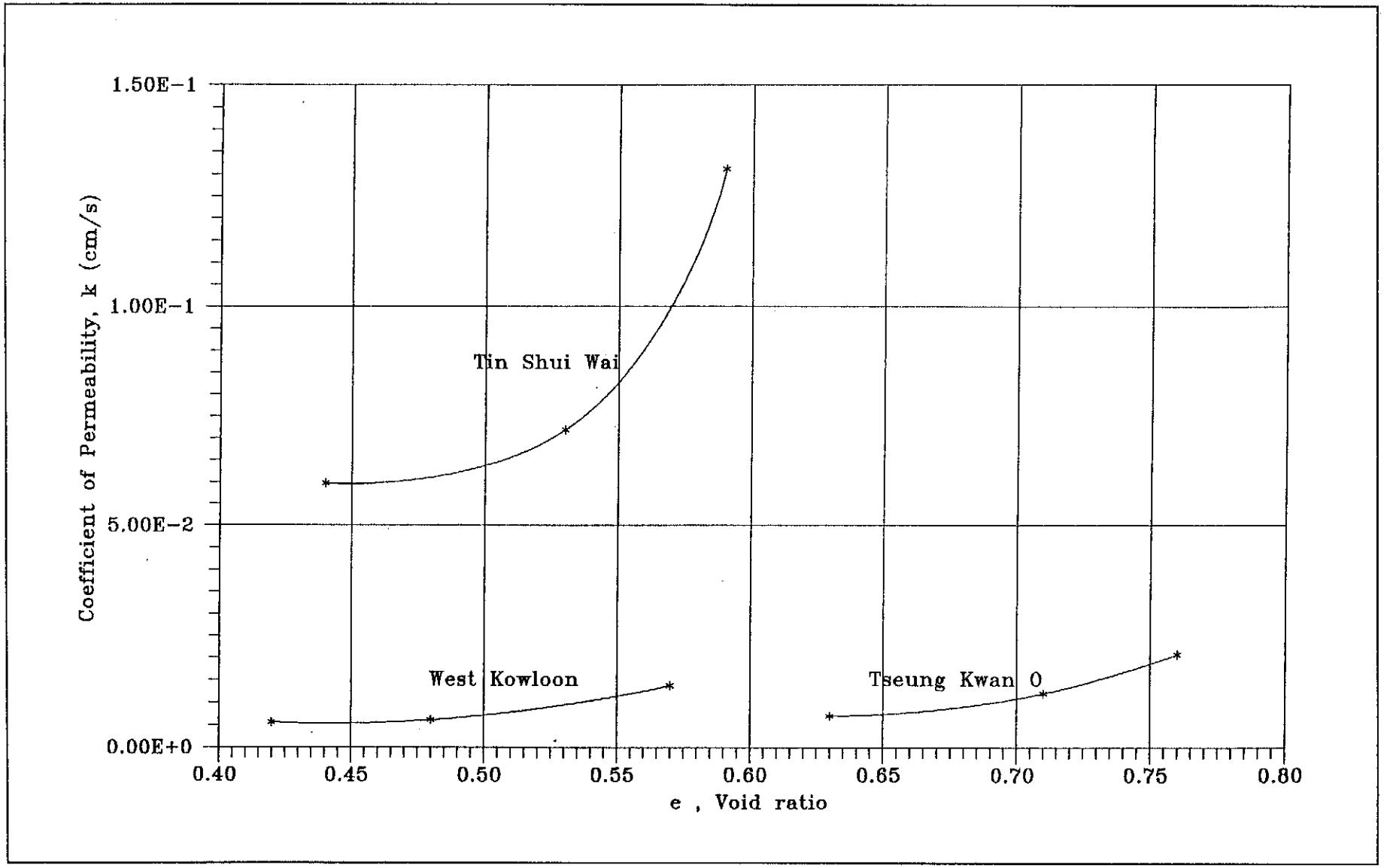

Figure 4.6 - Relationships Between Coefficient of Permeability and Void Ratio for Soils from the Three Sites

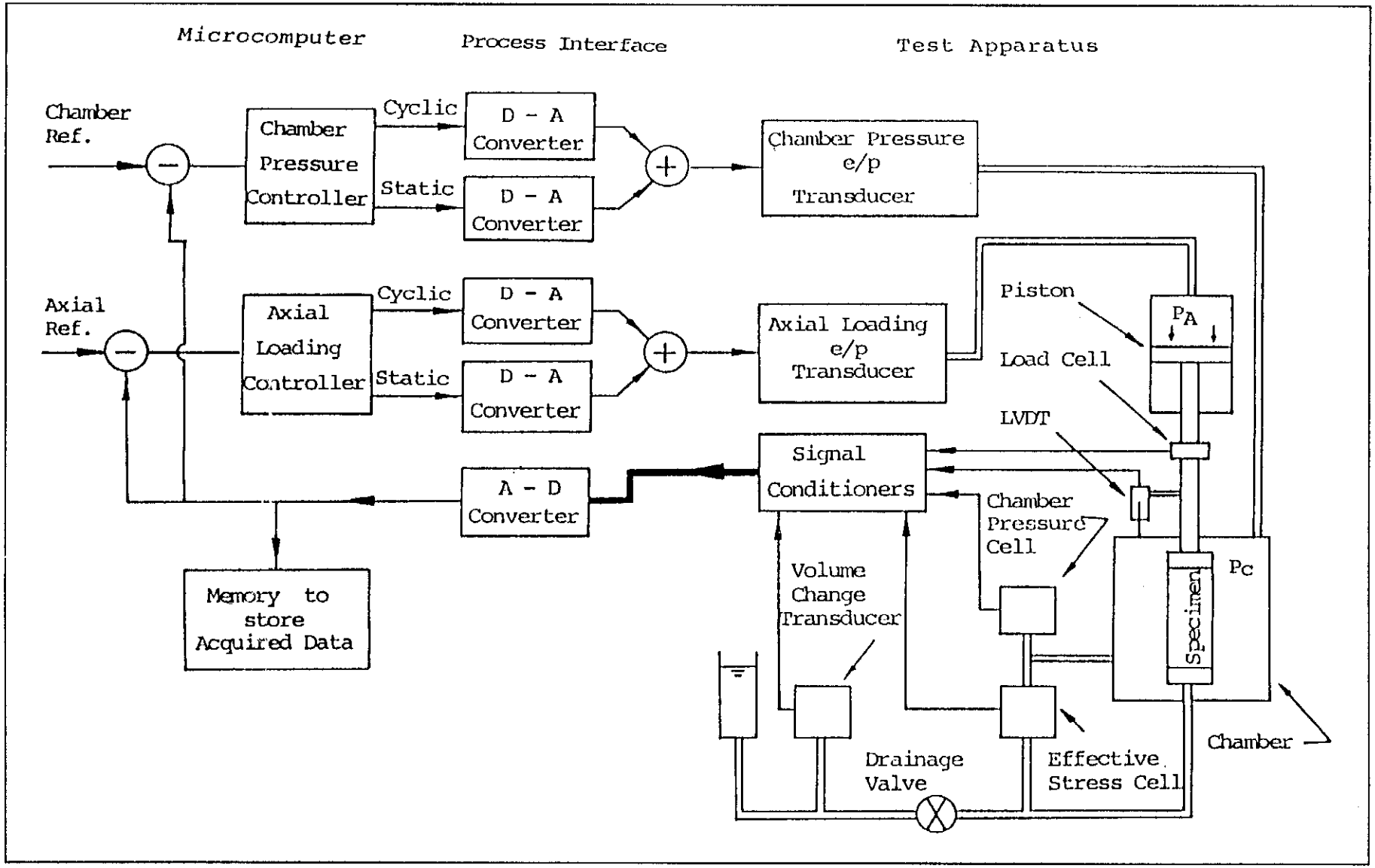

Figure 5.1 - The General Layout Assembly for Automatic Cyclic Triaxial Test System

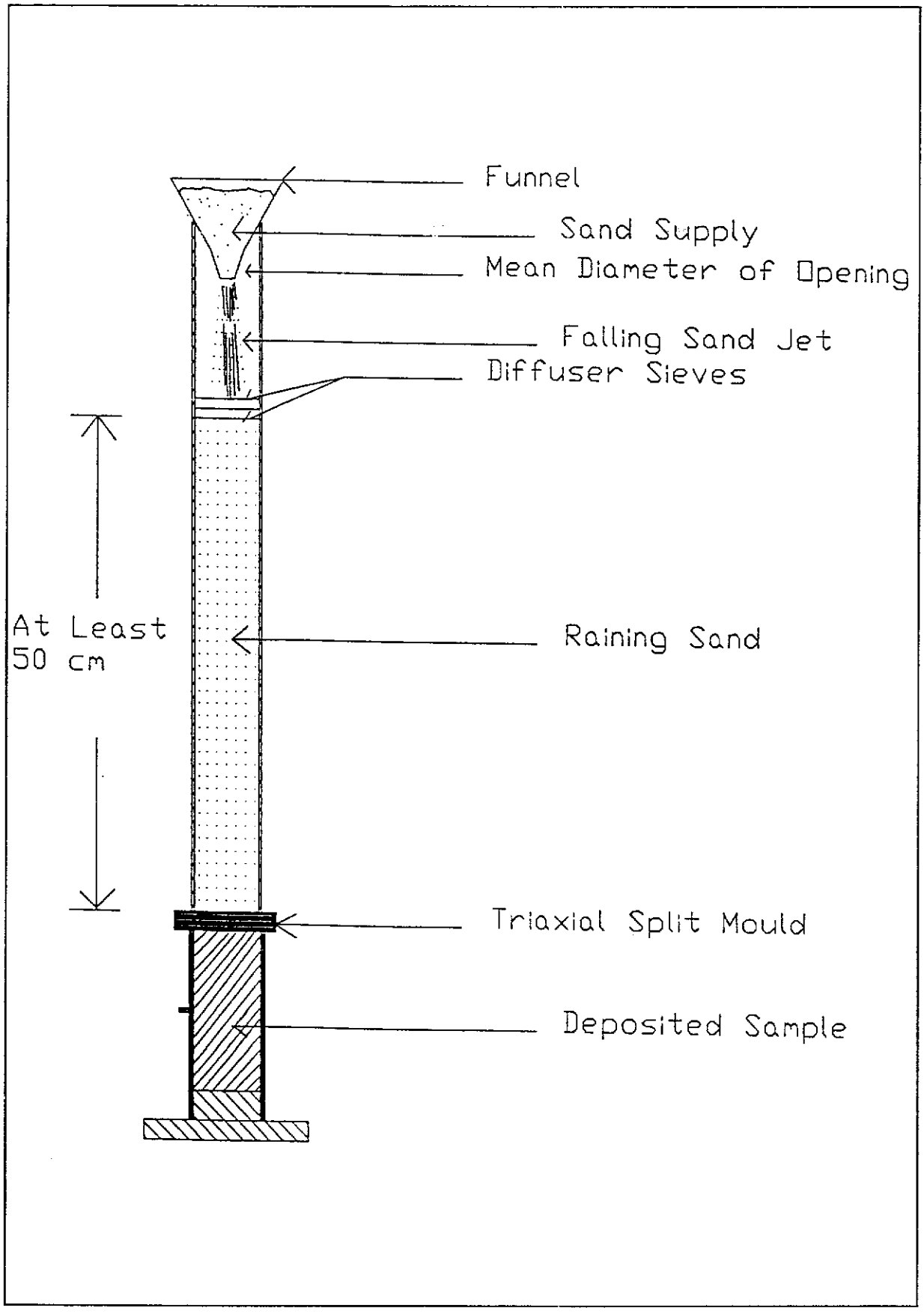

Figure 5.2 - Schematic of Sand Pluviation Apparatus

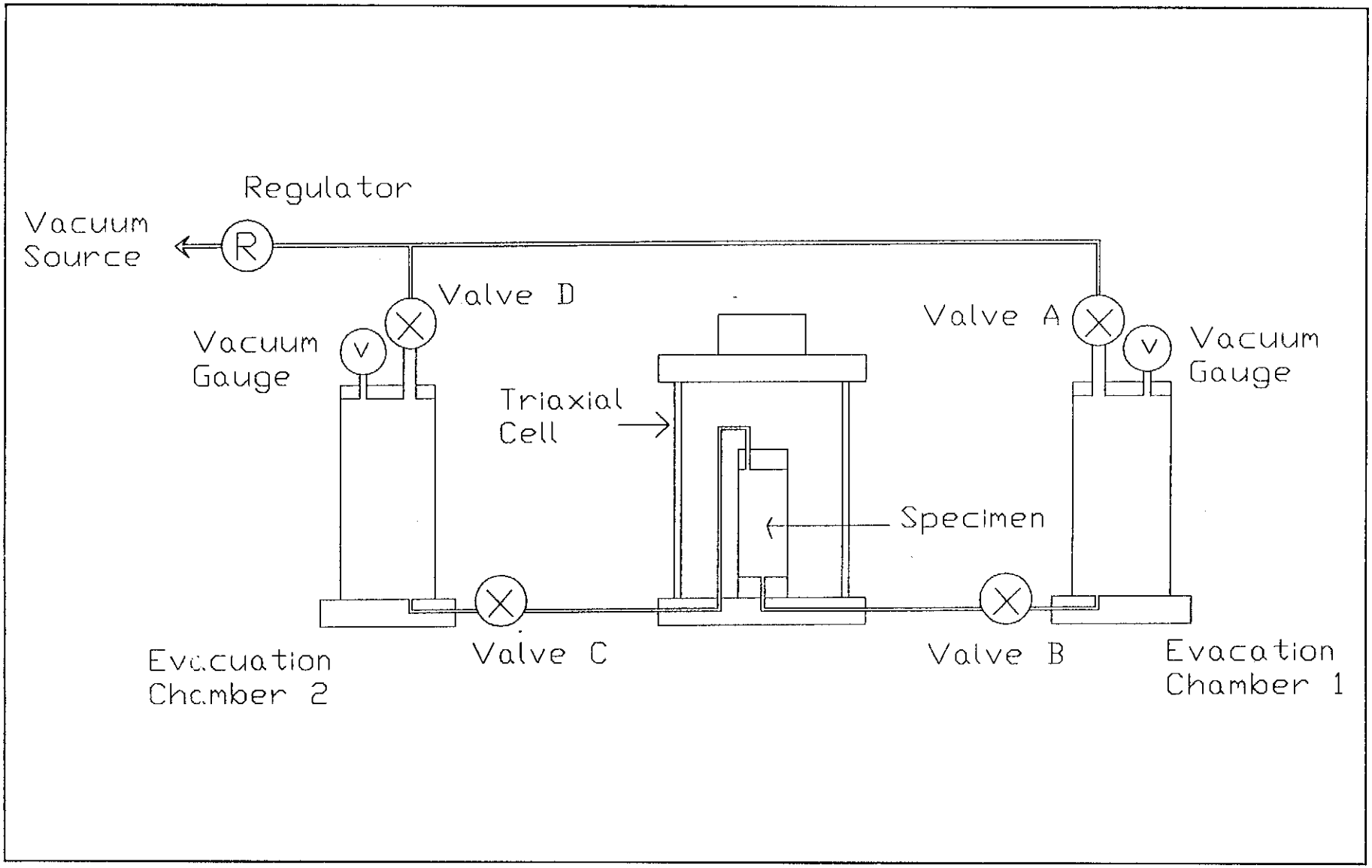

Figure 5.3 - Schematic of Dual Evacuation Chambers Method for Sample Saturation

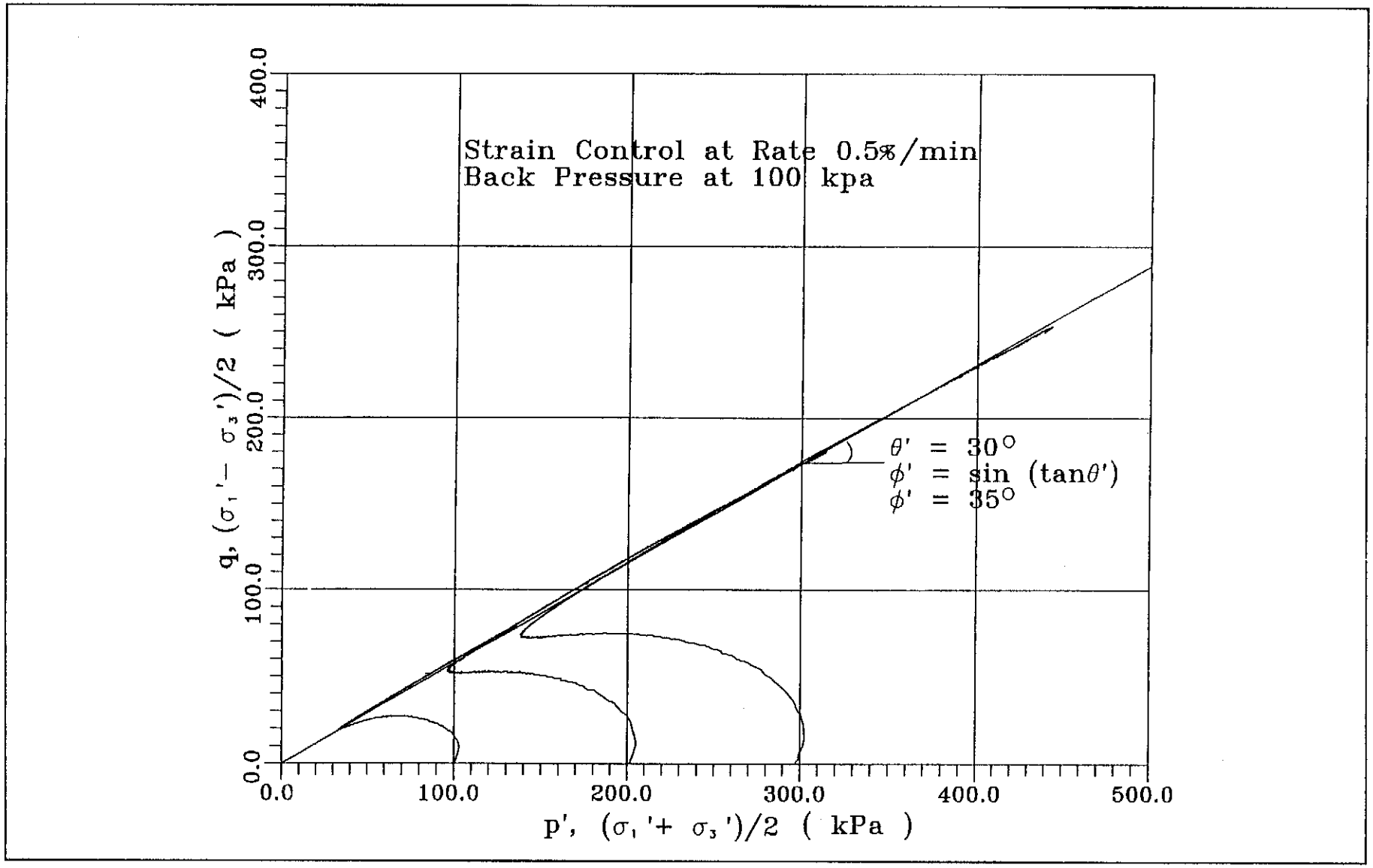

Figure 5.4 - Stress Path Plot for CS1 Sand With Relative Density (BS) about 35%

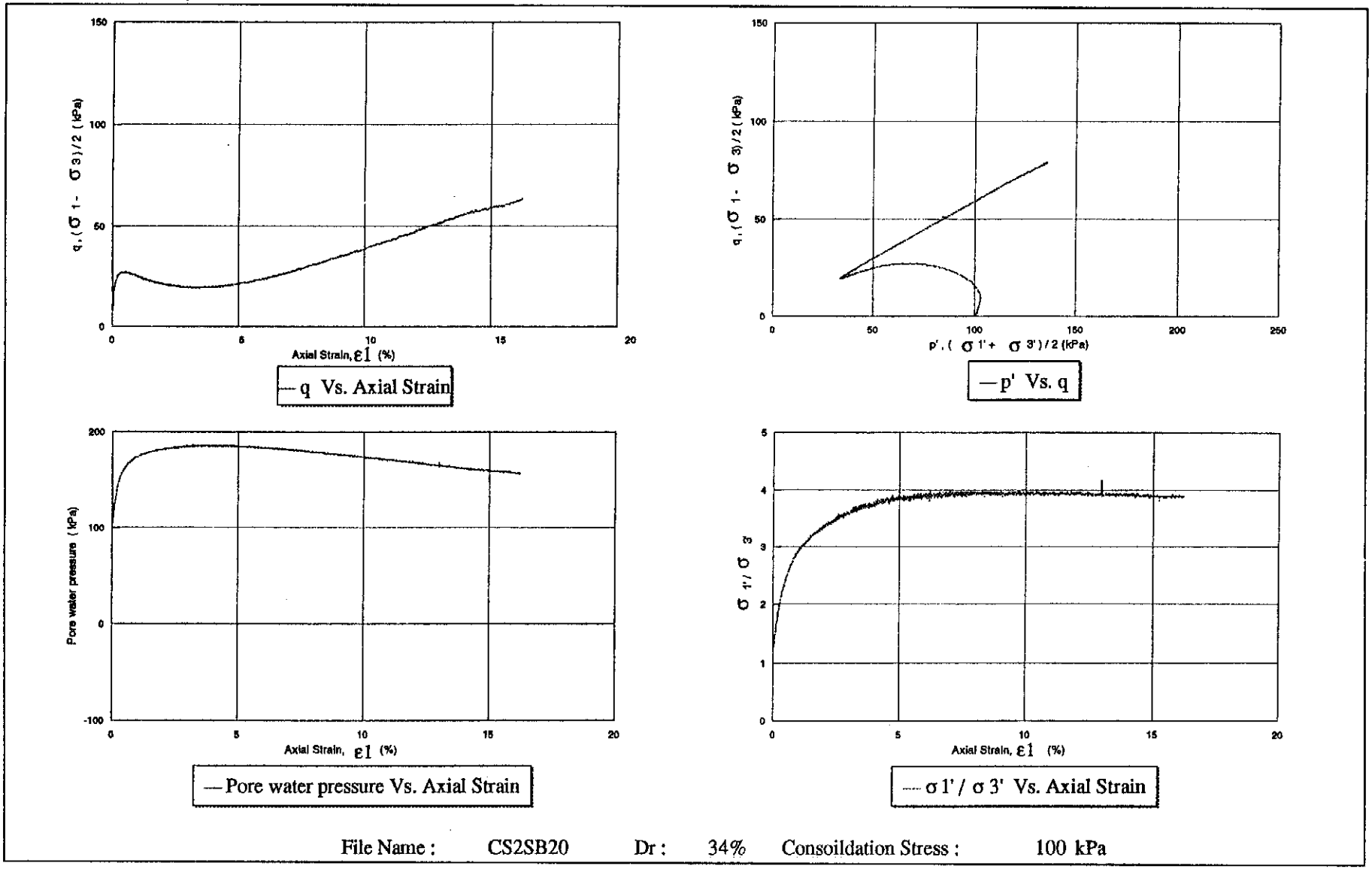

Figure 5.5 - Static Triaxial Test Results for CS1 Sample ($D_{r(BS)}$ = 34%) at Consolidation Stress = 100 kPa

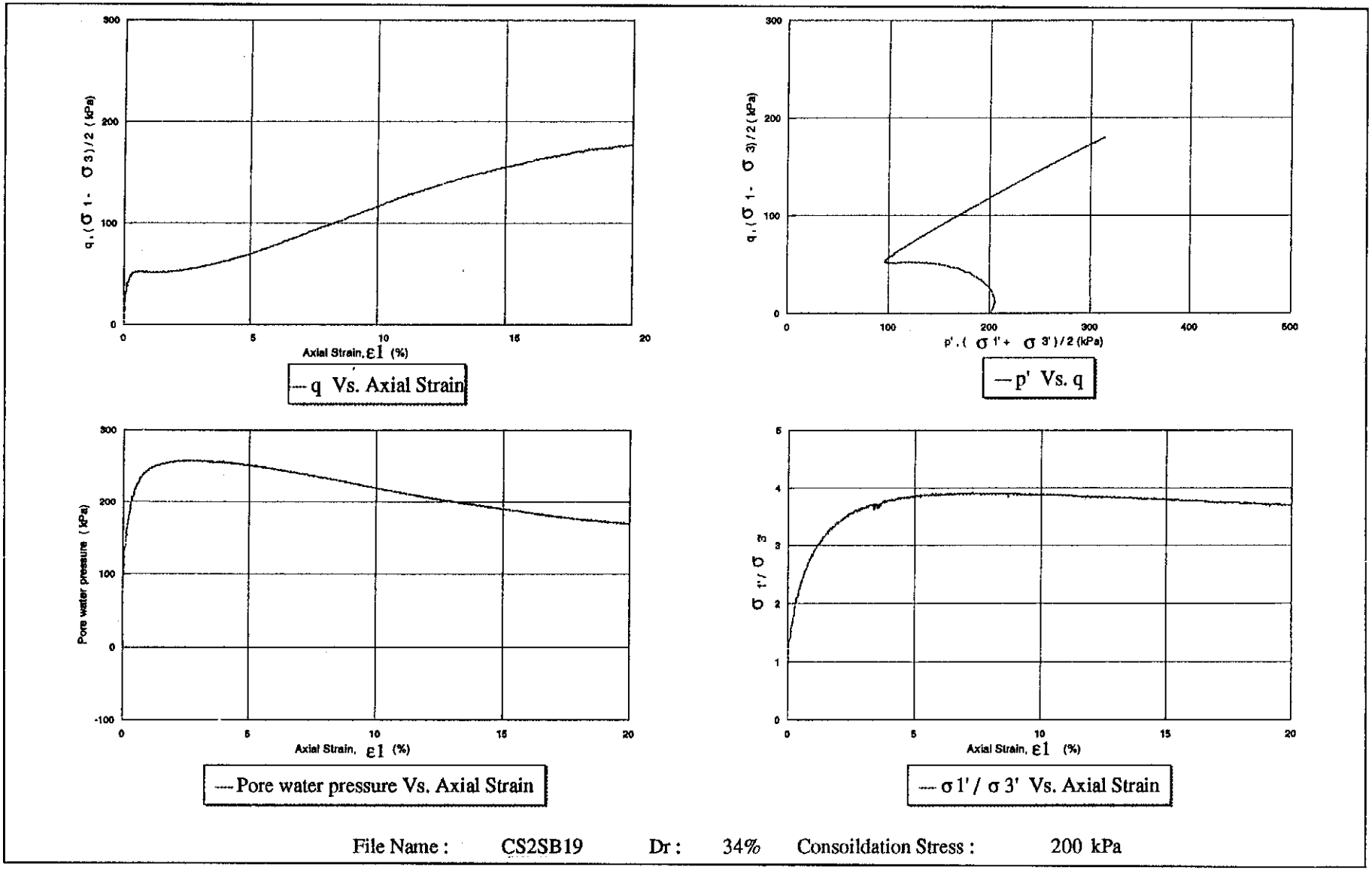

Figure 5.6 - Static Triaxial Test Results for CS1 Sample ($D_{r(BS)}$ = 34%) at Consolidation Stress = 200 kPa

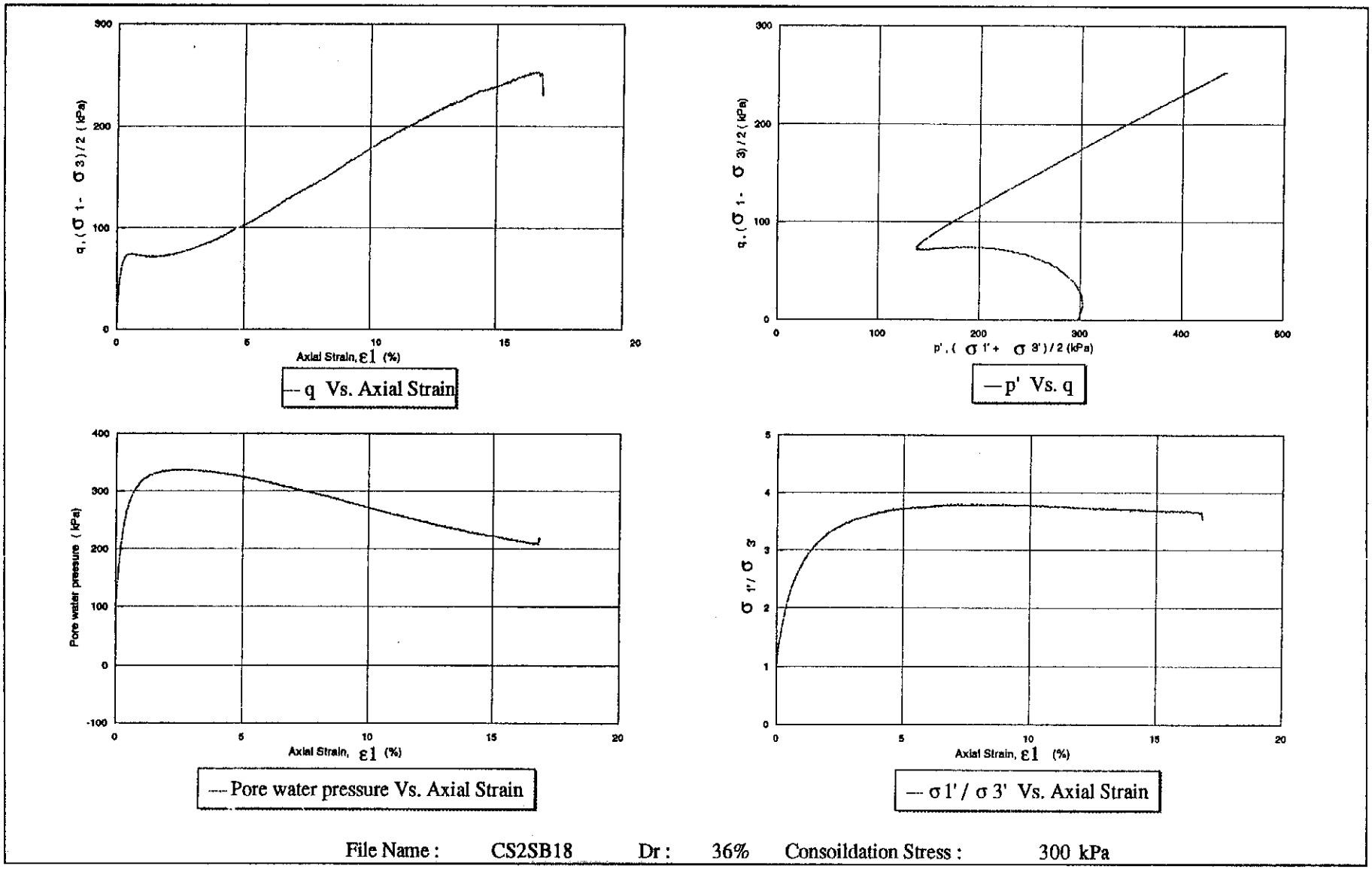

Figure 5.7 - Static Triaxial Test Results for CS1 Sample ($D_{r(BS)}$ = 36%) at Consolidation Stress = 300 kPa

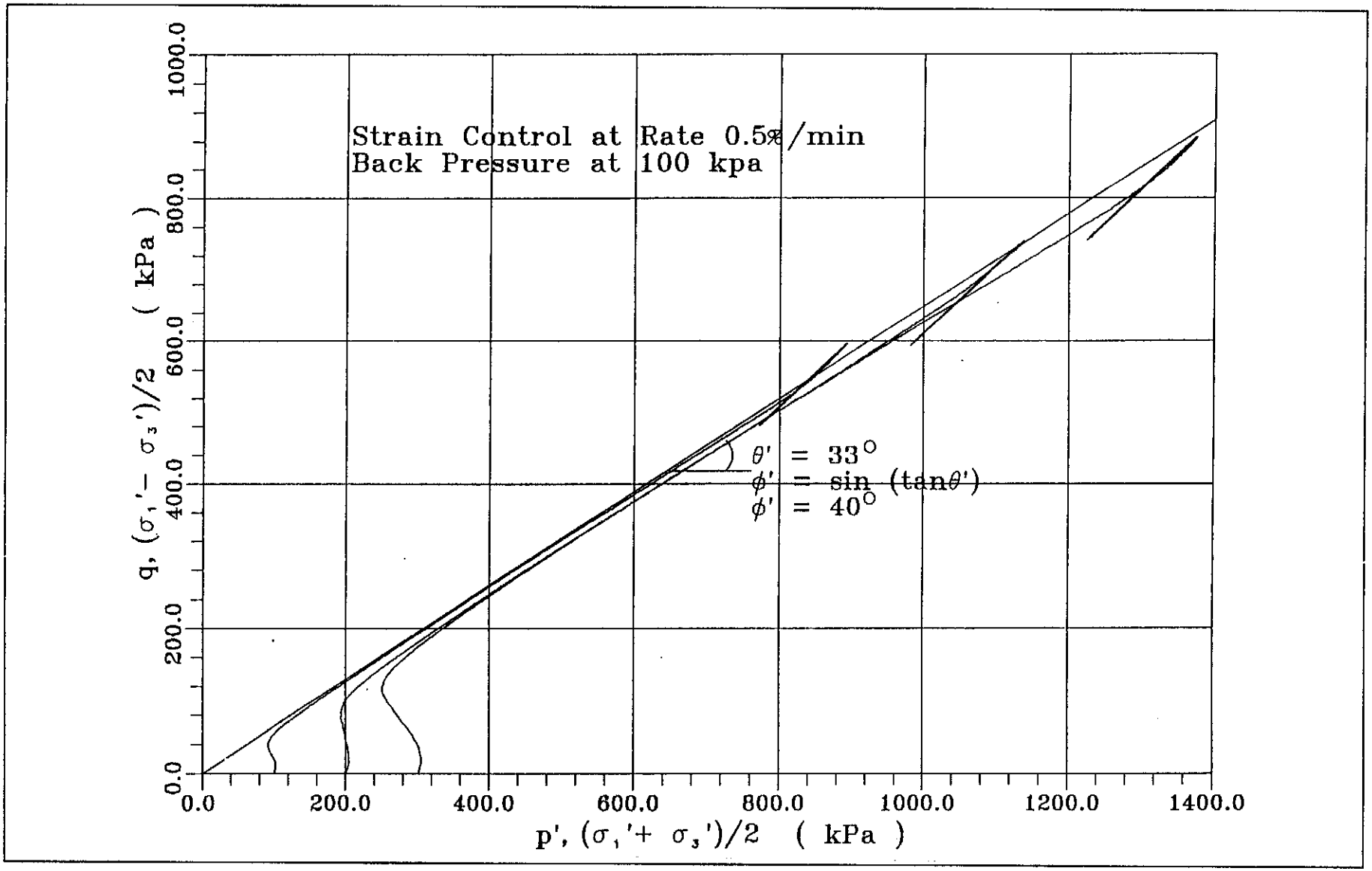

Figure 5.8 - Stress Path Plot for CS1 Sand with Relative Density (BS) about 73%

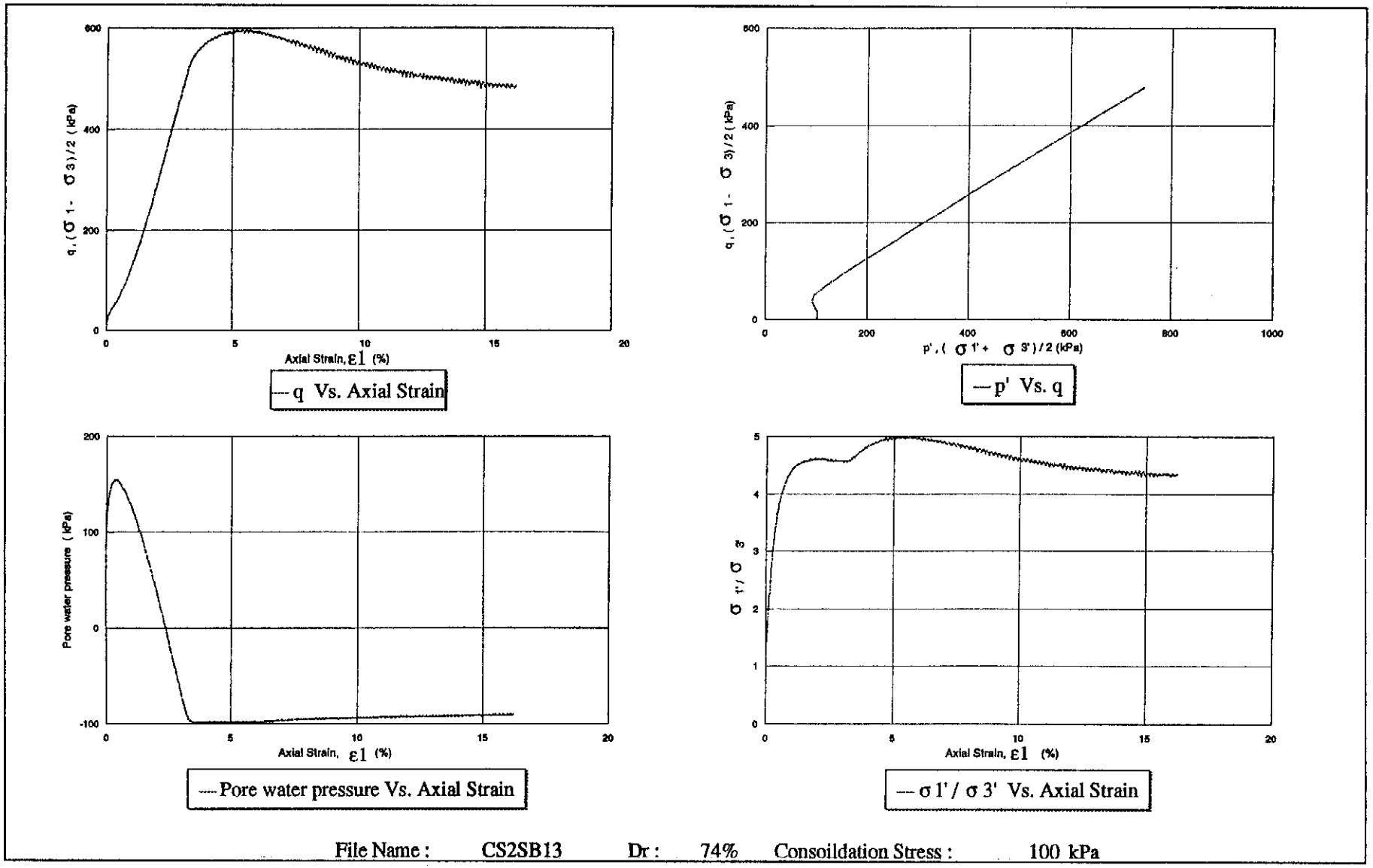

Figure 5.9 - Static Triaxial Test Results for CS1 Sample ($D_{r(BS)}$ = 74%) at Consolidation Stress = 100 kPa

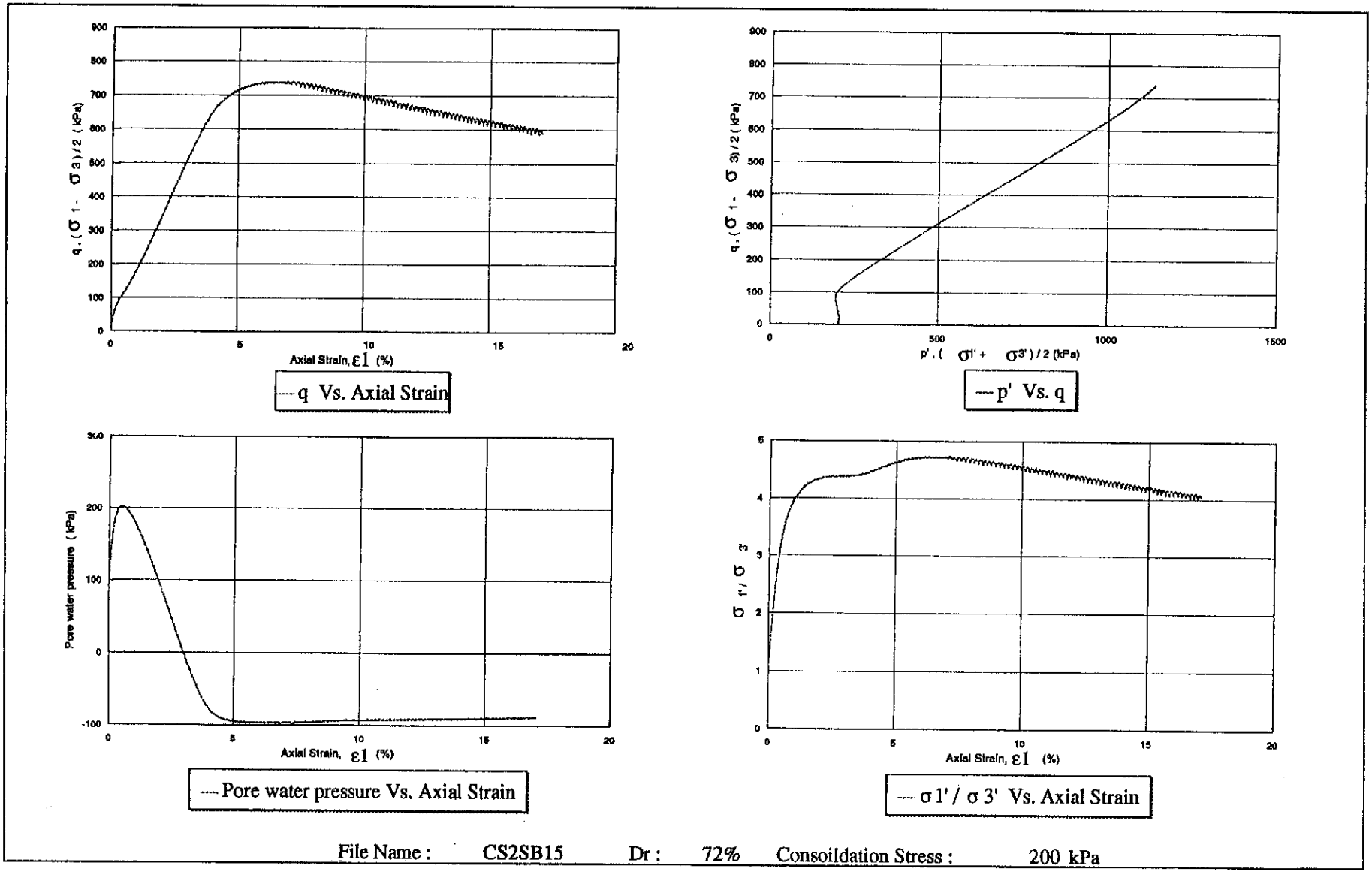

Figure 5.10 - Static Triaxial Test Results for CS1 Sample ($D_{r(BS)}$ = 72%) at Consolidation Stress = 200 kPa

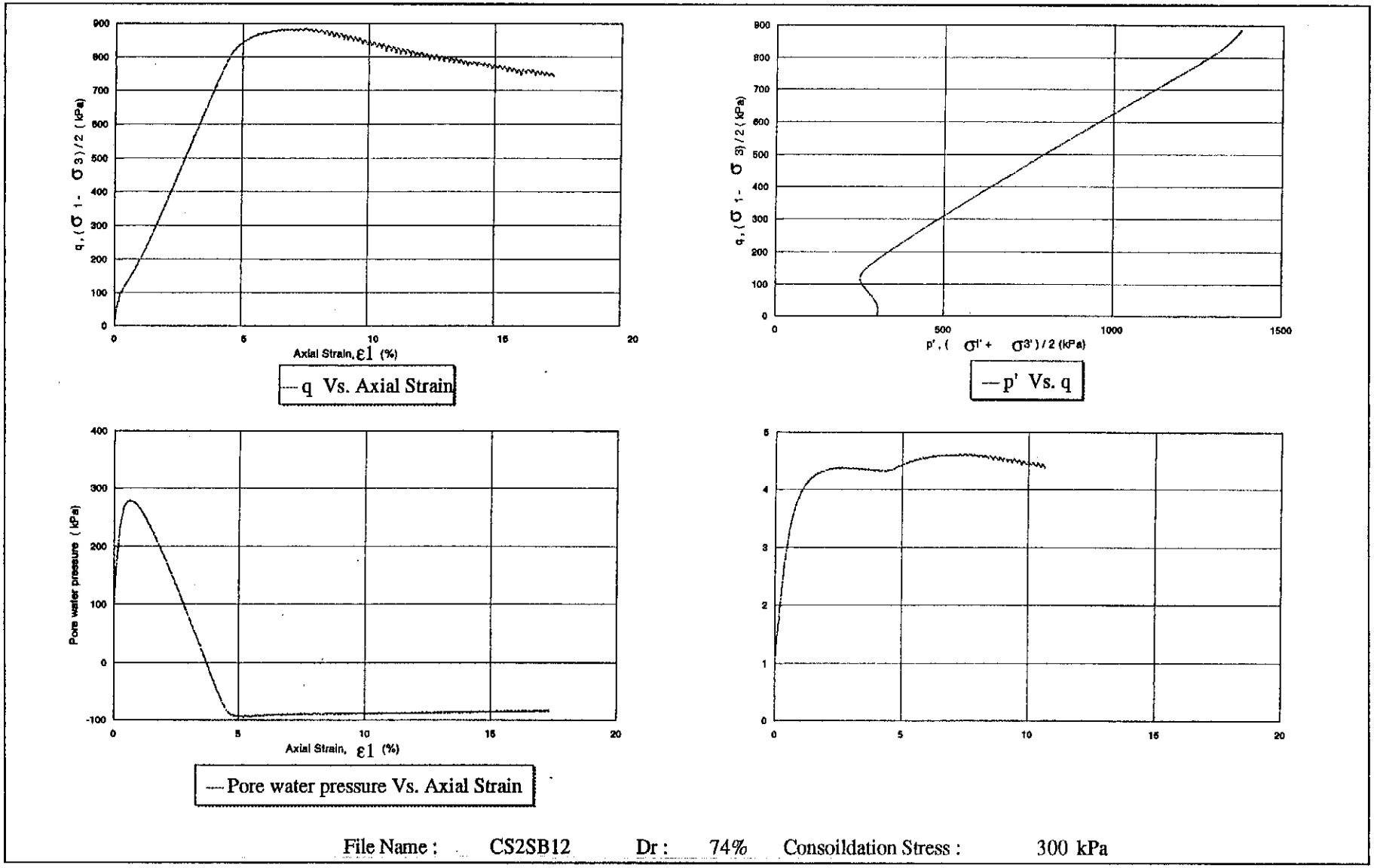

Figure 5.11 - Static Triaxial Test Results for CS1 Sample ($D_{r(BS)}$ = 73%) at Consolidation Stress = 300 kPa

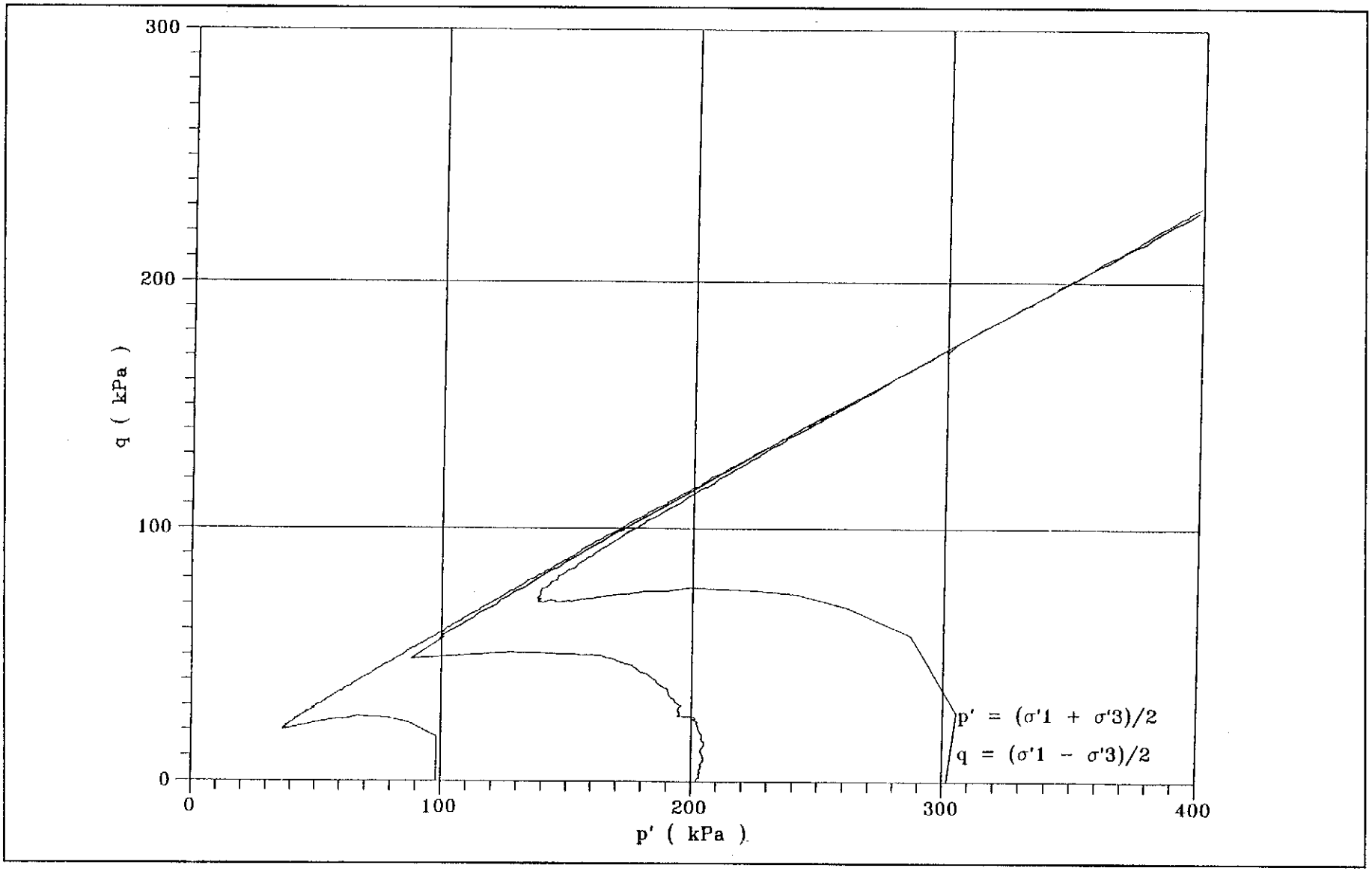

Figure 5.12 - p' Versus q' for Static Tests for TKO Sample (Average $D_{r(BS)}$ = 36.5%)

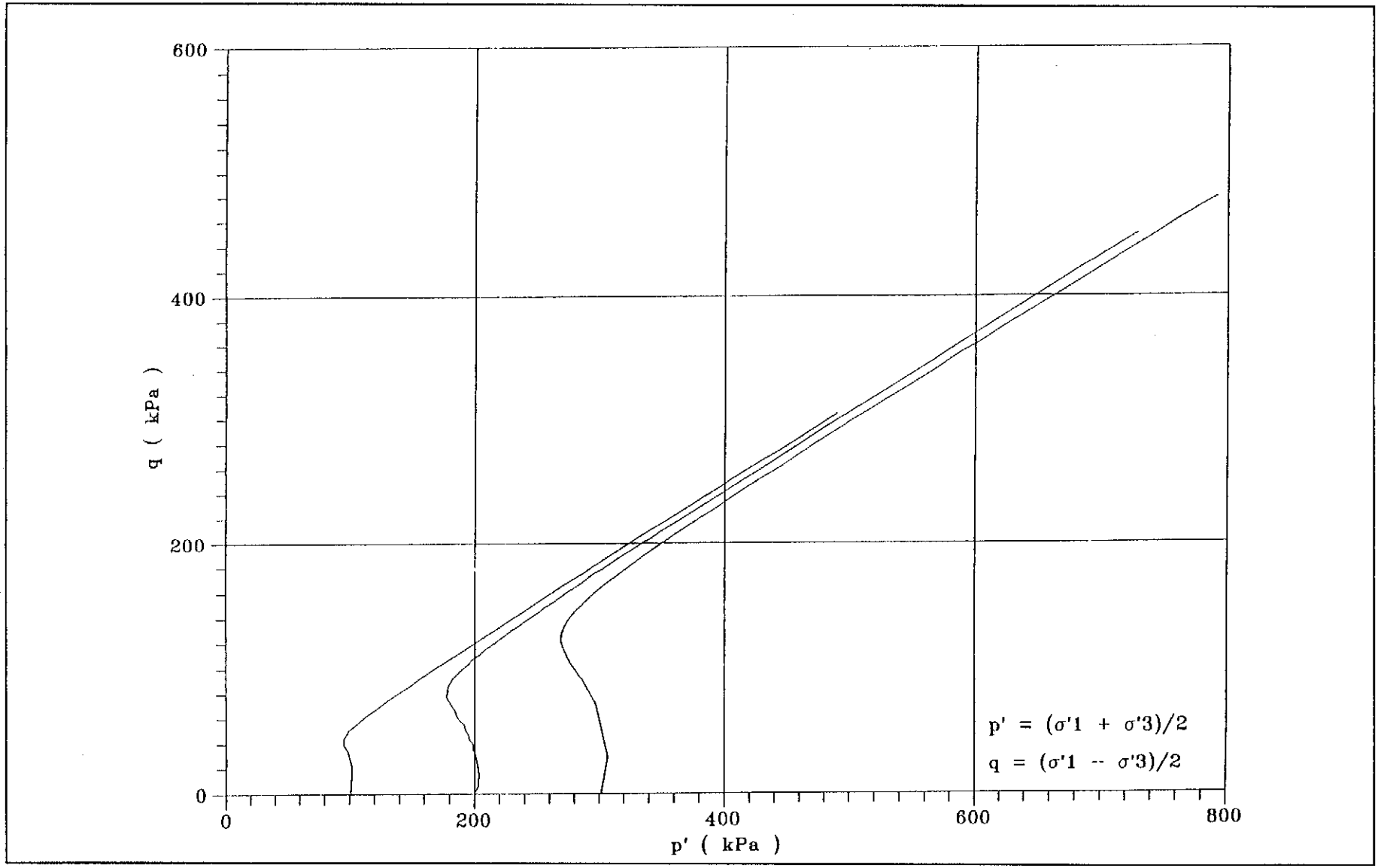

Figure 5.13 - p' Versus q' for Static Tests for TKO Sample (Average $D_{r(BS)}$ = 68.5%)

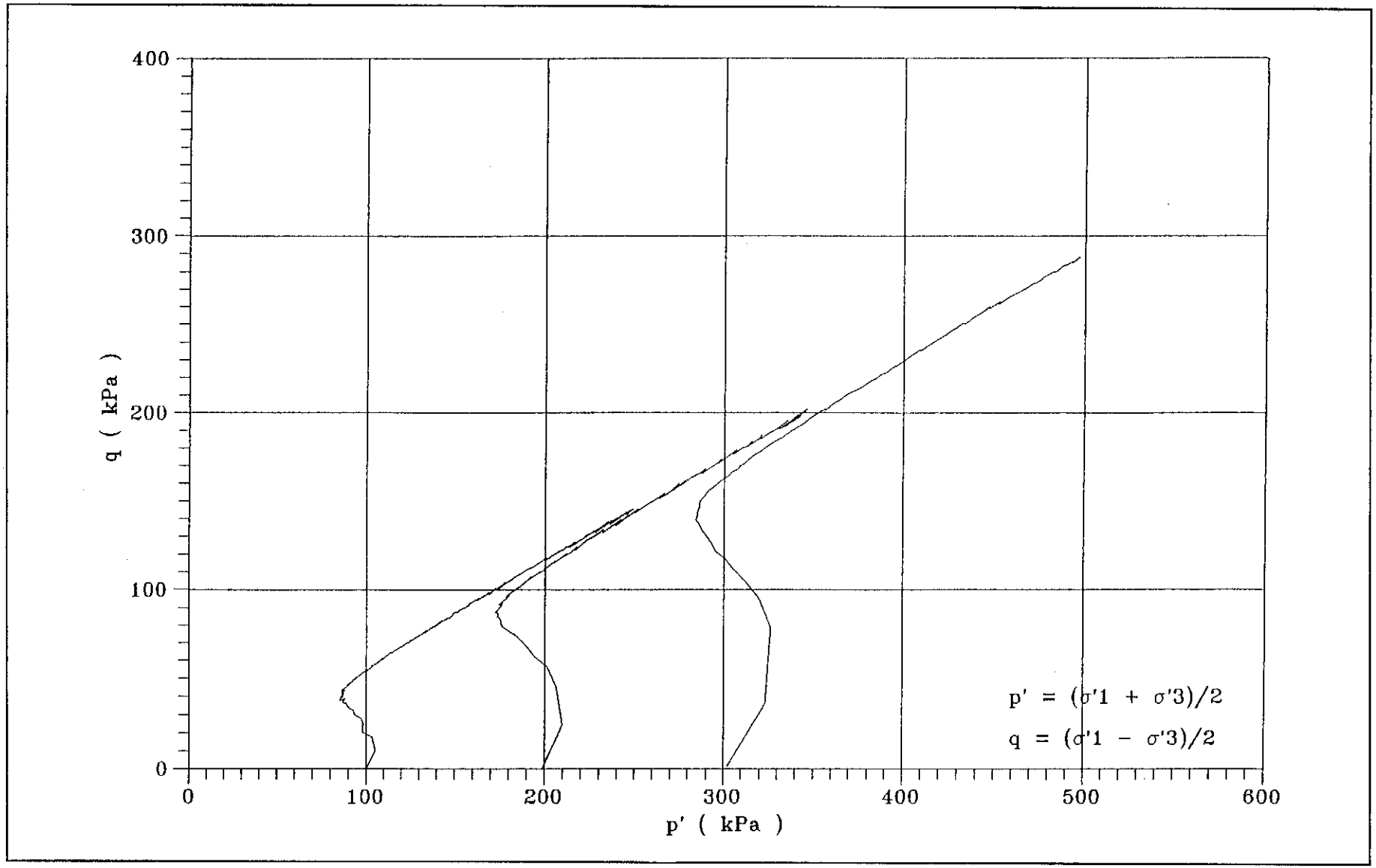

Figure 5.14 - p' Versus q' for Static Tests for TSW Sample (Average $D_{r(BS)}$ = 38.5%)

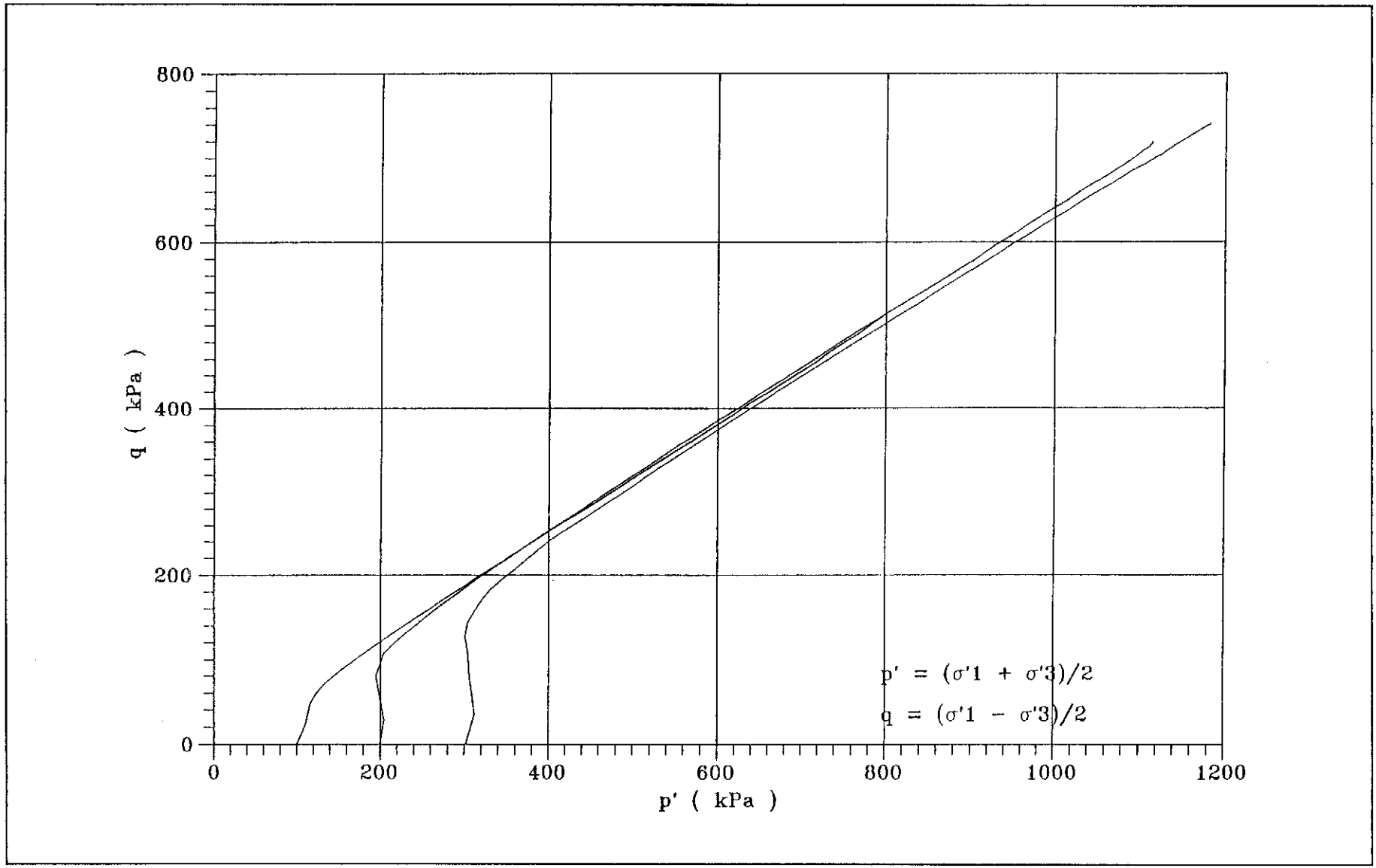

Figure 5.15 - p' Versus q' for Static Tests for TSW Sample (Average $D_{r(BS)}$ = 68.9%)

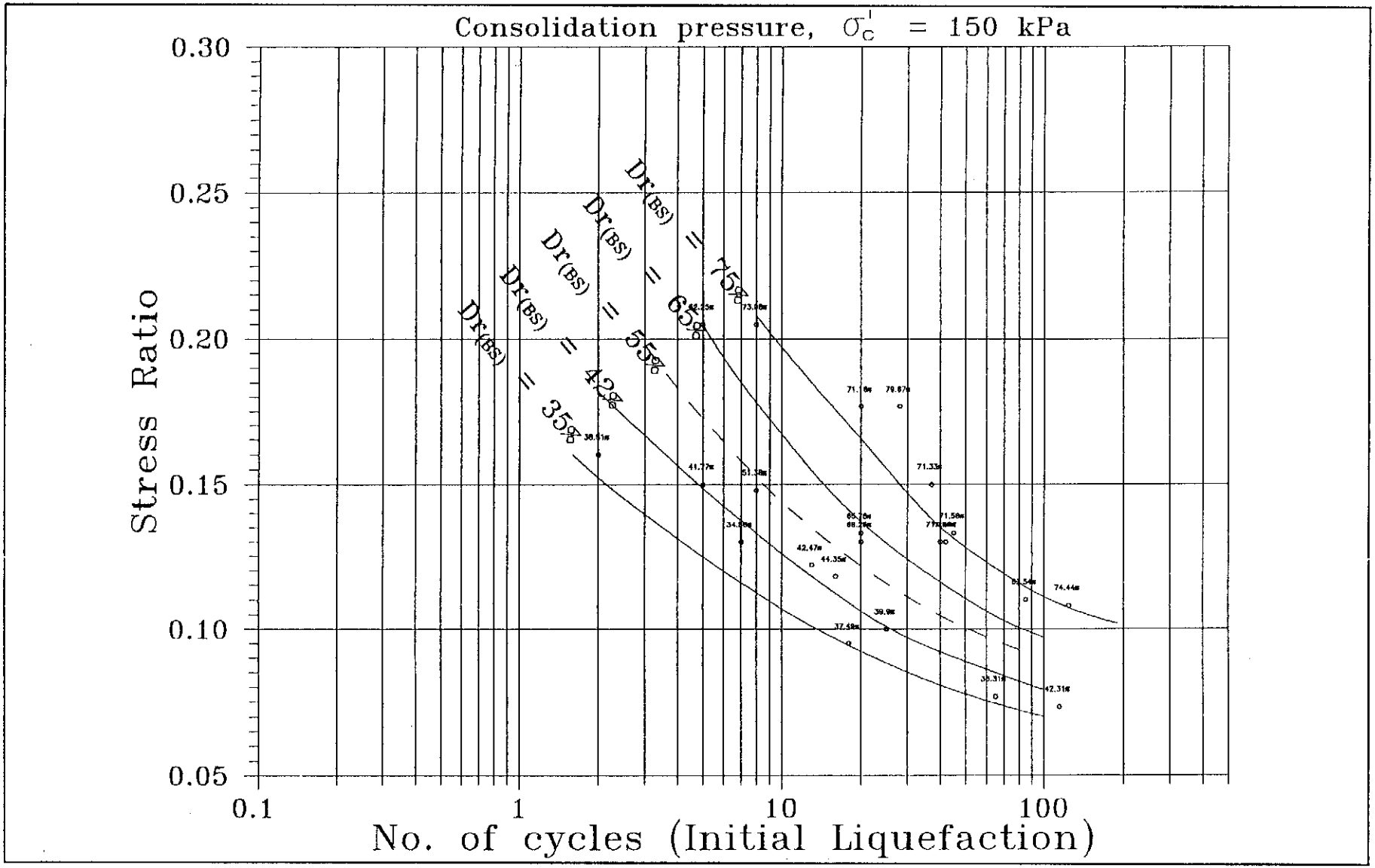

Figure 5.16 - Normalized Liquefaction Curves for Samples Obtained from the West Kowloon Reclamation Site

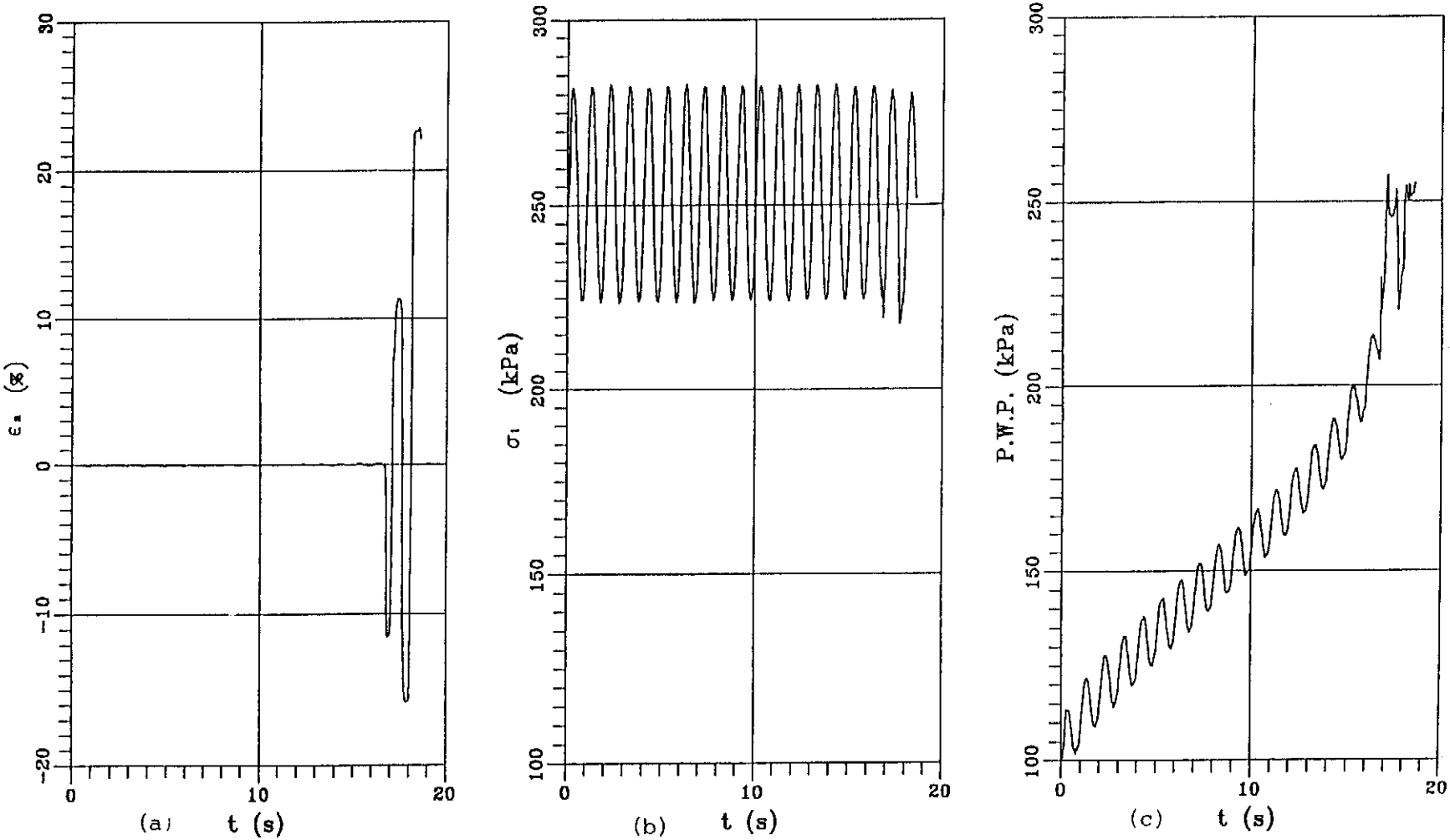

Note : Relative density = 37.49%; Stress ratio = 0.095

Figure 5.17 - Typical Result of Dynamic Triaxial Loading Test on CS1 Loose Sand (Sheet 1 of 3)

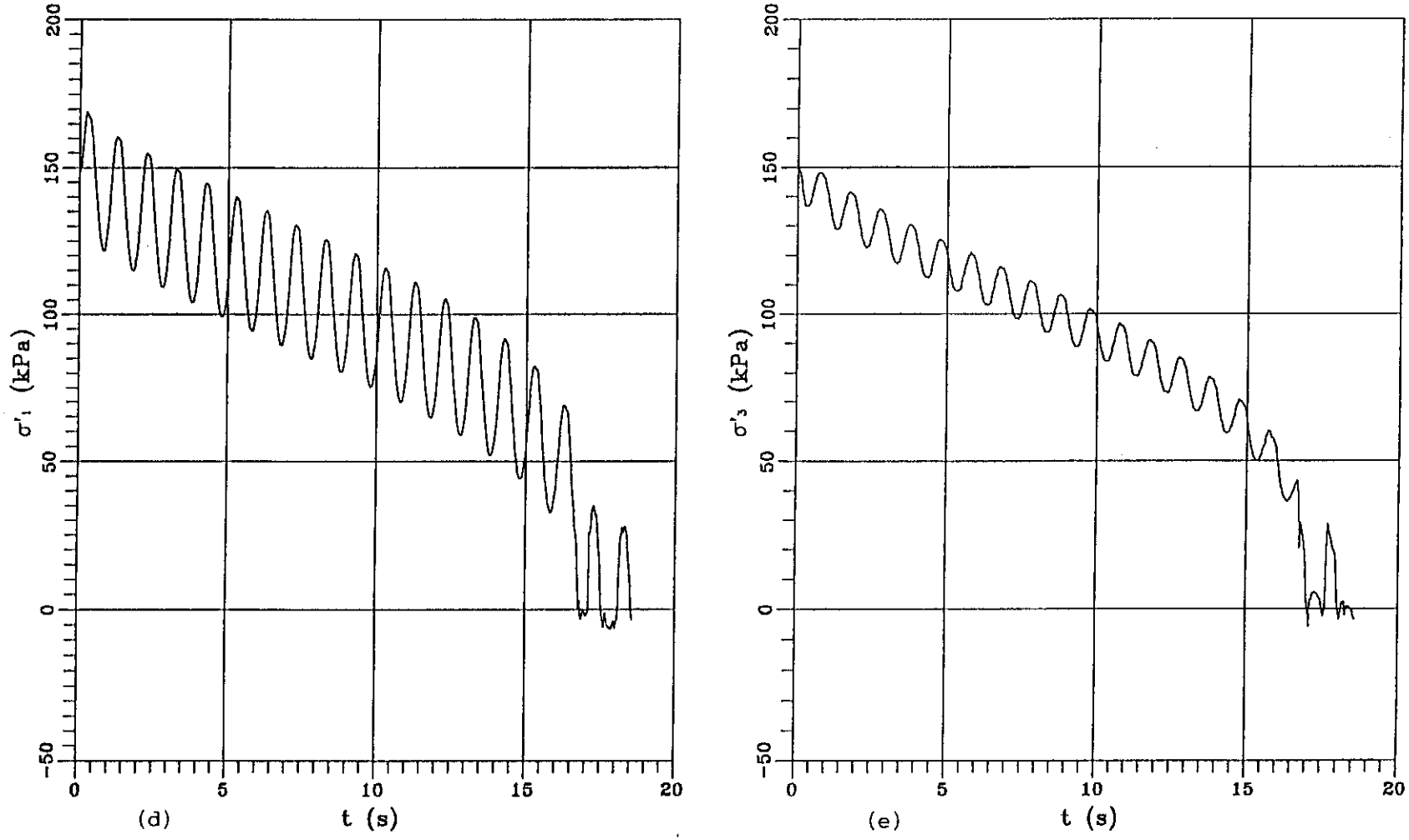

Note : Relative density = 37.49%; Stress ratio = 0.095

Figure 5.17 - Typical Result of Dynamic Triaxial Loading Test on CS1 Loose Sand (Sheet 2 of 3)

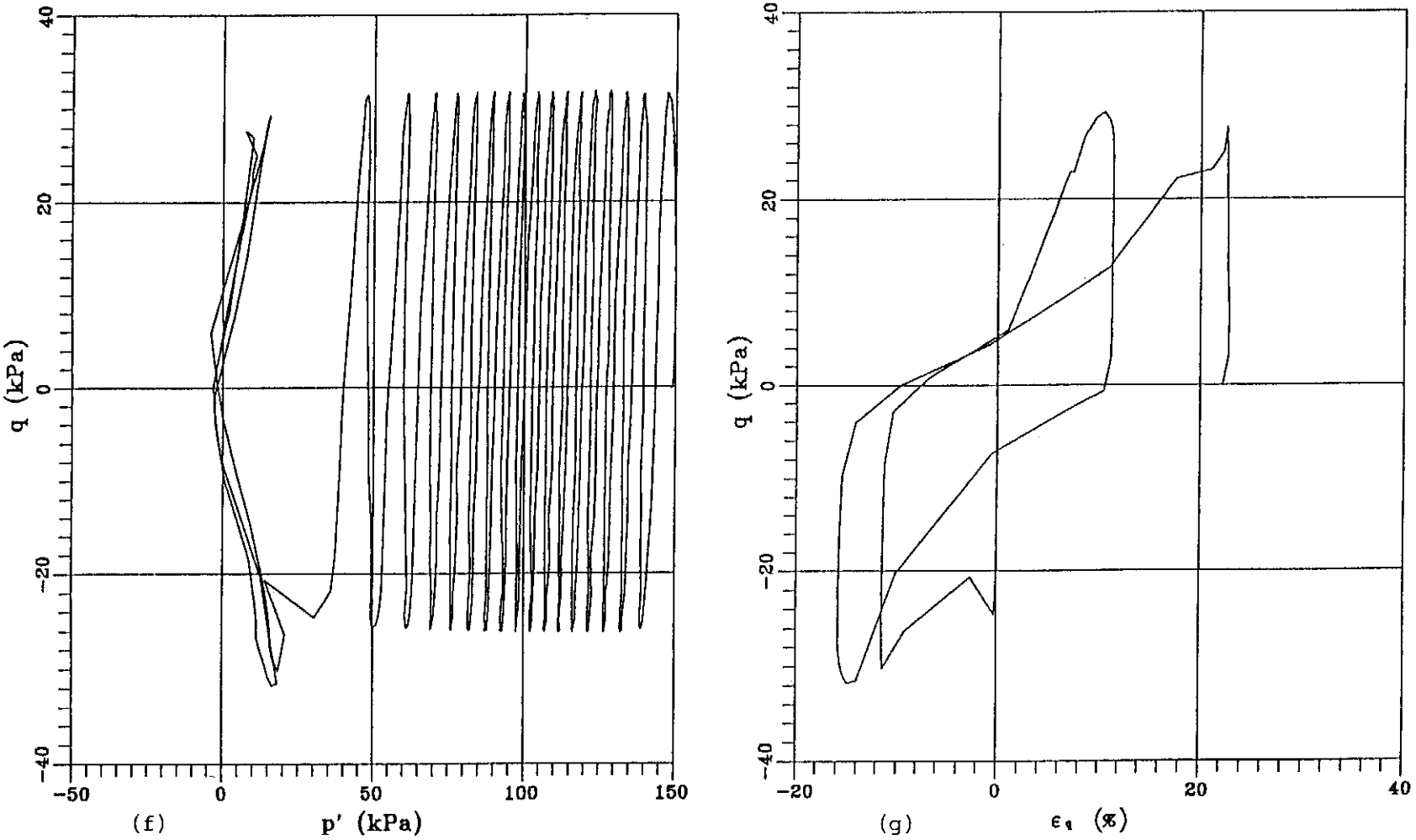

Note : Relative density = 37.49%; Stress ratio = 0.095

Figure 5.17 - Typical Result of Dynamic Triaxial Loading Test on CS1 Loose Sand (Sheet 3 of 3)

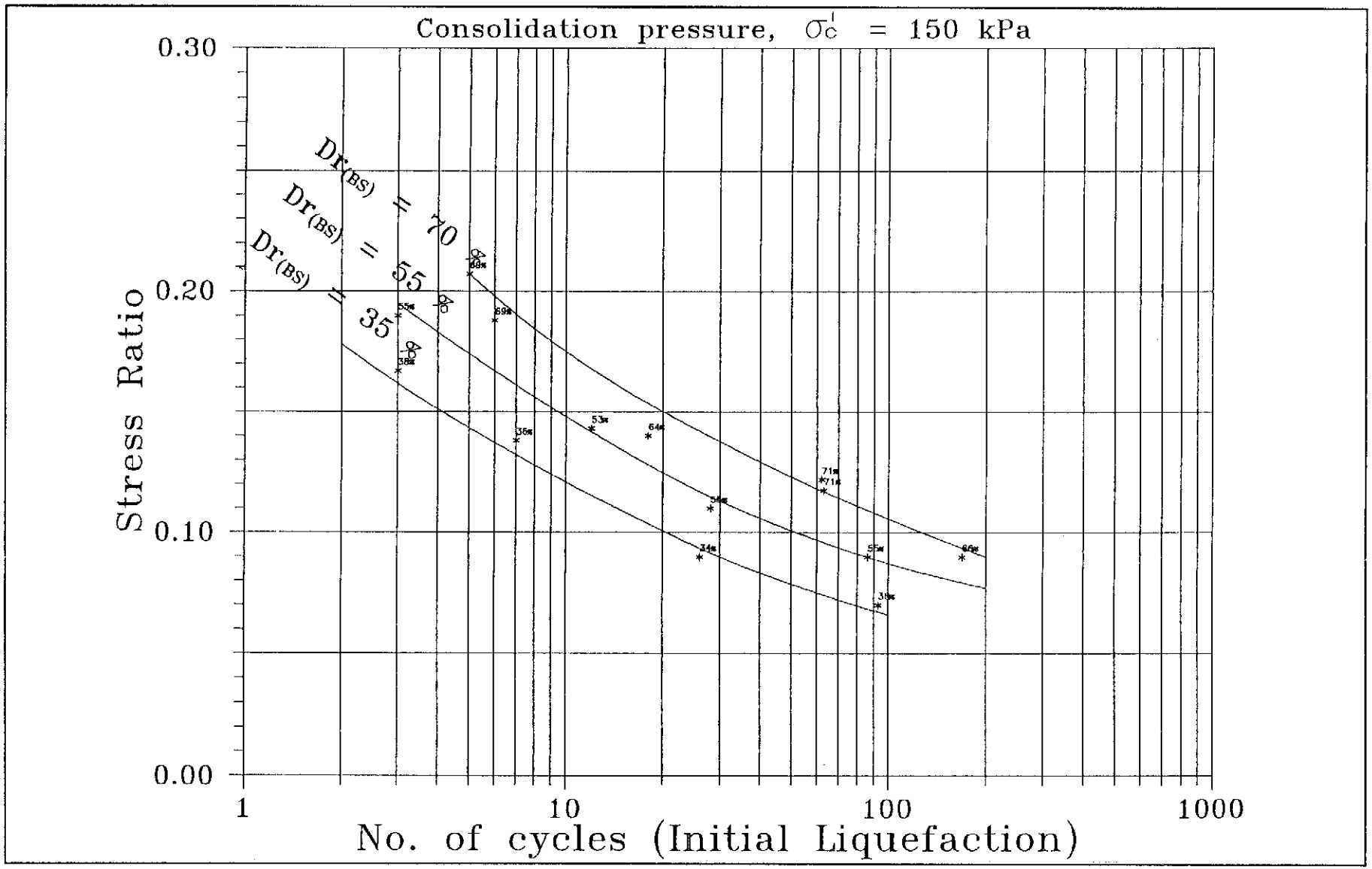

Figure 5.18 - Normalized Liquefaction Curves for Samples Obtained from the Tseung Kwan O Reclamation Site

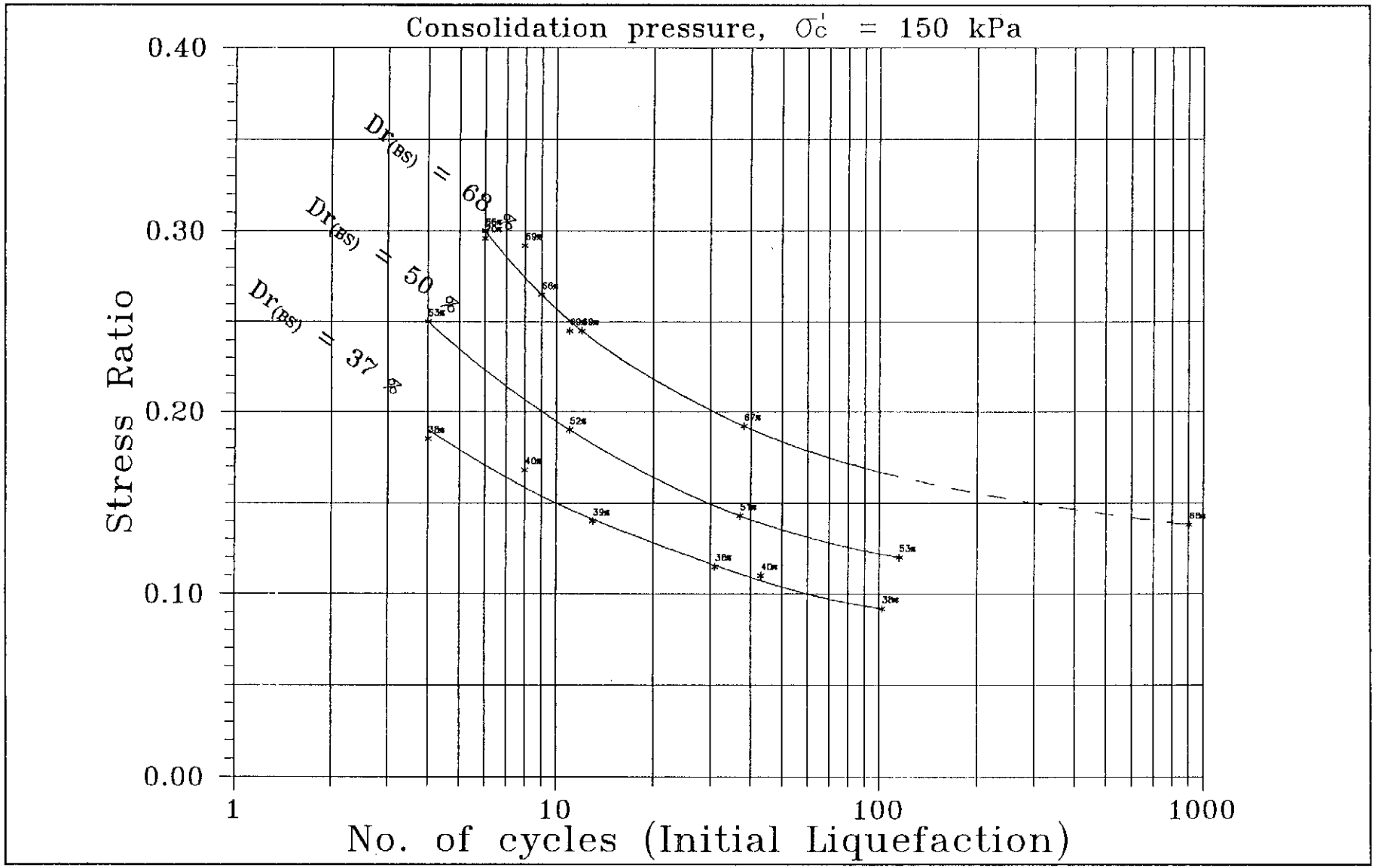

Figure 5.19 - Normalized Liquefaction Curves for Samples Obtained from the Tin Shui Wai Reclamation Site

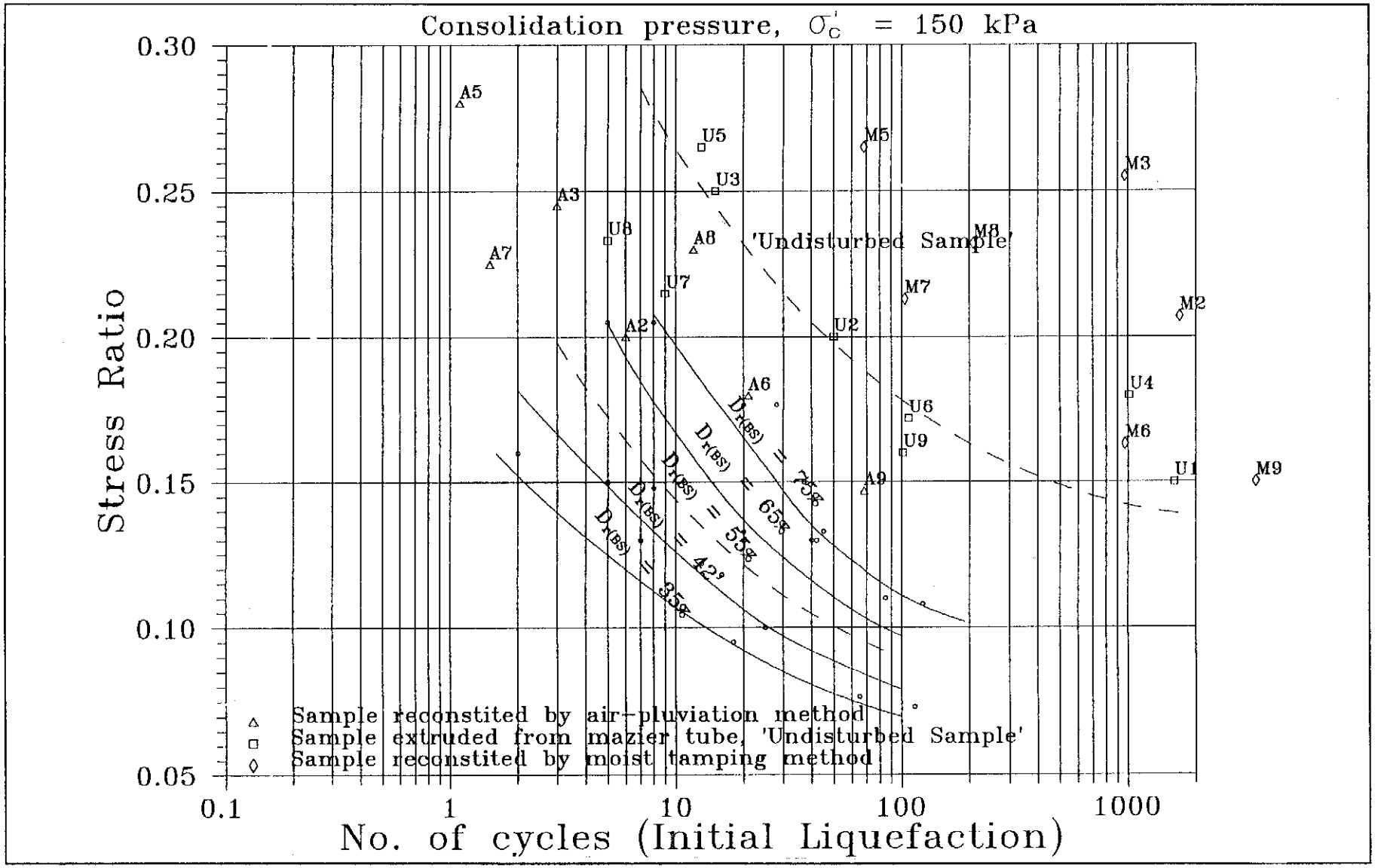

Figure 5.20 - Normalized Liquefaction Curves for Samples Obtained from the West Kowloon Reclamation Site

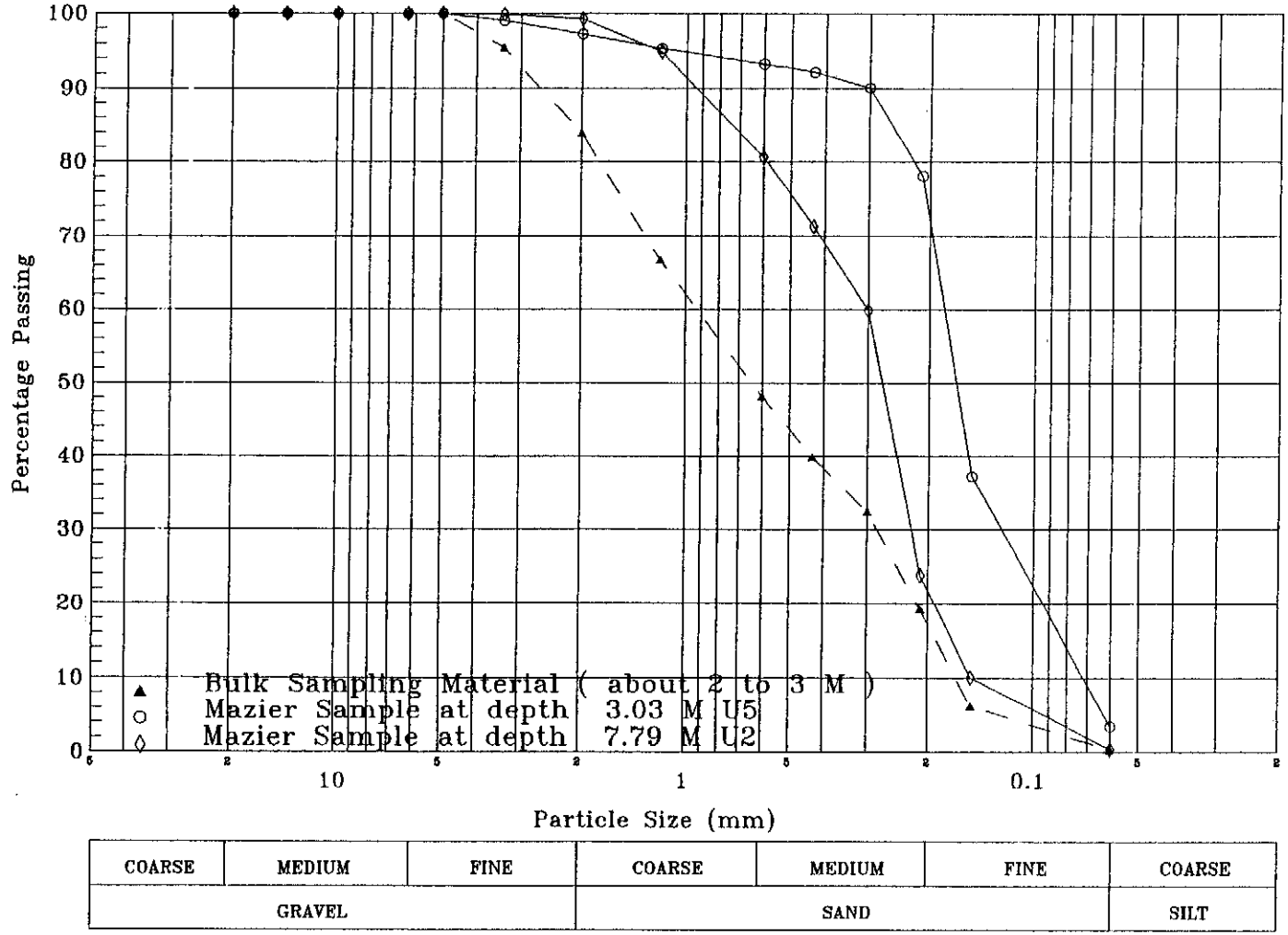

Figure 5.21 - Grain Size Variation of Mazier Samples at Different Depths (CS1)

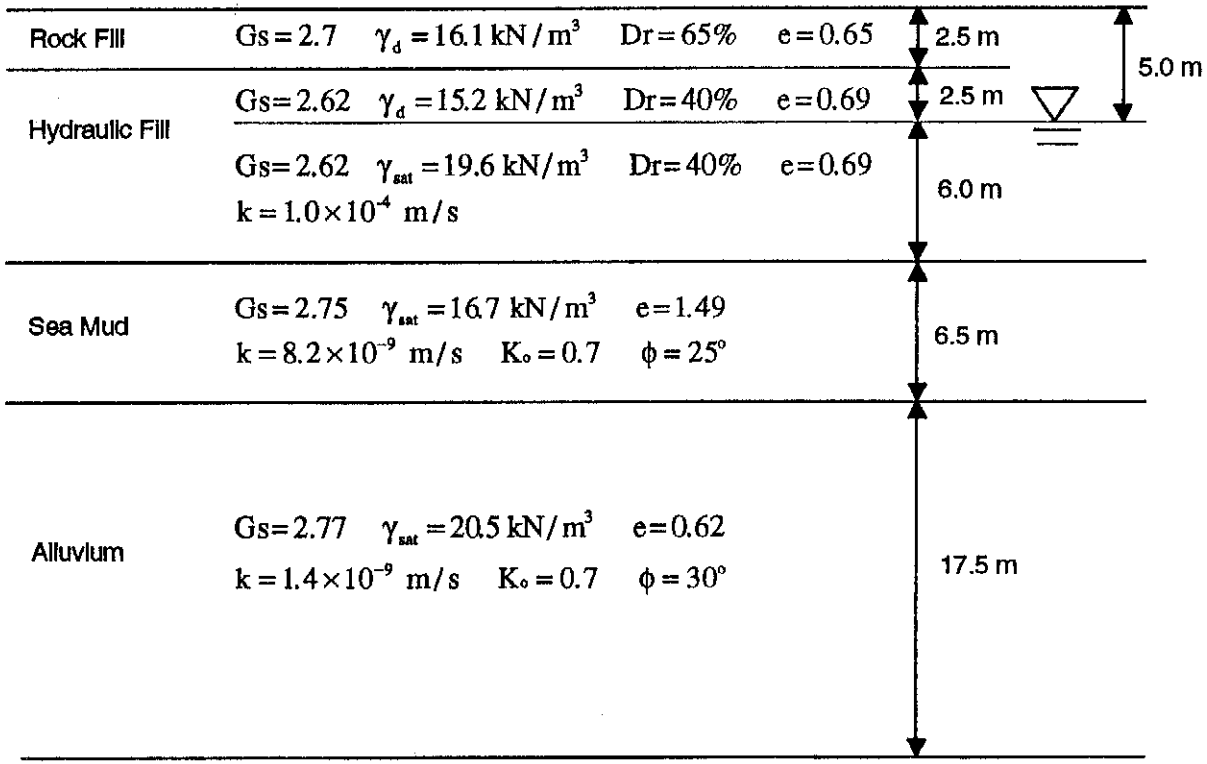

Figure 6.1 - Soil Profile of TKO Site Used in the Analysis

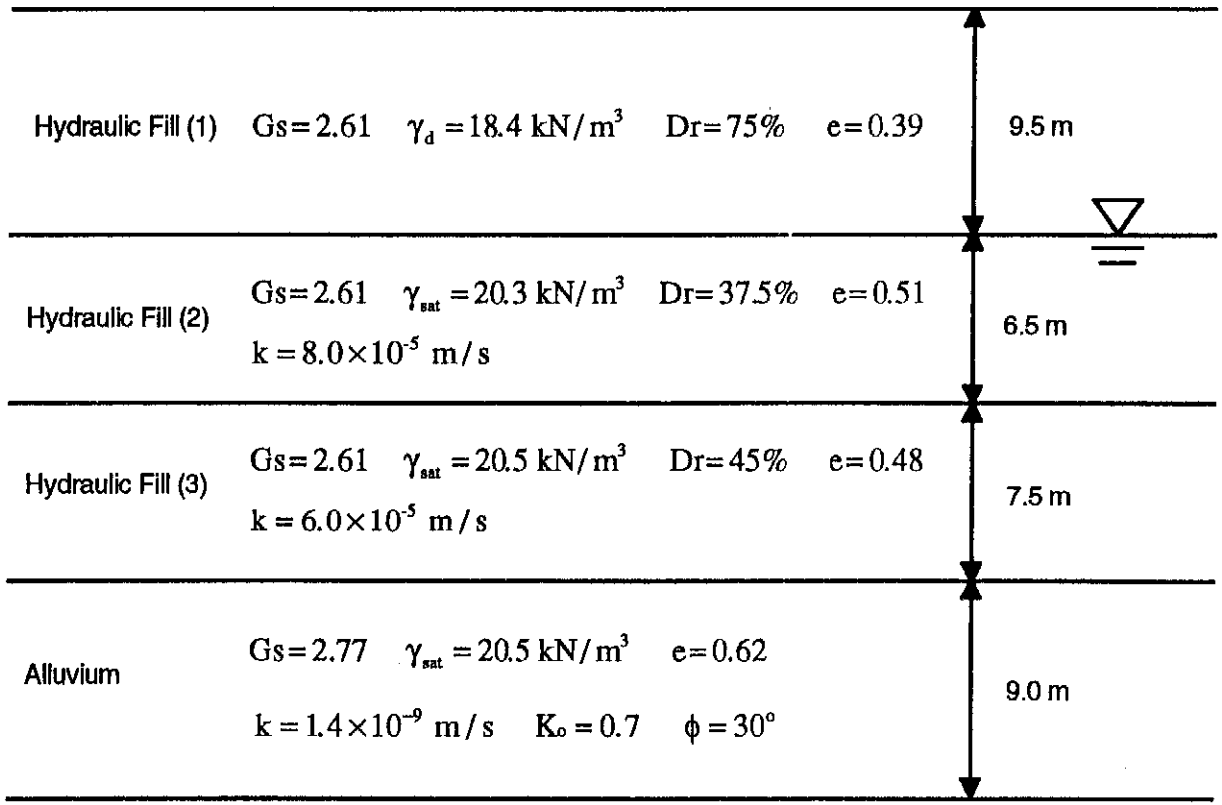

Figure 6.2 - Soil Profile of CS1 Site Used in the Analysis

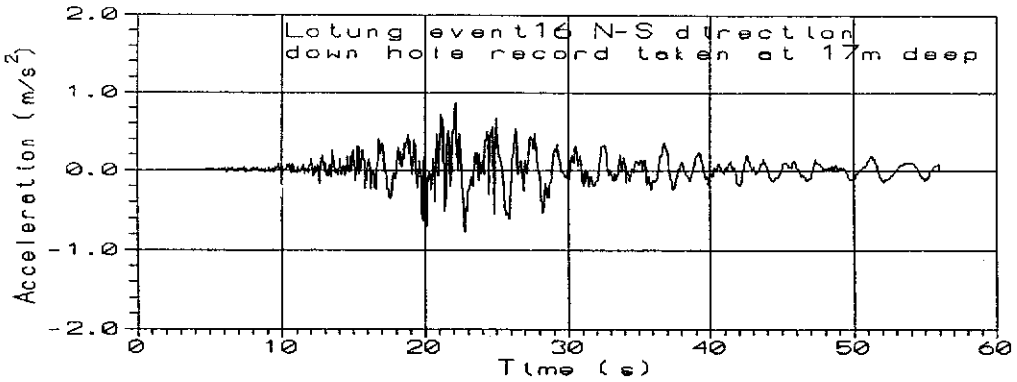

(a) Time History of Original Lotung Motion at N-S Direction (Direction 1)

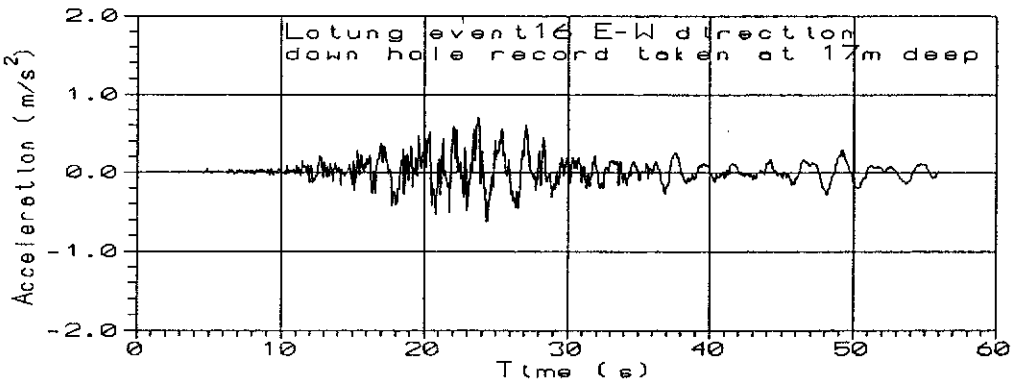

(b) Time History of Original Lotung Motion at E-W Direction (Direction 2)

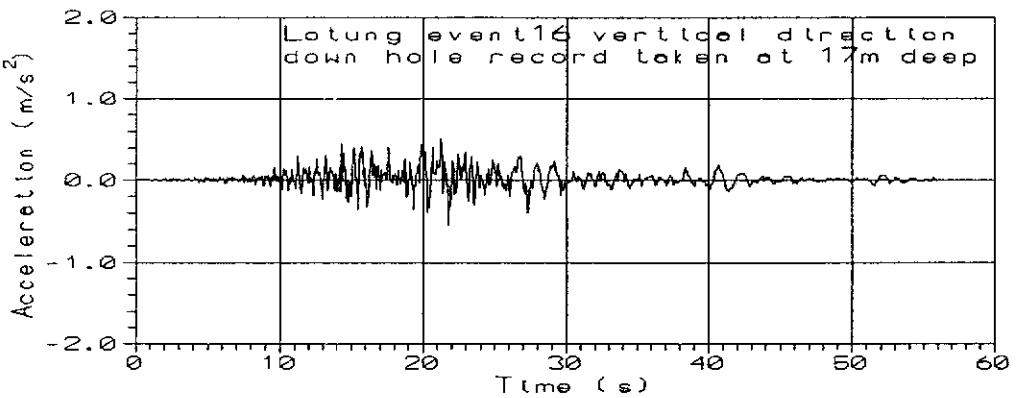

(c) Time History of Original Lotung Motion at Vertical Direction

Figure 6.3 - Time History of Original Lotung Motion

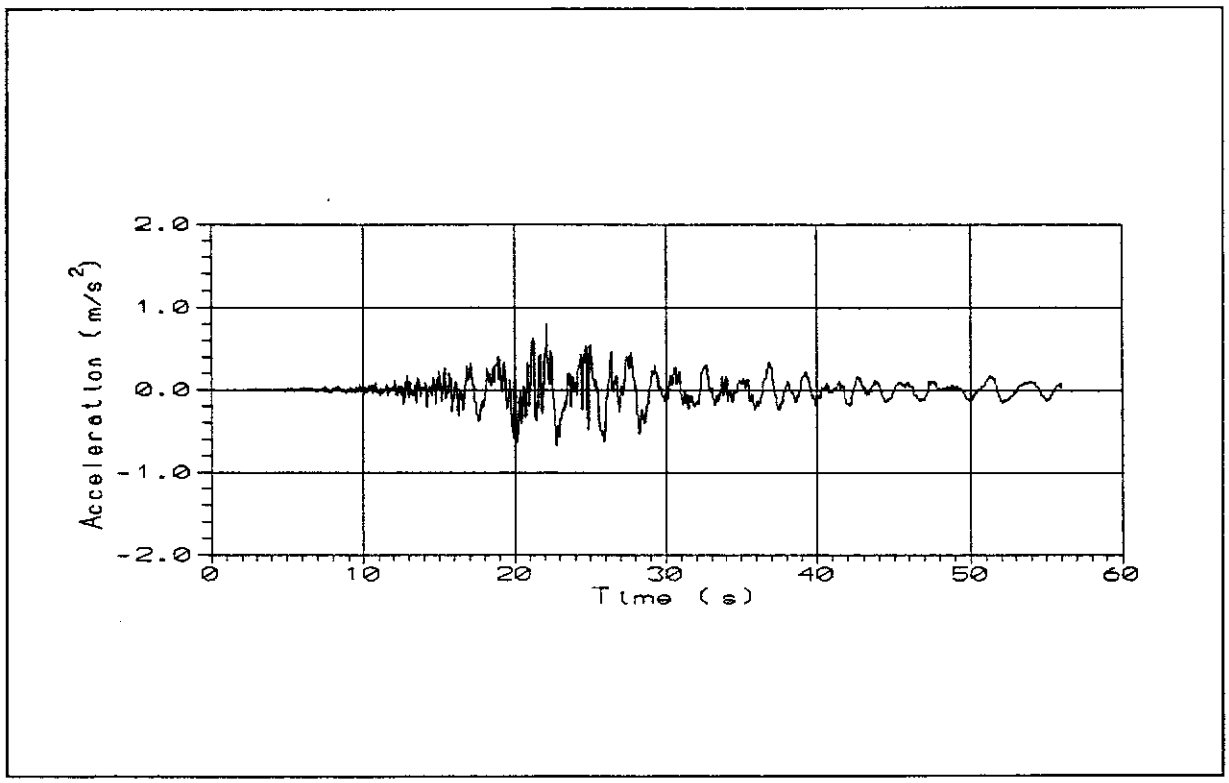

Figure 6.4 - Acceleration Time History at Bottom Boundary in Direction 1

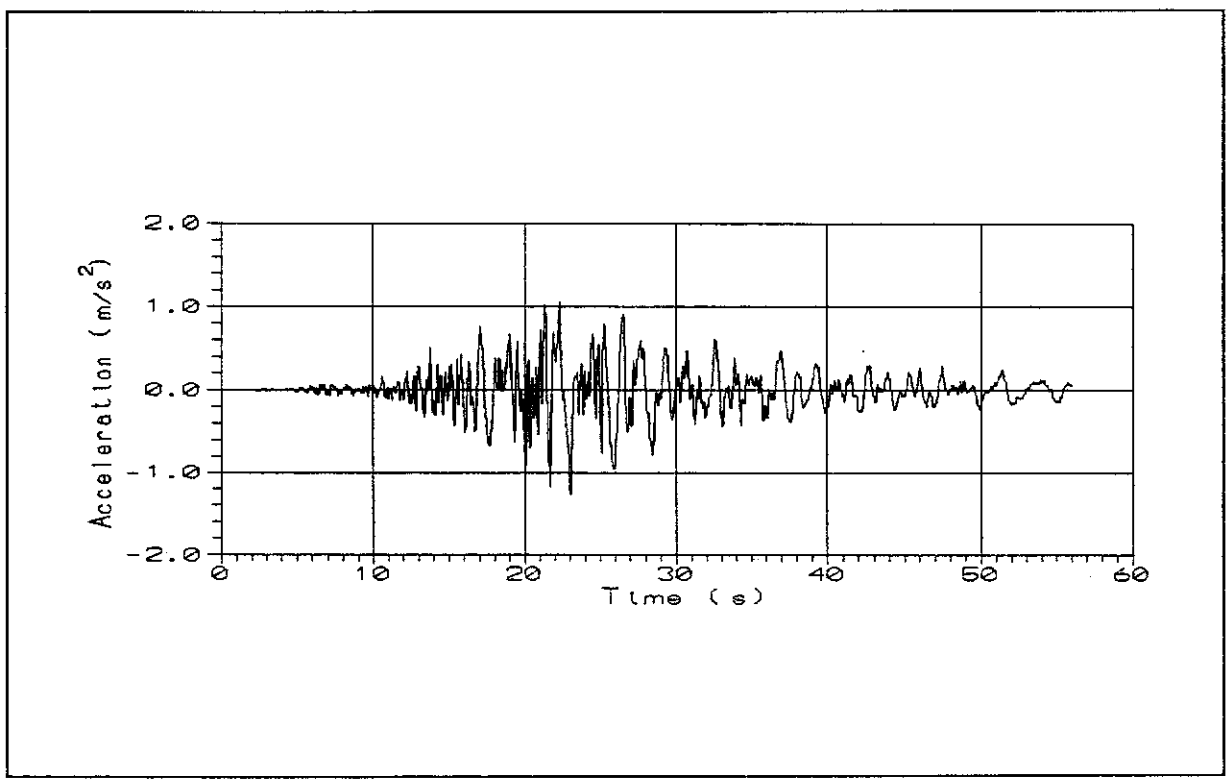

Figure 6.5 - Acceleration Time History at Ground Surface in Direction 1

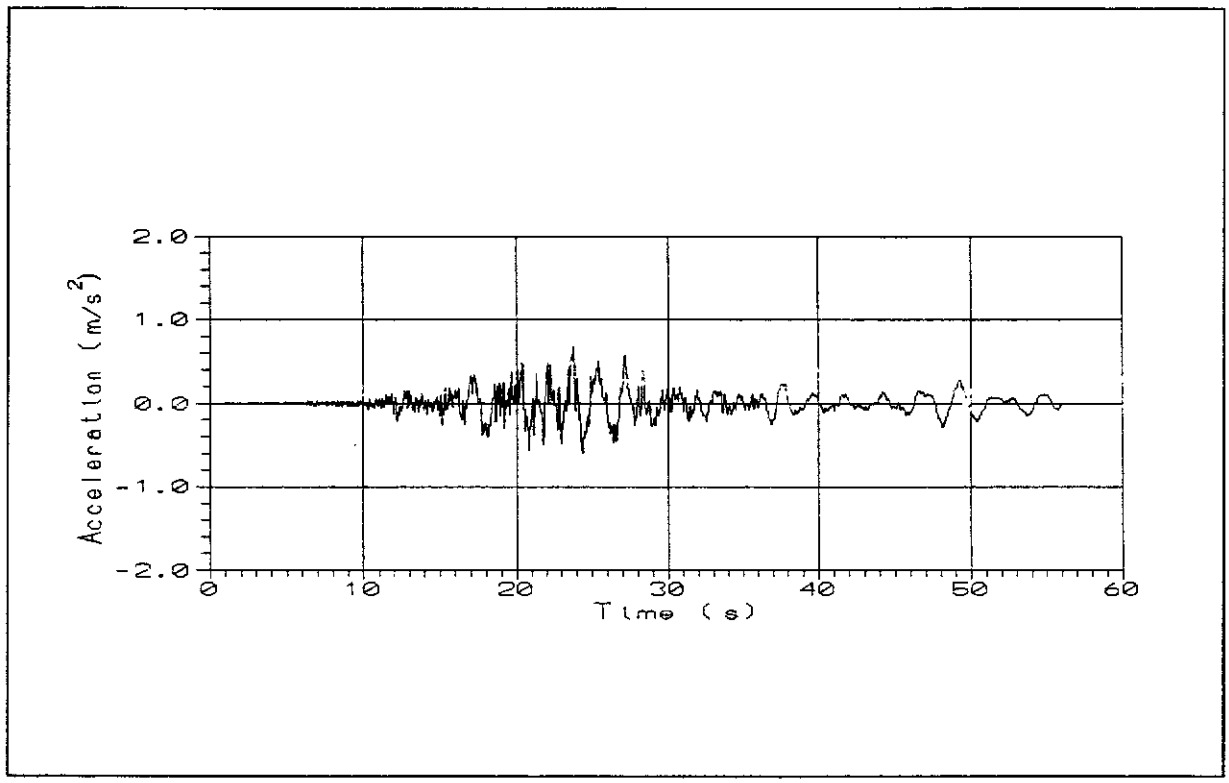

Figure 6.6 - Acceleration Time History at Bottom Boundary in Direction 2

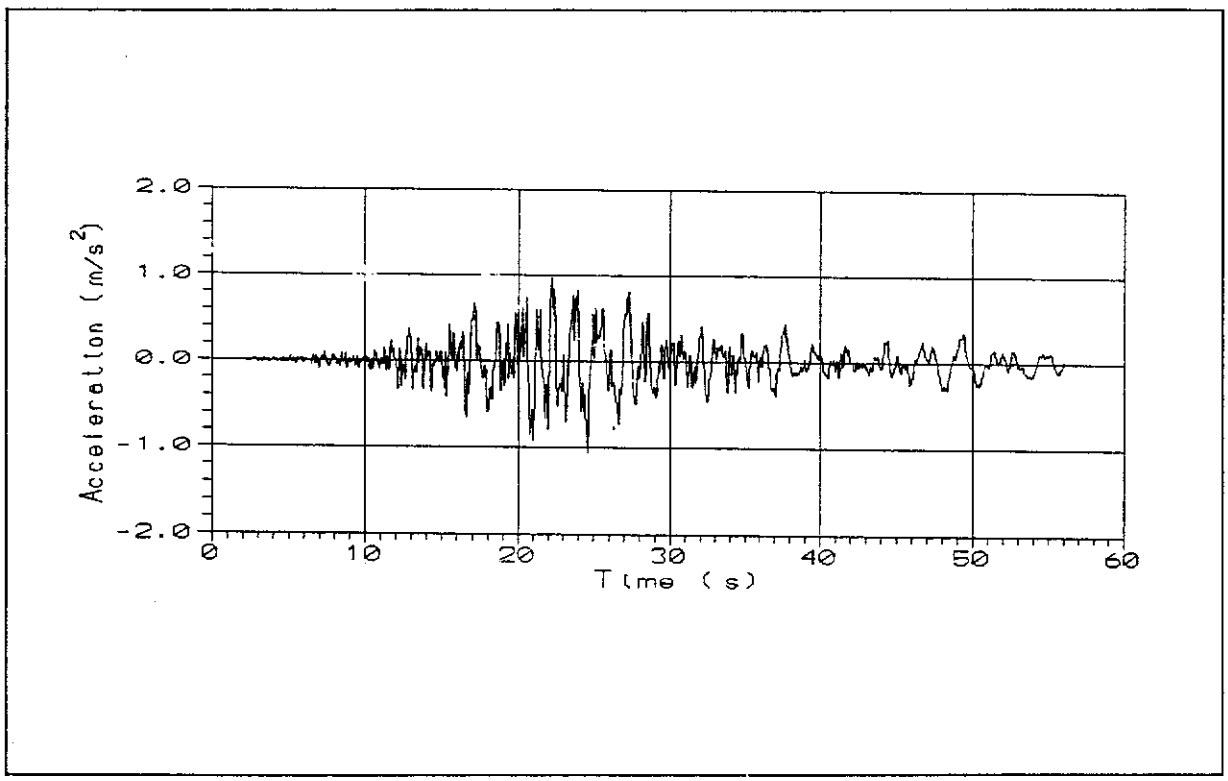

Figure 6.7 - Acceleration Time History at Ground Surface in Direction 2

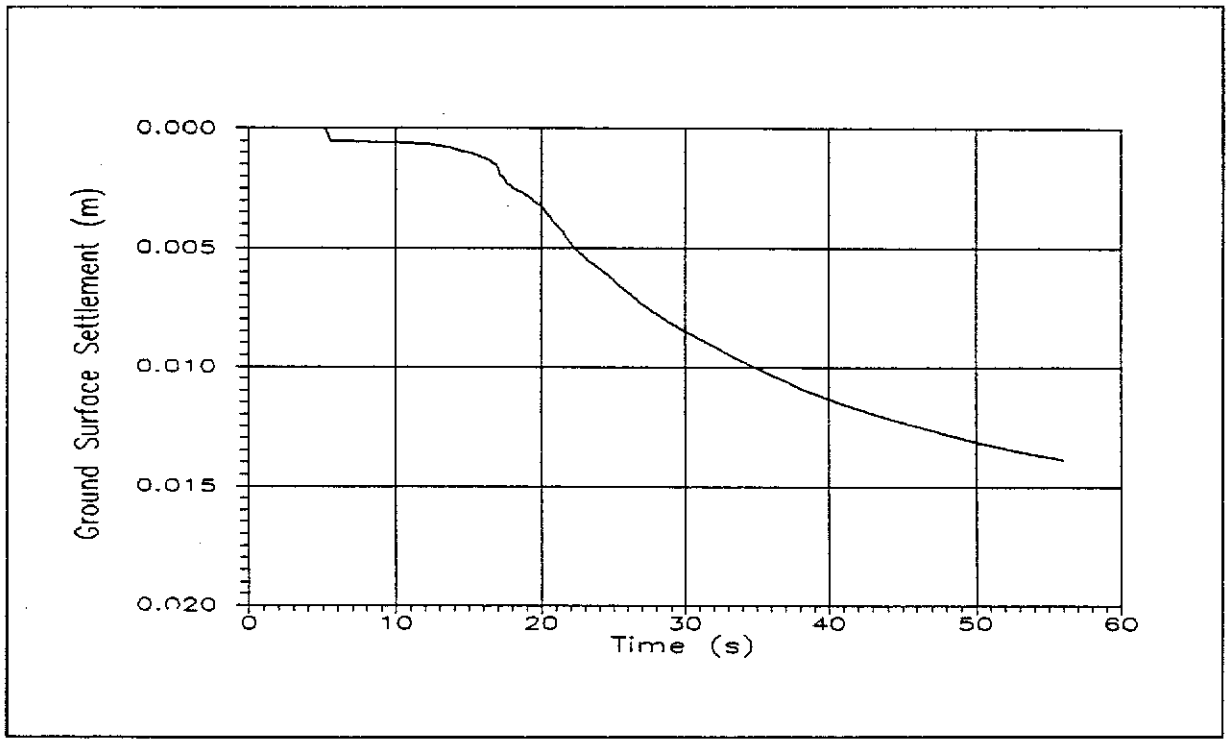

Figure 6.8 - Time History of Ground Surface Settlement

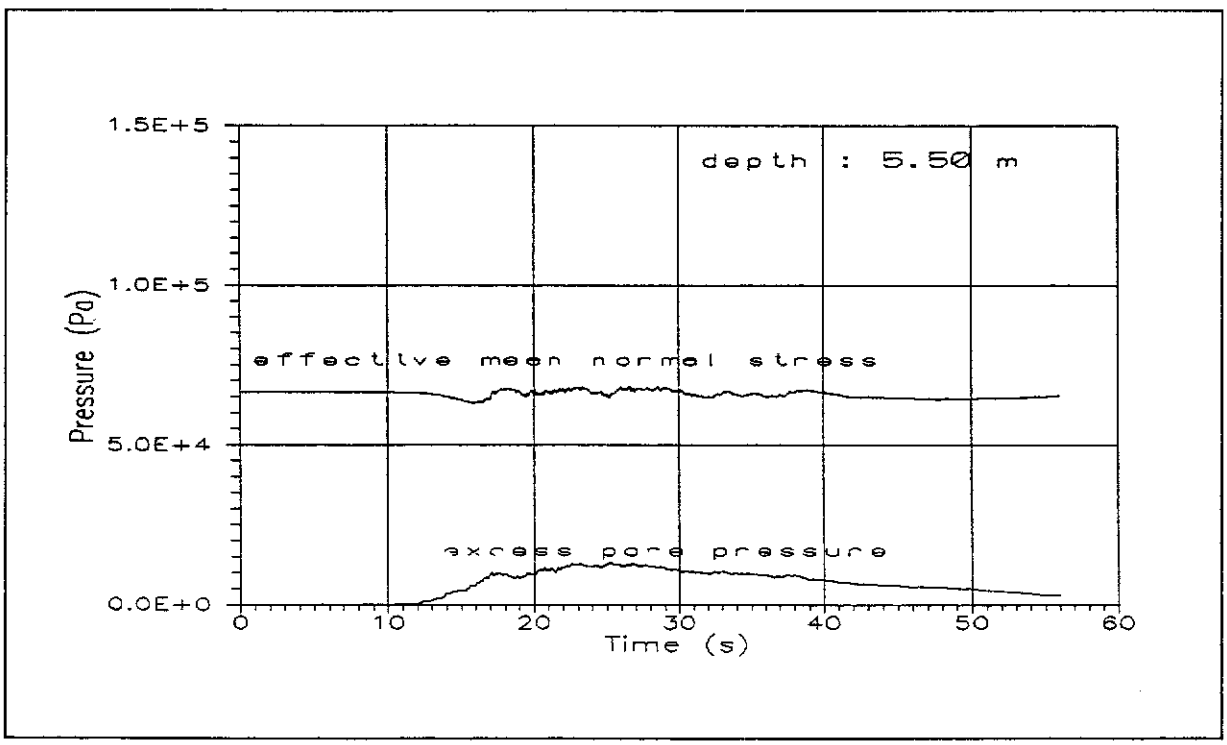

Figure 6.9 - Time History of Effective Mean Normal Stress
and Excess Pore Pressure at 5.5 m

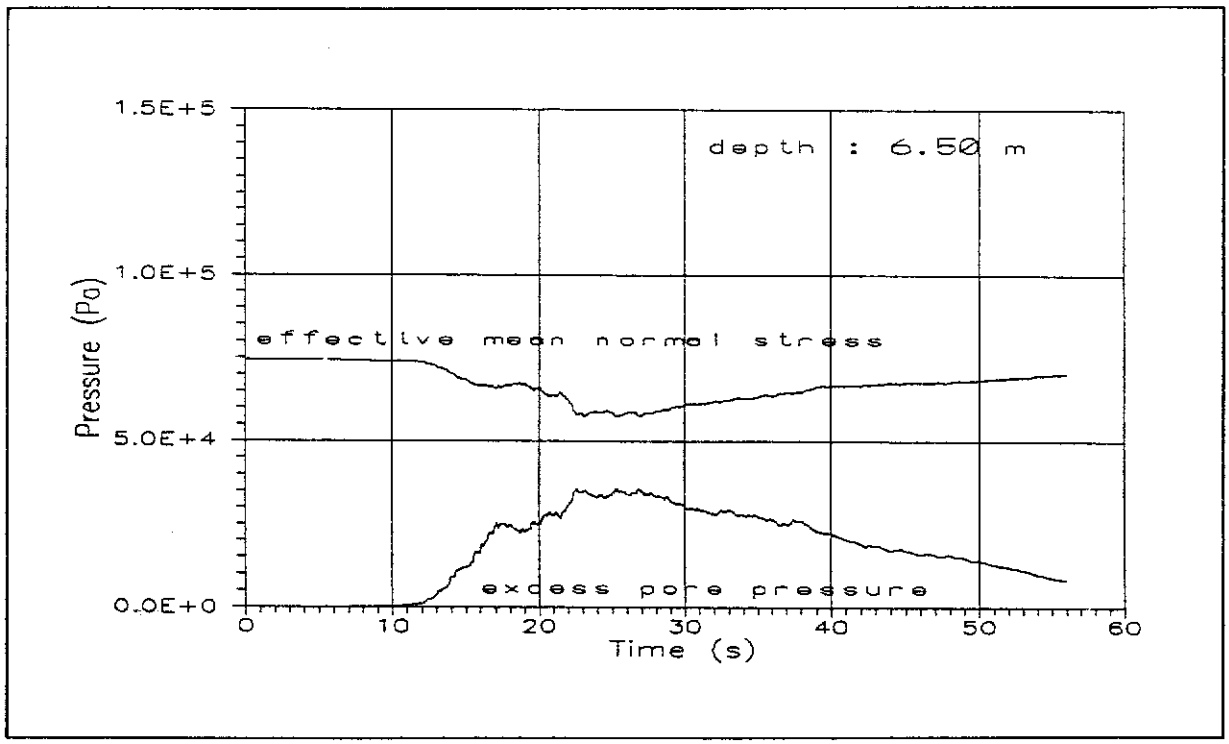

Figure 6.10 - Time History of Effective Mean Normal Stress and Excess Pore Pressure at 6.5 m

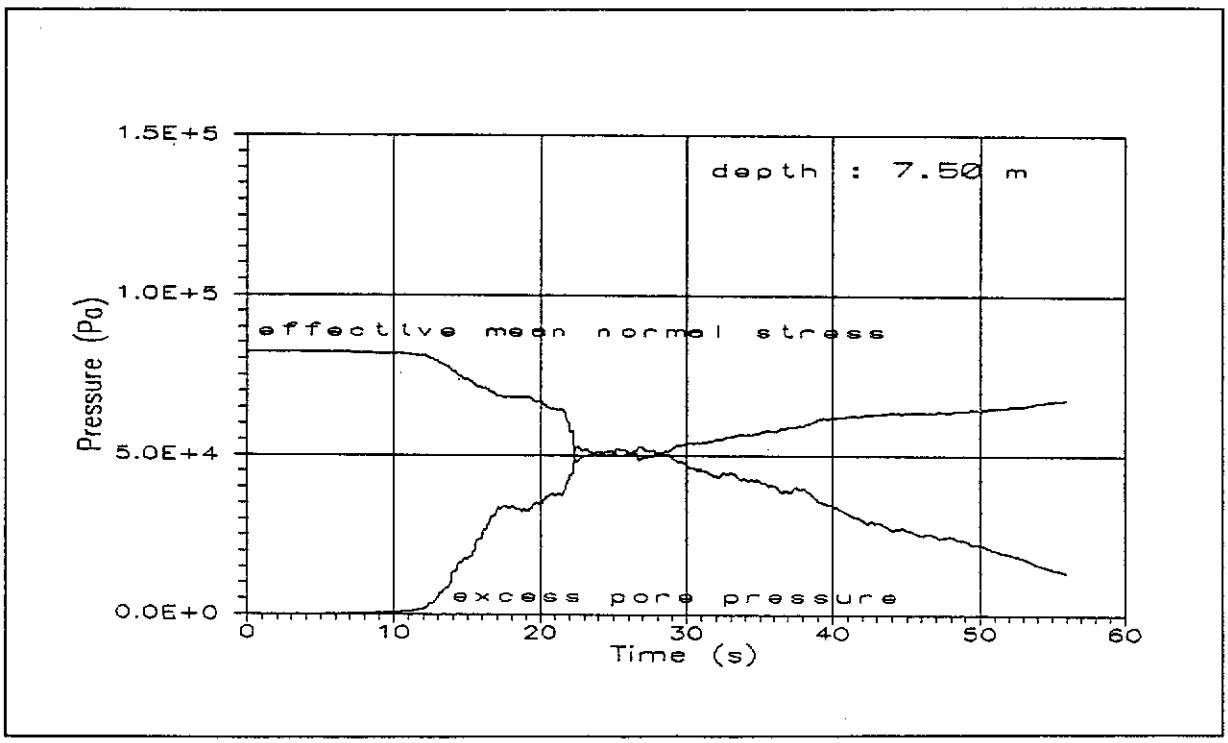

Figure 6.11 - Time History of Effective Mean Normal Stress and Excess Pore Pressure at 7.5 m

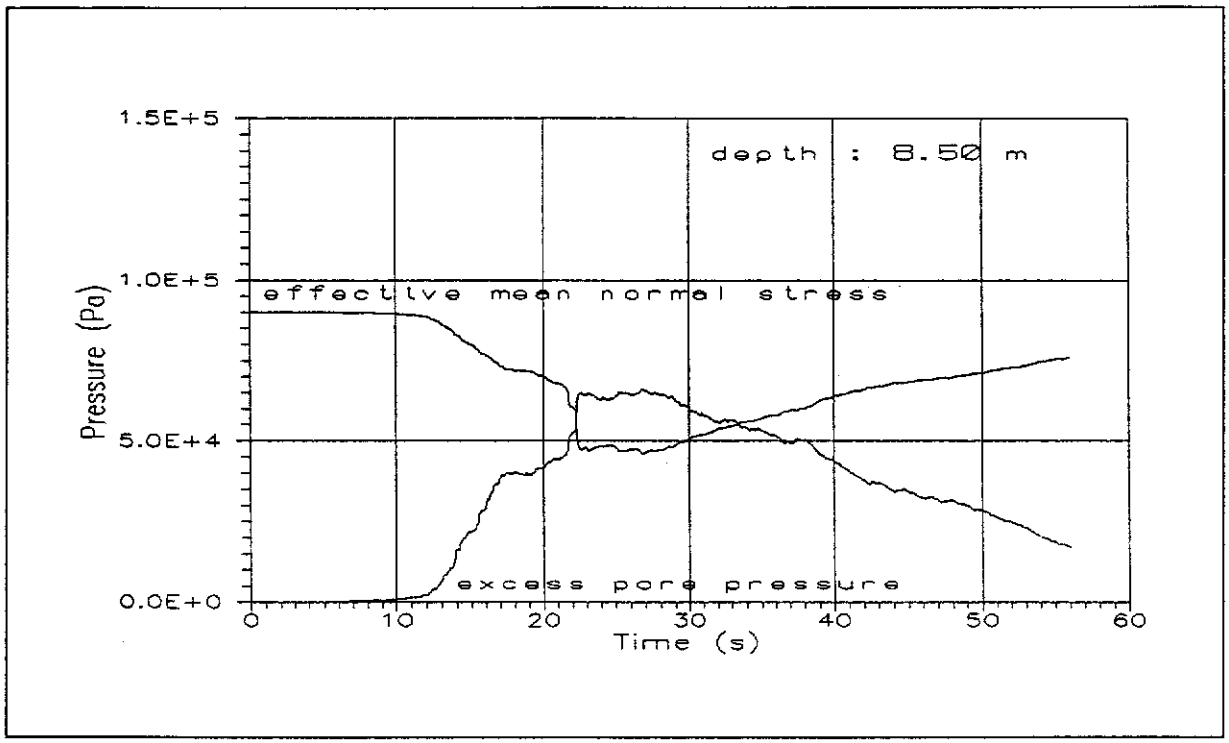

Figure 6.12 - Time History of Effective Mean Normal Stress and Excess Pore Pressure at 8.5 m

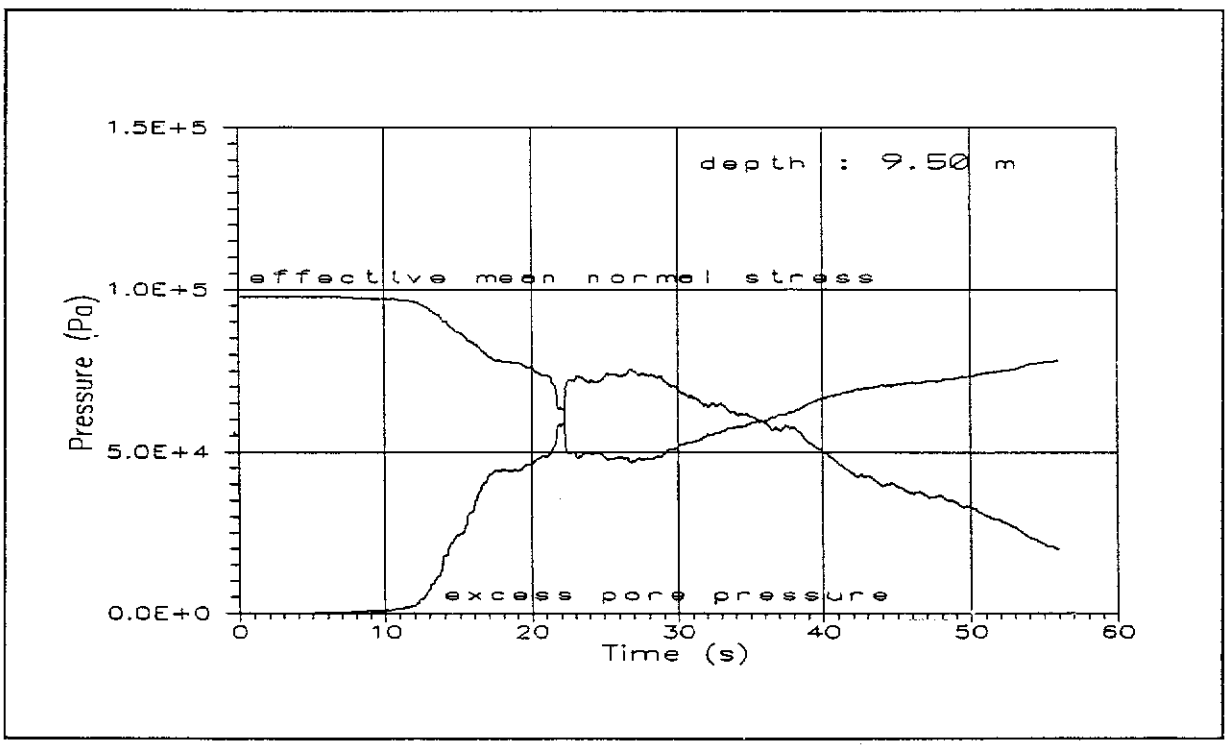

Figure 6.13 - Time History of Effective Mean Normal Stress and Excess Pore Pressure at 9.5 m

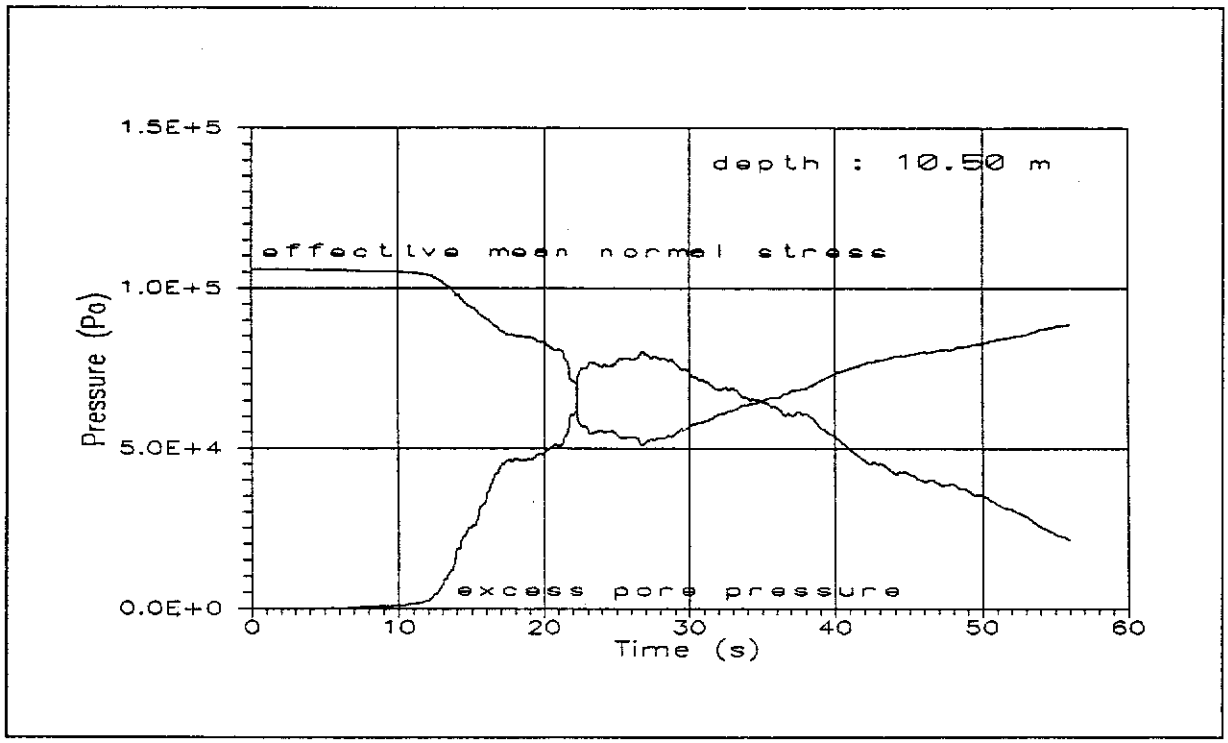

Figure 6.14 - Time History of Effective Mean Normal Stress
and Excess Pore Pressure at 10.5 m

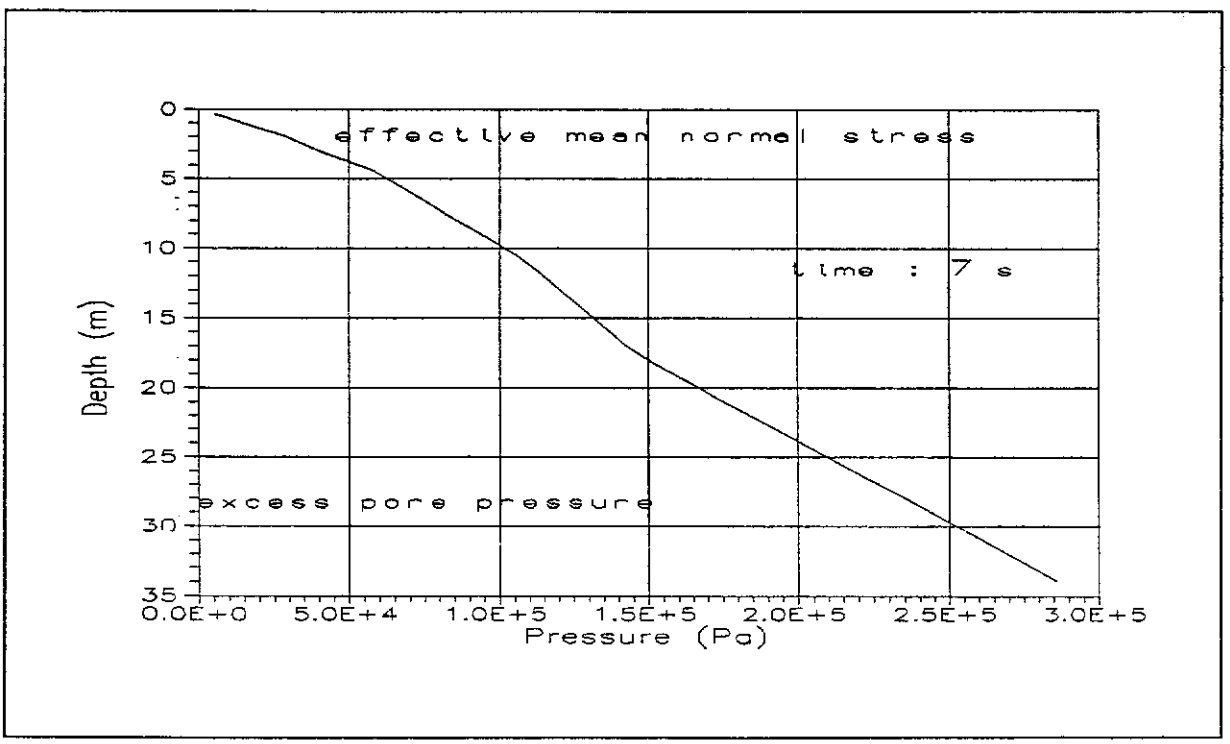

Figure 6.15 - Distribution of Effective Mean Normal Stress
and Excess Pore Pressure at 7 s

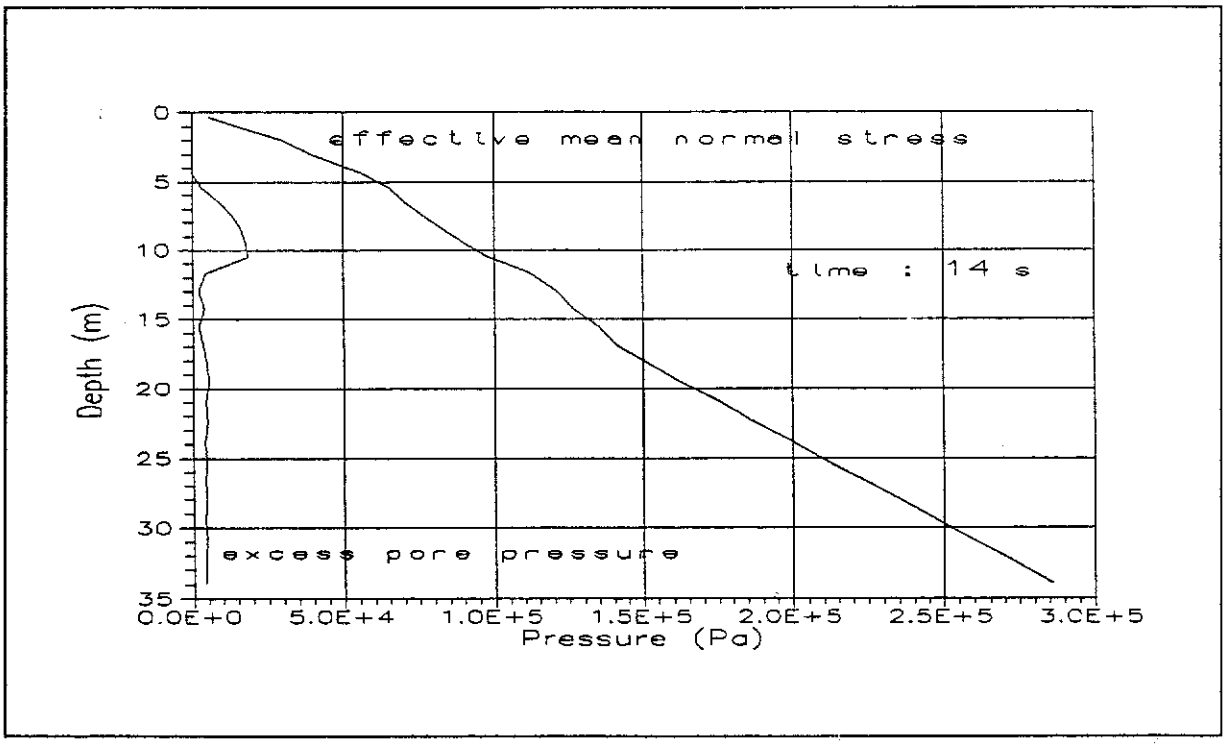

Figure 6.16 - Distribution of Effective Mean Normal Stress and Excess Pore Pressure at 14 s

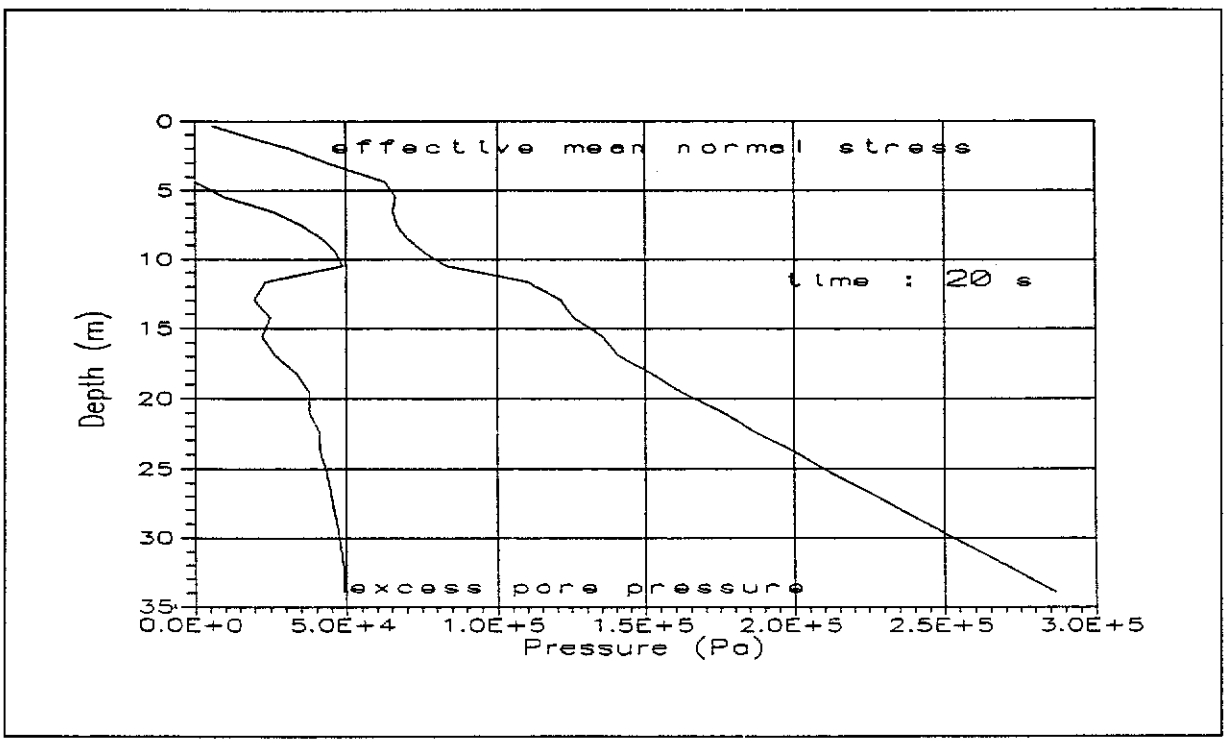

Figure 6.17 - Distribution of Effective Mean Normal Stress and Excess Pore Pressure at 20 s

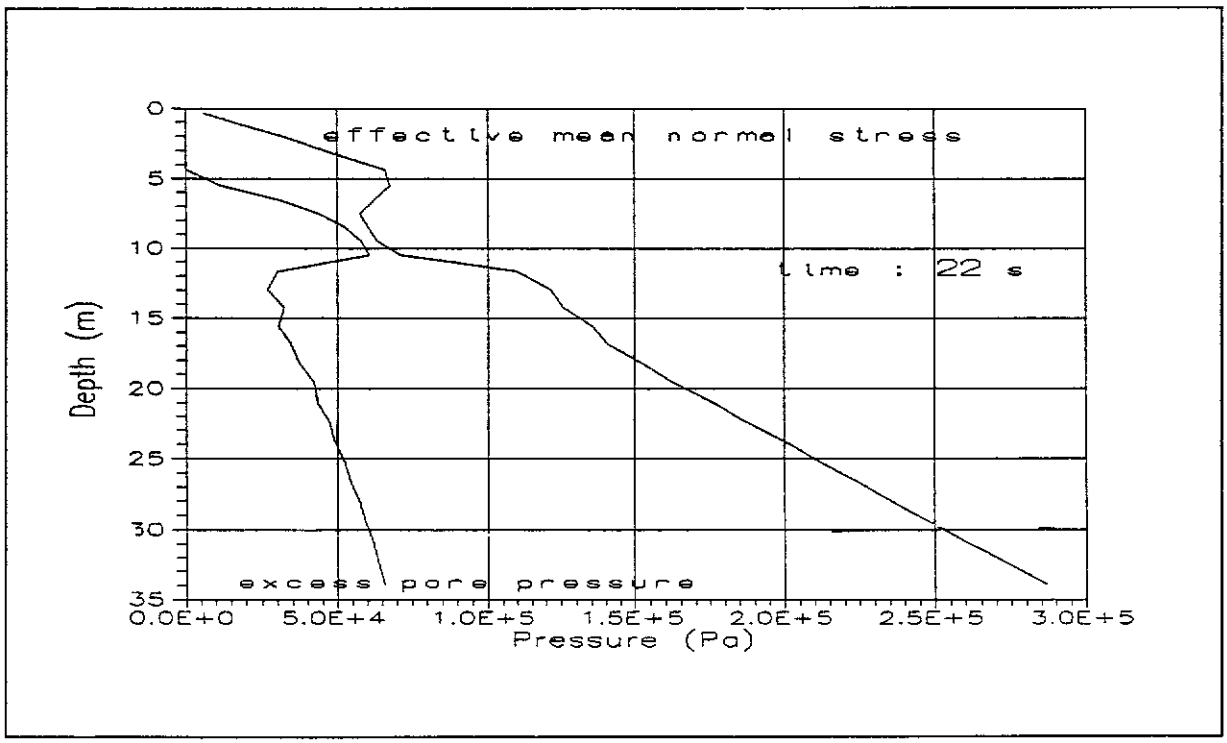

Figure 6.18 - Distribution of Effective Mean Normal Stress and Excess Pore Pressure at 22 s

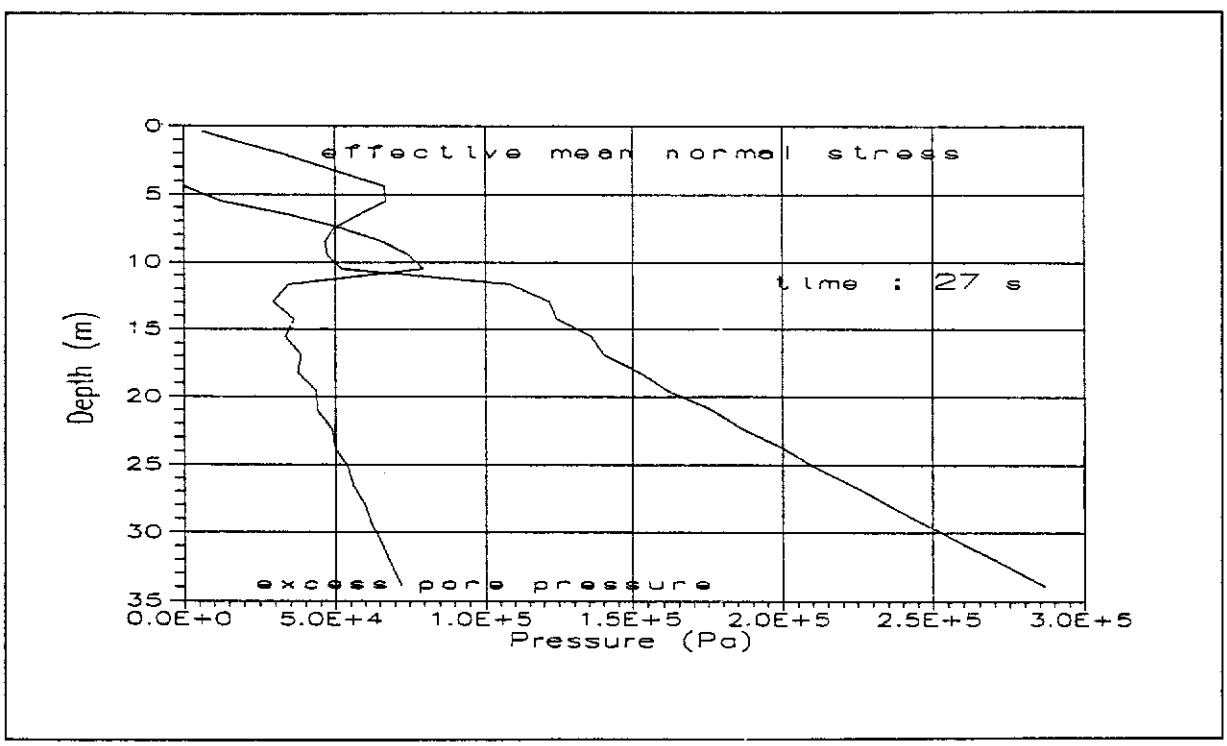

Figure 6.19 - Distribution of Effective Mean Normal Stress and Excess Pore Pressure at 27 s

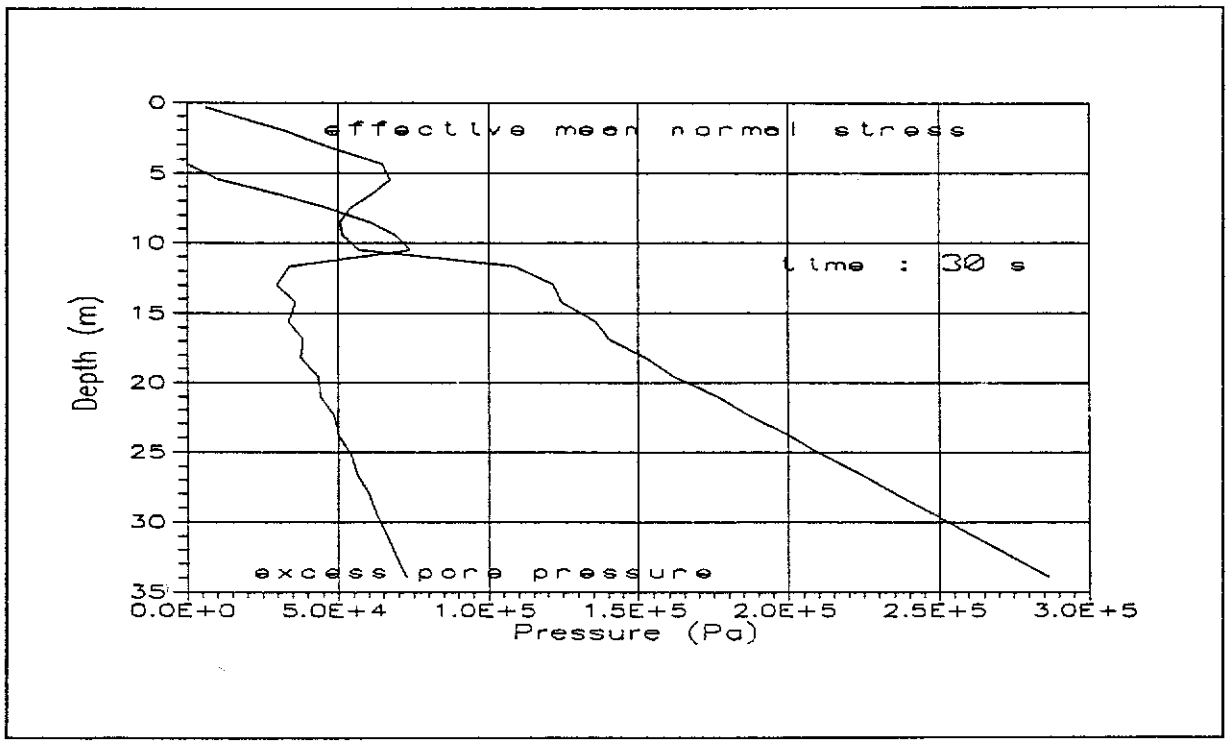

Figure 6.20 - Distribution of Effective Mean Normal Stress and Excess Pore Pressure at 30 s

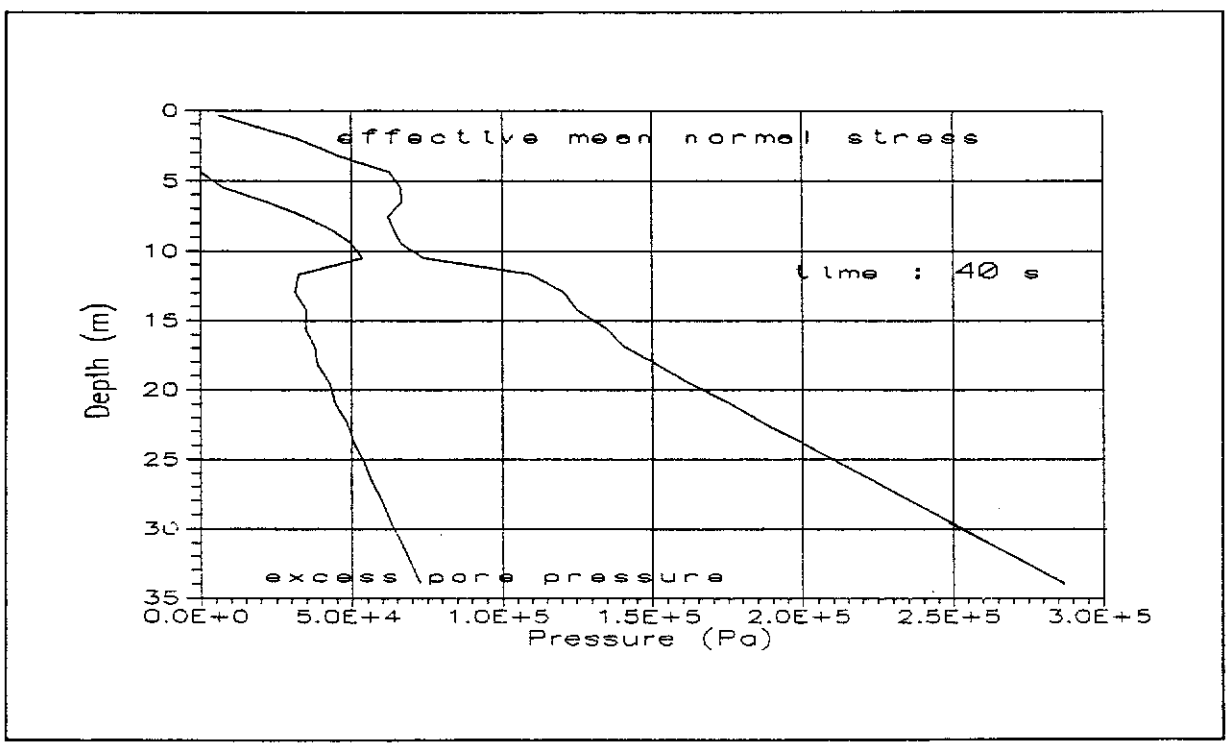

Figure 6.21 - Distribution of Effective Mean Normal Stress and Excess Pore Pressure at 40 s

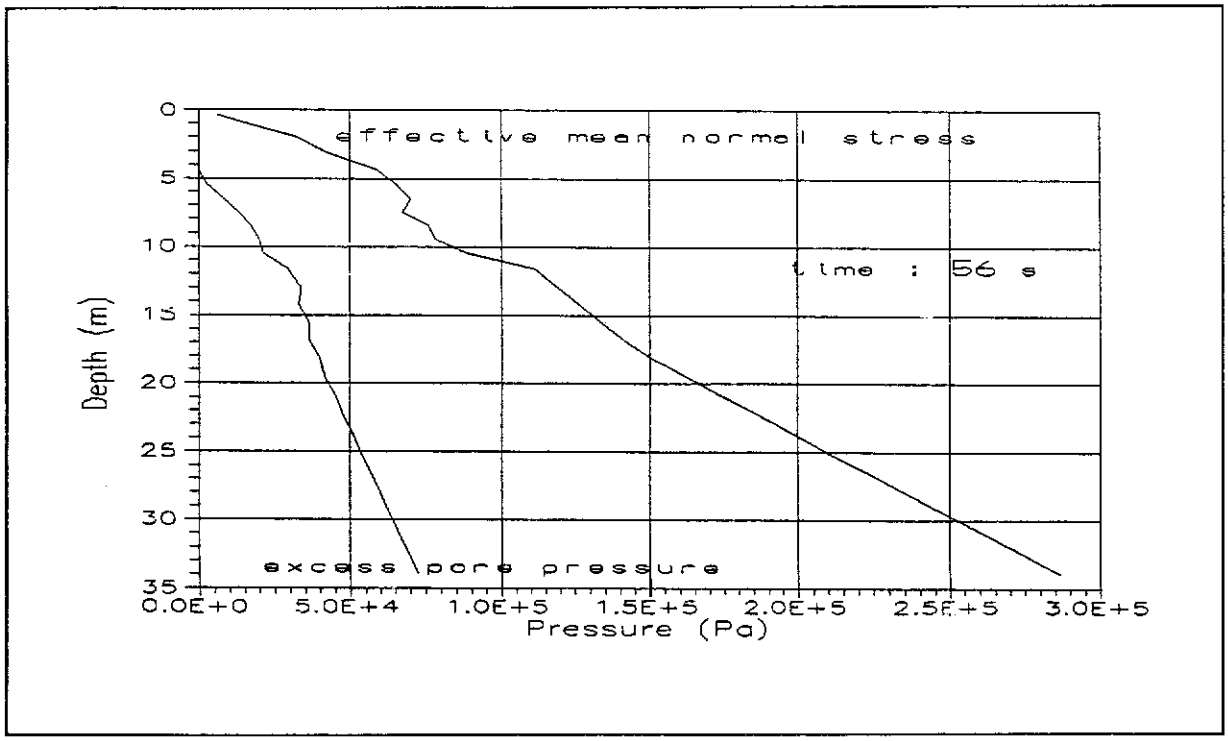

Figure 6.22 - Distribution of Effective Mean Normal Stress and Excess Pore Pressure at 56 s

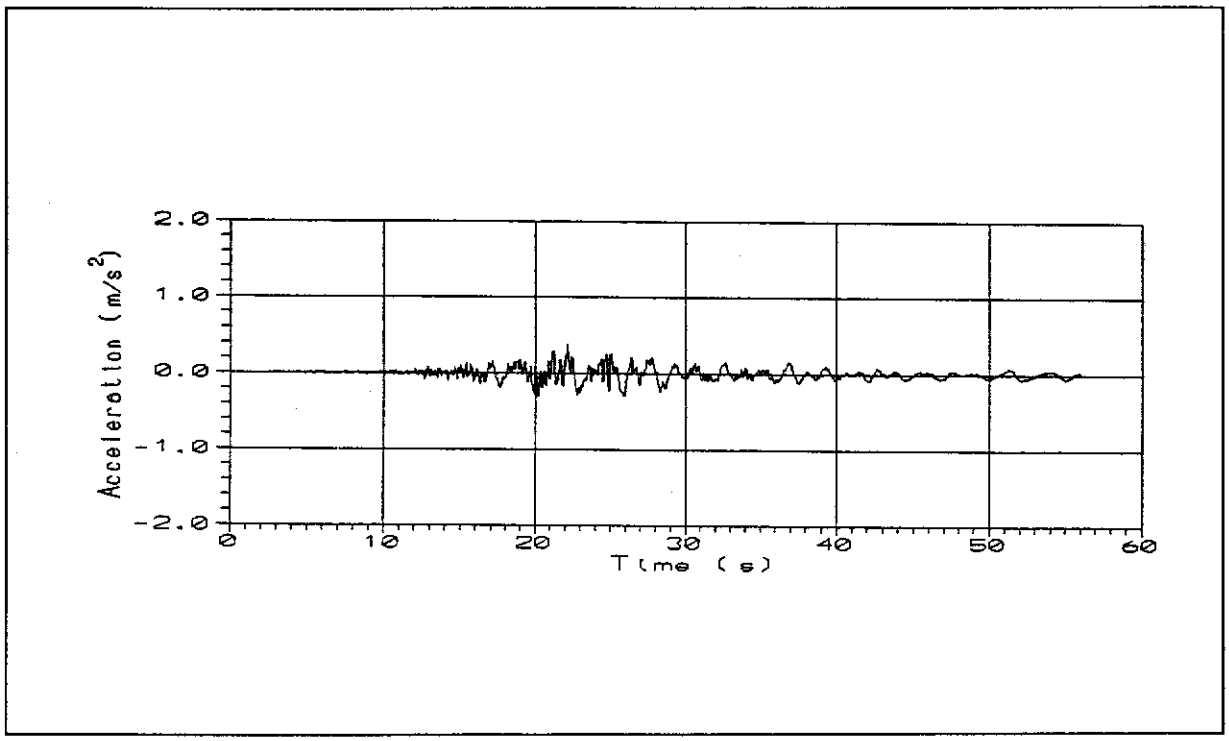

Figure 6.23 - Acceleration Time History at Bottom Boundary in Direction 1 (Scaled down by a Factor of 0.45)

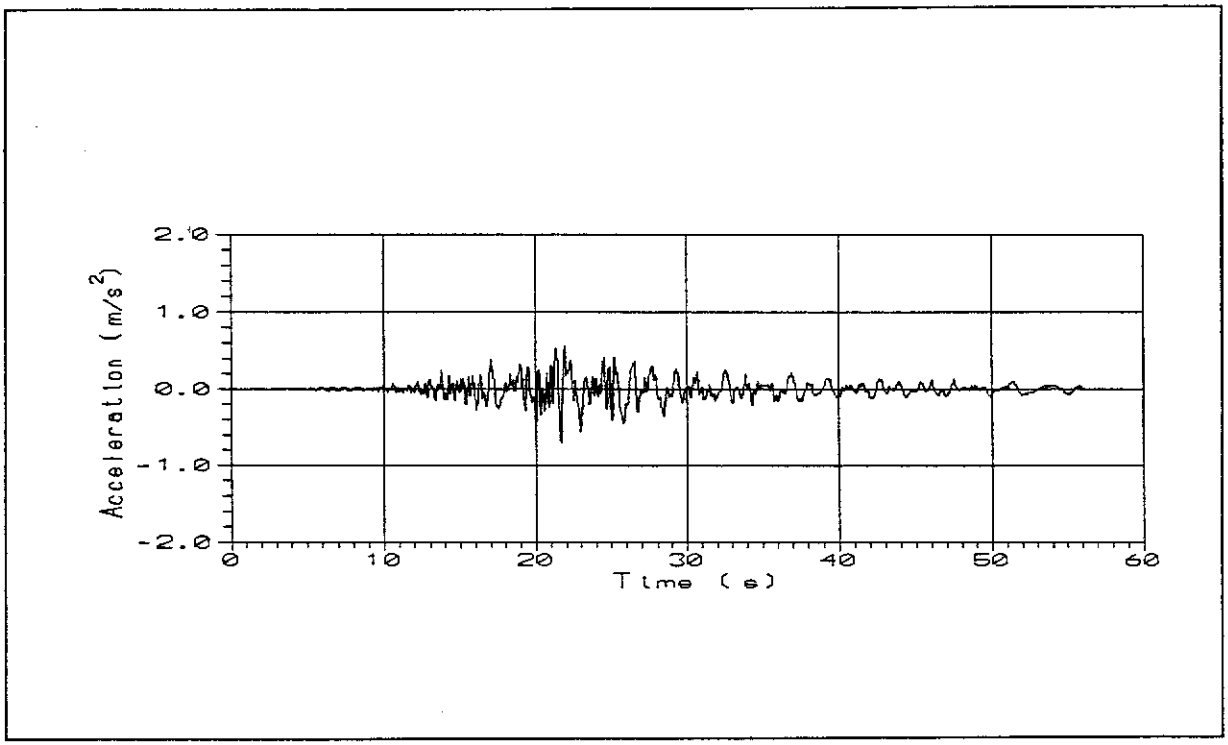

Figure 6.24 - Acceleration Time History at Gound Surface in Direction 1
(Scaled down by a Factor of 0.45)

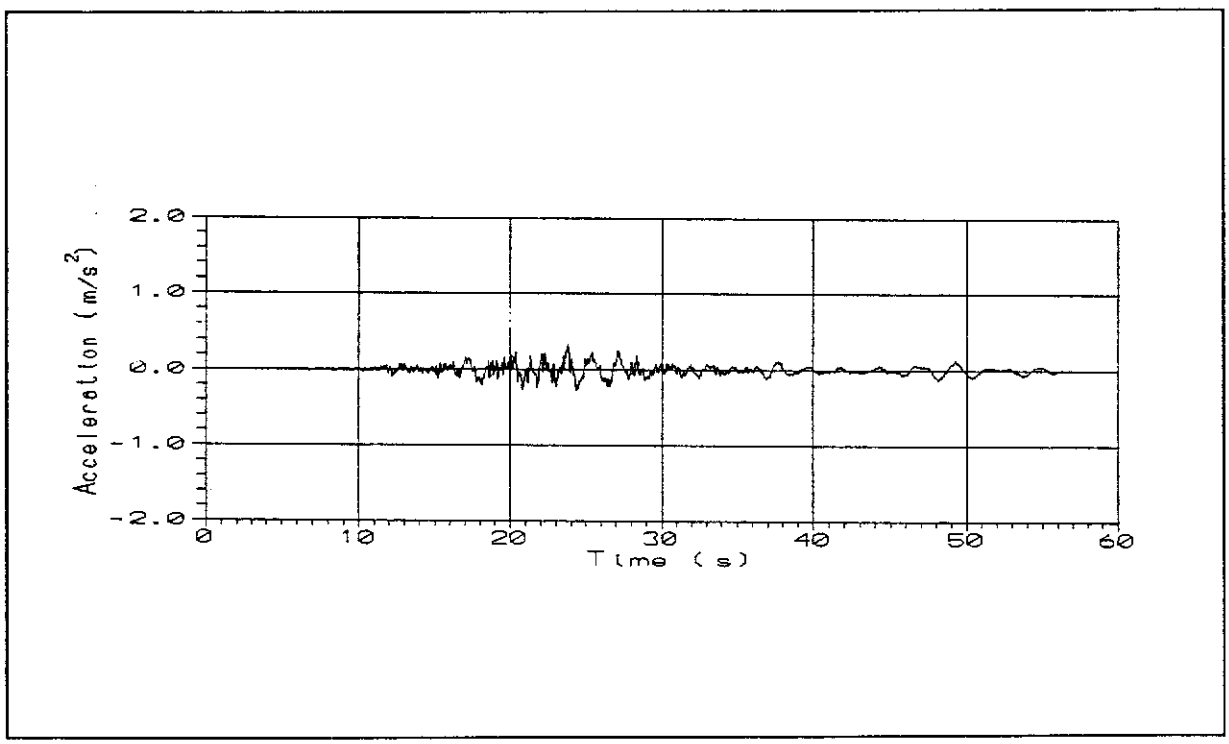

Figure 6.25 - Acceleration Time History at Bottom Boundary in Direction 2
(Scaled down by a Factor of 0.45)

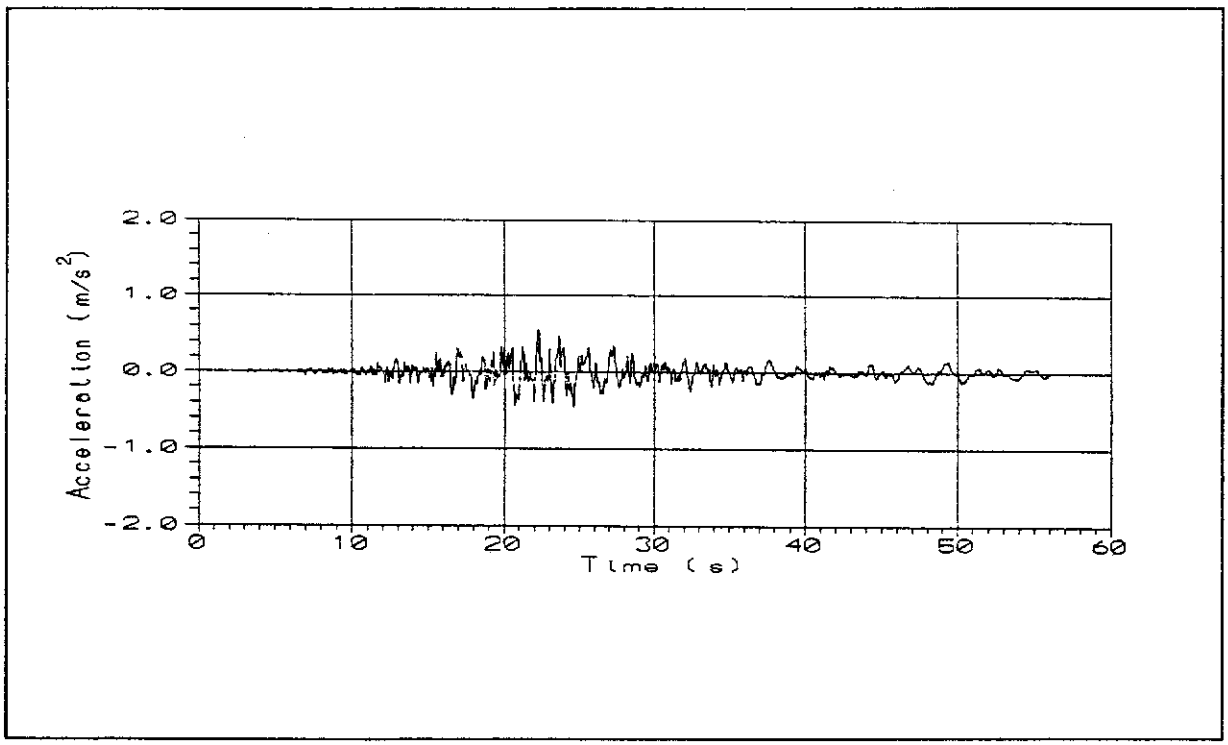

Figure 6.26 - Acceleration Time History at Gound Surface in Direction 2
(Scaled down by a Factor of 0.45)

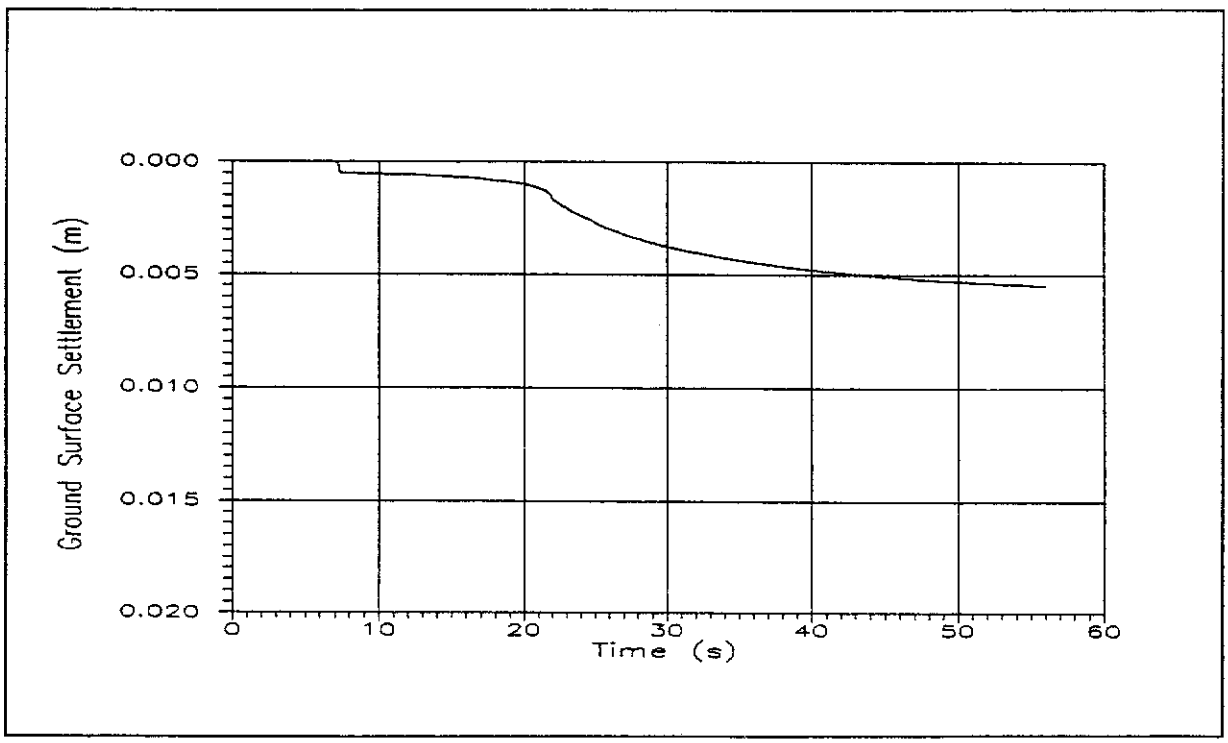

Figure 6.27 - Time History of Ground Surface Settlement
(Scaled down by a Factor of 0.45)

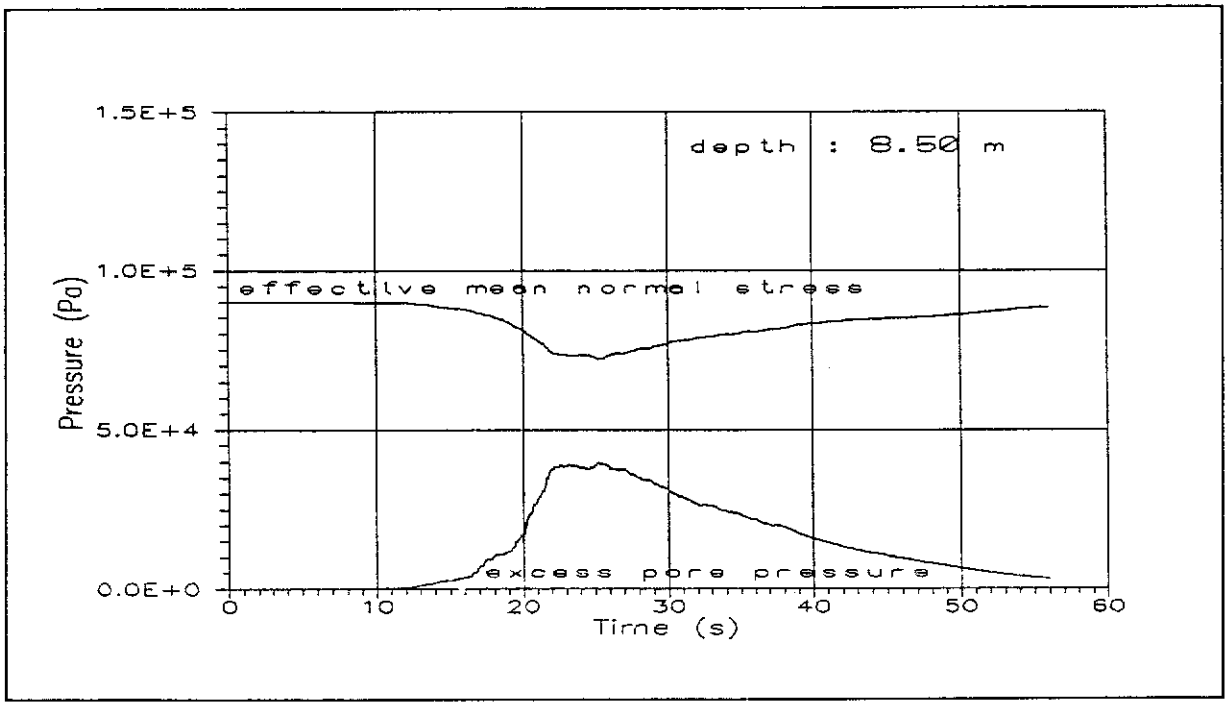

Figure 6.28 - Time History of Effective Mean Normal Stress
and Excess Pore Pressure at 8.5 m
(Scaled down by a Factor of 0.45)

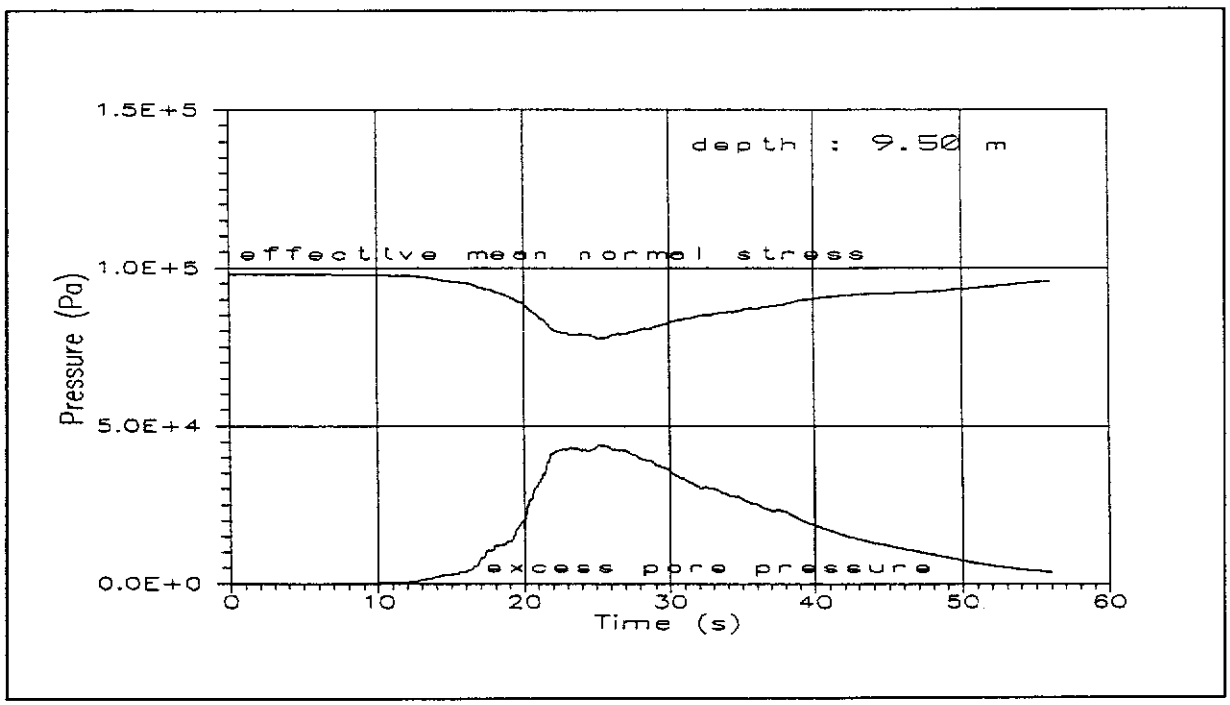

Figure 6.29 - Time History of Effective Mean Normal Stress
and Excess Pore Pressure at 9.5 m
(Scaled down by a Factor of 0.45)

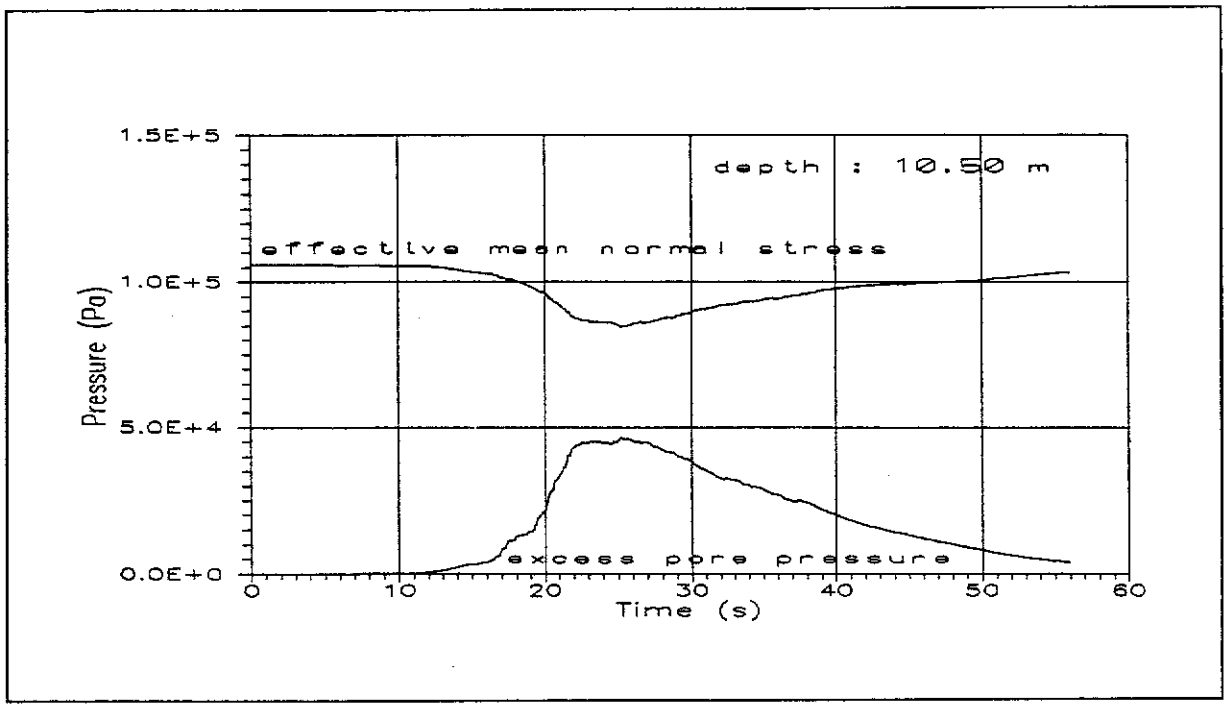

Figure 6.30 - Time History of Effective Mean Normal Stress
and Excess Pore Pressure at 10.5 m
(Scaled down by a Factor of 0.45)

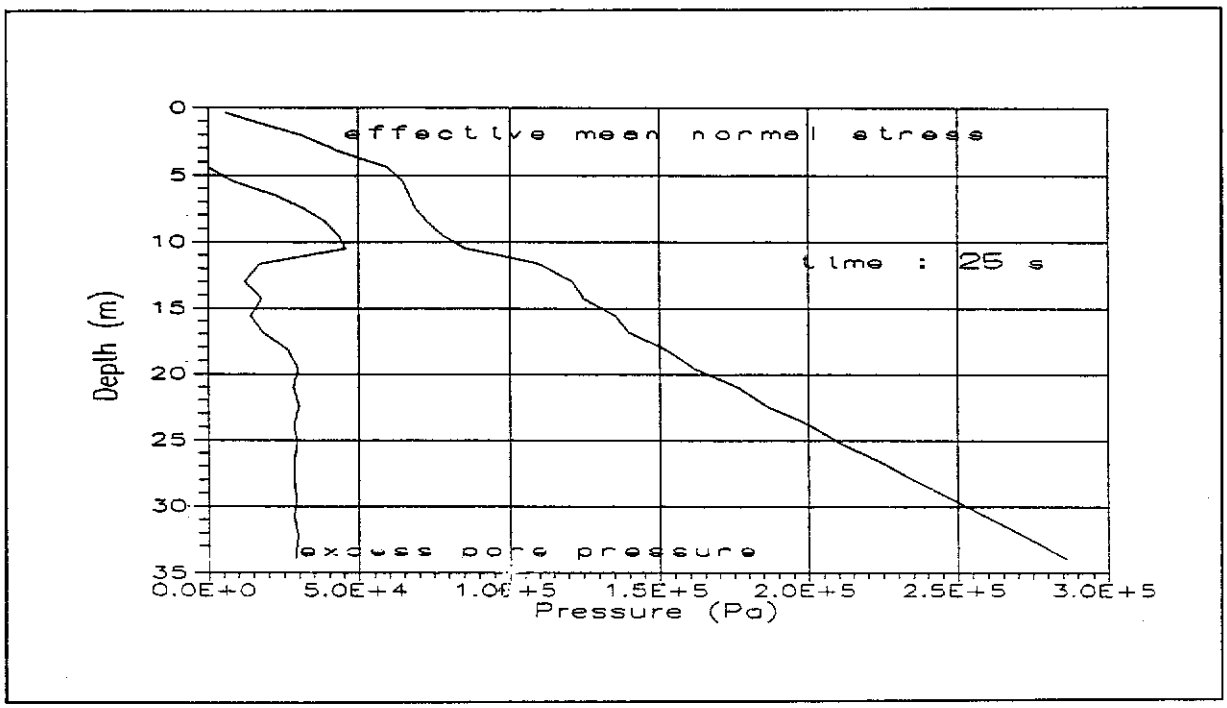

Figure 6.31 - Distribution of Effective Mean Normal Stress
and Excess Pore Pressure at 25 s
(Scaled down by a Factor of 0.45)

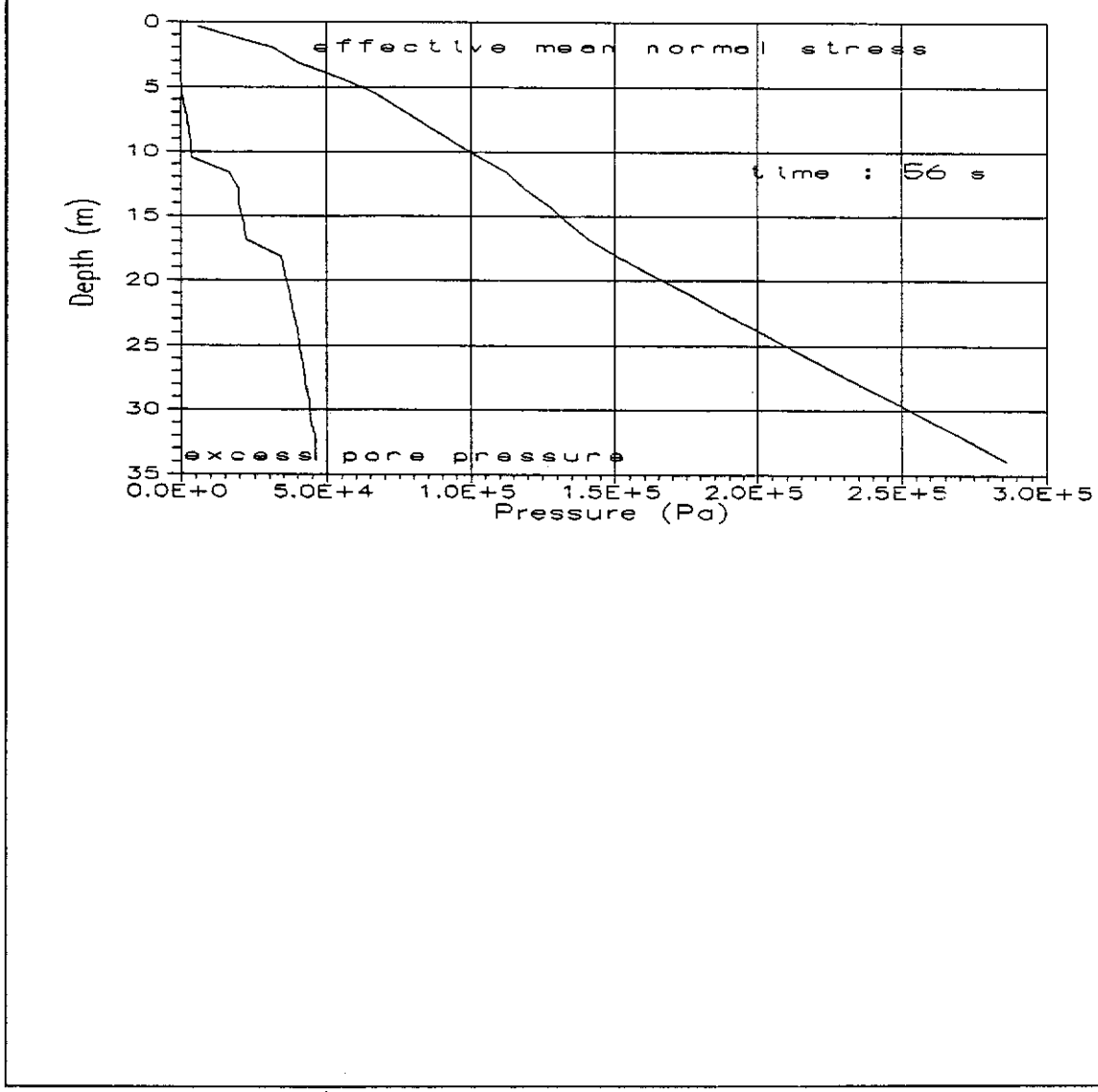

Figure 6.32 - Distribution of Effective Mean Normal Stress
and Excess Pore Pressure at 56 s
(Scaled down by a Factor of 0.45)

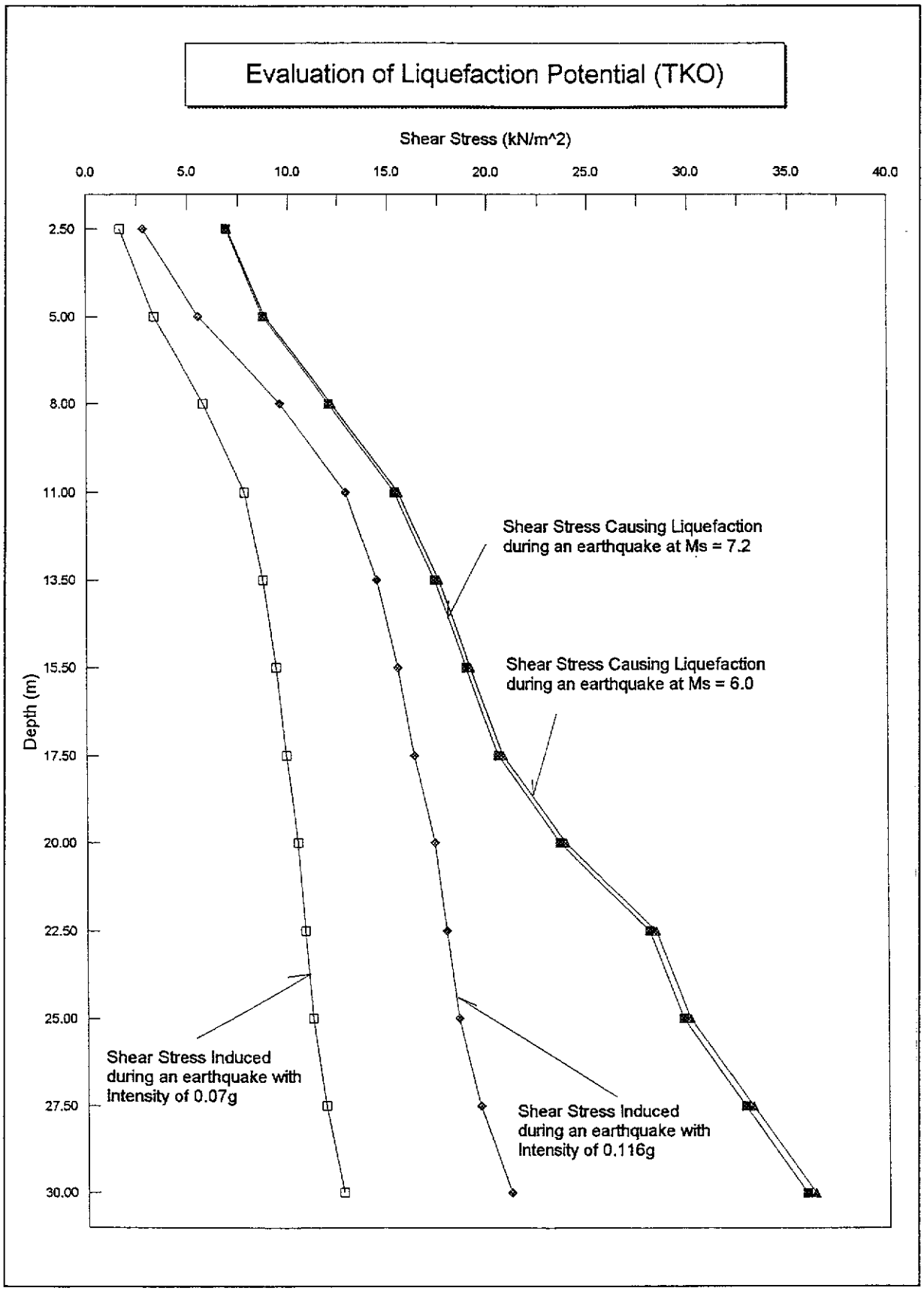

Figure 6.33 - Evaluation of Liquefaction Potential by Seed and Idriss' Simplified Method (TKO Reclamation Site)

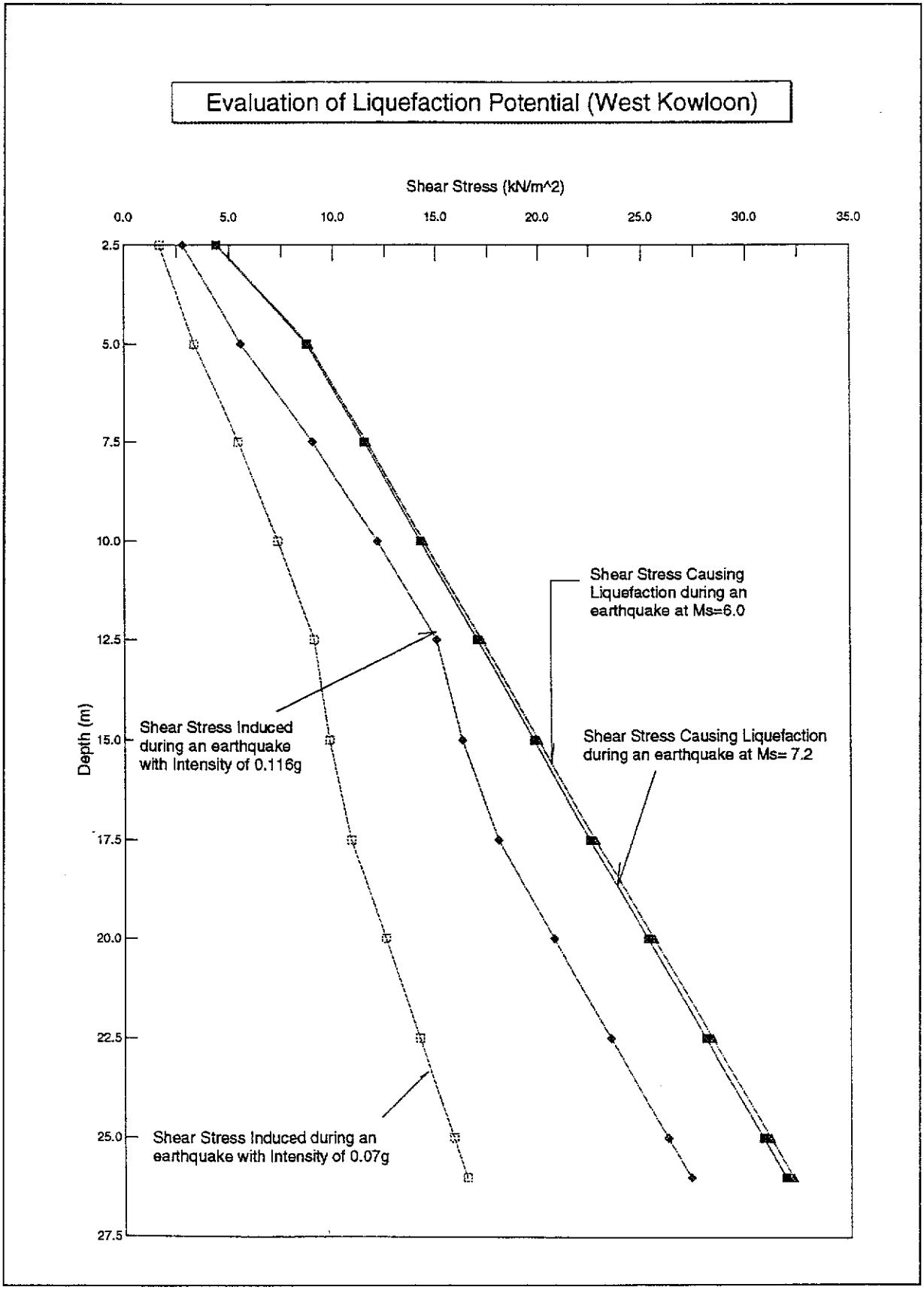

Figure 6.34 - Evaluation of Liquefaction Potential by Seed and Idriss' Simplified Method (West Kowloon Reclamation Site)

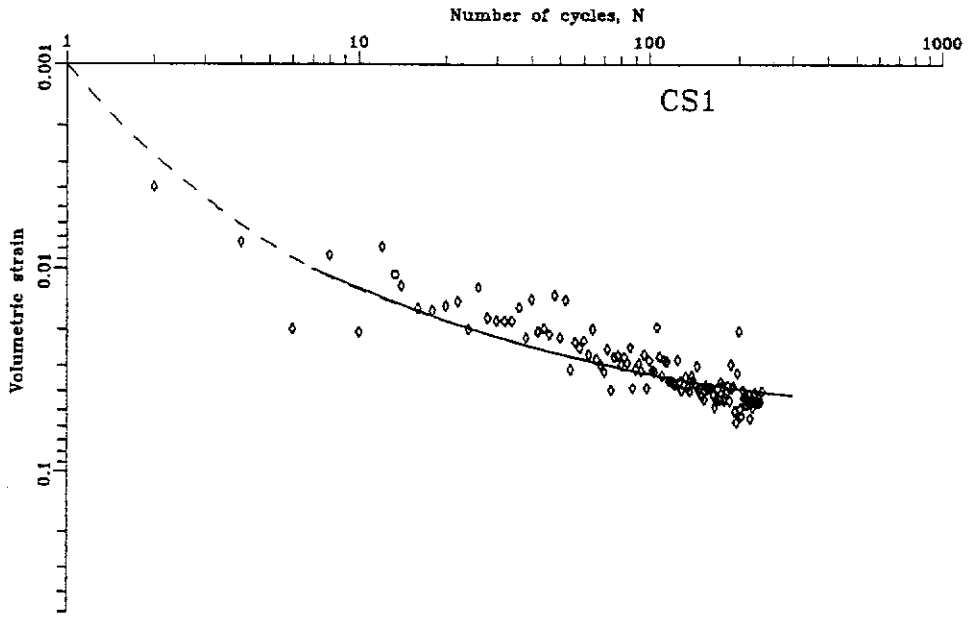

(a) Volumetric Strain Vs. No. of Loading Cycles on Cyclic Triaxial Test
(Deviator Stress = 10.8 kPa and Relative Density = 40%)

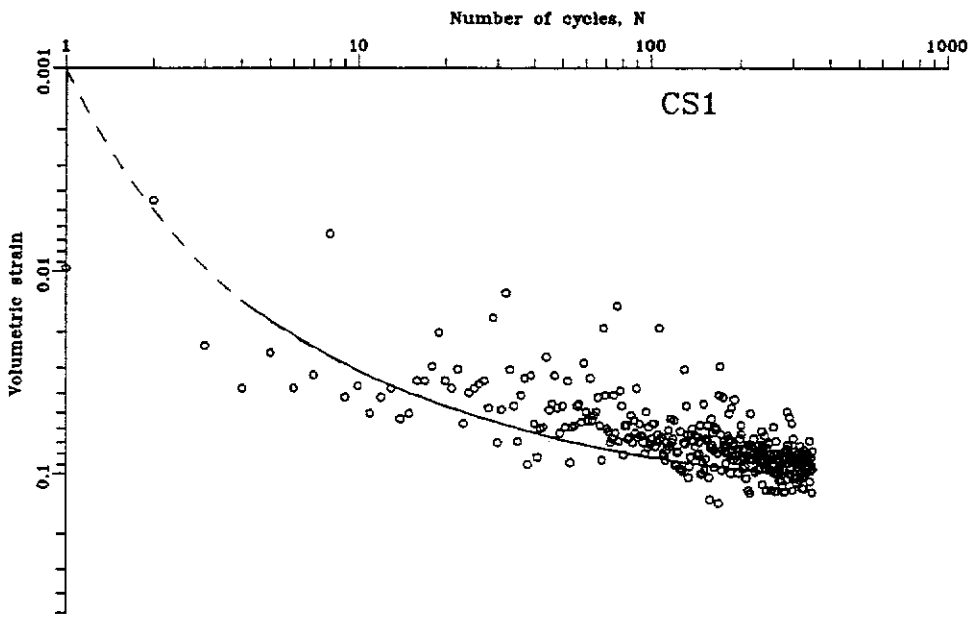

(b) Volumetric Strain Vs. No. of Loading Cycles on Cyclic Triaxial Test
(Deviator Stress = 21.5 kPa and Relative Density = 45%)

Figure 6.35 - Volumetric Strain Versus No. of Loading Cycles on Cyclic Triaxial Test (Sheet 1 of 2)

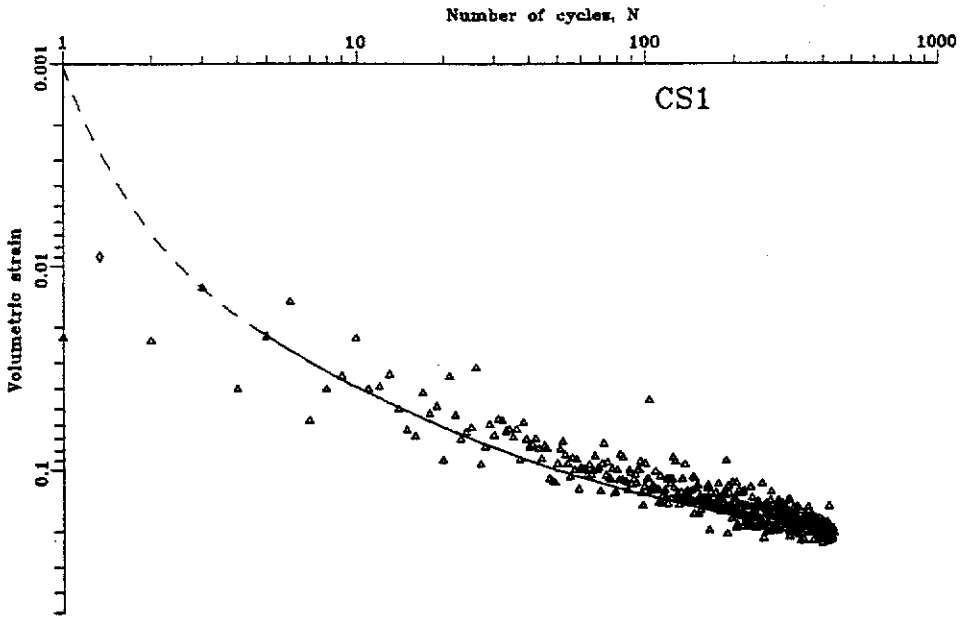

(c) Volumetric Strain Vs. No. of Loading Cycles on Cyclic Triaxial Test
(Deviator Stress = 23.0 kPa and Relative Density = 53%)

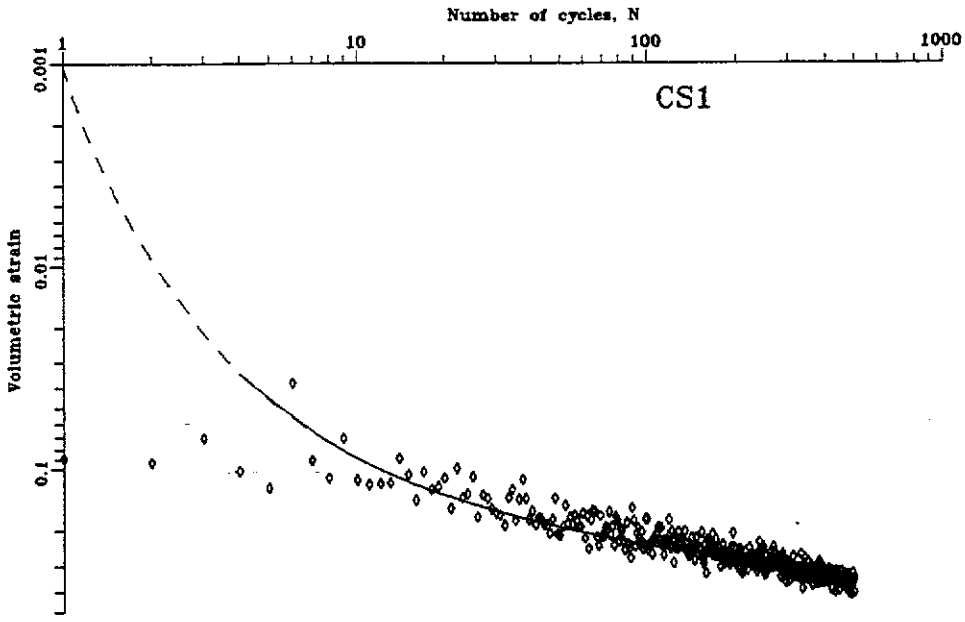

(d) Volumetric Strain Vs. No. of Loading Cycles on Cyclic Triaxial Test
(Deviator Stress = 34.5 kPa and Relative Density = 53%)

Figure 6.35 - Volumetric Strain Versus No. of Loading Cycles on Cyclic Triaxial Test (Sheet 2 of 2)

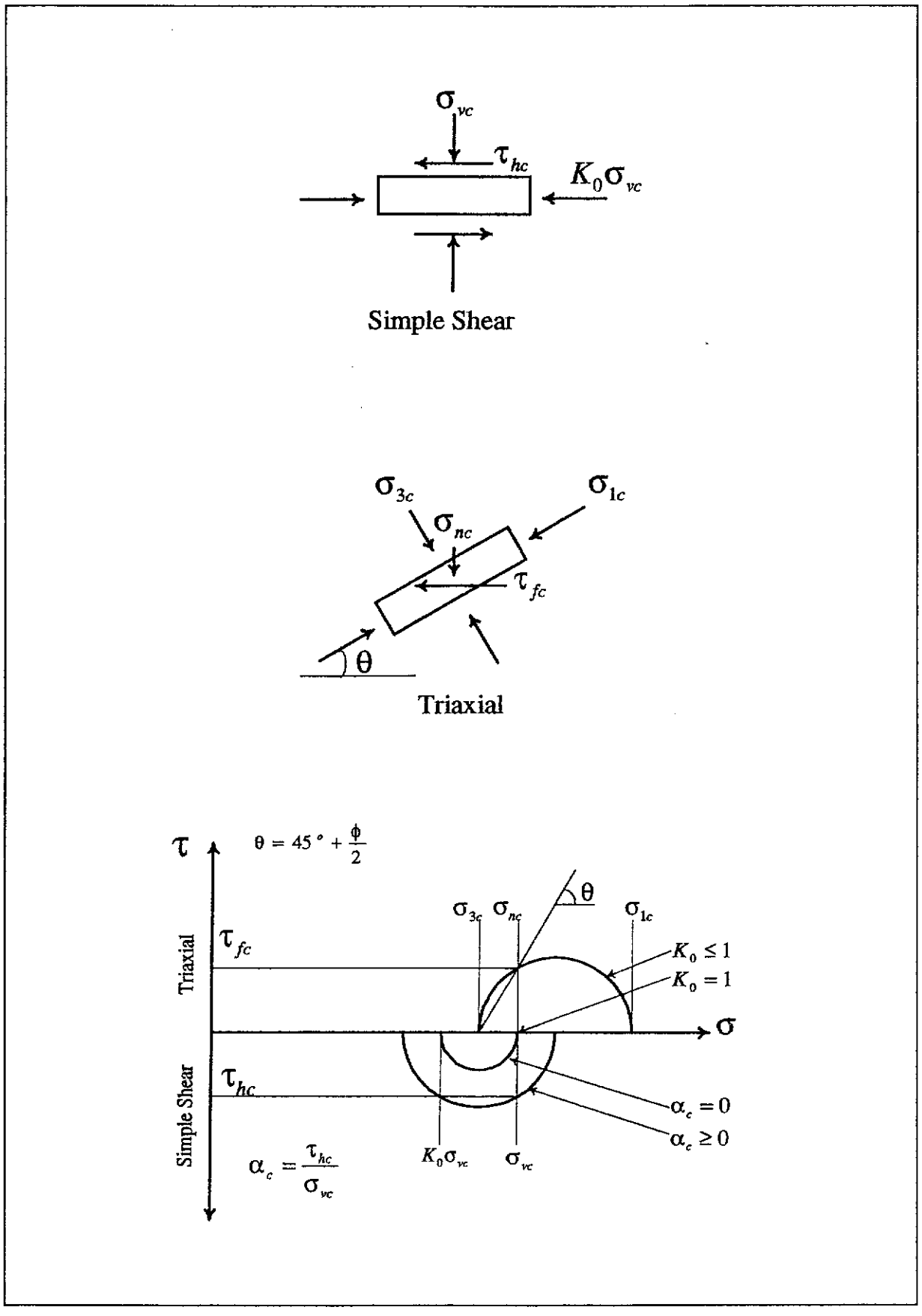

Figure 6.36 - Initial Stress Conditions for Cyclic Laboratory Tests

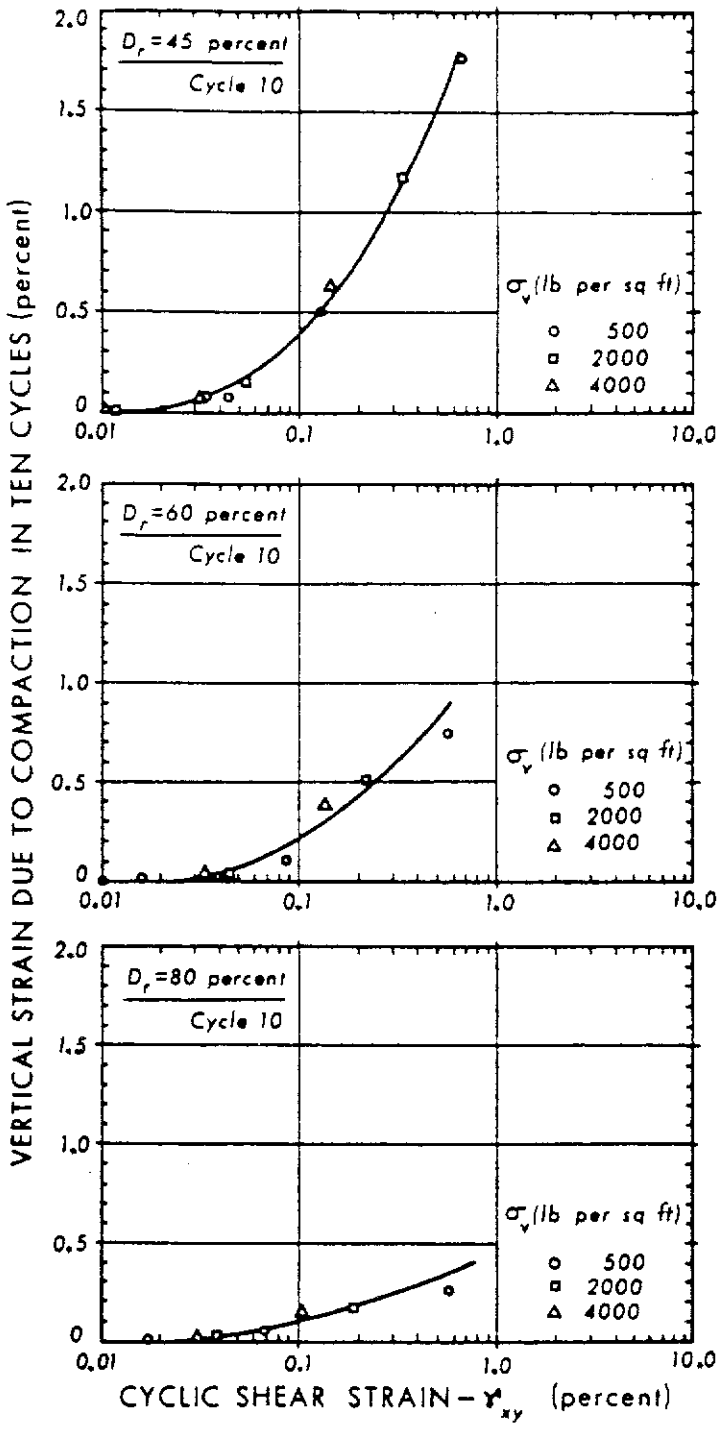

Figure 6.37 - Effect of Confining Pressure on Settlement in 10 Cycles (after Silver & Seed, 1971)

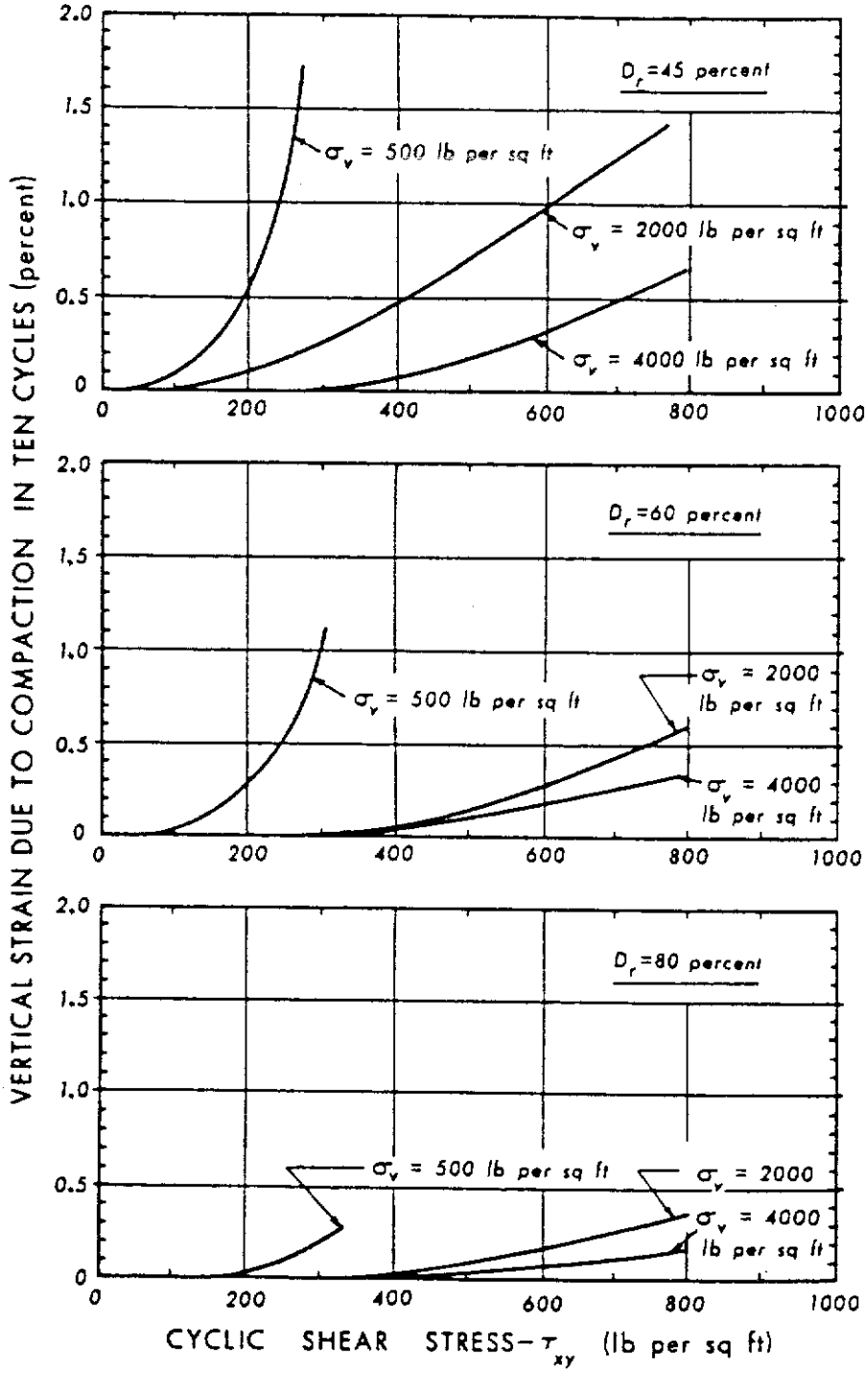

Figure 6.38 - Effect of Confining Pressure on Vertical Settlement in 10 Cycles - Maximum Cyclic Shear Stress Relationship (after Silver & Seed, 1971)

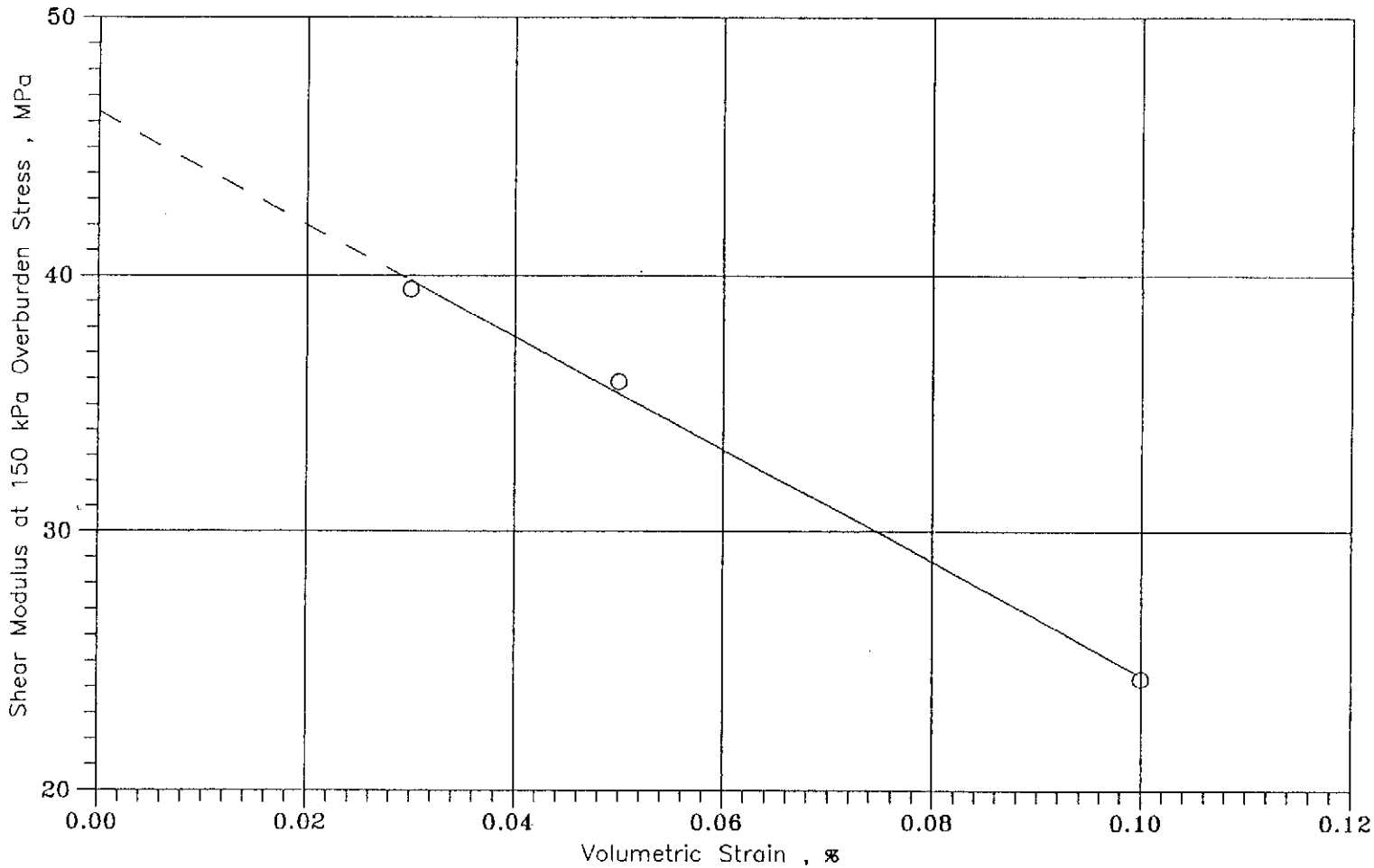

Figure 6.39 - Shear Modulus Under 150 kPa Overburden Stress Versus Volumetric Strain from Cyclic Simple Shear Test

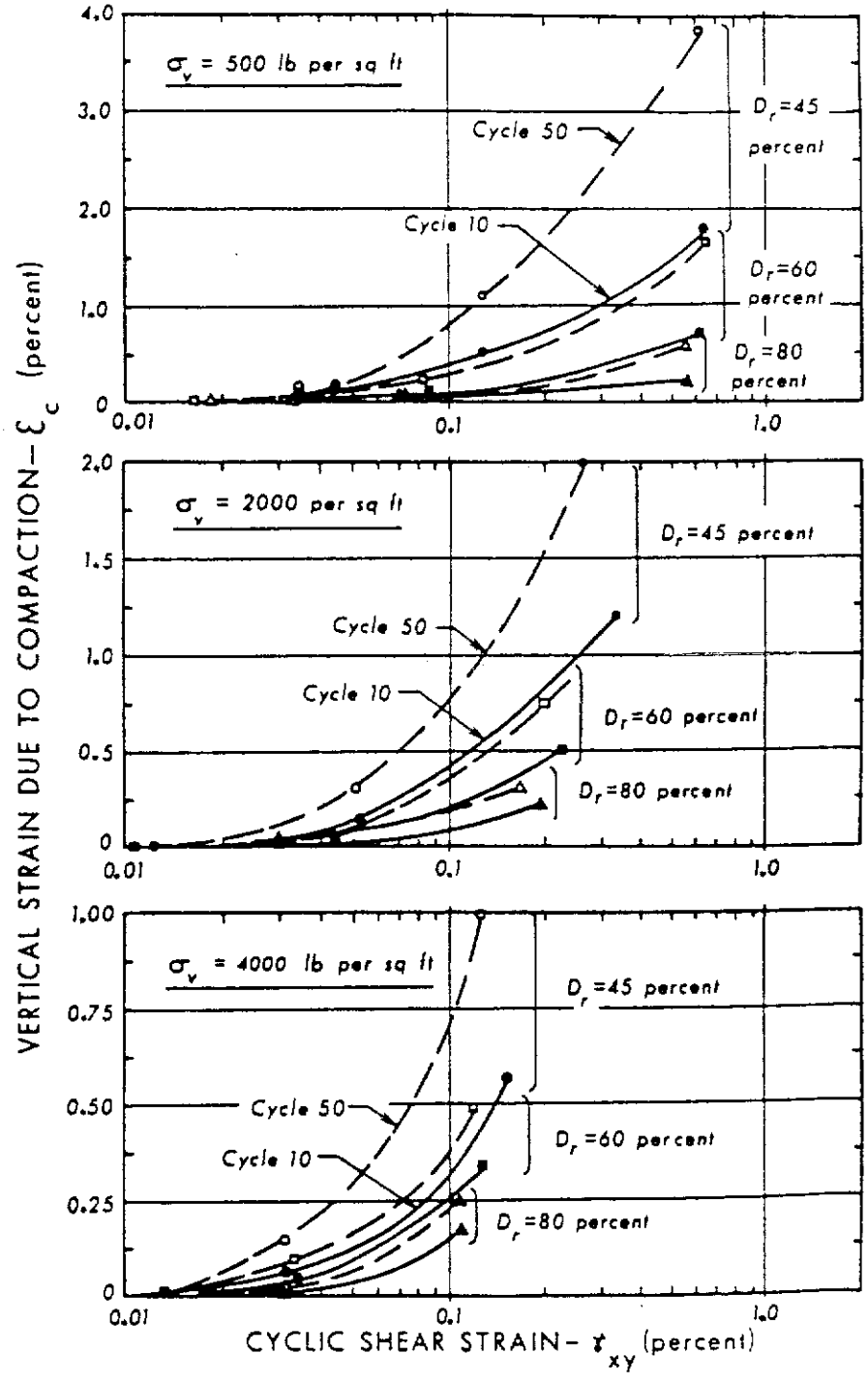

Figure 6.40 - Effect of Number of Strain Cycles on Sand Settlement (after Silver & Seed, 1971)

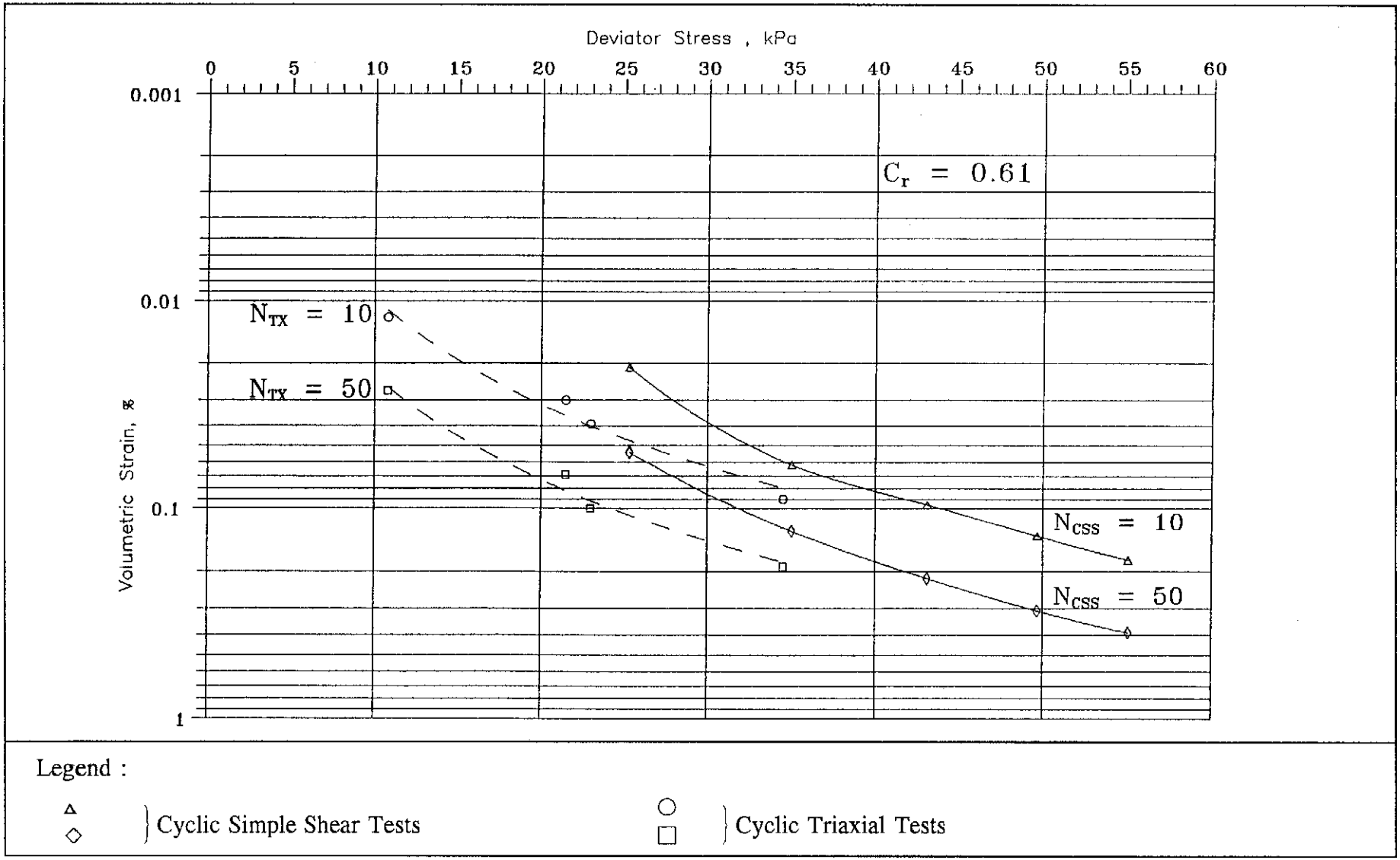

Figure 6.41 - Deviator Stress Versus Volumetric Strain at Different Loading Cycles (N) (C_r = 0.61)

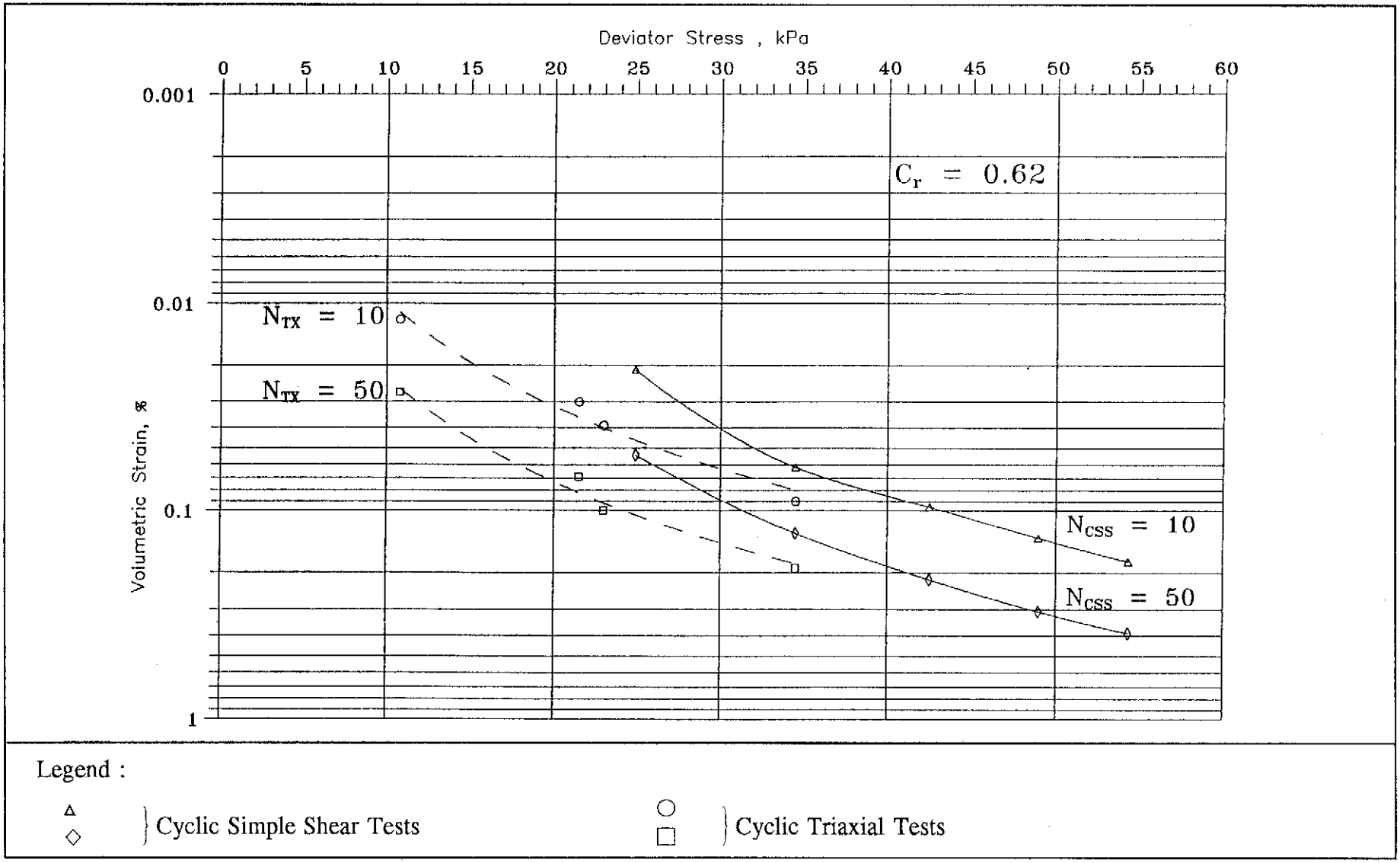

Figure 6.42 - Deviator Stress Versus Volumetric Strain at Different Loading Cycles (N) (C_r = 0.62)

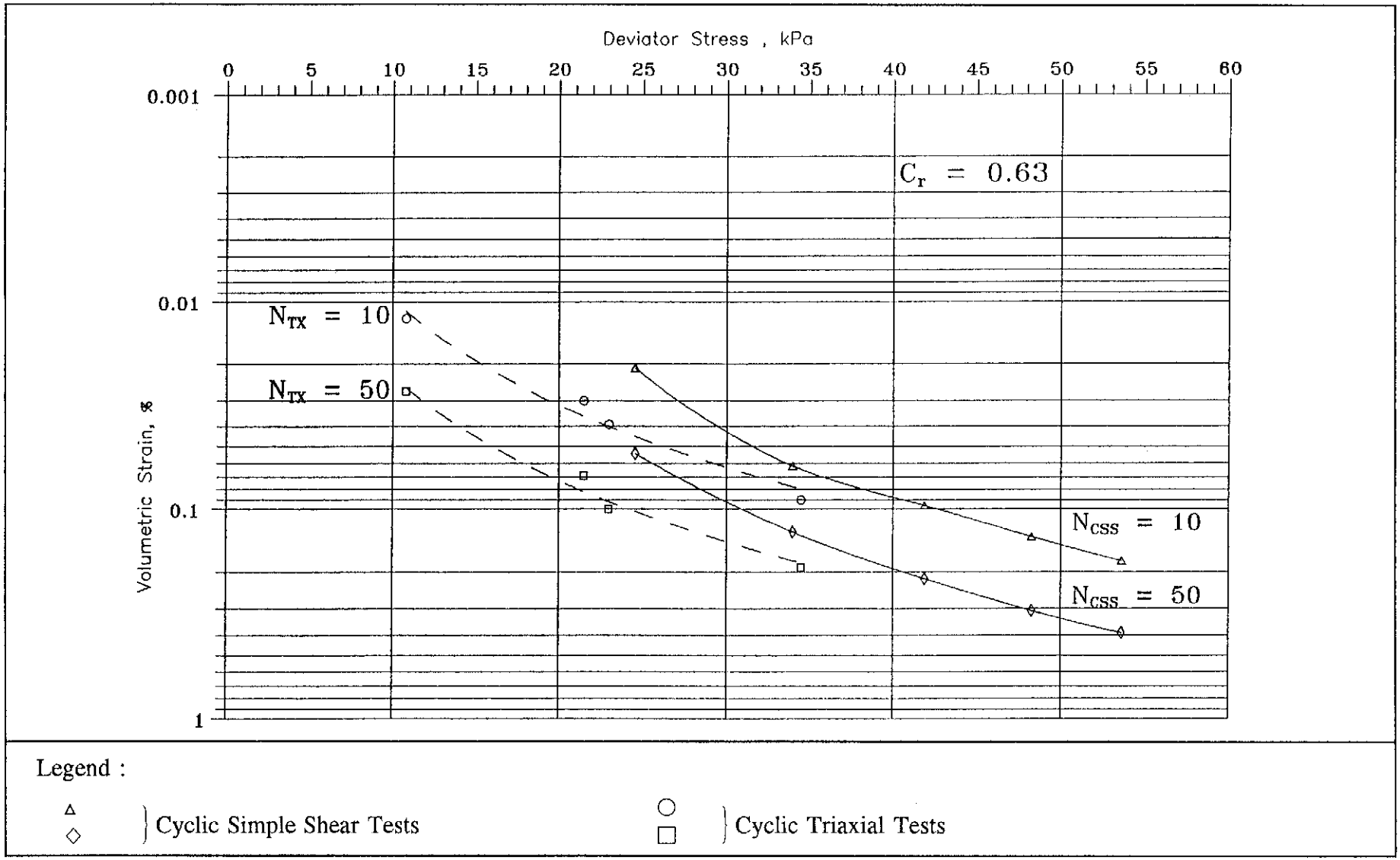

Figure 6.43 - Deviator Stress Versus Volumetric Strain at Different Loading Cycles (N) (C_r = 0.63)

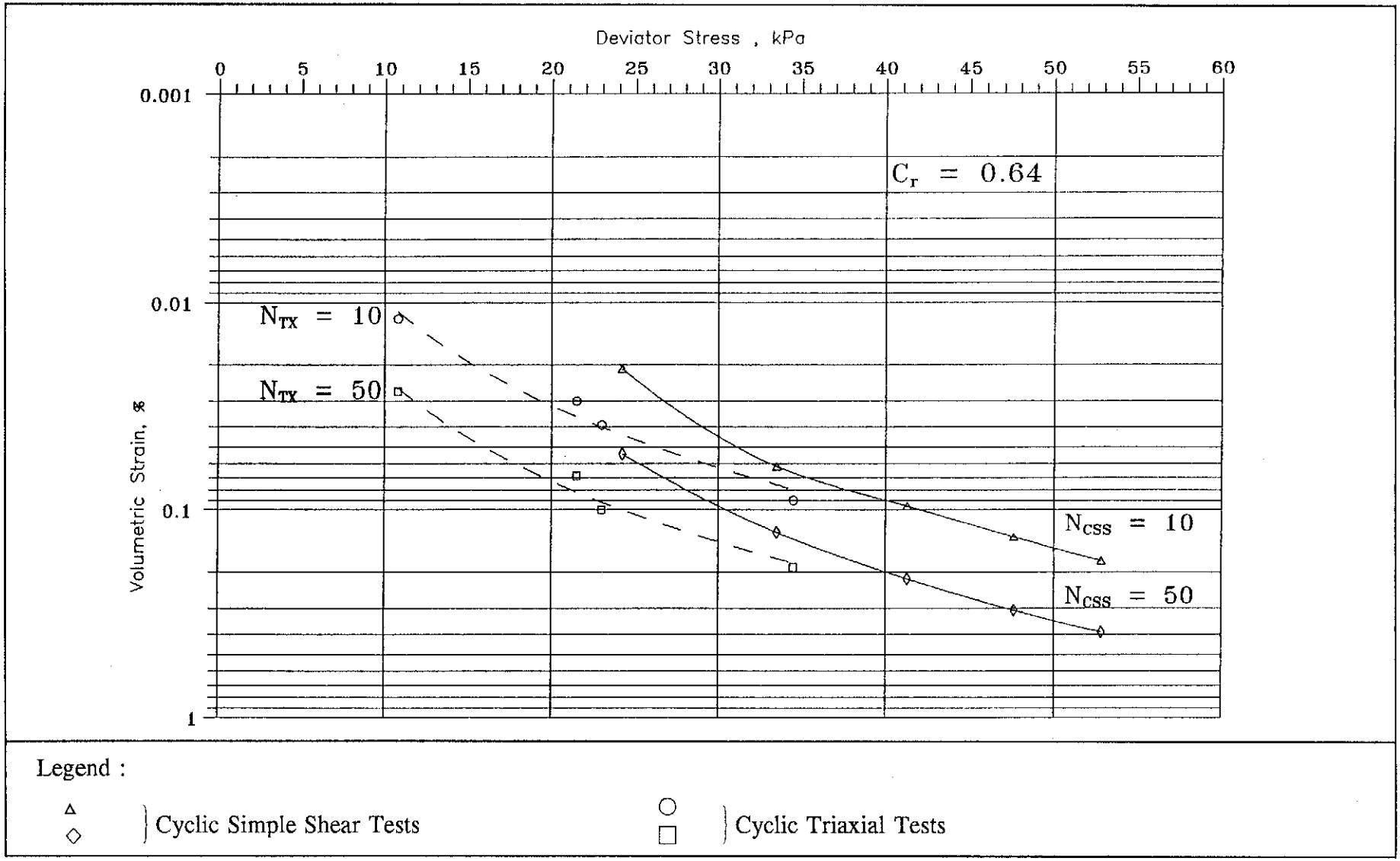

Figure 6.44 - Deviator Stress Versus Volumetric Strain at Different Loading Cycles (N) (C_r = 0.64)

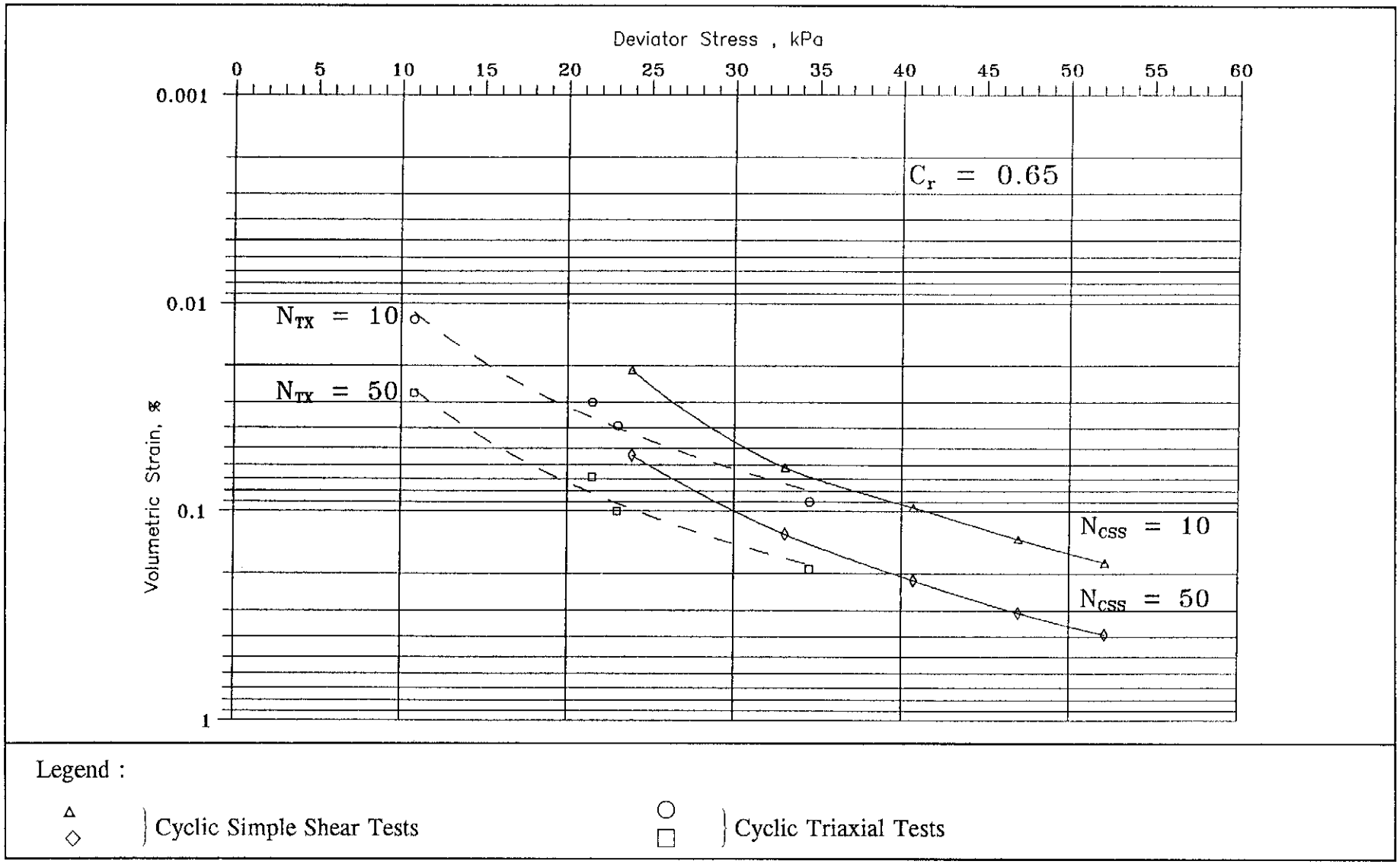

Figure 6.45 - Deviator Stress Versus Volumetric Strain at Different Loading Cycles (N) (C_r = 0.65)

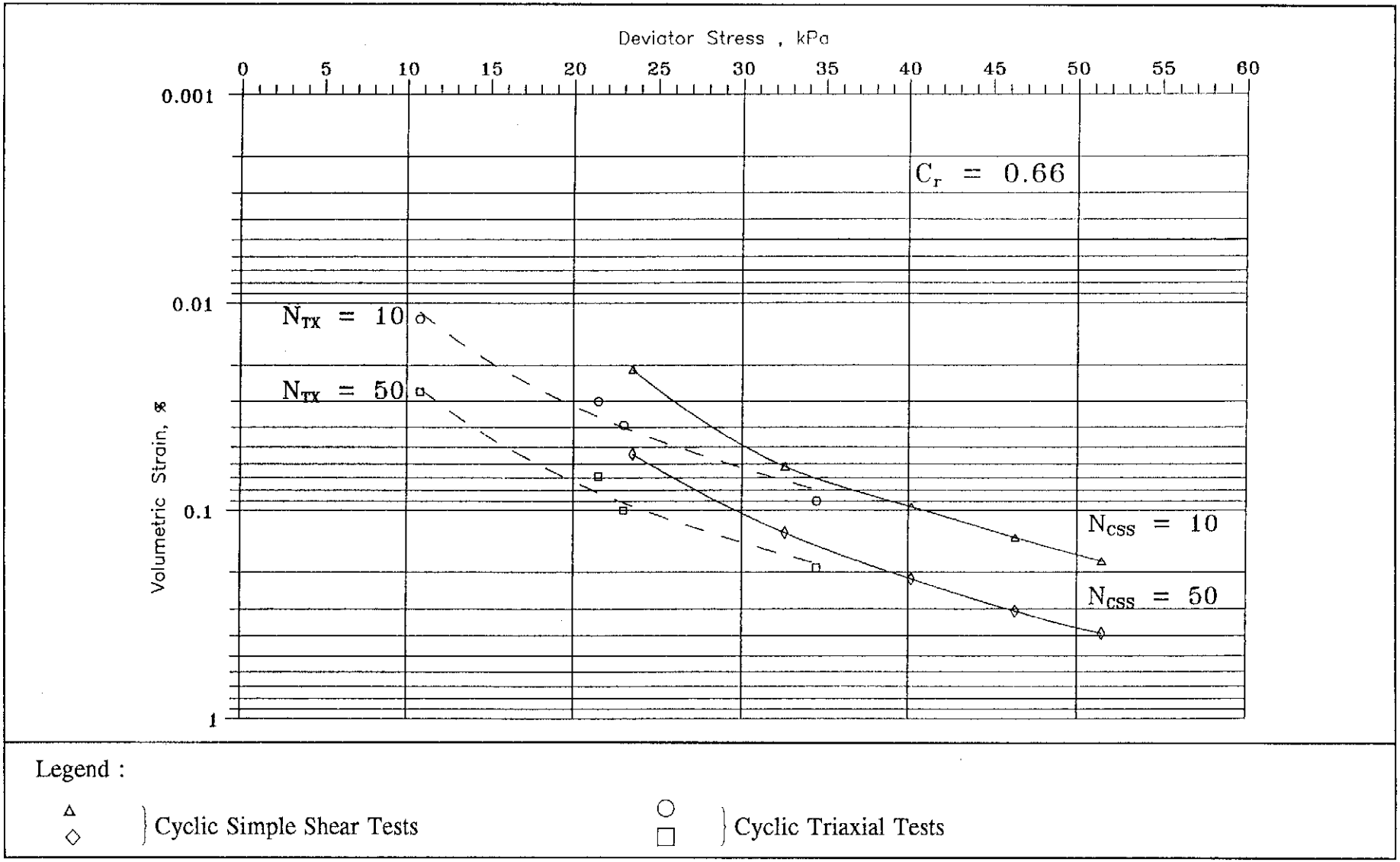

Figure 6.46 - Deviator Stress Versus Volumetric Strain at Different Loading Cycles (N) (C_r = 0.66)

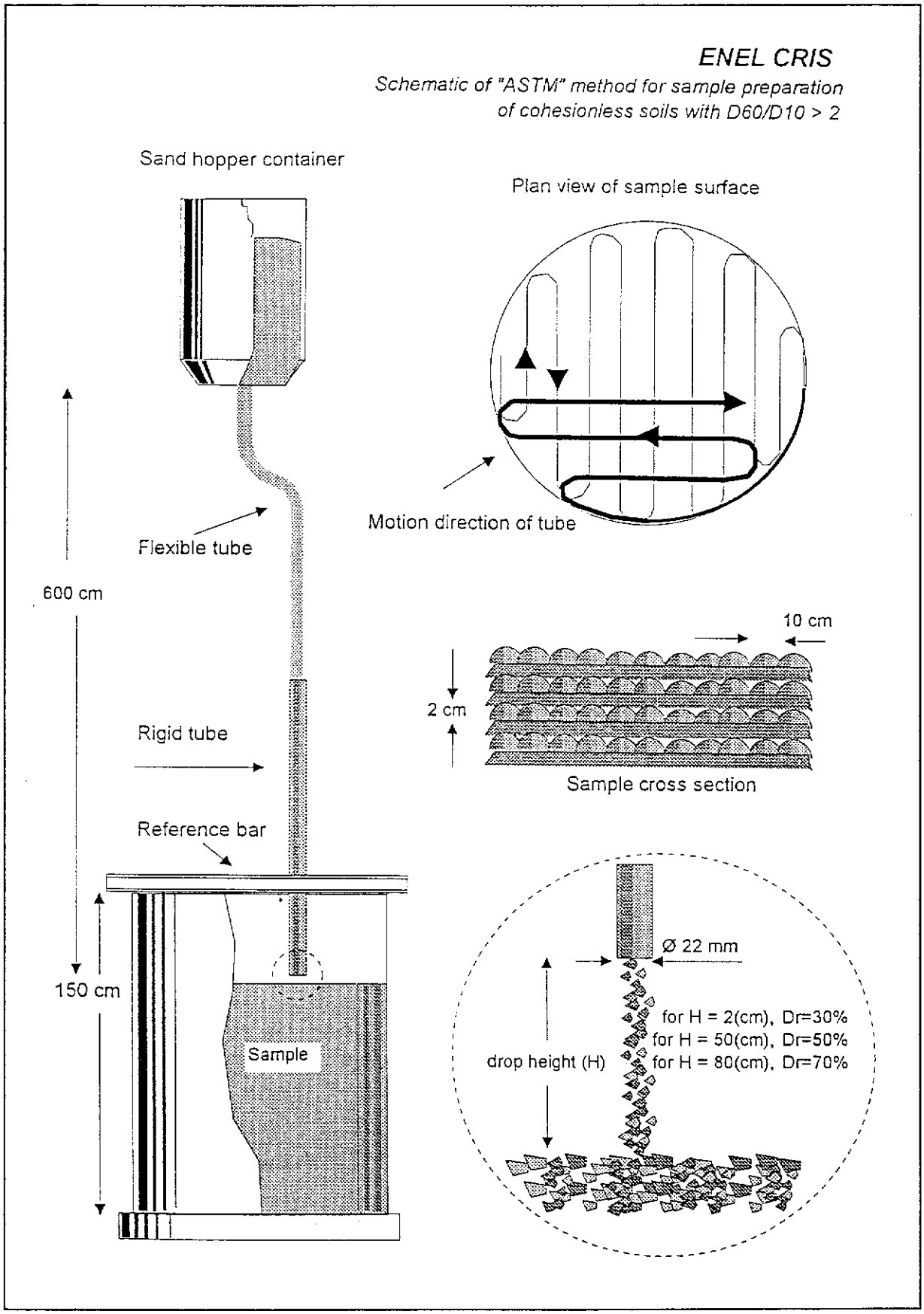

Figure 7.1 - Schematic of "ASTM" Method for Sample Preparation of Cohesionless Soils

ISMES

Environmental department
Calibration Chamber testing - Penetration stage

Test n.:	443	H,c:		141.9 (cm)	Cone diameter: 20 (mm)
Sand type:	Honk Kong CS	V,c:		1.595 (m3)	Cone n.: 125 -
Sand conditions:	saturated	γ d,min.:	(ASTM)	1.573 (t/m3)	Penetration rate: 2 (cm/sec)
σ v',c:	51.8 (KPa)	γ d,max.:	(")	1.837 (t/m3)	qc (50:60cm): 1338.3 (KPa)
σ h',c:	33.5 (KPa)	γ d,c:		1.654 (t/m3)	qc (90:100cm): 2659.7 (KPa)
Back pressure:	30.3 (KPa)	Dr,c:		33.5 (%)	Test date: 30.04.1993
OCR:	1	γ d,cc:		1.658 (t/m3)	Revision date: 3.05.1993
Boundary conditions,p:	BC 1	Dr,cc:		35.8 (%)	Technicians: F.C.-S.M.

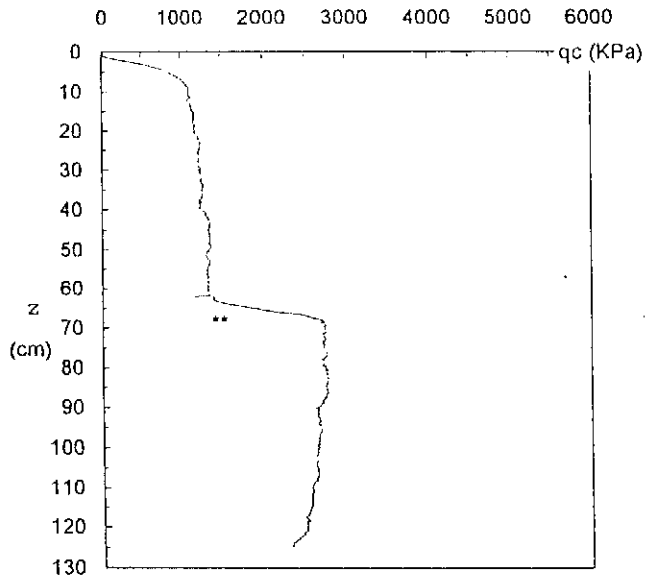

depth (cm)	qc (KPa)	fs (KPa)	Rf (%)	δ h (mm)	δ v (cm3)	σ h' (KPa)*	σ v' (KPa)*	K (-)	σ oct' (KPa)	
0	3.0	-	-	0.000	0	33.8	51.8	0.652	39.8	(c)
5	658.7			0.000	14	20.6	36.9	0.559	26.0	
10	1104.7			0.000	7	33.8	51.9	0.651	39.8	
15	1150.0			0.000	9	33.5	51.7	0.648	39.5	
20	1180.2			0.003	9	33.4	51.6	0.649	39.5	
25	1228.5			0.009	12	33.7	51.7	0.651	39.7	
30	1234.5			0.000	10	33.4	51.5	0.649	39.4	
35	1273.8			0.009	12	33.2	51.2	0.649	39.2	
40	1270.7			0.006	12	33.1	51.0	0.650	39.1	
45	1337.2			0.009	12	33.1	50.8	0.651	39.0	
50	1349.2			0.015	12	33.1	51.0	0.649	39.0	
55	1328.1			0.018	10	33.1	51.0	0.649	39.1	
60	1316.0			0.018	10	32.8	50.4	0.651	38.7	
65	1889.9			-0.003	11	65.9	101.1	0.652	77.6	(cc)
70	2741.2			-0.003	28	65.7	100.9	0.651	77.4	
75	2733.0			0.000	33	65.7	100.7	0.652	77.3	
80	2765.3			-0.003	34	65.6	100.8	0.651	77.3	
85	2753.2			0.000	38	65.7	101.2	0.650	77.6	
90	2647.6			-0.018	38	66.0	101.3	0.651	77.8	
95	2665.7			-0.015	44	65.7	100.9	0.651	77.5	
100	2665.7			-0.024	38	65.9	101.2	0.651	77.7	
105	2638.5			-0.012	46	65.6	100.5	0.653	77.2	
110	2581.2			-0.009	49	65.6	100.7	0.652	77.3	
115	2545.0			-0.015	46	65.7	100.5	0.654	77.3	
120	2502.7			-0.009	49	65.7	100.7	0.652	77.3	
125	2324.6			-0.015	49	65.7	101.0	0.650	77.4	
130										

*Effective stresses are measured at 75 cm of depth

**At 62 cm of depth , the insertion of the cone was stopped and the stress state had been modified(see the stress history data sheet).

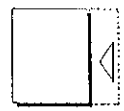

δ v<0

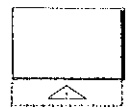

δ h>0

Figure 7.2 - Typical Calibration Chamber Test Result

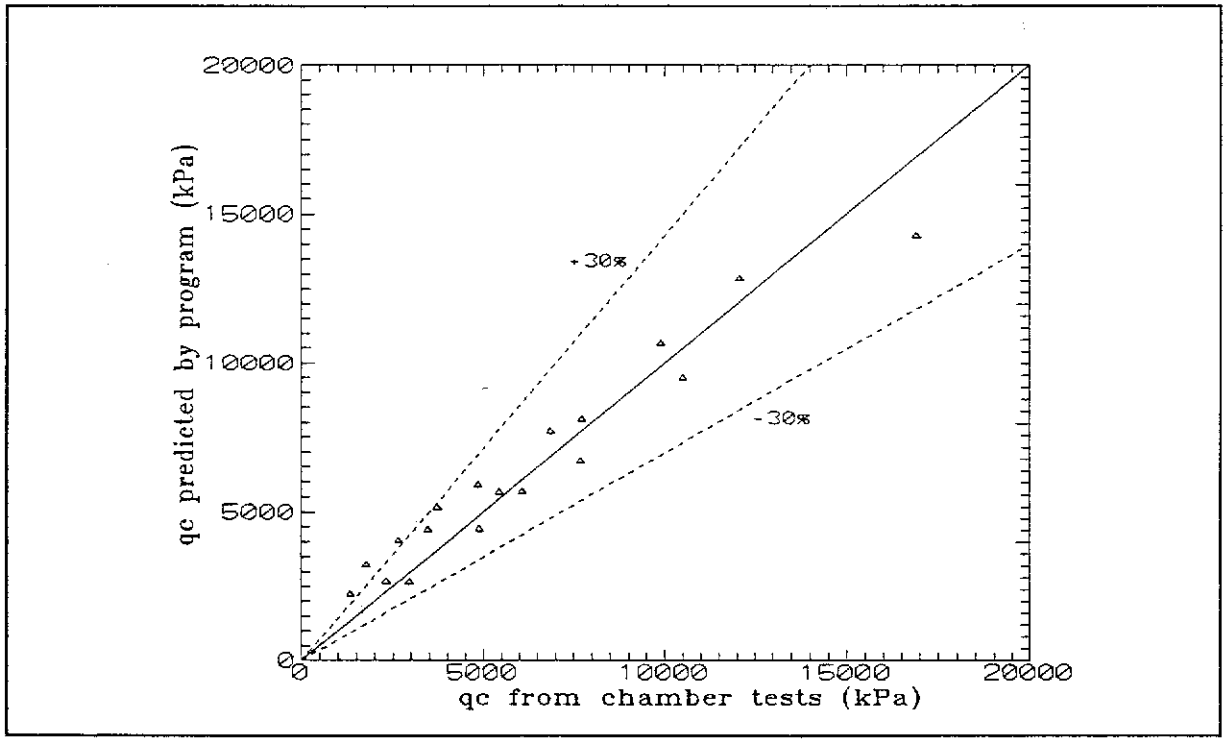

Figure 7.3 - Comparison between q_c Predicted by the F.E. Program and the Actual Chamber Test Results for CS1 Sand

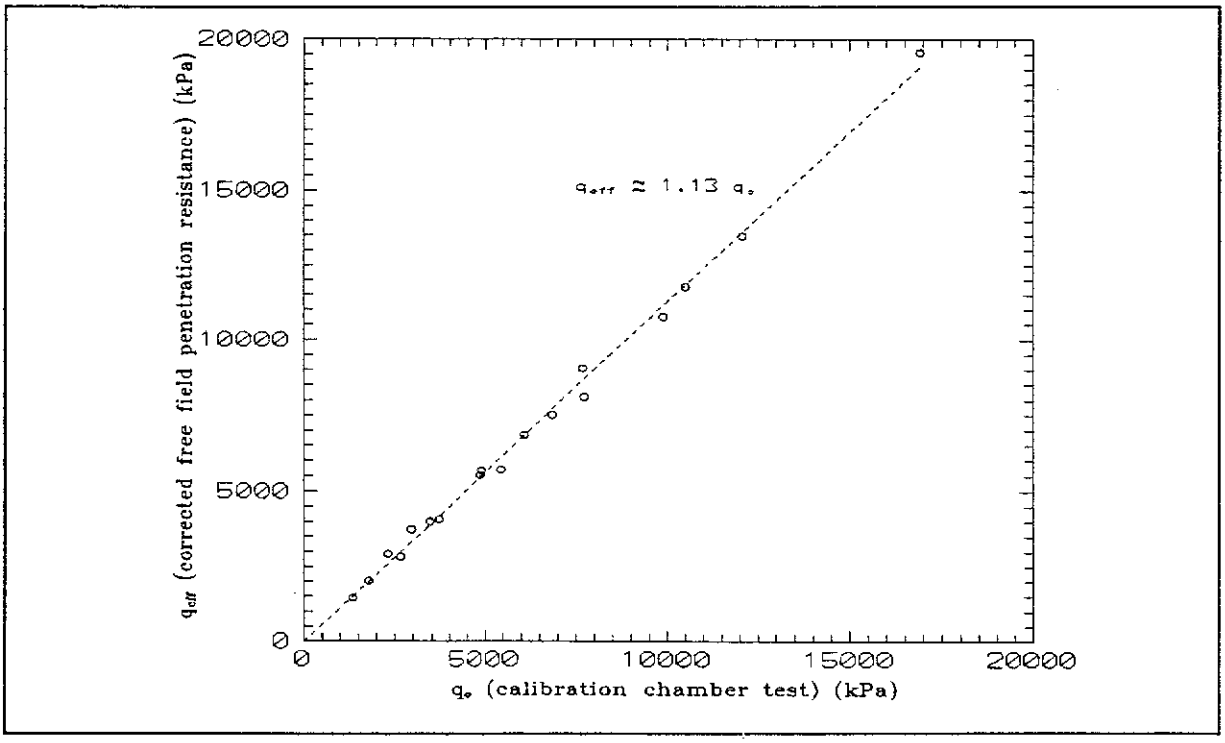

Figure 7.4 - Relationship between q_c Obtained from Calibration Chamber Tests and Predicted Free Field Penetration Resistance (q_{cff}) for CS1 Sand

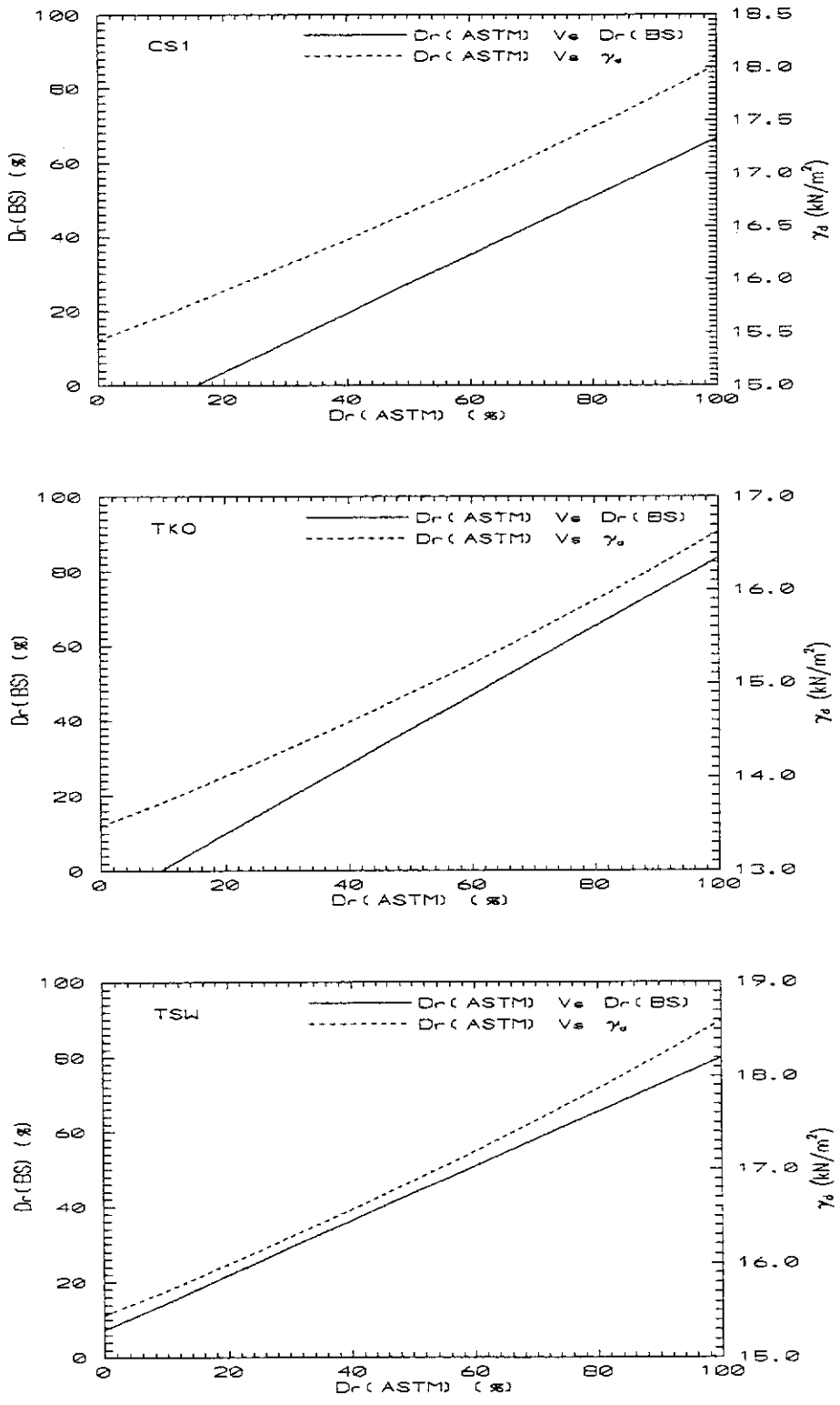

Figure 7.5 - Conversion between $D_{r(ASTM)}$ and $D_{r(BS)}$ for CS1, TKO and TSW Sands

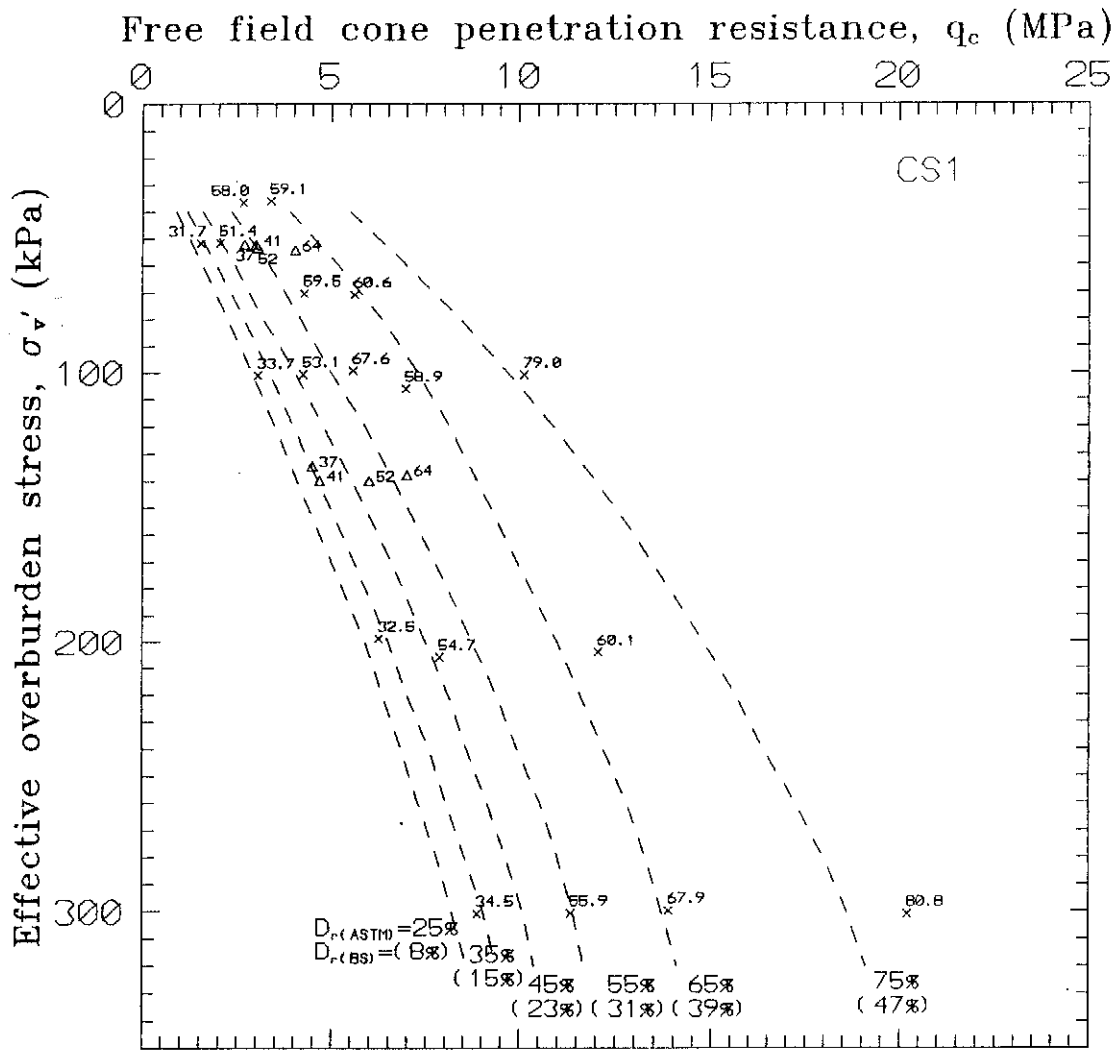

Figure 7.6 - σ_v' - q_c - D_r Correlations for CS1 Hydraulic Fill Sand

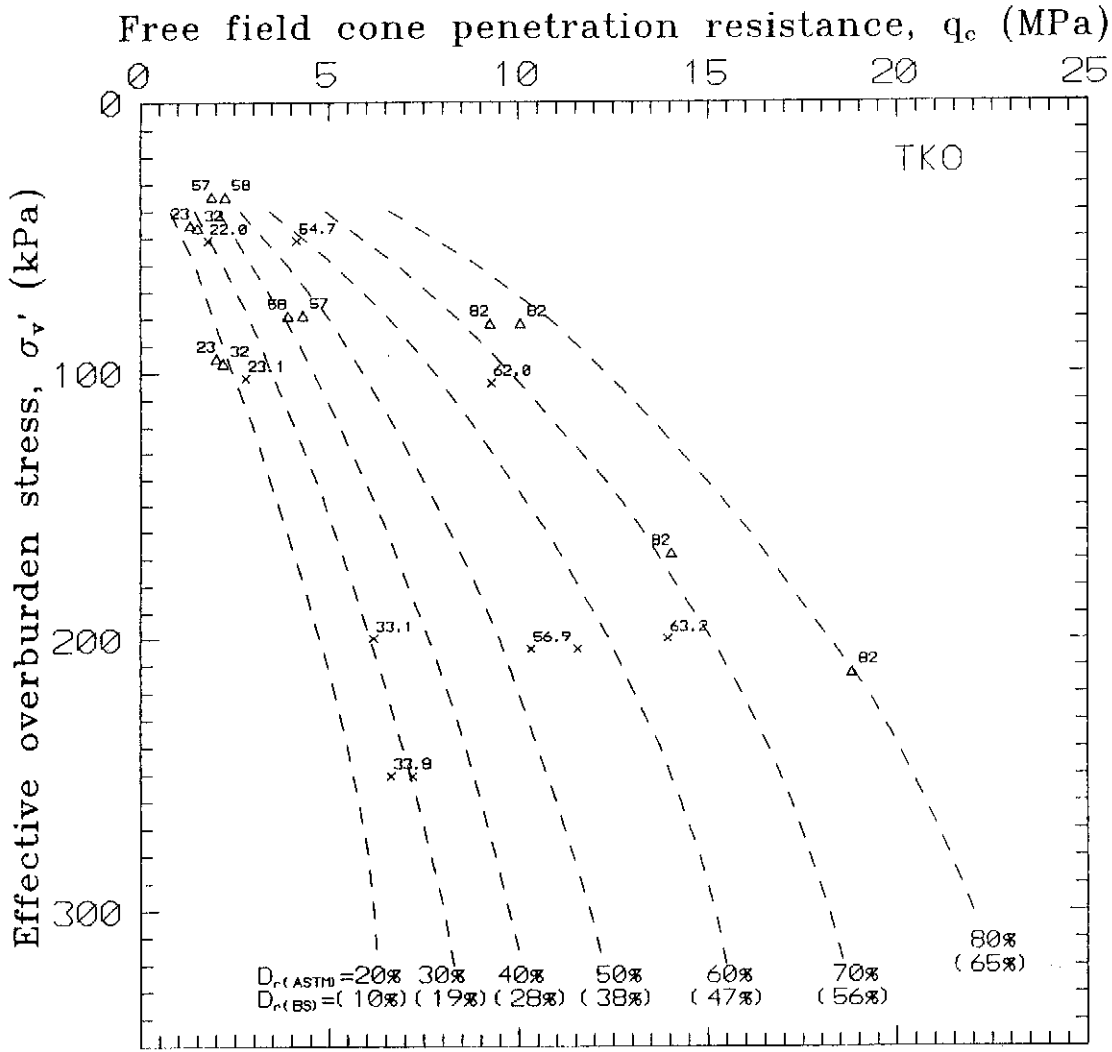

Figure 7.7 - σ_v' - q_c - D_r Correlations for TKO Hydraulic Fill Sand

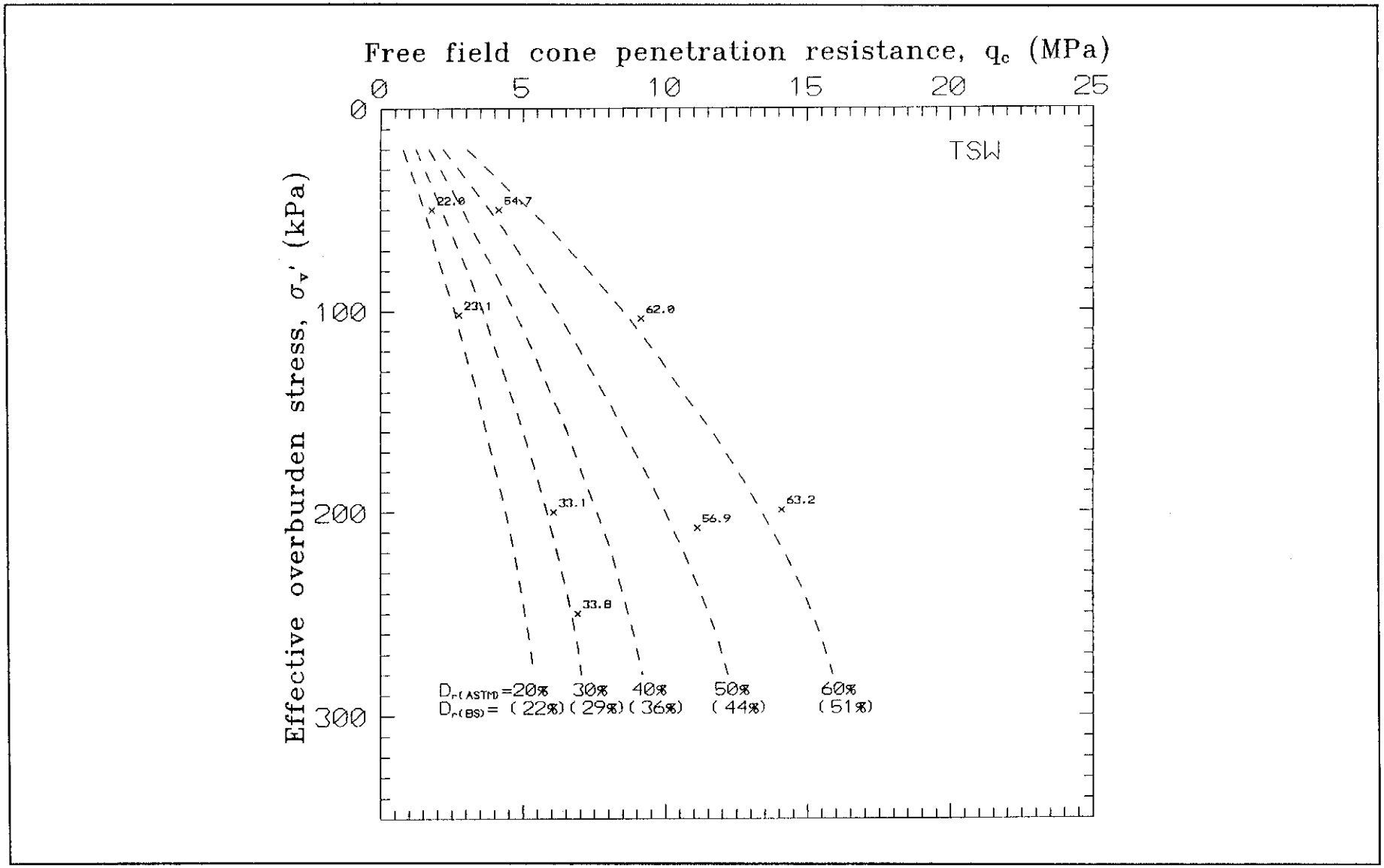

Figure 7.8 - σ_v' - q_c - D_r Correlations for TSW Hydraulic Fill Sand

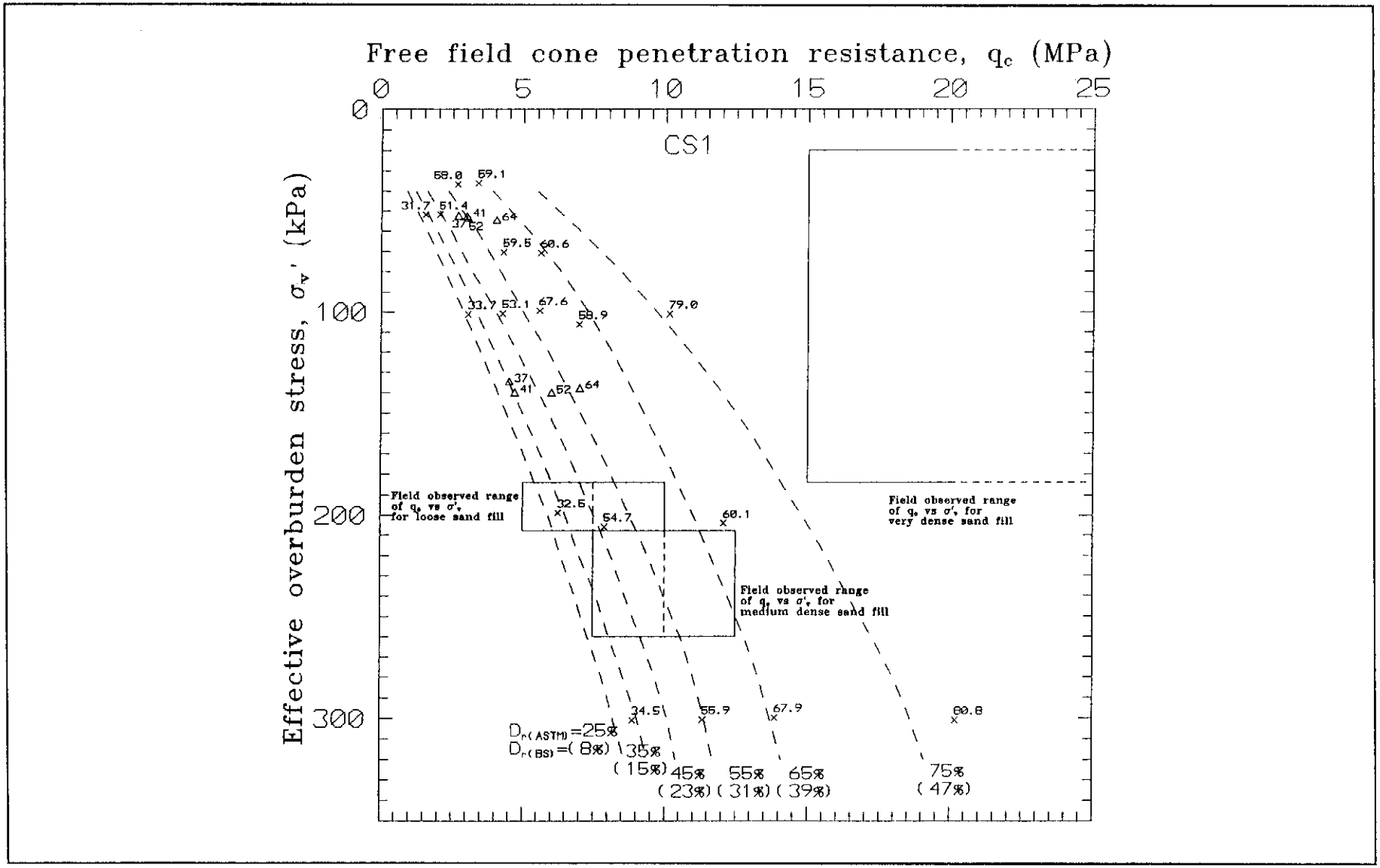

Figure 7.9 - Comparison of q_c Versus σ_v' for Insitu Observed Values and Calibration Chamber Test Results for CS1 Sand

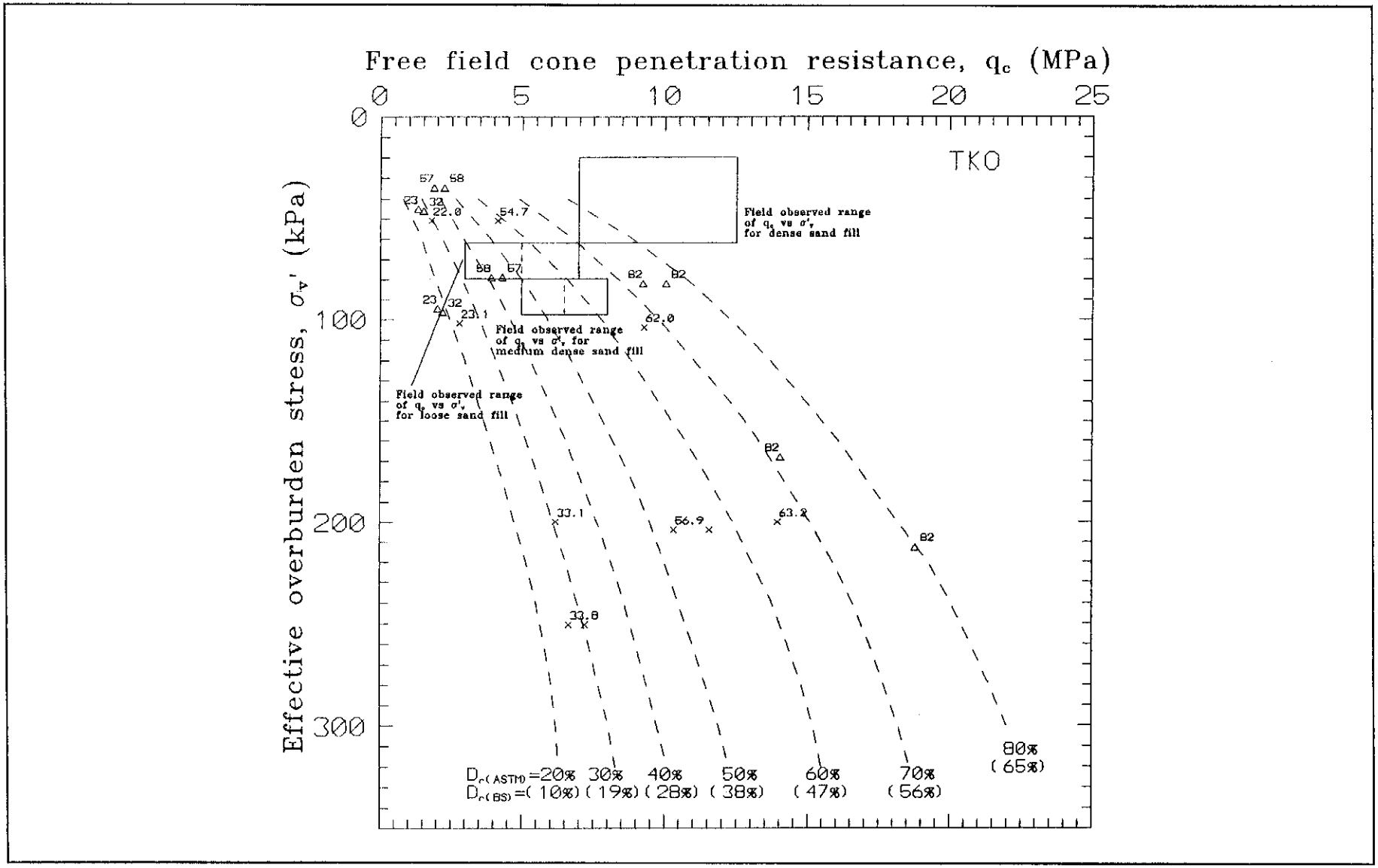

Figure 7.10 - Comparison of q_c Versus σ_v' for Insitu Observed Values and Calibration Chamber Test Results for TKO Sand

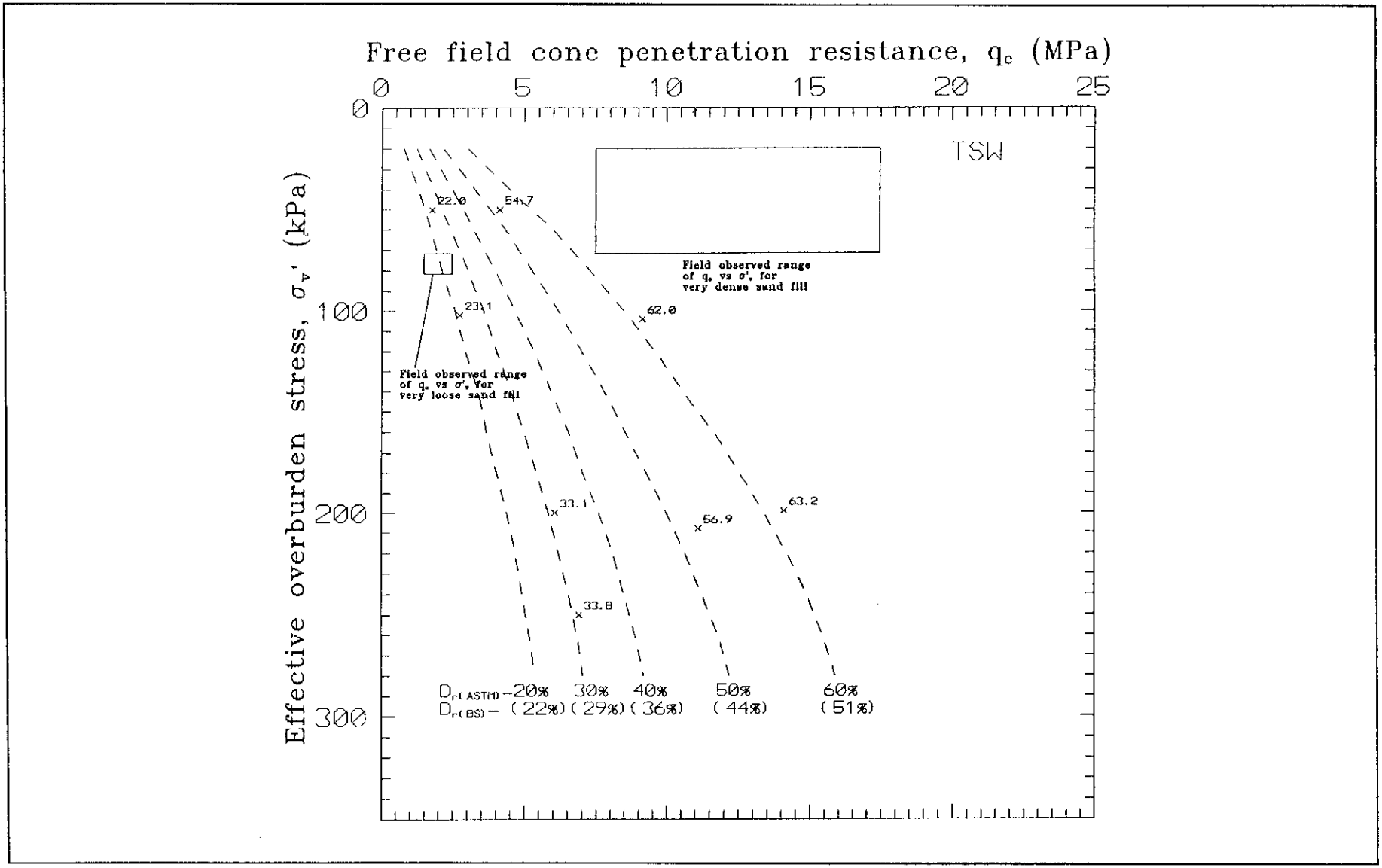

Figure 7.11 - Comparison of q_c Versus σ_v' for Insitu Observed Values and Calibration Chamber Test Results for TSW Sand

LIST OF PLATES

Plate 3.1 - Undisturbed Sample Obtained by Mazier Sampler (CS1)

Plate 3.2 - Hydraulic Filling by Spigotting

Plate 3.3 - Hydraulic Filling by Pump-out

Plate 4.1 - Excavation for Bulk Sample

Plate 4.2 - Steel Barrels Holding Marine Sand Fill to be Shipped out to Italy for Stress Chamber Testing

Plate 4.3 - Segregation Marks of Fine-to-coarse Sands at the West Kowloon Reclamation Site

Plate 4.4 - Segregation Marks of Fine-to-coarse Sands at the Tseung Kwan O Site

Plate 4.5 - Segregation Marks of Fine-to-coarse Sands at the Tin Shui Wai Site

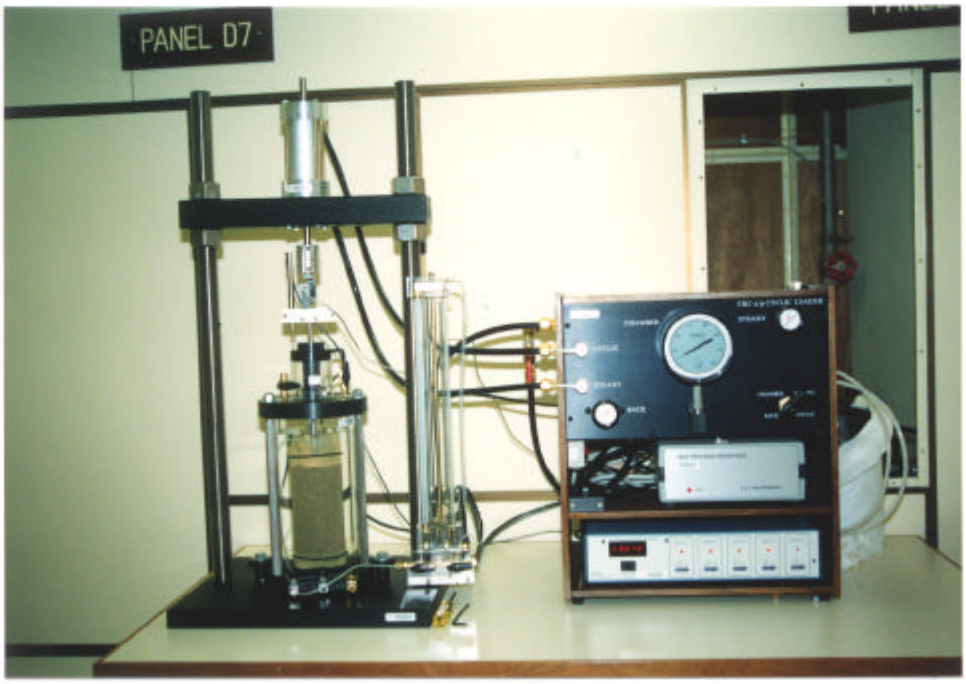

Plate 5.1 - Automated Triaxial Testing System

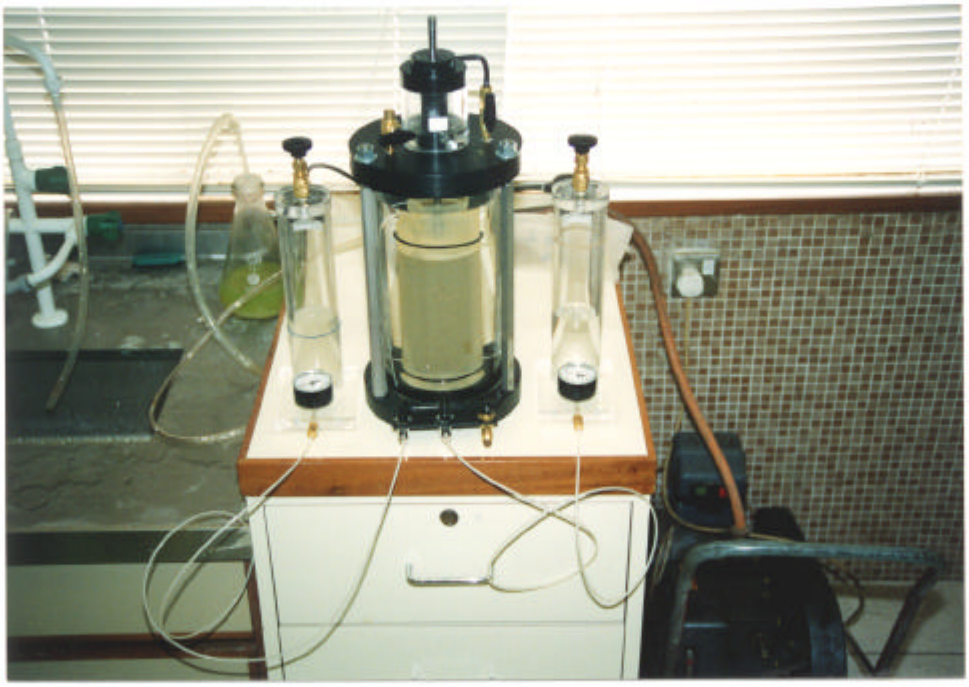

Plate 5.2 - Dual Evacuation Chambers Method for Sample Saturation